Saline Waste Use for Subgrade Soil Improvement

by

Ali Fakih

A Dissertation Presented in Partial Fulfillment
of the Requirements for the Degree
Doctor of Philosophy

Approved June 2017 by the
Graduate Supervisory Committee:

Kamil Kaloush, Chair
Claudia E. Zapata
Peter Fox

ARIZONA STATE UNIVERSITY

August 2017

ABSTRACT

Chloride solutions have historically been used to stabilize roads and to prevent dust; however, very little work has been done on investigating the soil stabilizing benefits from interactions between salt solutions and different soil types. The primary goal of this research was to analyze the feasibility of utilizing a salt waste product as an economically and environmentally responsible means of dust control and/or soil stabilization. Specifically, this study documents an investigation leading to the understanding of how the addition of saline based waste products, when using a soil stabilizer, modifies the strength behavior of soils.

The scope of work included the evaluation of current literature, examination of the main challenges meeting relevant governmental regulations, and exploring the possibility of using saline waste to improve roadways.

Three soils were selected, treated with varying amounts of salt (calcium chloride, $CaCl_2$), and tests included soil composition and classification, correlation of soil characteristics and salt, and obtaining strength parameters that are typically used in pavement design and analysis. The work effort also included the determination of the optimum dosage of salt concentration for each soil. Because Lime treatment is also commonly used in soil stabilization, one of the soils in this study included a treatment with Lime for comparison purposes.

Results revealed that when salt concentration was increased, a decrease in the plasticity index was observed in all soils. A modest to considerable strength gain of the treated material was also observed for two of the soils; however, a strength loss was observed for the third soil, which was attributed to its low clay content.

When comparing the soil corrosive potential, the additional salt treatment showed promise for increasing strength, to an extent; however, it changes the chemical properties of the soil. The soils prior to treatment were corrosive, which could be

managed with appropriate techniques, but the salt increases the values to levels that could be potentially cost prohibitive if salt was used by itself to treat the soil.

The pavement design and performance investigation revealed that the Vineyard soil treated at 16% $CaCl_2$ had an improvement that is comparable to the Lime treatment. On the other hand, the Eager soil showed very little pavement performance improvement at 8% $CaCl_2$; this goes back to the effect of acid on the clay mineralogy. It was also postulated that using salt by-products to stabilize highway shoulders could be beneficial and save a lot of maintenance money when it comes to cleaning unwanted vegetation. A salt saturated soil structure could help in dust control as well.

Future environmental challenges for salt leaching that could affect agriculture in developing countries will still need to be carefully considered. The chlorine levels in the soil would increase, and if not treated, can potentially have corrosive effects on buried structures. Future research is recommended in this area and to also evaluate soil stabilizing properties of varying proportions of Lime and salt using the approach provided in this study.

DEDICATION

To my wife, Rashel, for your understanding and support;

To my daughter, Malak and my son Ali;

To my Parents;

I love you all, each one of you has contributed to this achievement.

ACKNOWLEDGMENTS

Firstly, I would like to express my sincere gratitude to my Advisor, Professor Dr. Kamil Kaloush, for the continuous support of my PHD study and related research. I could not have wished for a better friend, mentor, and adviser for my PHD study.

Besides my advisor, I would like to thank the rest of my thesis committee Dr. Claudia Zapata and Dr. Peter Fox whom, without their guidance and inspiration, this dissertation would not have been accomplished.

I thank my colleagues at SEG, clients, and friends for their support and motivation to conduct this research; in particular, Susan Houston, Jose Medina, and Dr. Daniel Rosenbalm for their encouragement and help to finalize this project.

Finally, one should never forget the support and encouragement family: My wife, Rashel, my two beautiful kids, Malak and Ali, my Parents, my two brothers and two sisters for supporting me spiritually and leading me here.

TABLE OF CONTENTS

Page

CHAPTER Page

CHAPTER Page

CHAPTER Page

LIST OF TABLES

Table Page

Table Page

LIST OF FIGURES

Figure Page

Figure Page

Chapter 1

Introduction and Objectives

1.1. Introduction

A strong emphasis is placed on clean air throughout the world. In the United States, the Clean Air Act required the Environmental Protection Agency (EPA) to set National Air Quality Standards for all pollutants that may be harmful to the human and environmental health of a community. Primary standards are enforceable limits set to preserve the health of the public.

The six principal pollutants identified by the EPA are:

Carbon Monoxide (CO)

Lead (Pb)

Particulate Matter (PM)

Ozone (O_3)

Nitrogen Dioxide ($NO_{2)}$

Sulfur Dioxide ($SO_{2)}$

Within the Particulate Matter (PM) standards that regulate suspended particulate matter in the air is particle pollution, a mixture of solid particles and liquid droplets found in the air. (Environmental Protection Agency, National Ambient Air Quality Standards (NAAQS), 2015). Particle pollution includes PM_{10} and $PM_{2.5}$ (particulate matter less than 10 micrometers and 2.5 micrometers, respectively) are inhaled and are emitted from sources such as construction sites, unpaved roads, fields, smokestacks and fires. These microscopic droplets represent the great harm as they can be inhaled and cause major health problems. (Environmental Protection Agency, National Ambient Air Quality Standards (NAAQS), 2015). Standards continue to be stricter, as discussions may further restrict coarse PM, primarily composed of suspended dust and dirt, as part of the Clean Air Act's Five-Year Review (Reske, 2011).

Dust Control is becoming a serious environmental challenge worldwide. Despite the existence of many opportunities for dust suppression, there are still unresolved issues that need to be addressed. Many products and processes currently in the marketplace do not offer long-term solutions. Other unresolved issues include analysis of human and environmental health and safety. Within the U.S., some cities and states are supportive of alternative technologies, while others are not. The burden is on the manufacturers to prove the safety of their products.

Beyond the United States, there are many countries throughout the world faced with problems of dust. Regions such as Asia, Africa, the Middle East and Australia are also heavily impacted by dust. Dust storms in these dry areas are often highlighted in the news due to their impacts upon human health with the transfer of bacteria, viruses and other microorganisms along with the particulate matter of the dust. Countries within these regions are also very interested in utilizing improved methods of dust control that will conserve their small resources of water and may only dampen the dust. This problem is clearly a global issue. Recent air pollution emergencies in China and India have forced the closure of schools and construction sites, suggesting that citizens stay indoors and where masks due, in part to uncontrolled air born dust (Newsmax, 2017) (Krausz, 2016). Additional research for a sustainable and lasting dust suppressant material is needed.

Notably, the long-term sustainability of dust suppression products based primarily on potable water use will not be applicable in areas of drought, or in the future when water conservation will undoubtedly be increased. These countries must conserve their small resources of water and rather than well wet the dusty areas, may only dampen the dust.

In addition to water, there are many organic and manufactured products currently available for dust control. The EPA recognizes Chlorides (Calcium and

Magnesium Chloride), Resins, Natural clays, Asphalts, Soybean Oil, and other commercial binders (Environmental Protection Agency, 2015), with each manufacturer claiming to have the best technology and application process. The majority of these products are water or oil-based and do not stand the tests of time when they are applied to roadways or other typical dusty areas.

Chlorides can be detrimental to animals and plants. Calcium chloride is corrosive to vehicles and application equipment (University of Wisconsin, 1997). Resins are by-products of manufacturing processes. They need to be evaluated in terms of effectiveness and safety, depending on specific road conditions (Environmentally Sensitive Maintenance for Dirt and Gravel Roads; EPA, Chapter 7, 2010). Natural Clays must contain the correct moisture content and can be difficult to apply (Environmental Protection Agency, 2003). Asphalt requires considerable energy to produce. (Environmental Protection Agency, 2003). Soybean Oil (Acidulated Soybean Oil Soapstock), although a bi-product of soybean oil refining, is effective in controlling dust on limited road surfaces and must be applied to a dry road surface (U.S.Roads, 1998). Other commercial binders such as Lime, lignins, polymers and other synthetic products may improve soil stability but also produce undesired physical or environmental reactions; further discussed in Chapter 2.

Superior techniques with sustainable components must be used to phase out these unsustainable products. Such sustainable components would include lower energy use in production, maximized use of by-products, less dependence on water usage, and be environmentally friendly, recyclable, long lasting and cost effective. Long term impact analysis of these existing products must also be completed in order to compare fair market economies and find a reasonable equilibrium point.

With the exception of Soybean Oil, existing dust suppression products do not consider using recycled waste to address the environmental challenges. There are very

few studies that present the use of Saline Solutions, as an industrial waste product, to address growing dust control challenges. For example, North Dakota has approved the use of salt brine formed through the process of oil and gas drilling; the safety of this method is still under dispute (Macpherson, 2008). Canada considers the application of this and any salt-based product to be toxic. Inorganic chlorides, with or without ferrocyanide salts, may be having an immediate or long term effect on surface water organisms, terrestrial vegetation, and wildlife. These chlorides may also constitute a danger to the environment on which life depends through its impacts on aquatic systems, soils, and terrestrial habitats. Thus, road salts that contain inorganic chloride salts, with or without ferrocyanide salts, should be considered toxic because of tangible threats of serious or irreversible environmental damage (Environment Canada and Health Canada, 2001).

Chloride solutions have historically been used to stabilize roads and to prevent dust; however, very little work has been done on investigating the soil stabilizing benefits from interactions between salt solutions and different soil types.

This study expands the research and testing in this focus area to provide further guidance and address potential uses of saline waste. On a basic level, salt has been used for many years in research for dust control and roadway stabilization (Salt Institute, 1982). Salt waste products are not being used for dust control and roadway stabilization today; many challenges in the technology need to be improved prior to vast commercialization of these products. More advanced techniques for water and wastewater treatment and use of these salt waste products should be employed (such as typical desalination as well as ion exchange) in order to utilize the salts naturally found in the wastewater.

1.2. Research Objective

The primary goal of this research is to analyze the feasibility of utilizing a salt waste product as an economically and environmentally responsible means of dust control and/or soil stabilization. Specifically, this study documents an investigation leading to the understanding of how the addition of saline based waste products, when used a soil stabilizer, modifies the strength behavior of soils. With a positive determination of feasibility, the longer term goal of creating the technology and associated products for the saline waste usage is researched and developed.

The scope of work includes:

1. Analyzes of salt impact on soil structure, uncover any potential environmental hazard and emphasis on using waste as a source of salt solutions. Sources to be considered are solid waste, brine solutions and wastewater effluent.
2. Examines some of the main challenges meeting all of the relevant governmental regulations including dust control mandates, water quality regulations, and water reuse regulations. The level of salt allowed in groundwater according to the EPA must be less than the chloride maximum of 250 mg/L (Thorstensen Laboratory, Inc., 2011).
3. Explores the possibility of using dissolved solids from wastewaters that are high in salts to improve rural transportation and urban construction dust control procedures.

Wastewater is often released into streams or rivers by treatment plants, inefficiently losing the possible use of the water prior to its return to the natural environment. In the United States, wastewater is usually treated to a secondary level, including disinfection. Many times, the levels of total dissolved solids (TDS) may have

a great impact upon downstream ecology when the wastewater is released at that stage of treatment (Martinet, 2008).

1.3. Organization

Following this introduction, Chapter 2 presents background information covering soil stabilizing techniques currently in use. A discussion on how improved strength parameters of soils may reduce the required pavement section for certain roadways is also presented.

In Chapter 3, the design of experiment is discussed which includes the laboratory testing program used and soil strength parameters used for pavement design.

In Chapter 4, the laboratory testing data is collected to evaluate the research objectives.

Chapter 5 presents the pavement design analysis and modeling.

Summary and Conclusions are presented in Chapter 6. Soil strength parameters of soils for use in pavement sections are considered and empirical data are illustrated.

Recommendations for future research efforts are provided in Chapter 7.

Chapter 2

Literature Review

2.1. Current Dust Suppression and Soil Stabilization Methods

2.1.1. Water

The scientific principle at work is that by increasing the moisture content of dust, the particles are weighed down and cannot be aerosolized and therefore decrease airborne particles. The benefits of using water are that it is initially inexpensive, readily available in most parts of the world, easy to apply, effective immediately upon application and has no negative environmental impacts after application. The negative aspect is that water does not have a long-term impact as it is only beneficial as long as the moisture content in the dust is above 9% (Marine 3 Technologies Ltd., 2008). Water's real limitations relate to evaporating readily and thereby its short-term control. This means it becomes very labor intensive and costly due to the need for repeated applications for effective control (Environmentally Sensitive Maintenance for Dirt and Gravel Roads; EPA, Chapter 7, 2010).

Techniques which use less potable water help to conserve this limited resource and may maintain the desired properties of the soil for a longer period of time.

2.1.2. Polymers

There are many polymer products that are designed solely for the purpose of maintaining a longer dust suppression time. Lignin is an organic polymer that binds soil particles together. Synthetic polymers include polyvinyl acrylics and acetates (Air Quality Division, Alaska, 2006). Polymers bind the soil particles and form semi-rigid film on the road. Most of these chemicals are applied as part of an emulsion in water. As they have greater binding properties than water alone, most of these emulsion applications have a life many times that of the water application, but at most, they still are only effective for between 1 and 24 months (Soilworks, LLC, 2011). Rain tends

to re-emulsify the material, increasing the potential for run-off. Although lignins can be called a natural substance, if they leach into the stream they will deplete the oxygen and destroy stream life.

Polymers are designed and produced by companies and manufacturers who patent these products and sell them to consumers (Environmentally Sensitive Maintenance for Dirt and Gravel Roads; EPA, Chapter 7, 2010).

2.1.3. Organics

Organic products such as branches, oils and lignins are also being used today. Stabilization of slopes using plant products such as willow branches is done throughout the world (Florineth & Gerstgraser, n.d., p. 1998). Spraying oils such as canola, soybean, or petroleum is another popular technique used on roads, properties, and even in farming locations where dust may cause severe health effects (Senthilselvan, et al., 1997). The application of Soybean Oil by-products is dependent upon the temperature of the oil and the road surface, environmentally friendly biodegradable material, and may be effective for several months. As it does not emulsify with water, it is recommended that the road surface be dry prior to application (Road Management & Engineering Journal, 1998). On a greater engineering scale, lignin-based products combine the natural organics with polymeric technology to create emulsions similar to that of synthetic polymers (Midwest Industrial Supply, Inc., 2011). Disadvantages of lignins include foul smell, sticky surface, and clinging to vehicles. Lignin derivatives are highly acidic, foul smelling, slippery when wet, brittle when dry, and being a natural substance, decompose over time. With lignin derivatives, the road should have a silt/clay content of 4% to 8% for them to be effective in controlling dust. Being an organic material, they decompose over time (Environmentally Sensitive Maintenance for Dirt and Gravel Roads; EPA, Chapter 7, 2010).

2.1.4. Lime

Lime is used to treat many soils in order to improve their workability and load-bearing characteristics in a number of situations. Lime can substantially increase the stability, impermeability, and load-bearing capacity of the subgrade. Soil stabilization occurs when Lime is added to a reactive soil to generate long-term strength gain through a pozzolanic reaction which may remain effective for decades with correct amount of Lime and pH levels. (NLA - Soil Stabilization, n.d.). However, many clays contain soluble sulfate that can also react with Lime to form Ettringite. This corresponds to an increase in volume, referred to as heave (Michael J McCarthy, 2011). Using Lime stabilization is still costly in comparison to using salt waste.

The production of Lime includes a calcination process where limestone, mostly Calcium Carbonate ($CaCO_3$), is heated to produce quick Lime (CaO) (Greenhouse Gas Protocol, 2007). Carbon dioxide is a byproduct of this reaction and is usually emitted to the atmosphere. Greenhouse gases indirectly contribute to the carbon footprint created from the production of Lime (Greenhouse Gas Protocol, 2007).

2.1.5. Others

Ligninsulfonates, asphalt emulsions, petroleum byproducts (coal tar or synthetic fuel distillates), and hygroscopic salts are some of the chemicals used for controlling fugitive dusts. Depending upon methods of application, when ligninsulfonates, asphalt emulsions, and petroleum byproducts are used, they penetrate through the soil matrix, so that soil particles are glued together to form a crusty layer or a solid block which is too heavy to be picked up by the wind. Tar-based additives are derived from coal tar or synthetic fuel distillates to which solvents are added to improve penetration. They are used in a similar way to bitumen additives, however, tars, in general, are known carcinogens and hence their use could have serious health and environmental implications. Their source, composition and potential

carcinogenicity should be established prior to considering their use on roads. (Jones, James. Vitale, 2008).

Hydroscopic salts such as calcium chloride or magnesium chloride absorb moisture from the atmosphere and keep the salt treated surface wet (Li, Elmore and Hartley, 1983).

The use of coal fly ash for soil stabilization is a cost-effective stabilization method for certain soils and must be used in specific site conditions. It may be used alone or added to Lime stabilized soils to assist in the pozzolanic reactions. There is no adverse environmental impact with its application (Industrial Resources Council c2008-2016).

2.2. Pavement Design, Soil Strength & Soil Stabilization

The purpose of a stabilized base or subbase layer is to provide transitional load-bearing strata between pavement layers which directly receive the wheel loading of vehicular traffic, while reducing loading on the underlying subgrade soil. In a geotechnical subsurface investigation program for pavement design and construction, a thorough understanding is obtained of the subsurface conditions along the alignment that will constitute the foundation for support of the pavement structure. The specific emphasis of the subsurface investigation is to identify the impact of the base/subbase conditions on the construction and performance of the pavement, and to obtain design input parameters. This, supported by a laboratory testing program to classify subgrade material and evaluate support properties and moisture sensitivity (heave, collapse, softening), can affect long-term pavement performance.

In the construction of infrastructures, such as highways, earth dams and industry buildings, soil serves as the foundation to provide support and receive loads from upper structures. Soil stabilization is a technique introduced many years ago to enhance the strength of the soils so the soil is capable of meeting the specific

requirements of engineering projects. One of the most effective soil treatments is using salts. In expansive clays, the distance between soil particles is relatively longer and the soil structure is often dispersed. Monovalent cations such as sodium and potassium are widely found and can be replaced by higher valence cations, for example, calcium. Replacing monovalent cations with higher valence cations decreases the size of the bound water layer and enables soil particles to flocculate. The flocculation enhances the soil strength and turns soil into a more granular material.

2.2.1. Soil Testing

Soil testing consists of classification testing (i.e., gradation analysis, Atterberg Limits) and engineering properties testing (i.e., Resistance or R-value, unconfined compressive strength, and California Bearing Ratio or CBR).

2.2.2. Resistance

The Resistance Value (R- Value) is a material stiffness test that measures the response of a compacted sample of soil or aggregate to a vertically applied pressure. The California Pavement Design method uses the R-Value in pavement design for treated and untreated soil subgrades (California Test 301, 2000). The 1993 AASHTO method correlates the structure number (SN) for Subgrade material with the R-Value. A higher SN means a stronger pavement. Figure 2.1 shows the variation in granular subbase layer coefficient with various strength parameters.

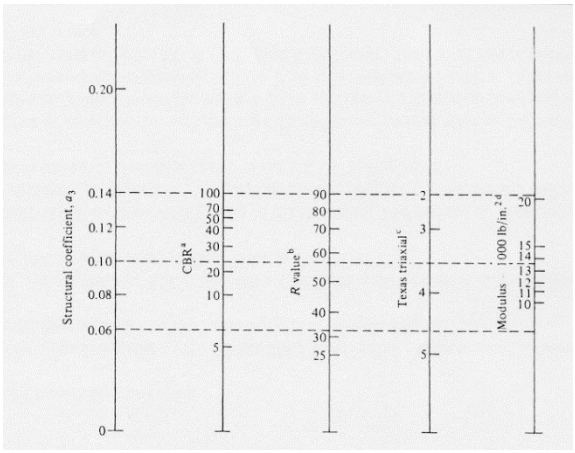

FIGURE 2.1: Variation in granular subbase layer coefficient with various strength parameters (AASHTO, 1993)

Stiffness is the most important mechanical characteristic of unbound materials in pavements. The relative stiffness of the various layers dictates the distribution of stresses and strains within the pavement system. Figures 2.2 and 2.3 illustrate respectively how the stiffness of the subgrade and the unbound base layer influence the horizontal tensile strain at the bottom of the asphalt and the compressive vertical strain at the top of the subgrade for a simple three-layer flexible pavement system. These pavement response parameters are directly related to asphalt fatigue cracking and subgrade rutting performance as used in mechanistic-empirical pavement design methodologies.

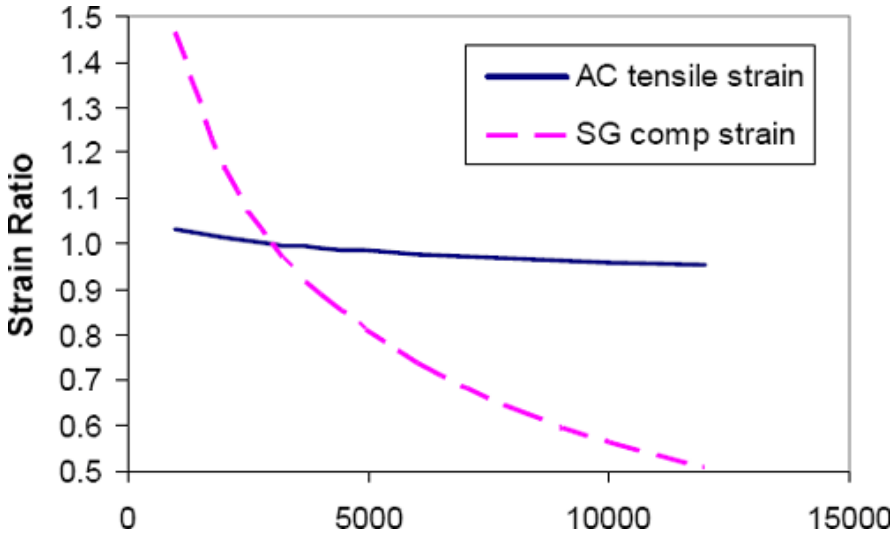

FIGURE 2.2: Influence of Subgrade Stiffness on Critical Pavement Strains. (Geotechnical Inputs for Pavement Design, FHWA, 2013)
(Elastic solution, 6 in./150 mm AC over 18 in./450 mm granular base. Reference elastic moduli: E_{AC} = 500,000 psi/3450 MPa; E_{BS} = 30,000 psi/207 Mpa; E_{SG} = 3000 psi/20.7 MPa. Load: 10 kip/44.5 kN single-wheel load, 100 psi/690 kPa contact pressure).

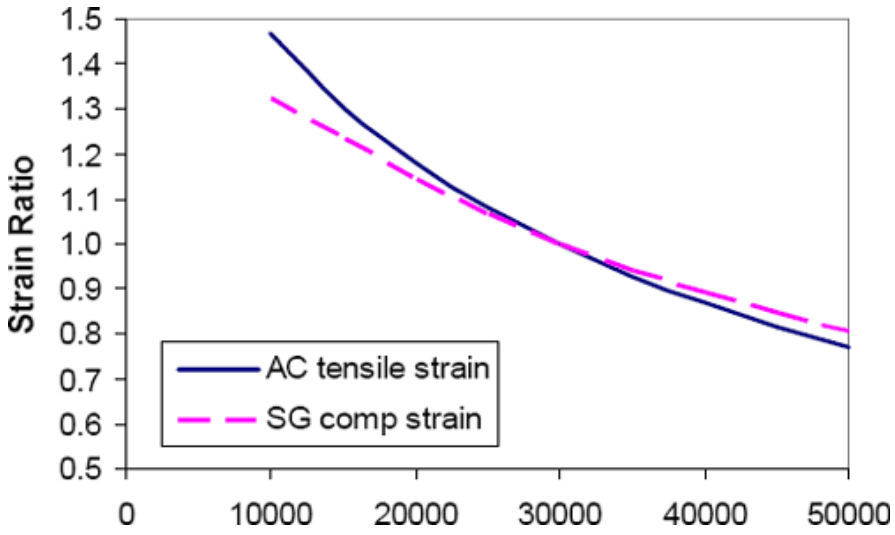

FIGURE 2.3: Influence of Granular Base Stiffness on Critical pavement Design (Geotechnical Aspects of Pavement Design, Chapter 5, FHWA, 2013)
(Elastic solution, 6 in./150 mm AC over 18 in./450 mm granular base. Reference elastic moduli: EAC = 500,000 psi/3450 MPa; EBS = 30,000 psi/207 Mpa; ESG = 3000 psi/20.7 MPa. Load: 10 kip/44.5 kN single wheel load, 100 psi/690 kPa contact pressure).

2.2.3. Sodic Soils

Sodic Soils or the Sodicity of a soil is defined as the amount of Sodium (Na^+), a cation, held in a soil. (Chapter D5. Sodic Soil Management, n.d.). By examining the Sodium Adsorption Rate (SAR), in the pore water, the ratio of sodium to the calcium and magnesium ions, studies can be done to determine the amount of sodium cations in a solution:

$$SAR = \frac{[Na^+]}{\sqrt{([Ca^{2+}] + [Mg^{2+}])/2}}$$

Based on the sodic conditions of a soil, when the SAR is larger, there is a higher level of sodium in the water causing a dispersion of the particulate matter in the soil, bringing expansion to the clay particles, weakening the structure, and closing off the soil pores causing the clay to become impermeable. This leads to the soil having properties that reduce the filtration rate of water, as seen in Figure 2.4.

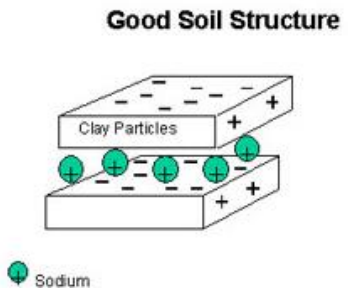

FIGURE 2.4: Good Soil Structure. Modified from (Horton Web Design, 2008)

Studies have shown that a decrease in the electrolyte concentration, or an increase in the level of the SAR, will lead to an increased capacity of clay to swell or retain water, thereby changing the pore size of the soil. This causes binding using ionic and Van der Waals forces to decrease infiltration and increase the strength of the soil. The higher the valence of the ion, the higher the bonding forces between the clay particles (Peng, Horn, Deery, Kirkham, & Blackwell, 2005).

The electrical conductivity of the soil is an important property; it defines the existing levels of salt in the soil as shown in Figure 2.5.

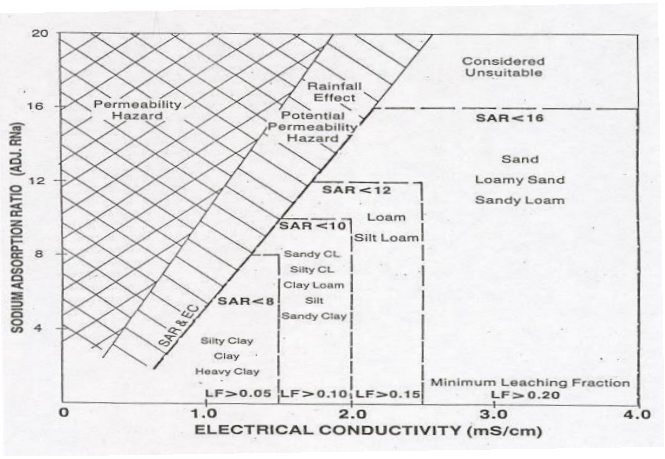

FIGURE 2.5: Relationship between Electrical Conductivity and Sodium Adsorption Rate (Warrence, Bauder, & Peterson, 2004)

2.2.4. Ion Exchange Reactions

Soils contain clay minerals which provide support for horizontal and vertical engineering properties. Clay minerals are negatively charged based on their structure and chemical composition (Onlelow & Okoafor, 2012).

Soil stabilization using salt depends on ion exchange and changes in diffuse layer interactions to alter inter-particle arrangements. The ease of cation replacement depends mainly on the valence, relative abundance of the different ion types and ion size. Divalent cations are held more tightly than monovalent cations. The rate of exchange depends on clay type, solution concentrations, and temperature. In general, exchange reactions in the Kaolin minerals are almost instantaneous. In Illite, a few hours may be needed for completion because a small part of the exchange site may be between unit layers. A longer time is required in Smectite because the major part

of the exchange capacity is located in the interlayer regions (James K. Mitchell, Third Edition).

In summary, fine-grained soils display rapid cation exchange and flocculation reactions when treated with salt that contains divalent cations in the presence of water. Divalent cations preferentially replace commonly present monovalent soil cations such as hydrogen and sodium.

2.3. Dust Control

2.3.1. Environmental Concerns

Unpaved roads are considered the largest source of particulate air pollution in the country. According to the Environmental Protection Agency, unpaved roads produce almost five times as much particulate matter as construction activities in the form of airborne soil particles (Environmentally Sensitive Maintenance for Dirt and Gravel Roads; EPA, Chapter 7, 2010).

Airborne particles or Aerosols are particulates suspended in the air. The particles, at sufficient concentration, are toxic to the body. They may cause adverse health effects in the respiratory system or may be deposited on the skin or the eyes causing irritation. Mechanical generation particles in dust or mist, on the small range of the scale, are smaller than bacteria, less than .01 micrometers. It takes particles smaller than 0.5 micrometers many hours to settle in still air, given the original source, secondary sources and aerosol losses, there is still a wide window of opportunity for these mechanically generated particles to become inhaled or otherwise absorbed into the human body (Baron, n.d.).

Serious health problems are attributable to fine grained airborne soil particles, especially particles with a nominal size of 10 micrometers or less (PM-10). PM-10 particles can penetrate deep into bronchial tubes causing asthma attacks, bronchitis, and other lung diseases. Primary standards are enforceable limits set to preserve the

health of the public. Two of the seven primary standards which regulate suspended particulate matter in the air include PM-10 and PM-2.5 particulates since these represent the greatest potential harm (Environmental Protection Agency, 2011). The EPA's five-year review of the Clean Air Act may further restrict coarse PM primarily composed of suspended dust and dirt (Reske, 2011). Interdisciplinary, sustainable solutions are important to emphasize as the problem of dust control is often in areas with decreasing water availability, increasingly arid climates, or where soil for agricultural applications is misused.

Investigating alternative dust suppression technologies will assist in meeting the new standards and reduce the impact on human and environmental health.

Additionally, the proposed research will look into improving operating efficiency and maintenance costs for alternative energy plants, such as wind mills and solar plants, by reducing cleaning needs due to dust.

2.3.2. Dust Generation Experiments

This research used the experiment process prepared at Arizona State University laboratories to evaluate the wind-erosion resistance of soils. It is a simple low-cost setup consisting of aluminum pie plates (21.6 cm dia, 2.54 cm deep), aluminum ductwork (38 x 38 x 119 cm), and an industrial type stand fan. For each trial, an aluminum pie plate full of test soil was placed inside the aluminum conduit, 51 cm away from the end in contact with the fan and exposed to air flow for approximately 10 minutes. The aluminum conduit was used to direct the wind produced by the fan over the soil with minimal disturbance from the surrounding and allowed collection of the eroded soil. An anemometer placed within the conduit at the designated location of the aluminum pie plates measured the velocity of the air flow prior to the start of the experiments approximately 26 km/hr (E. Kavazanjian, 2009).

2.4. Sustainability and Soil Stabilization

2.4.1. Sustainability Concerns

In the past few years, there has been a growing awareness concerning sustainability in transportation. The sustainability aspects of transportation systems are yet to be completely defined, characterized and measured. The pavement network is one of the major components of transportation systems.

2.4.2. Salt Waste Recycle

Salt waste management is a major challenge to desalination processes (seawater or potable water desalination). The desalting by-products are commonly disposed of through one of five practices: 1- Sewer discharge, 2- Surface water discharge, 3- Deep well injection, 4- Evaporation ponds, or 5- Zero Liquid Discharge Thermal Processes. Controlling and reusing these salt wastes will provide great environmental and economic benefits.

2.4.3. Water Use Reduction

Application of water is the most popular and historical method of dust suppression. Water scarcity is among the main problems to be faced by many societies around the world in the 21st century. Almost one-fifth of the world's population (approaching 500 million people) lives in areas of physical scarcity. (International Decade for Action, Water For Life 2005 - 2015, 2011).

Conventional dust suppression products use water as a solvent. Most of these products are biodegradable, which require retreatment of the soil every three to six months or after every storm event. This adds to the scarcity of the most vital natural resource. In places water is so scarce that necessary dust control measures are not in place, airborne pollutants increase to potentially dangerous levels.

Using salt solutions as a sustainable dust suppression mean will potentially reduce the use of potable water during construction activities, in alternative energy power plants, at open sites, and on unpaved roads.

2.4.4. Effluent Salt Reuse

Wastewater effluent has a high salt content nationwide. Wastewater effluent is often released into streams or rivers by treatment plants, inefficiently losing the possible use of the water prior to its return to the natural environment. In the United States, wastewater is usually treated to a secondary level, including disinfection. Many times, the levels of total dissolved solids (TDS) have a great impact upon downstream ecology when the wastewater is released at that stage of treatment (Martinet, 2008). This research will analyze the possibility of using dissolved solids from wastewaters that are high in salts to improve rural transportation and urban construction dust control procedures.

2.5. Soil Strength Parameters

All aspects of soil stability, including bearing capacity and penetration resistance, depend on soil strength Fundamentals of Soil Behavior). Two tests that measure the strength of soils are:

1. The Standard Proctor test determines the water content needed to compact a soil to its maximum dry density, at which the soil will be its strongest.
2. The California Bearing Ratio (CBR) test compares the bearing capacity of a soil to that of a material having a CBR of 100%, the theoretical strongest bearing capacity (Pavement Interactive, 2007).

The dry density of the sample is used in conjunction with the %CBR to determine the optimum degree of compaction (Civil Engg. Dictionary, n.d.).

2.5.1. Compaction

The Standard Proctor Test

A compaction curve is plotted between the water content (%), abscissa, and the corresponding dry density (g/cc), ordinate, as shown in Figure 2.6. It is observed that the dry density initially increases with an increase in water content until the maximum dry density (ρ_d) max is attained. With further increase in water content, the dry density decreases. The water content corresponding to maximum dry density is called optimum moisture content (O.M.C.).

At water contents lower than the optimum, the soil is rather stiff and has a lot of void spaces, therefore the dry density is low. As the water content is increased, the soil particles get lubricated and slip over each other, move into densely packed positions, and the dry density is increased. However, at water contents more than the optimum, the additional water reduces the density, as it occupies the space that might have been occupied by the solid particles.

For a given water content, theoretical maximum dry density, $\rho_{d\ max,}$ is obtained corresponding to the condition when there are no air voids (i.e. degree of saturation=100%). Theoretical maximum dry density is also known as saturated dry density, $\rho_{d\ sat}$. In this condition, the soil becomes saturated by reduction of air voids to zero but with no change in water content. The soil can also become saturated by increasing the water content such that all air voids are filled. As we are interested in the dry density at given water content, the latter case is not considered.

An expression for theoretical maximum density is as given below.

$$\rho_{d,\max} = \frac{G\rho_w}{1 + wG},$$

The theoretical maximum dry density occurs when saturation =100%

G= Specific Gravity, w= water content (%)

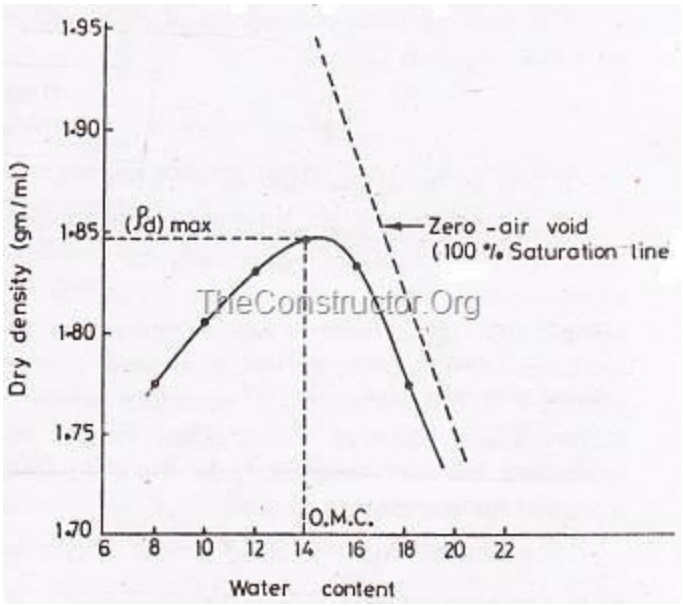

FIGURE 2.6: Compaction Curve Plot (The Constructor.org, n.d.).

2.5.2. Lime Stabilization of Clay Minerals and Soils

Research on soil stabilization with Lime treatment is easily found in literature. Bell (2006) performed a series of tests to compare the geotechnical engineering properties of two clays from the field to their corresponding part with Lime additive. The two clays used were Upper Boulder Clay and Tees Laminated Clay.

Samples of Upper Boulder Clay and Tees Laminate Clay were mixed with varied amounts of Lime additive. The soil properties, California Bearing Ratio, liquid limits, plastic limits, and compaction tests of all the samples were studied. Soil stabilization is most often used in subgrade and subbase material for road construction.

Both clays were added with 2%, 4%, 6%, and 8% Lime to investigate its influence in the consistency limit. In the case of Upper Boulder Clay, both plastic and liquid limits are increased due to the Lime additive. As for Tees Laminated Clay, the plastic limit increased after Lime was added, however, the liquid limit decreased. Results are in Table 2.1.

TABLE 2.1: Values of Plastic Limit, Liquid Limit, Plasticity index and Linear Shrinkage of Upper Boulder Clay and Tees Laminated Clary treated with various amounts of Lime (Bell, 2006)

Soil	Property	Amount of Lime added (%)				
		0	2	4	6	8
Upper Boulder Clay	PL (%)	14	25	23	21	18
	LL (%)	30	42	40	41	37
	PI (%)	16	17	17	20	19
	LS (%)	6	2	1	1	1
Tees Laminated Clay	PL (%)	26	36	34	3	31
	LL (%)	58	57	53	50	49
	PI (%)	32	19	19	17	18
	LS (%)	20	4	3	2	2

Compaction and California Bearing Ratios tests were both carried out on treated and untreated samples. As for compaction curves, an increase in optimum water content and decrease in maximum dry density (Table 2.3 and Figure 2.6) were found when Lime was added. An increase in California Bearing Ratio was found when Lime added (Table 2.2).

TABLE 2.2: Values of Compaction & California Bearing Ratio Tests on Upper Boulder Clay and Tees Laminated Clay (Bell, 2006)

Soil	Amount added (%)	Compaction		CBR	Property	Amount of lime added (%)*				
		Optimum moisture content (%)	Maximum dry density Mg/m³)			0	2	4	6	8
Upper Boulder Clay	0	18	1.81	9	UCS (kPa)	538	762	1056	1597	1452
	6	20	1.75	24	E (Mpa)	35	49	56	58	52
Tees Laminated Clay	0	22	1.65	5	UCS (kPa)	178	584	889	776	847
	4	25	1.60	19	E (Mpa)	15	21	43	38	40

* Soils were treated with optimum amounts of lime (quantities at which highest unconfined compressive strength achieved, cured at 20° after 7 days).
UCS: Unconfined Compressive Strength

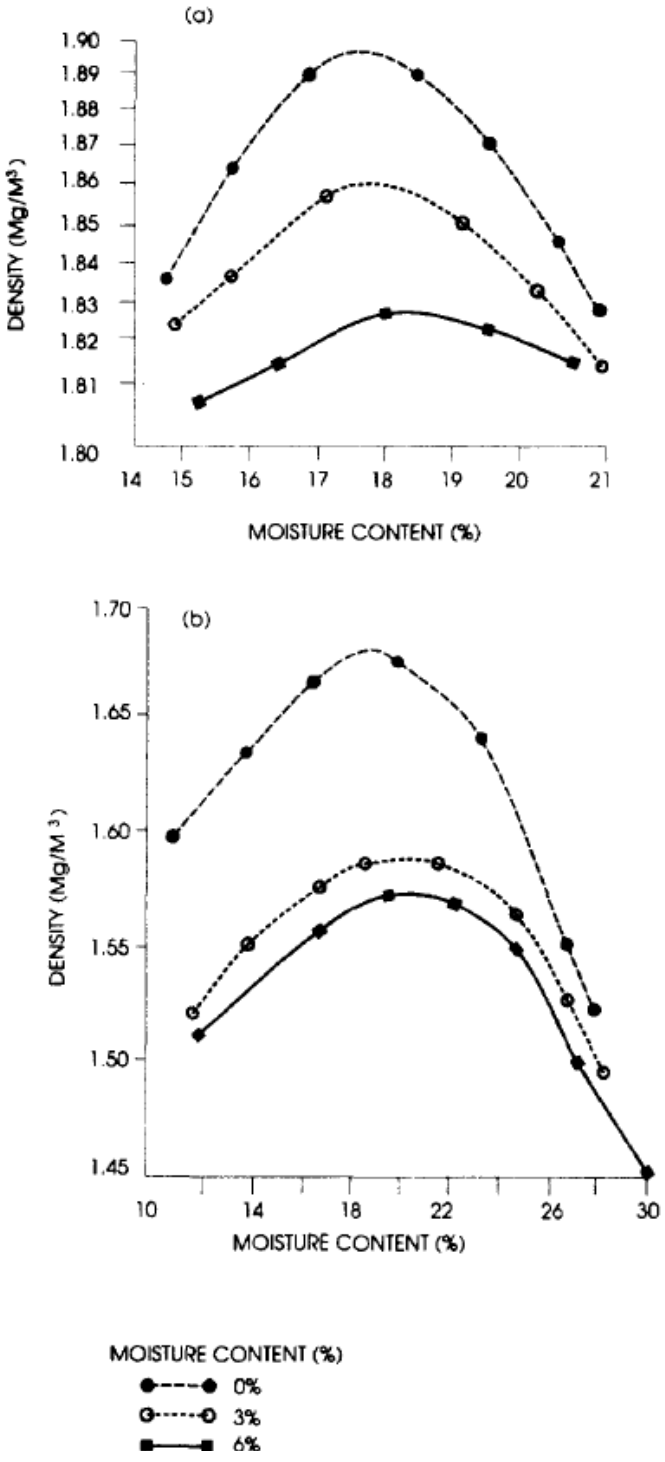

FIGURE 2.7: Examples of Compaction curves of Upper Boulder Clay (top) and Tees laminated Clay (bottom) (Bell, 2006)

2.5.3. Soil Stabilization by Chemical Agent

Maadith (2002) used Lime and sodium silicate to treat a brown sandy clay collected from Jordan. Standard proctor tests and California Bearing Ratio tests were performed to determine the influence of the addition of a mixture of Lime and sodium silicate. Figure 2.12 shows an increase of optimum water content and maximum dry density of treated sample when compared with untreated sample.

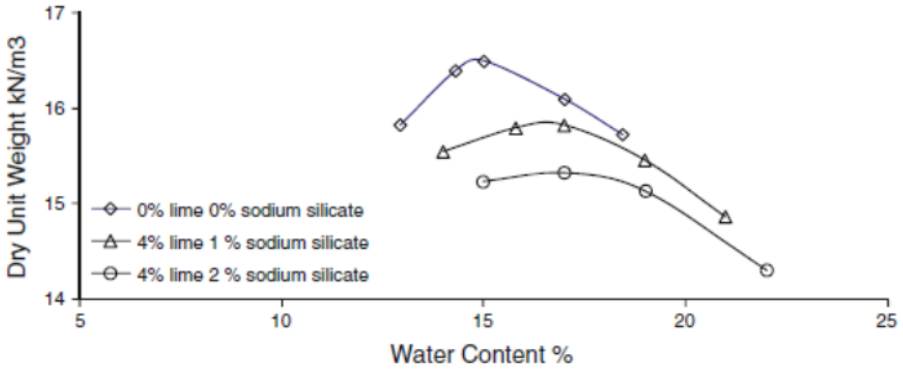

FIGURE 2.8: Effect of Soil Treatment on Standard Proctor Test (Maadith, 2002)

California Bearing Ratio test results are shown in Figures 2.13 and 2.14. It is obvious that the California Bearing Ratio value (soaked and unsoaked) increased as the concentration of Lime and sodium silicate additive increased.

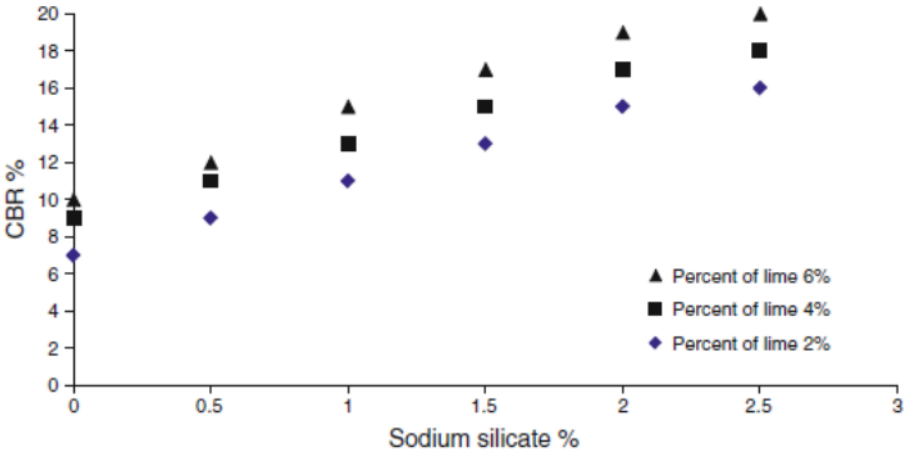

FIGURE 2.9: Effect of Lime and Sodium Silicate on soaked California Bearing Ratio Test (Maadith, 2002)

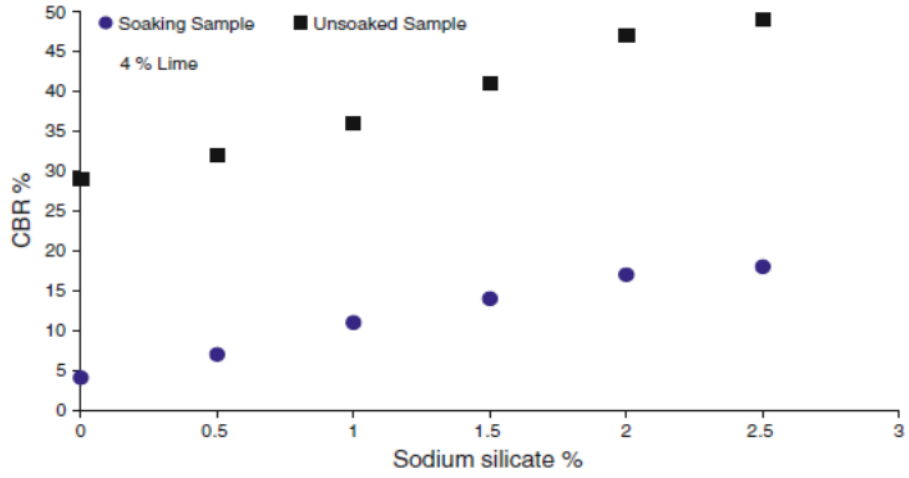

FIGURE 2.10: Comparison between soaked and unsoaked California Bearing Ratio Test (Maadith, 2002)

2.5.4. Stabilization of Clayey Soils with High Calcium Fly Ash and Cement

Kolias et al (2005) investigated the effect of high calcium fly ash and cement on stabilization of fine-grain clayey soils (CL, CH) in the laboratory. The tests conducted

were strength in uniaxial compression, direct tension, and California Bearing Ratio test on a 90-day soaked sample.

Three soils were tested in this research, one is classified as CH, the other two are CL. The soil Atterberg limits and grain size distribution curves are shown in Figure 2.16.

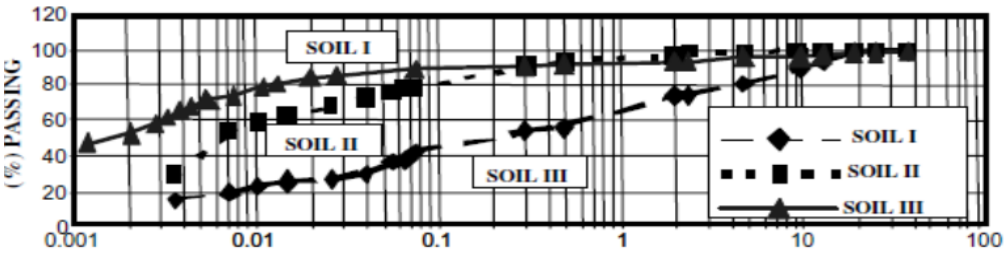

NOMINAL GRAIN DIAMETER (mm)

SOIL SAMPLES	ATTERBURG LIMITS			AASHTO CLASSIFICATION	UNIFIED SOIL CLASSIFICATION	
	PL	LL	PI		GROUP SYMBOL	GROUP NAME
SOIL 1	20	38	18	A-6	CL	LEAN CLAY
SOIL 2	23	53	30	A-7-6	CH	FAT CLAY
SOIL 3	18	43	25	A-7-6	CL	SILTY CLAY

FIGURE 2.11: Atterberg Limits, Gradation and Soil Classification of Soil Samples (Kolinas et al, 2005)

Two fly ashes, named "FA Ⅰ" and "FA Ⅱ" are found in Greece. The percentage of free Lime is 18% and 16.7% respectively. The compaction tests results of soil 1, CH, with different amounts of Fly Ash are shown in Figure 2.17 in terms of initial moisture content and measure moisture content.

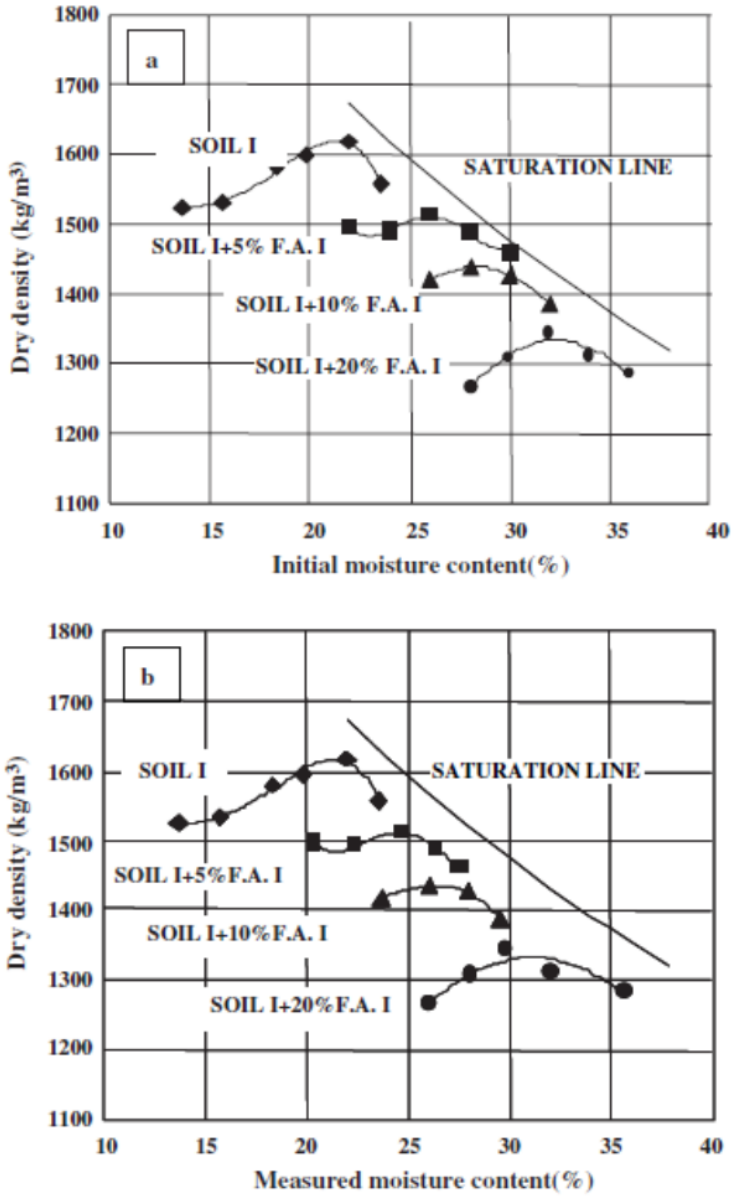

FIGURE 2.12: Stand Compaction Test for Clay I:
(top) Initial moisture (bottom) Measure moisture (Kolias et al, 2005)

As Fly Ash was increased, the optimum moisture content of compaction curves enhanced and maximum dry density reduced.

For the three soils, the soaked California Bearing Ratio increased as the percentage of fly ash increased as shown in Figure 2.18.

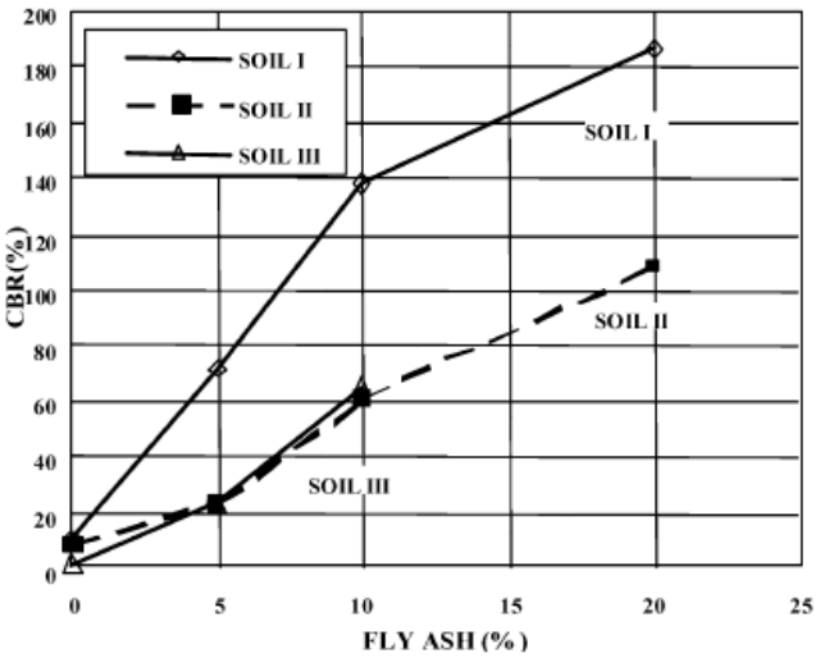

FIGURE 2.13: Variation of California Bearing Ratio for Clays I, II, III stabilized with Fly Ash (Kolias et al, 2005)

2.5.5. Soil Stabilization by Calcium Carbide Residue and Fly Ash

Calcium Carbide Residue (CCR) contains a high percentage of $Ca(OH)_2$ while Fly ash is a pozzolanic material. Horpibulsuk et al (2012) investigated the possibility of using a mixture of Calcium Carbide Residue and Fly Ash to improve the strength of a silty clay in northeast Thailand.

Standard proctor tests have been done to investigate the effect of the CCR additive to control soil. As the CCR is added in, the compaction curve flattens. The optimum water content increased and maximum dry density decreased. Figure 2.19 shows compaction curves of varies samples.

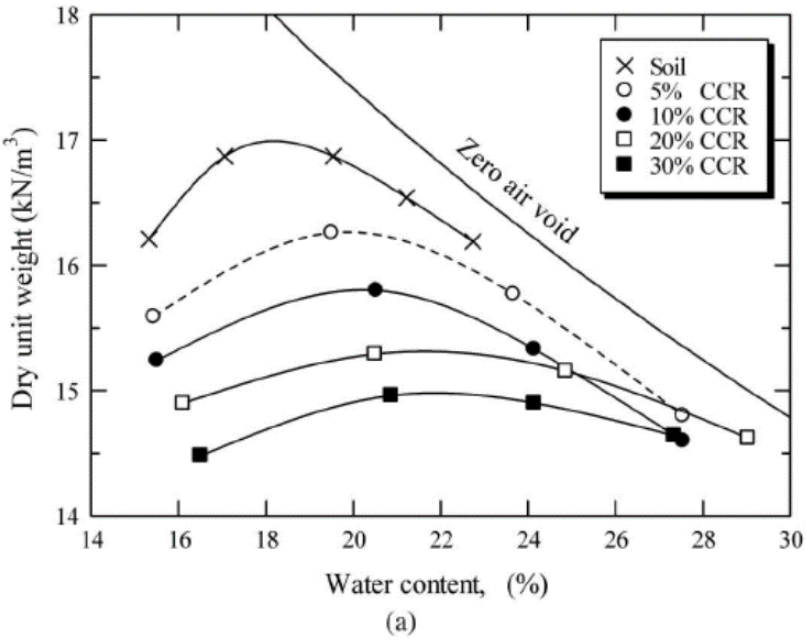

FIGURE 2.14: Compaction Curves of samples with varying CCR additive concentrations (Horpibulsuk et al, 2012)

2.5.6. Salt Stabilization

Literature shows that as the soil has an increased salt concentration, the compaction curve will shift up and to the left, which corresponds to a higher maximum dry density and lower optimum moisture content (Abdullah et al.1999). In addition, all the soils were compacted to the optimum moisture content of the control specimens. The reduction in the unconfined compressive strength corresponds to using the optimum moisture content and the maximum dry density of the control specimen. If the compaction curves of the soils with salts were known and the optimum moisture content was used for the comparison, the strength of the material would have expectedly increased. Figure 2.20 shows and example of how the maximum dry density changes with the addition of salts.

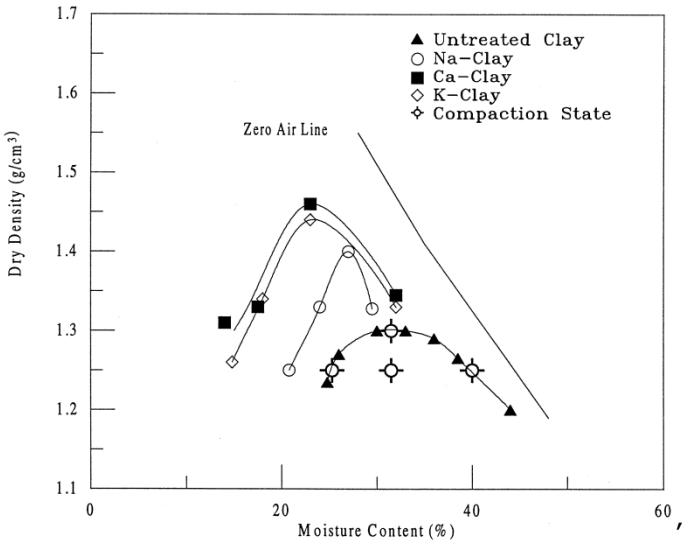

FIGURE 2.15: Maximum Dry Density Changes (Abdullah et al.1999)

Chapter 3

Design of Experiment

Questions that need to be answered by this study include determining the optimum dosage of salt concentration for each area or volume of soil; ensuring that the process is easily operable and safe for the public and environment; and analyzing the effects of this mixture upon the groundwater and other natural systems. Each of these challenges were addressed by the tasks outlined below.

Laboratory testing in this research is focused primarily on using calcium chloride ($CaCl_2$) as a salt additive to improve performance of fine grained materials. Calcium chloride is both hygroscopic and deliquescent. Thus, under common ambient conditions, solid material will absorb moisture from the air until it dissolves. Calcium chloride solutions will absorb moisture until equilibrium is reached between the water vapor pressure of the solution and that of the air. If the humidity of the air increases, more moisture is absorbed by the solution. If it decreases, water evaporates from the solution into the air (Occidental Chemical Corporation, 2009).

As Lime treatment is commonly used in soil stabilization, one of the soils in this study included the treatment with Lime for comparison purposes. The same tests are performed on treated and untreated samples.

The work in this laboratory testing include:

1. Soil Composition and Classification
2. Correlation of Soil Characteristics and Salt
3. Pavement Design Parameter Analysis
4. Potential Challenges and Impact Analysis

3.1. Task 1: Soil Composition Analysis and Classification of Soil Properties

Typical soils which need dust suppression include Aeolian soils. Aeolian soils are typically loose and can become aerosolized when subjected to a wind force. Fine-

grained soil samples from locations throughout rural, suburban, and urban areas in Arizona that have been classified as needing to apply dust suppression techniques were utilized. At each of the test locations, a minimum 10-kilogram sample from the top 12-inches were collected using hand sample equipment (i.e., shovel, soil probe, bucket sampler).

A total of three soils samples were analyzed in this task to represent variability in characteristics of each sample type; gradation tests were performed on each sample as per ASTM D6913.

The Unified Soil Classification System (USCS) was employed to give an initial soil classification of the sample. Initial soil classification consisted of sieve analysis; Atterberg limits tests, and further classification of fine grained soils.

Presented in Table 3.1 are the laboratory tests that were performed on the soils collected from around Arizona. Note that not all of the soils collected were subjected to all the laboratory tests or tested at the listed treatment level presented.

TABLE 3.1: Laboratory Tests and Treatments

Laboratory Tests	Treatment Solution	Treatment Level(s)
Atterberg Limits	Distilled Water/ Lime/ $CaCl_2$	N/A 16% 2%, 4%, 8%, 12%, 16%
Standard Proctor Density	Distilled Water/ $CaCl_2$	N/A 8%, 12%, 16%
Unconfined Compressive Strength	Distilled Water $CaCl_2$	N/A 2%, 4%
California Bearing Ratio	Distilled Water/ Lime/ $CaCl_2$	N/A 16% 2%, 4%, 8%, 12%, 16%
Gradation	Distilled Water	N/A

3.1.1. Atterberg Limits

The Atterberg limits are a basic measure of the nature of a fine-grained soil. Depending on the water content of the soil, the soil may appear in one of the following four states: solid, semi-solid, plastic, and liquid. In each state, the consistency and behavior of a soil is different and consequently so are its engineering properties. Thus, the boundary between each state can be defined based on a change in the soil's behavior. The Atterberg limits can be used to distinguish between silt and clay, and it can distinguish between different types of silts and clays.

The liquid limit (LL) is the water content at which a soil changes from plastic to liquid behavior. The original liquid limit test involved mixing a pat of clay in a round-bottomed porcelain bowl of 10–12 cm diameter. A groove was cut through the pat of clay with a spatula, and the bowl was then struck many times against the palm of one hand. The moisture content at which it takes 25 drops of the cup to cause the groove to close over a distance of 13.5 millimeters (0.53 in) is defined as the liquid limit. Now

the test is performed using a brass cup attached to an apparatus that allows the brass cup to fall at from a specified height until the soil pat close at least 13.5 mm. The typical test setup for the liquid limit is presented in Figure 3.1. The soils per the ASTM standard were prepared following the wet preparation method.

FIGURE 3.1: Casagrande Device (Liquid Limit Test Device)

The plastic limit is determined by rolling out a thread of the fine portion of a soil on a flat, non-porous surface. The procedure is defined in ASTM Standard D 4318. (ASTM International). If the soil is plastic, this thread will retain its shape down to a very narrow diameter without crumbling. The sample can then be remolded and the test repeated until the thread begins to crumble at the desired diameter. The plastic limit is defined as the moisture content where the thread begins to crumble apart at a diameter of 3.2 mm (about 1/8 inch) as depicted in Figure 3.2.

FIGURE 3.2: Crumbled Thread of *Anthem Clay* in Plastic Limit Test

The plasticity index (PI) is a measure of the plasticity of a soil. The plasticity index is the size of the range of water contents where the soil exhibits plastic properties. The PI is the difference between the liquid limit and the plastic limit (PI = LL-PL). Soils with a high PI tend to be clay, those with a lower PI tend to be silt, and those with a PI of 0 (non-plastic) tend to have little or no silt or clay. (Seed, 1967).

3.1.2. Standard Proctor Density

The Proctor Density is the relationship between soil density and moisture content. The Proctor density was established for compaction theory in the 1930's by R.R. Proctor. The Proctor test established the relationship between dry density, moisture content, compactive effort, and soil type. The compactive effort is governed by the size of rammer, number of blows, and number of lifts. For this research study, the procedure used to obtain the Proctor Density is defined in ASTM D698 Method C. (ASTM International). Figure 3.3 depicts the typically Proctor Density setup used in the laboratory testing.

FIGURE 3.3: Compaction Tools

Before compaction, the mold was clamped with an extension collar attached to the base plate. A spacer disk was placed on the top of base plate with a piece of filter paper placed on top of the spacer disk. The soil was then placed and compacted per ASTM D698 Method C protocols. After compaction was completed, the extension collar was removed and the soil sample was carefully trimmed with a straight edge to make the surface of the testing sample even.

3.1.3. Unconfined Compressive Strength

The unconfined compressive strength (UCS) test determines the compressive strength at which unconfined cylindrical specimen of soil will fail in a simple compression. Additionally, the USC test is a measure of the shear strength of the material, which is determined by dividing the UCS result by 2 (ASTM International).
For this test, the target density was 95% of the Maximum Dry Density (MDD) Determined by the Standard Proctor. However, when using the Humboldt compaction

hammer and mold, the density achieved range from 100% to 105% of the MDD, for the only soil tested.

3.1.4. California Bearing Ratio

As presented earlier, the CBR test is used in evaluating the strength properties of the subgrade, subbase, and base materials that are used to aid in pavement design. The laboratory test uses a circular piston to penetrate material compacted in a mold at a constant rate of penetration. The CBR is expressed as the ratio of the unit load on the piston required to penetrate 0.1 in. (2.5 mm) and 0.2 in (5.1 mm) of the test material to the unit load required to penetrate a standard material of well-graded crushed stone.

The CBR test specimen is prepared in a similar manor as the Standard Proctor; however, the mold height is different. The test is performed at loading rate of 0.05 inches/minute. The load and deformation are recorded during testing. A penetration measure device (LVDT), reading to the nearest 0.001 inches, is mounted with the loading tracking system. Prior to testing, the samples were unsoaked and soaked and a 10-pound perforated surcharge weight was used to represent traffic and pavement surcharge loading. After a specified amount of time, the samples were removed from the soak tank and tested using the aforementioned testing procedure with the 10-lb surcharge weight in-place.

3.1.5. Gradation

This test method is used to separate particles into size ranges and to determine quantitatively the mass of particles in each range. These data are combined to determine the particle-size distribution (gradation). This test method uses a square opening sieve criterion in determining the gradation of soil between the 3-in. (75-mm) and No. 200 (75-μm) sieves (ASTM International).

3.1.6. Soil Corrosion Testing Suite

Soil corrosion testing is integral to determining which types of building materials can be used to withstand the corrosive nature of the native soils during the estimated design life. Typically, the soil corrosion suite will includes determining the soil pH, soil resistivity, chloride (Cl) content, and sulfate content (SO_4). The soil corrosion testing suite is used to determine minimum corrosion rate for buried ferrous material or corrosive nature to Portland cement structures that are either reinforced or unreinforced.

The soil pH was measure by following ASTM D4972. In this test, the soil is mixed with water to create a 1:1 ratio of soil to water. Prior to testing, the pH meter is calibrated with known stock solutions (i.e., solutions with pH of 4, 7, or 10) to determine the pH of the solution. The pH is useful in determine the corrosion rate in galvanized coated steel (FHWA 2009).

The soil resistivity was measured in the laboratory using the Werner 4-Pin resistivity box following the ASTM G57 testing procedure. The soil resistivity is another tool to determine the soil corrosion potential. If the soil resistivity is less than 1,000 Ohm-cm, the soil is determined to be corrosive and corrosion counter-measured should be used (FHWA 2009). When testing the soil in the laboratory, the moisture content is varied until either three readings in a row are similar or the reading after increasing the soil moisture content increases over the last reading.

The chloride content was determined following ARIZ 736b testing standard. This test requires the use of chloride standard solution, demineralized water, and a centrifuge. After the sample is prepared the voltage of the solution is measured and then convert to a parts-per million (ppm) value. The chloride content is considered corrosive once the value exceeds 100 ppm (FHWA 2009).

The sulfate content was determined following ARIZ 733b testing standard. This test is performed similarly as ARIZ 736, with the additional measurement of turbidity. The sulfate content is used to determine the sulfate attack potential or the type of Portland cement that should be used in construction.

3.2. Task 2: Correlation of Soil Characteristics and Salt

In this task, a calcium chloride salt solution, at varying concentration levels, was used to treat the three fine-grained soil samples to document the changes in their index properties. All the soils were treated with one percentage level of Lime, for comparison purposes.

3.3. Task 3: Pavement Design Parameters Analysis

In this task, the CBR and laboratory test results were analyzed to predict impacts on pavement structural design and load carrying capacity. A comparison with Lime stabilization practices was also performed in this task.

3.4. Task 4: Potential Challenges and Impact Analysis

This task includes data analysis and future recommendations into the implications of the findings; such as, long-term sustainability of using salt as a means of dust control and soil stabilization, especially upon the groundwater, agricultural products, wildlife implications and potential ecological interactions.

Chapter 4

Laboratory Testing

As mentioned in Chapter 3, a total of three soils were collected for the laboratory testing as part of Task 1. The four soils were sourced from different areas around Arizona. The soils sourced for this study were collected from the following locations:

- Anthem, Arizona (One soil) – Collected by Arizona State University for previous research
- Apache Junction, Arizona (one soil) – Collected by Smith & Annala Engineering Co. (SAECO)
- Eagar, Arizona (one soil) – Collected by SAECO

Prior to the laboratory testing, the three soils were dried out to a residual moisture content (i.e., 6 to 8 percent). The soil was spilt for the various laboratory tests. For the treated material, the appropriate amount of calcium chloride by weight was weighed out and the appropriate amount of water was weighed out and added to the calcium chloride under a fume hood to allow the chemical reaction to occur between the calcium chloride and the water, as depicted in the equation below:

$$CaCl_2 + H_2O_{(l)} \xrightarrow{t\ ^0C} Ca(OH)_2 + HCl_{(aq)}$$

Once the chemical reaction has occurred, it is an approximate 1:1 ratio of the calcium hydroxide to hydrochloric acid. The calcium chloride/water solution was then mixed with the soil. After mixing the solution with the soil occurred, the soil was then placed in a container and allowed to meld for a minimum of 24 hours prior to testing. Finally, after the melding time was deemed complete, the various laboratory tests were performed.

4.1. USCS Soil Classification Results

The laboratory testing of the selected soils was performed at Arizona State University and SAECO. The unified soil classification system (USCS) soil classification as well as the visual classification for the three soils are as follows:

- Anthem, Arizona – Reddish brown LEAN CLAY
- Vineyard Road #1 – Reddish brown, SAND LEAN CLAY
- Eagar, Arizona – Grayish brown, FAT CLAY with SAND

Table 4.1 outline the changes in USCS classification for the three soils.

TABLE 4.1: USCS Classification of the Three Soils

Treatment Level	Anthem	Vineyard Road	Eager
None	CL	CL	CH
%2 $CaCl_2$	CL	--	--
%4 $CaCl_2$	CL	--	--
%8 $CaCl_2$	CL	CL	CL
%12 $CaCl_2$	--	CL	CL
%16 $CaCl_2$	--	CL	CL
%16 CaO	--	CL	MH

4.2. Gradation Results

The gradation results for the three soils are presented in Figure 4.1. The particle size analysis based on the gradation results are presented in Table 4.2. The clay content of the three soils varied by 15 to 32.2 percent.

TABLE 4.2: Soil Particle Composition

Particle Size	Anthem	Eager	Vineyard
%Gravel (-76mm to +4.76mm)	0.0%	8.2%	1.2%
%Sand (-4.76mm to +0.074mm)	11.3%	52.2%	38.4%
%Silt (-0.074 to +0.002 mm)	56.5%	24.6%	41.2%
%Clay (-0.002 mm)	32.2%	15.0%	19.2%

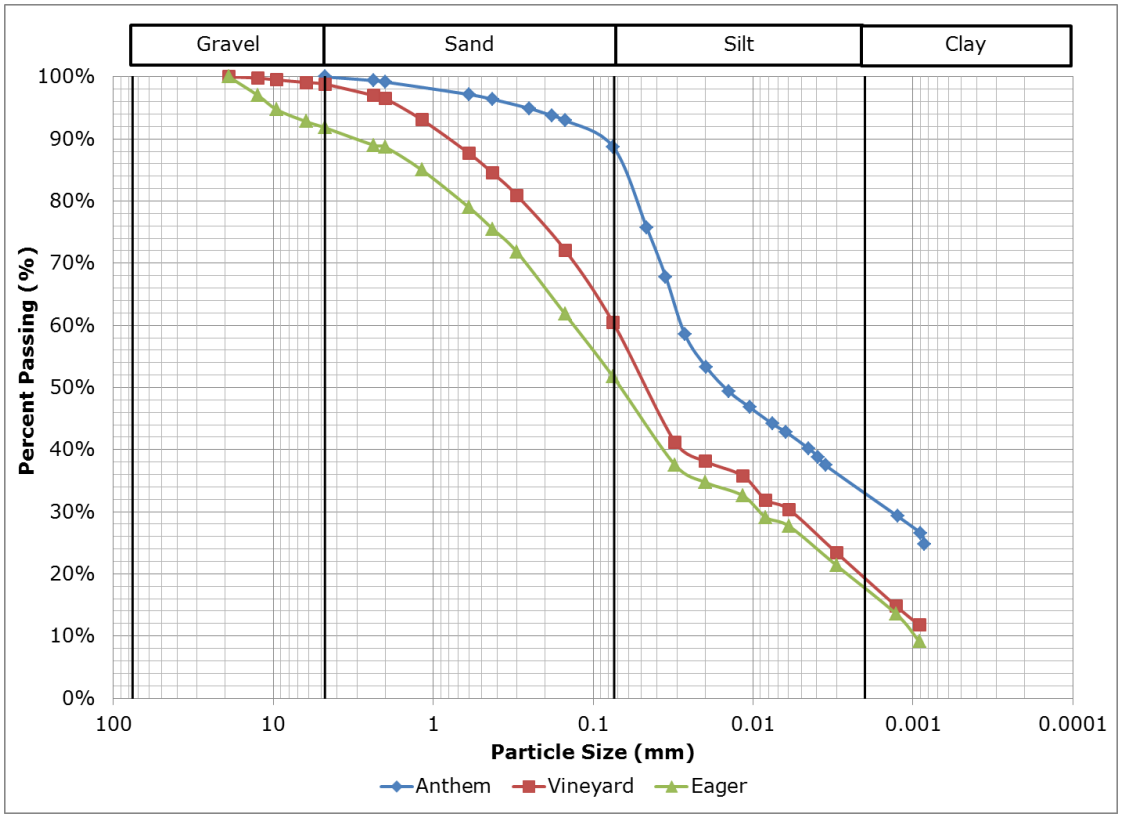

FIGURE 4.1: Gradation Results for the Three Soils.

4.3. Atterberg Limit Results

For the liquid limit test, the Casagrande device was used (see Figure 3.1). A portion of the previously mixed soil was placed into the cup of Casagrande apparatus and soil was squeezed to eliminate air pockets on the base of the cup. Soil was spread in the cup to a depth of 10mm at the deepest point. After the soil was evenly spread using a grooving tool to cut a clean straight groove down the center of the cup. The crank on the apparatus was turned at a rate of approximately two drops per second, the number of drops, N, was counted until the soil parted into two halves and the soil pat come into contact at the bottom of the groove along a distance of 13 mm. Several attempts were made to make the one N value between 15 and 25, 20 and 30, and 25 and 35. The water content of each attempt been measured using an oven. Table 4.3

presents the Atterberg Limit results for the three soils. Figures 4.2, 4.3, and 4.4 show the changes in the Atterberg Limits for the three soils.

TABLE 4.3: Atterberg Limit Results of the Three Soils

Treatment Level	Anthem			Vineyard Road			Eager		
	LL	PL	PI	LL	PL	PI	LL	PL	PI
None	48.7	21.3	27.4	38.5	17.2	21.3	49.8	22.5	27.3
%2 $CaCl_2$	44.2	20.9	23.3	--	--	--	--	--	--
%4 $CaCl_2$	42.5	19.8	22.7	--	--	--	--	--	--
%8 $CaCl_2$	39.9	19.2	20.7	33.5	14.9	18.6	46.1	22.7	23.4
%12 $CaCl_2$	--	--	--	33.4	16.0	17.4	43.1	21.4	21.7
%16 $CaCl_2$	--	--	--	31.9	15.0	16.9	43.1	21.1	22.0
%16 CaO	--	--	--	42.5	24.3	18.2	53.2	36.7	16.5

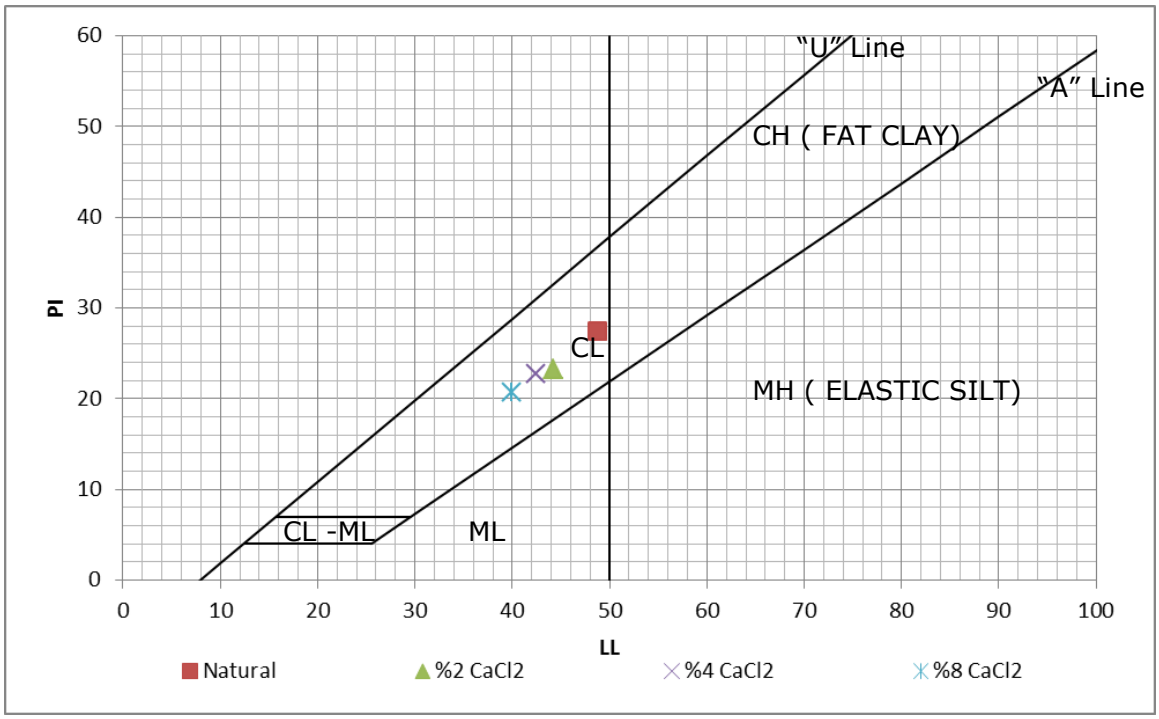

FIGURE 4.2: Anthem's Reduction in the Atterberg Limits.

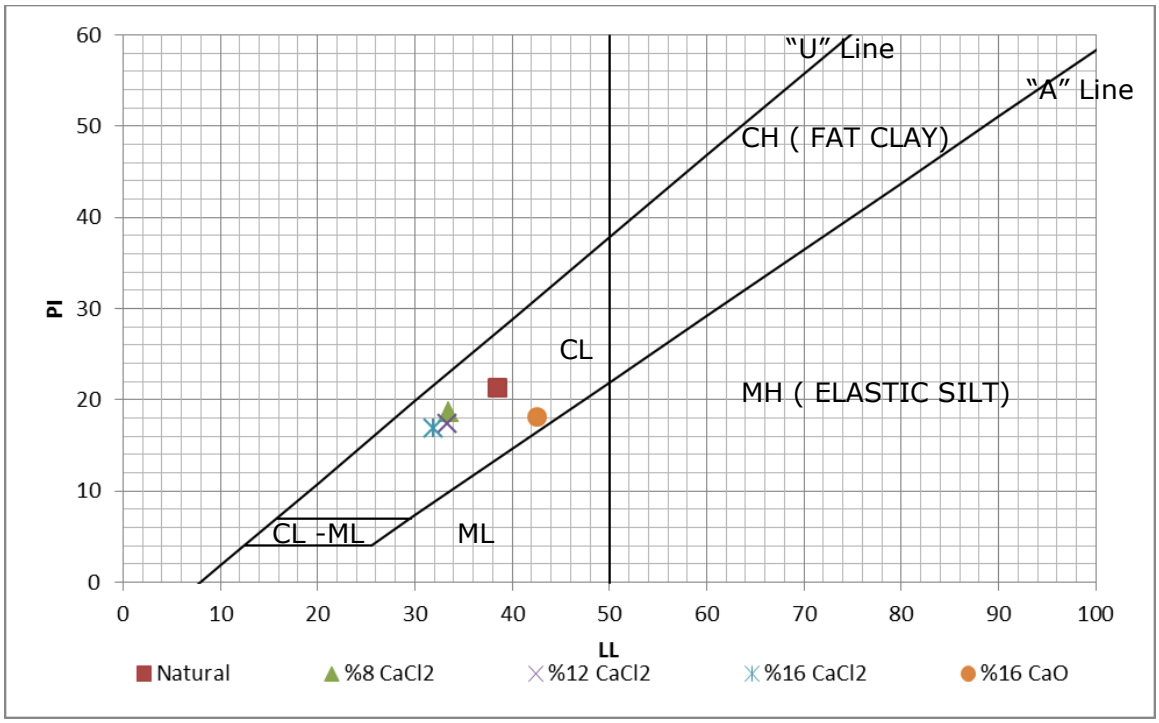

FIGURE 4.3: Vineyard's Reduction in the Atterberg Limits.

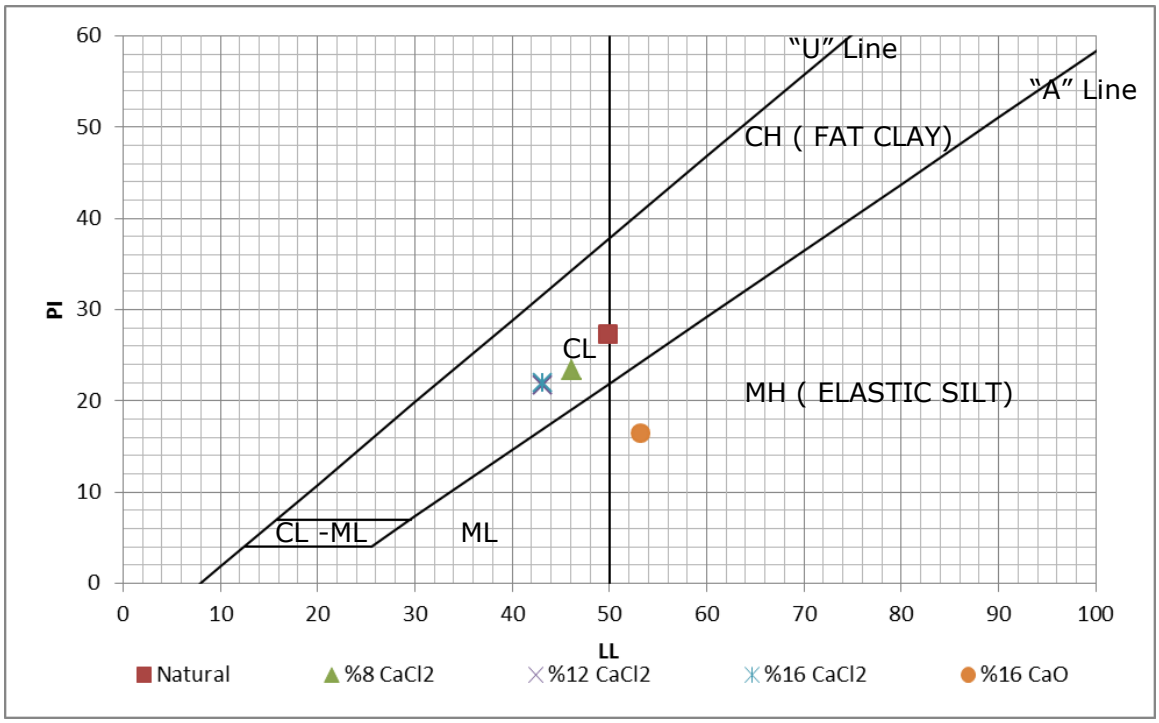

FIGURE 4.4: Eager's Reduction in the Atterberg Limits.

As seen in the test results, the addition of salt had a marginal reduction in the plastic limit. The major reduction in the plasticity index is due to the reduction in the liquid limit as the salt concentration increased.

4.4. Standard Proctor Density Results

The Standard Proctor Density results for the three soils are presented in Figures 4.5, 4.6, and 4.7.

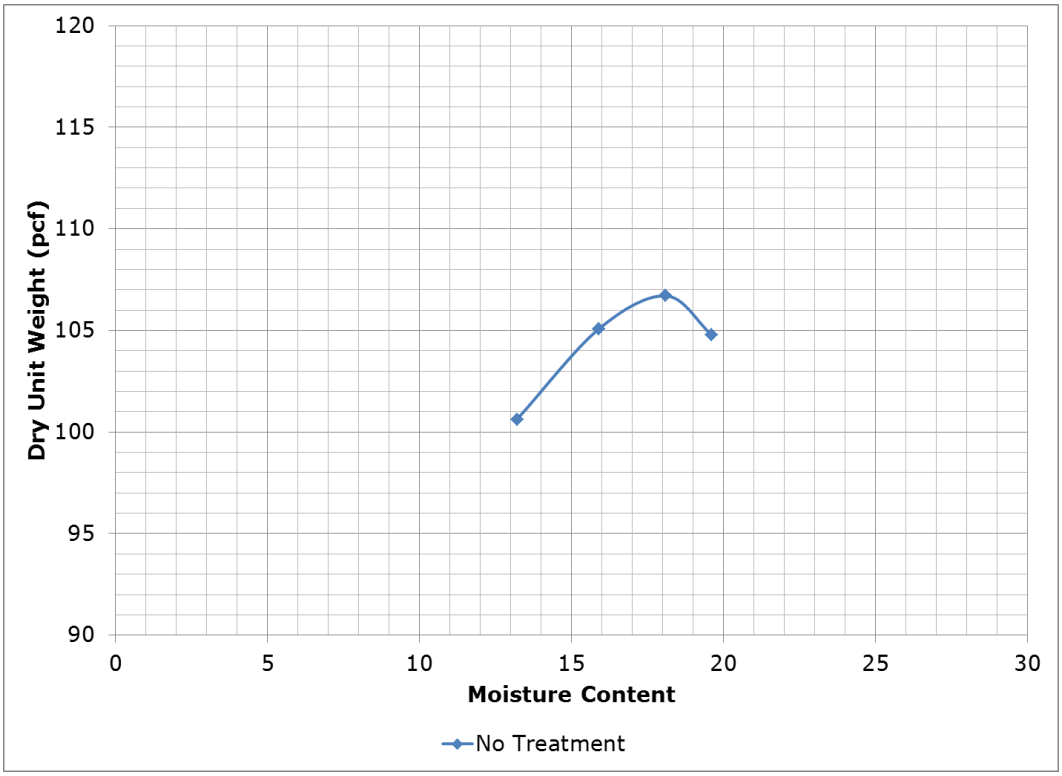

FIGURE 4.5: Anthem Standard Proctor Results.

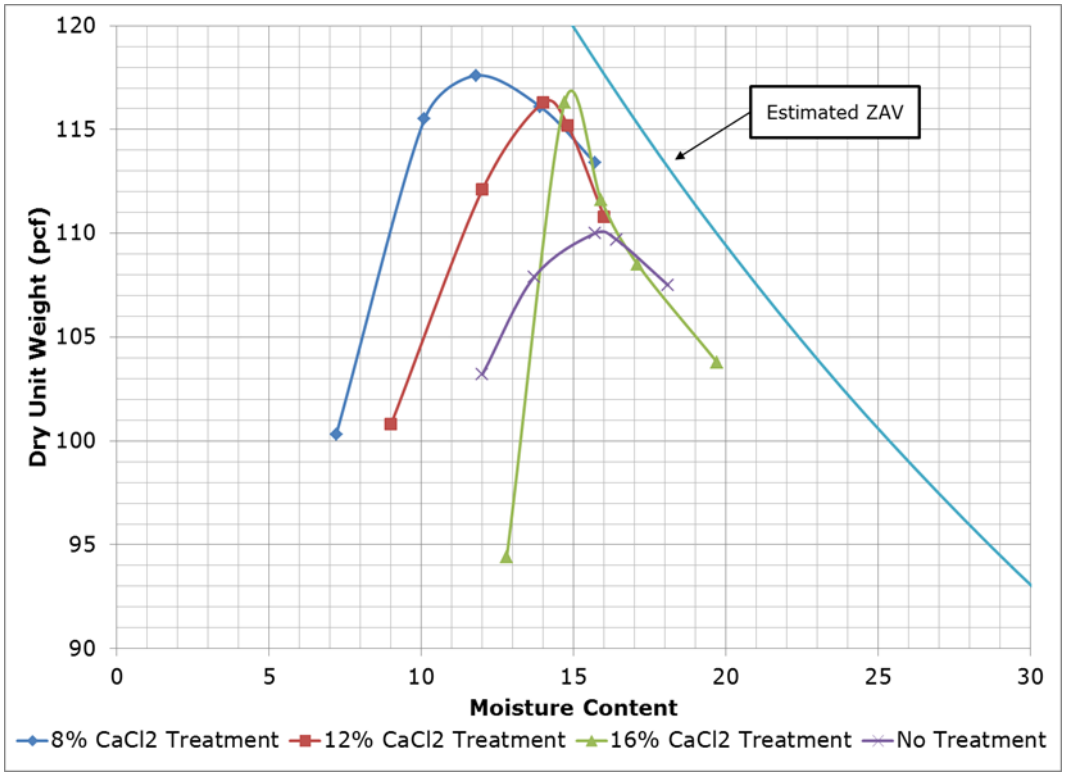

FIGURE 4.6: Vineyard Standard Proctor Results.

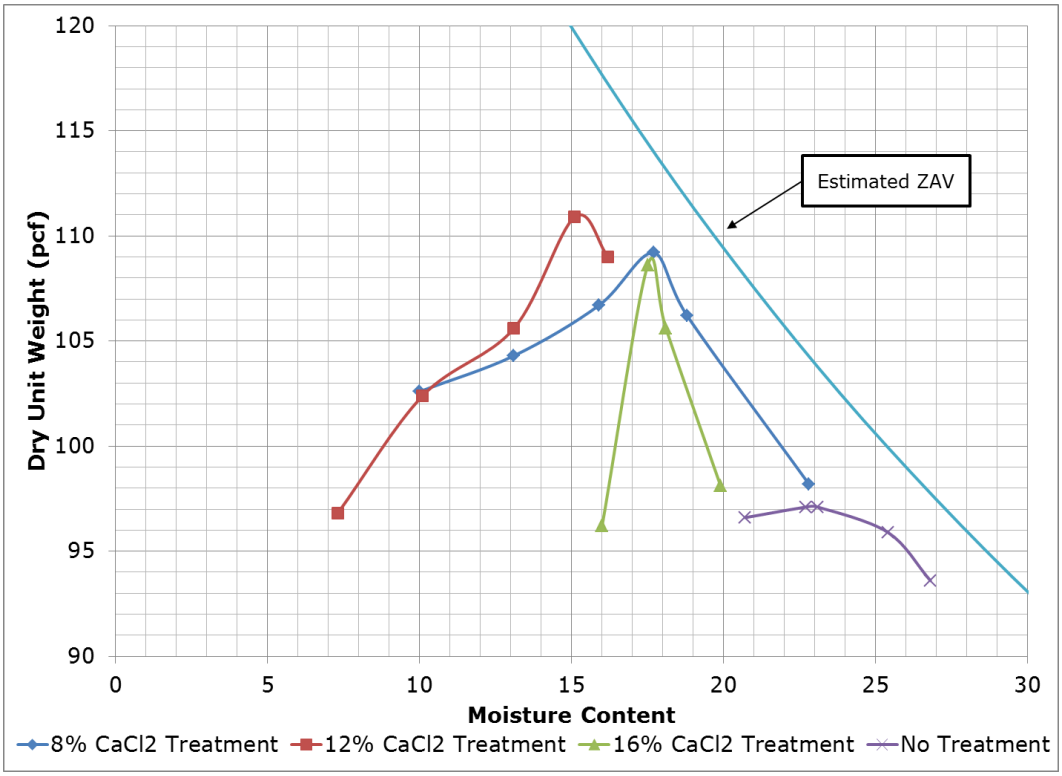

FIGURE 4.7: Eager Standard Proctor Results.

4.5. Unconfined Compressive Strength Results

The results of the unconfined compressive strength are shown in Table 4.4 for the Anthem soil only. A total of nine specimens were tested including the control, 2% $CaCl_2$, and 4% $CaCl_2$ with three replicates each. The fabrics of the soil with salts were in the dispersed category, while the control was at the ideal conditions. The coefficient of variation between the densities was less than a percent, which allows for comparison, even though the fabric of the soils is different. The q_u is Unconfined Compressive Strength in kPa, the ρ_{dry} is the dry density of the sample, and the RC is relative compaction of the sample.

TABLE 4.4: Unconfined Compressive Strength

Control (No $CaCl_2$)				**2% $CaCl_2$**			**4% $CaCl_2$**		
Specimen ID	**RC (%)**	**ρ_{dry}**	**q_u (kPa)**	**RD (%)**	**ρ_{dry}**	**q_u (kPa)**	**RC (%)**	**ρ_{dry}**	**q_u (kPa)**
1	102.7	1.761	326.9	102.6	1.759	261.3	102.8	1.762	280.9
2	102.6	1.759	305.1	102.5	1.758	300.4	103.1	1.767	289.6
3	101.9	1.748	293.8	101.8	1.745	266.7	102.0	1.749	280.8
μ	102.4	1.756	308.6	102.3	1.754	276.1	102.6	1.76	283.8
σ	0.40%	0.007	16.8	0.4	0.007	21.2	0.5	0.9	5
CV (%)	0.4	0.4	5.45	0.43	0.43	7.68	0.53	0.53	1.78

The above results presented in Table 3.4, show the unconfined compressive strength ranged from 309kPa for the control to 284 kPa for the 4% salt concentration. It is interesting to note that the relative density is based on the compaction curve for the control specimens. The compaction curves for the soils with salts were not obtained for the preliminary testing. The main objective was to compare the control and the two soils with salt solutions at the same dry density; however, as referenced in the literature review and seen in the results below the Proctor density increases as the salt concentration increases.

4.6. California Bearing Ratio Results

For the California Bearing Ratio test, the samples were prepared in a mold similarly to the Standard Proctor; however, the mold is approximately 7 inches tall and during compaction a 2.416-inch spacer is placed in the bottom of the mold, which then simulates the same volume as a 6-inch Proctor mold. Once the sample is prepared in the mold, the samples were then loaded with a 10-pound surcharge weight tested accordingly per the testing standard. The surcharge weight of 10-pounds "represents" traffic loading. The bolded values represent in the tables the optimum moisture as determined by the Standard Proctor.

TABLE 4.5: Anthem CBR Test results

Treatment Level	**Moisture Content**					
	11%	12%	14%	16%	18%	20%
Control			4.0		2.7	
2%$CaCl_2$		3.6	2.8		**3.7**	2.1
4%$CaCl_2$			4.5		2.7	
8%$CaCl_2$	5.7			2.4	3.8	
16%$CaCl_2$				4.0	**7.5**	5.1
16% CaO				7.9	**11.0**	9.2

TABLE 4.6: Vineyard CBR Test results

Treatment Level	**Moisture Content**										
	7.2	9.0	10.1	12.0	12.8	14.0	14.8	15.7	16	17.1	19.7
Con-trol	--	--	--	--	--	--	--	**11.1**	--	--	--
8% $CaCl_2$	22.0	--	**20.9**	11.7	--	5.8	--	4.1	--	--	--
12% $CaCl_2$	--	27.0	--	**19.4**	--	12.0	5.8	--	1.8	--	--
16% $CaCl_2$	--	--	--	--	**22.3**	--	13.2	8.7	--	1.5	0.4
16% CaO	--	--	--	--	--	--	--	**42.0**	--	--	--

TABLE 4.7: Eager CBR Test results

Treatment Level	Moisture Content								
	7.3	**10.0**	**13.1**	**15.1**	**16.0**	**17.5**	**18.1**	**19.9**	**23.1**
Control	--	--	--	--	--	--	--	--	**12.3**
8% $CaCl_2$	--	28.1	22.3	--	**17.6**	12.0	8.0	--	1.8
12% $CaCl_2$	30.7	19.8	**14.8**	9.9	4.7	--	--	--	--
16% $CaCl_2$	--	--	--	--	**13.6**	5.0	1.5	0.7	--
16% CaO	--	--	--	--	--	--	--	--	**33.7**

4.7. Soil Corrosion Results

Two of the three soils were tested for corrosive potential after treatment to determine if there would be an adverse impact to the environment. The results for the Vineyard soil are presented in Table 4.8 and the results for the Eager soil are present in Table 4.9.

TABLE 4.8: Vineyard Soil Corrosion Test Results

Treatment Level	pH	Resistivity Ohm-cm	Cl ppm	SO_4 ppm
No Treatment	7.8	1,200.0	143	55
%8 $CaCl_2$	6.6	22.0	21,806	88
%12 $CaCl_2$	6.4	17.0	63,477	105
%16 $CaCl_2$	6.4	13.0	72,093	116

TABLE 4.9: Eager Soil Corrosion Test Results

Treatment Level	pH	Resistivity Ohm-cm	Cl ppm	SO_4 ppm
No Treatment	8.1	1,100.0	115	51
%8 $CaCl_2$	6.9	23.0	21,070	54
%12 $CaCl_2$	6.7	20.0	58,656	63
%16 $CaCl_2$	6.5	16.0	84,874	93

4.8. Dust Control Experiment

The third evaluation test consisted of placing the soil in a wind tunnel (E. Kavazanjian, 2009). The specimens were prepared by passing the soil through a number four sieve, placing the soil in tins, and adding 200 grams of water with or without the salts, depending on the specimen. Table 3.5 shows the results of the wind tunnel experiment. The relative density for all the specimens was at 74.6% of the maximum dry density. The natural water content of the soil is 6%, which when the water was added to the soil, the moisture content increased to 23.4%. With the increase in moisture content, the degree of saturation increased from 15% to 56.4%. After the soil was inundated with water, the specimen was then allowed to dry in the laboratory for two days. The weight of the specimens was recorded, then placed in the wind tunnel. Even though the specimens were placed in the wind tunnel for 10 minutes, each specimen gained weight. The weight gained by the specimens was due to the matric and osmotic potential of the soil. The samples were stored in a relative humidity and temperature controlled environment; the wind tunnel was located in a storage shed, which is not a relative humidity or temperature controlled environment. The lab space was at 23 degrees Celsius, while the shed was a roughly 15 degrees Celsius. Just the drop of 8 degrees Celsius increased the amount of water in the air, which caused the specimens to pull water in to achieve moisture equilibrium. Once the specimens were placed back in the laboratory, the specimens began to lose mass, which is due to the matric and osmotic potential of the soil coming back into equilibrium with the laboratory temperature. It was also interesting to note the crack propagation of the soils with the salts. It appeared that the crack propagation of the soils with salts was less than the control. There was no quantitative measurement taken of the cracks.

TABLE 4.10: Wind Tunnel Results

PASSED SOIL THROUGH #4 SIEVE			
volume	**900 cm^3**	**moist soil**	**1220g**
ρ_{dry}	1.279 g/cm^3	Relative Density	74.6%
Gs	2.723	void ratio	1.129
w% before	6.0%	w% after water	23.4%
%S before water	14.5%	%S after water	56.4%
WIND TUNNEL			
Specimen ID	**Before (g)**	**After (g)**	**% Change**
4% $CaCl_2$	1345.61	1346.71	0.08%
2% $CaCl_2$	1335.55	1336.76	0.09%
Control	1325.71	1327.08	0.10%

Chapter 5

Pavement Design Analysis and Modeling

The Mechanistic-Empirical Pavement Design Guide (MEPDG) is a tool for pavement design that considers fundamental engineering principles. In the past, design was limited to empirical performance equations developed by AASHTO. MEPDG (now referred to as PavementME) was developed by a large number of recognized engineers in the field of pavement design, completed in 2004.

The objectives of this design guide were to provide a tool for the design of new pavement structures and overlays based on mechanistic-empirical principles.

Parameters to be considered in pavement design are the site conditions of traffic, climate, subgrade, materials, existing pavement conditions and construction conditions.

Once all the factors have been determined for a trial design, the pavement structure is evaluated with prediction models for the primary distresses in a pavement structure.

Users input their design information into three different design modules. The design modules include traffic module, bound materials module, and a soils module. The traffic module allows the user to input the traffic count information, and growth behavior to estimate the traffic loading that will occur during the design period. The bound materials module is used to predict either the Portland cement concrete (PCC) or the Asphaltic Concrete (AC) behavior during the design life. The soils module is used to determine the behavior of the unbound soils during the design period.

Within each of the modules, a hierarchical level approach is used for the data input and analysis. The hierarchical level approach within each of the modules allows for all known data input (Level 1) typically determined from field or laboratory measurements, less data input (less than Level 1 and more than Level 3) and limited

use of correlations (Level 2), and limited data input or use of default values and heavily relying on correlations (Level 3).

5.1. Input Summary

The analysis performed utilitzed a combination of Level 2 and Level 3 heirarchical level of inputs. In the analysis, the pavement structure, the traffic loading, and the soil conditions were varied. The soil conditions used from the analysis, were the three soils tested as party of this research. Both the soaked and unsoaked tests results were utilized.

The pavement structures were selected from two Long Term Pavement Performance (LTPP) design sections. Pavement Structure 1 information was obtained from InfoPave LTPP Section 4-509 and Pavement Structure 2 information was obtained from InfoPave LTPP Section 4-1003. Both design pavement sections were located within Arizona. Section 4-509 utilized an AC thickness of 5.4 inches, unbound Granular Base of 14.8 inches and an infinite Subgrade. Section 4-1004 utilitzed an AC thickness of 13 inches, and unbound granular base of 6 inches and an infinite subgrade.

Although two pavement structures were analyzed, both pavements utilized the same AC layer information. The AC layer parameters that were used in the analysis are as follows: asphalt Performance Grade (PG) of 76-16, 5% Effective Binder Content, and 5% Air voids. The remainder of the AC data used default gradation values and correlations were used to estimate the remaining mechanisitic properities of the AC material.

Since there were two different pavement sections utilitized for the analysis, the traffic loading for each pavement structure was varied. Pavement Section 1 (Section 4-509 Interstate 8 and approximately Fuqua Road, Pinal County, Arizona) was analyzed using an Average Annual Daily Truck Traffic (AADTT) of 900 (Low Volume) and 4,500 (High Volume). Pavement Section 2 (Section 4-1003 Interstate 10 and

Winertersburg Road, Tonopah, Arizona) was analyzed using an AADT of 2,000 (low volume) and 10,000 (high volume). For both pavement structures a 20 year design life was used and an Annual Growth Rate of 1.1 percent was utilized. The default values for vehicle class distribution were utilized (Level 3).

The laboratory testing data presented in Chapter 4 was utilized for the soils for the infinite subgrade layer. The information that was inputted in the MEPDG include the Gradation, Liquid Limit, Plastic Limit, Optimum Moisture Content, Maximum Dry Density, In-situ Moisture Content, In-situ Density, CBR (Level 2 data input). The CBR was used to estimate the Resilient Modulus for each of the soils. Each of the soils were subjected to the two pavement structures and two traffic levels.

For CBR, OMC values were used for the pavement analysis. It was also determined that minus 2 percent from OMC would be used for the pavement analysis, for the salt treated soils due to the strength gains observed over OMC. The strength gain for the salt treatment could be due to the soil structure of the samples. The flocculated behavior of the clay increased at minus 2 percent created an edge-to-face orientation that was harder to shear when compared to the face-to-face orientation associated with a dispersed soil structure. Additionally, this level of compaction is achieveable in the field during construction and it can be controlled to maintain this strength level with a compaction specification that limits the moisture content from minus 4 to minus 2 percent from OMC.

Furthermore, the unsoaked value was used since the Resilient Modulus testing protocol outlines using the soil moisture condition that best represents the field condition and as part compaction requirement, minus 2 percent best represents the field condition. Furthermore, the MEPDG soils module uses an environmental factor to adjust the tested/estimated resilient modulus value based on moisture content that the soil module estimates using soil behavior and climatic conditions.

5.2. Comparison of Tested Soils to Listed Pavement Section Soils

The pavement sections that were evaluated are located within the greater Phoenix Area. Pavement Section 1 was from Interstate 8 located near the Interstate 8 and Standfield Road Traffic Interchange. The subgrade soils mapped within this study area were considered a silty gravel with sand (GM). Pavement Section 2 was from Interstate 10 located near the Interstate 10 and Wintersberg Road Traffic Interchange. The subgrade soils for this pavement section were mapped as clayey sand with gravel (SC). These soils encountered in the two pavement sections are considered not limited or commonly found in the greater Phoenix Area when compared to Carlson et al. 2008 soil criteria.

The soils tested as part of this study, when compared to the soils mapped in the greater Phoenix area are considered somewhat limited (Carlson et al. 2008).

5.3. Pavement Design Characteristics of Interest

For all three of the design categories, a reliability level of 90 percent was established as the design criteria. At any reliability level, the design distress value is calculated by applying a statistical analysis to destress value by using the mean and variance calculated for the distress value. The terminal International Roughness Index (IRI), total permanent deformation (total rutting), and Asphaltic Concrete (AC) bottom up cracking were the three design parameters that were evaluated.

The IRI is an index of the pavement smoothness with time. The MEPDG estimates the IRI with time given the following: initial IRI value of the roadway after construction, estimated pavement distresses with time, and the maintenance program performed for the roadway. Once the IRI value reaches 172.00 inches per mile, it exceeds the 90 percent reliability level.

The total permanent deformation is an estimate of the rutting that is aggregated from the asphaltic concrete, granular base material, and the subgrade. The failure criteria for 90 percent reliability is considered when the total exceeds 0.75 inches. The majority of the total rutting occurred within the subgrade and base layer for the pavement structures analyzed.

The Asphaltic Concrete (AC) bottom up cracking is an estimate of the "alligator" cracking for the pavement structure. The failure criteria for 90 percent reliability is considered when the fatigue cracking exceeds more than 25 percent of the pavement surface per lane mile.

5.4. Principles of the Mechanistic Procedure

The mechanistic-empirical principles for calculating the pavement design characteristic of interested are calculated as follows.

The MEPDG uses the concept of multi-layer elastic system or theory to calculate the responses to loading. Some of the assumptions in layered elastic analysis are the material properties of each layer are homogeneous, each layer is isotropic, full friction is developed between each layer interface, there are not shearing forces, the only to material properties used is the elastic modulus E and Poisson's ratio μ, each layer has a finite thickness except for the last layer which is assumed to have infinite thickness, all layers are infinite in the lateral direction. Based on these assumptions, the strains can be determined from the triaxial stress state of any element by the following equations:

$$\varepsilon_z = \frac{1}{E}\left(\sigma_z - \mu\left(\sigma_r + \sigma_t\right)\right)$$

$$\varepsilon_r = \frac{1}{E}\left(\sigma_r - \mu\left(\sigma_t + \sigma_z\right)\right)$$

$$\varepsilon_t = \frac{1}{E}\left(\sigma_t - \mu\left(\sigma_r + \sigma_z\right)\right)$$

When we know the types of stresses applied to pavement structures, using these equations, strains can be calculated and then the mechanistic-empirical models used to estimate performance of the pavement structure.

The International Roughness Index (IRI) is calculated using the following equation:

$$S(t) = S_0 + \left(a_1 S_{D(t)1} + a_2 S_{D(t)2} + ... + a_n S_{D(t)n}\right) + b_j S_j + c_j M_j$$

Where:

S(t) = pavement smoothness at a specific time in in/mi,

S_0 = initial smoothness immediately after construction in in/mi,

$S_{D(t)n}$ = change of smoothness due to i^{th} distress at a given time,

a_i, b_j, c_j = regression constants,

S_j = change in smoothness due to site factors, and

M_j =change in smoothness due to maintenance activities.

AC Fatigue Coefficients:

k1 = 0.007566

k2 = 3.9492

Bf1 = 1

Bf2 = 1

Bf3 = 1

The MEPDG model used for AC Fatigue Cracking is given by:

$$N_f = 0.00432 \times C \times \beta_{f1} k_1 \left(\frac{1}{\varepsilon_1}\right)^{k_2 \beta_{f2}} \left(\frac{1}{E}\right)^{k_3 \beta_{f3}}$$

$$C = 10^M$$

$$M = 4.84\left(\frac{V_b}{V_a + V_b} - 0.69\right)$$

The MEPDG model used for AC Rutting is given by:

$$\frac{\varepsilon_p}{\varepsilon_r} = k_z \beta_{r1} 10^{k_1} T^{k_2 \beta_{r2}} N^{k_3 \beta_{r3}}$$

$$k_z = (c_1 + c_2 * depth) * 0.328196^{depth}$$

$$c_1 = -0.1039 - H_\alpha^2 - 2.4868 * H_\alpha - 17.342$$

$$c_2 = 0.0172 * H_\alpha^2 - 1.7331 * H_\alpha + 27.428$$

Where:

ε_p =plastic strain,

ε_r =resilient strain,

T = layer temperature in °F,

N = number of load repetitions and

H_{ac} = total AC thickness in inches.

AC Rutting Coefficients:

k1 = -3.3512

k2 = 1.5606

Bf1 = 1

Bf2 = 1

Bf3 = 1

The MEPDG model used for Subgrade Rutting is given by:

$$\delta_a(N) = \beta_{s1} k_1 \varepsilon_v h \left(\frac{\varepsilon_o}{\varepsilon_r} \right) \left| e^{-\left(\frac{\rho}{N}\right)^{\beta}} \right|$$

Where:

δa = permanent deformation for the layer,

N = number of repetitions,

εv = average vertical strain,

$\varepsilon 0, \beta, \rho$ = material properties, and

εr = resilient strain

Subgrade Rutting Coefficients:

k1 fine = 1.35

k1 granular = 2.03

Bs1 = 1

5.5. Results of the Analysis

TABLE 5.1: Eager Soil - Results of the Analysis

SN	Traffic	Treatment	PI	CBR	Terminal IRI (in/mile)	Total Rutting (in)	AC Cracking (% lane mile)
1	900	Control	27.3	12.3	147.6	0.61	22.8
		%16 CaO	16.5	33.7	143.9	0.53	21.8
		8%CaCl2	23.4	17.6	147.2	0.6	22.3
		12%CaCl2	21.7	14.8	149.8	0.67	22.8
		16%CaCl2	22	13.6	148.3	0.63	22.6
	4500	Control	27.3	12.3	178.2	1.03	41.5
		%16 CaO	16.5	33.7	172.6	0.92	38
		8%CaCl2	23.4	17.6	177.3	1	39.9
		12%CaCl2	21.7	14.8	180.8	1.09	41.7
		16%CaCl2	22	13.6	179	1.04	40.9
2	2000	Control	27.3	12.3	135.9	0.44	1.6
		%16 CaO	16.5	33.7	131.4	0.37	1.5
		8%CaCl2	23.4	17.6	134.9	0.43	1.6
		12%CaCl2	21.7	14.8	137.7	0.49	1.6
		16%CaCl2	22	13.6	136.1	0.46	1.6
	10,000	Control	27.3	12.3	148.9	0.74	2.4
		%16 CaO	16.5	33.7	143.6	0.65	1.9
		8%CaCl2	23.4	17.6	147.6	0.72	2.1
		12%CaCl2	21.7	14.8	151.1	0.8	2.5
		16%CaCl2	22	13.6	149.2	0.76	2.3

TABLE 5.2: Vineyard Soil - Results of the Analysis

SN	Traffic	Treatment	PI	CBR	Terminal IRI (in/mile)	Total Rutting (in)	AC Cracking (% lane mile)
1	900	Control	21.3	11.1	151.4	0.7	23
		%16 CaO	18.2	42	146.6	0.6	22.8
		8%CaCl2	18.6	20.9	150.8	0.69	22.8
		12%CaCl2	17.4	19.4	148.3	0.63	22.3
		16%CaCl2	16.9	22.3	147	0.59	22.1
	4500	Control	21.3	11.1	182.3	1.13	42.5
		%16 CaO	18.2	42	175.2	0.96	38.6
		8%CaCl2	18.6	20.9	181.7	1.11	41.5
		12%CaCl2	17.4	19.4	178.5	1.03	40
		16%CaCl2	16.9	22.3	176.6	0.99	39
2	2000	Control	21.3	11.1	139.2	0.52	1.7
		%16 CaO	18.2	42	134.6	0.42	1.6
		8%CaCl2	18.6	20.9	138.4	0.5	1.6
		12%CaCl2	17.4	19.4	135.9	0.45	1.6
		16%CaCl2	16.9	22.3	134.4	0.42	1.6
	10000	Control	21.3	11.1	153	0.83	2.7
		%16 CaO	18.2	42	145.8	0.69	2
		8%CaCl2	18.6	20.9	151.8	0.81	2.4
		12%CaCl2	17.4	19.4	148.8	0.75	2.2
		16%CaCl2	16.9	22.3	147	0.72	2

5.6. Discussion of the Results

As we learned so far in this study, the Eager soil was the most vulnerable to the acidic condition that the salt mix created; therefore, the Eager soil showed less CBR improvement with the increase of salt concentration (Eager has less clay particles than Vineyard, refer to Chapter 3). It was expected that the Vineyard soil would perform better when it comes to cracking and deformation.

Tables 5.3 and 5.4 presents percentage of changes between the untreated soils, Lime treated soils and salt treated soils:

TABLE 5.3: Eager Soil - % of Change from Control

SN	Traffic	Treatment	PI	CBR	Total Rutting (in)	AC Cracking (% lane mile)	AC Cracking change from control %	Total Rutting Change from Control %
1	900	Control	27.3	12.3	0.61	22.8		
		%16 CaO	16.5	33.7	0.53	21.8	4.39%	13.11%
		8%CaCl2	23.4	17.6	0.6	22.3	2.19%	1.64%
		12%CaCl2	21.7	14.8	0.67	22.8	0.00%	-9.84%
		16%CaCl2	22	13.6	0.63	22.6	0.88%	-3.28%
	4500	Control	27.3	12.3	1.03	41.5		
		%16 CaO	16.5	33.7	0.92	38	8.43%	10.68%
		8%CaCl2	23.4	17.6	1	39.9	3.86%	2.91%
		12%CaCl2	21.7	14.8	1.09	41.7	-0.48%	-5.83%
		16%CaCl2	22	13.6	1.04	40.9	1.45%	-0.97%
2	2000	Control	27.3	12.3	0.44	1.6		
		%16 CaO	16.5	33.7	0.37	1.5	6.25%	15.91%
		8%CaCl2	23.4	17.6	0.43	1.6	0.00%	2.27%
		12%CaCl2	21.7	14.8	0.49	1.6	0.00%	-11.36%
		16%CaCl2	22	13.6	0.46	1.6	0.00%	-4.55%
	10,000	Control	27.3	12.3	0.74	2.4		
		%16 CaO	16.5	33.7	0.65	1.9	20.83%	12.16%
		8%CaCl2	23.4	17.6	0.72	2.1	12.50%	-10.77%
		12%CaCl2	21.7	14.8	0.8	2.5	-4.17%	-11.11%
		16%CaCl2	22	13.6	0.76	2.3	4.17%	5.00%

TABLE 5.4: Vineyard Soil - % of Change from Control

SN	Traffic	Treatment	PI	CBR	Total Rutting (in)	AC Cracking (% lane mile)	AC Cracking change from control %	Total Rutting Change from Control %
1	900	Control	21.3	11.1	0.7	23		
		%16 CaO	18.2	42	0.6	22.8	0.87%	14.29%
		8%CaCl2	18.6	20.9	0.69	22.8	0.87%	1.43%
		12%CaCl2	17.4	19.4	0.63	22.3	3.04%	10.00%
		16%CaCl2	16.9	22.3	0.59	22.1	3.91%	15.71%
	4500	Control	21.3	11.1	1.13	42.5		
		%16 CaO	18.2	42	0.96	38.6	9.18%	15.04%
		8%CaCl2	18.6	20.9	1.11	41.5	2.35%	1.77%
		12%CaCl2	17.4	19.4	1.03	40	5.88%	8.85%
		16%CaCl2	16.9	22.3	0.99	39	8.24%	12.39%
2	2000	Control	21.3	11.1	0.52	1.7		
		%16 CaO	18.2	42	0.42	1.6	5.88%	19.23%
		8%CaCl2	18.6	20.9	0.5	1.6	5.88%	3.85%
		12%CaCl2	17.4	19.4	0.45	1.6	5.88%	13.46%
		16%CaCl2	16.9	22.3	0.42	1.6	5.88%	19.23%
	10,000	Control	21.3	11.1	0.83	2.7		
		%16 CaO	18.2	42	0.69	2	25.93%	16.87%
		8%CaCl2	18.6	20.9	0.81	2.4	11.11%	2.41%
		12%CaCl2	17.4	19.4	0.75	2.2	18.52%	9.64%
		16%CaCl2	16.9	22.3	0.72	2	25.93%	13.25%

The positive percentage in the above tables presents an improvement from the control sample. As seen from the results, the Vineyard soil treated at 16% CaCl2 showed an improvement that is comparable to the Lime treatment. On the other hand, the Eager soil showed very little improvement at 8% CaCl2; cracking increased from control. This goes back to the effect of acid on the Eager Clay mineralogy.

Chapter 6

Summary and Conclusions

The following subsections outline the changes in soils properties for the three soils that were tested. Those changes in the Atterberg Limits, California Bearing Ratio, and the soil corrosion characteristics.

6.1. Changes in Atterberg Limits

The reduction in the plasticity index as a value and reduction as a percentage from the untreated samples are shown in Table 6.1 and 6.2 respectively.

TABLE 6.1: Reduction in Plasticity Index Compared to Untreated

Soil	No Treatment	%2 $CaCl_2$	%4 $CaCl_2$	%8 $CaCl_2$	%12 $CaCl_2$	%16 $CaCl_2$	%16 CaO
Anthem	0.0	-4.1	-4.7	-6.7	--	--	--
Vineyard	0.0	--	--	-2.7	-3.9	-4.4	-3.1
Eager	0.0	--	--	-3.9	-5.6	-5.3	-10.8

The values in Table 6.1 represent the difference between the treated sample and the untreated samples. The negative values correspond to a drop in the plasticity index.

TABLE 6.2: Percent Reduction in Plasticity Index Compared to Untreated

Soil	No Treatment	%2 $CaCl_2$	%4 $CaCl_2$	%8 $CaCl_2$	%12 $CaCl_2$	%16 $CaCl_2$	%16 CaO
Anthem	0.0%	-17.6	-20.7	-32.4	--	--	--
Vineyard	0.0%	--	--	-14.5	-22.4	-26.0	-17.0
Eager	0.0%	--	--	-16.7	-25.8	-24.1	-65.5

The values in Table 6.2 represent the percent change from the untreated sample (i.e., the difference between treated and untreated divided by the untreated value). The three soils exhibited reduction in the plasticity index. The acceptable range per ASTM 4318 to accept two test results performed by the same operator is 2 percent for CH soils and 1 percent for CL soils when comparing the plasticity index result. The

results indicate that the treated samples are statistically different when evaluated with the precision and bias statement outlined in ASTM 4318.

The reduction of the Atterberg Limits can be attributed to the introduction of calcium hydroxide and hydrochloric acid to the treated samples. Recall, when the calcium chloride is added to water, the by-product of the chemical reaction produces heat, calcium hydroxide (basic), and hydrochloric acid (acidic).

The research of Prakash and Arumairaj (2013) presented treating clay soil with various basic and acidic solutions. The results indicated the acidic solutions (hydrochloric acid) produced the highest reduction in the Atterberg Limits. The calcium hydroxide showed a marginal reduction in the Atterberg Limits, while other basic solutions showed an increase in the Atterberg Limits.

When comparing Prakash and Arumairaj (2013) research with the results of this research, it appears the hydrochloric acid by-product produced during the chemical reaction is governing the reduction of the Atterberg Limits.

Additionally, the results indicate a potential optimum treatment level maybe able to be determined from the reduction results. For the Vineyard soil, the optimum treated as determined by the highest reduction in plasticity index occurred between the 12 percent and 16 percent calcium chloride treatment, while the Eager soil occurred at 12% concentration. The Anthem soil on the other hand, did not receive a high enough treatment to determine the optimal reduction in the plasticity index.

6.2. Changes in the Standard Proctor Results

As observed in Figures 4.6, and 4.7, the maximum dry density and the optimum moisture content changed. In both soils, the optimum moisture content was reduced and the maximum dry density increased from the untreated Standard Proctor values. When comparing the results to the results presented by Prakash and Arumairaj (2013), the increase in maximum dry density is primarily due to the basic solution or the

calcium hydroxide. Additionally, their research also showed that both the basic and acidic solutions reduced the optimum moisture content similarly to results that were obtained in this research. Abood et al. (2007) showed that treating a clay sample with various amounts and types of salts increased the dry density and decreased the optimum moisture content.

6.3. Changes in California Bearing Ratio

The changes in the CBR observed in the samples are a direct correlation to the changes in strength of the material. In each of the samples tested, the CBR value either increased or decreased from the untreated sample. The increase in the CBR value, when the clay was treated, was not observed in all three soils. The Anthem and Vineyard soils showed an increase in CBR as the salt concentration increased when comparing the CBR value at optimum moisture content. The Eager soil, on the other hand, showed a minimum improvement in strength when the salt concentration was increased. The Anthem soil increased by almost 2.7 times when comparing the 16 percent salt treatment to untreated sample. At the same concentration of Lime, the 16 percent Lime treated sample increased the CBR by almost 4 times the untreated samples. The changes in CBR for the three soils are shown in Table 6.3 and Figure 6.1.

Additionally, the changes in the CBR strength of the soil as a percentage of the untreated samples are depicted in Figure 6.2.

TABLE 6.3: Percent Change in CBR Strength

Treatment Level	Anthem		Vineyard		Eager	
	CBR	% Change in CBR	CBR	% Change in CBR	CBR	% Change in CBR
No Treatment	2.7	0.0%	11.1	0.0%	12.3	0.0%
8% $CaCl_2$ Treatment	3.8	40.7%	20.9	88.3%	17.6	47.7%
12% $CaCl_2$ Treatment			19.4	74.8%	14.8	22.5%
16% $CaCl_2$ Treatment	7.5	177.8%	22.3	100.9%	13.6	11.7%

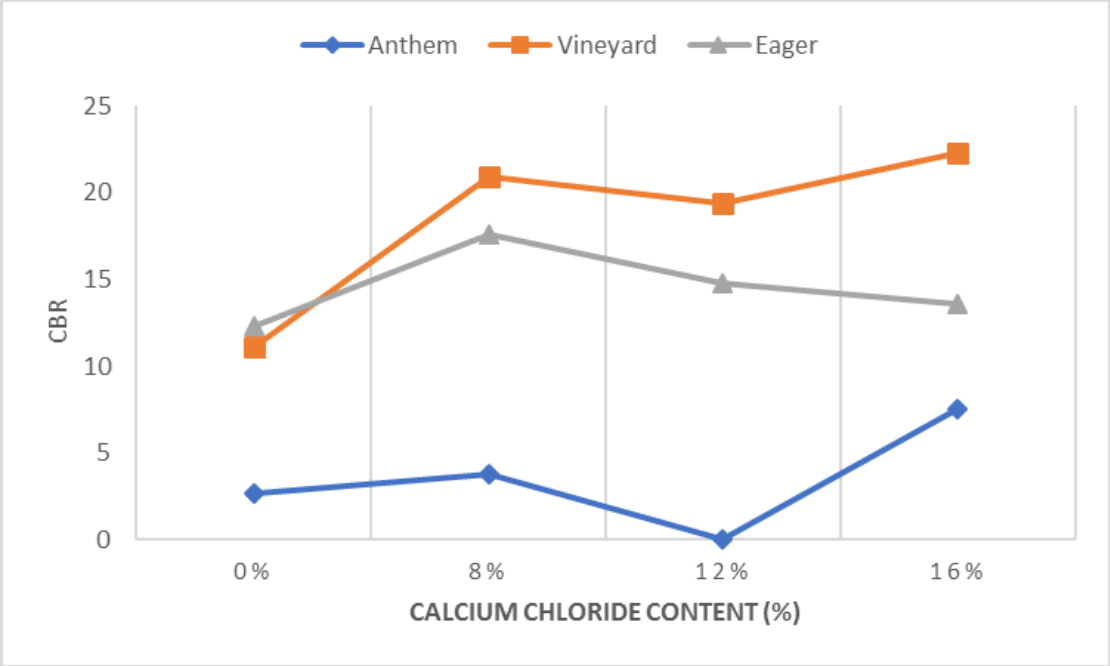

FIGURE 6.1: CBR Results for the Three soils at Optimum Moisture Content

As observed in Table 6.3 and Figure 6.1, the Anthem soil showed the most promising increases in strength when compared to the other two soils. The strength gains for the Anthem soil ranged from 40.7 percent to 174.5 percent, which shows the clay content/mineralogy reacted well with the salt treatment. The Vineyard soil showed strength gains ranging from 47.7 percent to 100.9 percent when treated with various

levels of the salt concentration. The Eager soil, on the other hand, showed the a sharp increase of CBR at 8 percent salt concentration; then it decreased to 11.7 percent (which still slightly higher than the control sample). The decrease in the CBR for the Eager soil when treated with the various salt concentration levels could be an indication that the optimum salt content of this soil is less than 8 percent. Additionally, this result for the Eager soil can be attributed to the clay content/mineralogy.

The reduction in the CBR strength value could be attributed to the amount of clay particles that were treated with salt. Recall back to Table 4.2, Anthem soil had approximately 32.2 percent, Vineyard soil had approximately 19.2 percent and Eager soil had approximately 15.0 percent clay. When comparing the CBR results to the Atterberg Limits, the reduction in the plasticity index was promising; this is potentially attributed to the hydrochloric acid destroying the clay mineralogy. As stated before, when clay is treated with acid, it reduces the plasticity index. Thus, it is possible the acid in the various treatment solutions destroyed all the clay minerals that would have benefited from the calcium hydroxide treatment. This is apparent when comparing the untreated to Lime treated Eager soil CBR results. The strength increases in the other soils could be potentially attributed to the clay mineralogy of the soils, which was not studied as part of this research.

Additionally, due to the low clay content in the Eager soil, it is possible that if the Eager soil was treated with a lower dosage of salt, there could be an increase in strength; however, the material was completely used during the laboratory testing. Additional material would be needed to determine if the Eager soil responds well to salt treatment.

Based upon Figure 6.1, it is possible for the salt treatment to be a viable option to increase strength, the minimum clay fraction as determined by a hydrometer analysis should be greater than 18 percent. It is quite possible that the Anthem and

Vineyard soils are comprised of similar clay mineralogy percentages and the Eager soil is comprised of entirely different clay mineralogy percentages, causing the observed results, then strength gains are not attributed to the clay percentage (i.e., smaller than 2 microns).

6.4. Changes in the Soil Corrosion Testing Suite

The addition of any salt to the soil will increase the corrosion potential due to the pore chemistry of the material. As outlined earlier, may factors affect soil corrosion and corrosion rates for buried ferrous and cementitious materials. Typically, the soil pH, soil resistivity, sulfate and chloride content are the contributing factors in determining the most corrosion rates for various materials.

The soil corrosion laboratory testing was performed only on the Vineyard and Eager soils. The results of the corrosion testing are presented in Tables 4.8 and 4.9, respectively and again in Tables 6.4 and 6.5 for ease of viewing.

TABLE 6.4: Vineyard Soil Corrosion Test Results

Treatment Level	pH	Resistivity Ohm-cm	Cl ppm	SO_4 ppm
No Treatment	7.8	1,200.0	143	55
%8 $CaCl_2$	6.6	22.0	21,806	88
%12 $CaCl_2$	6.4	17.0	63,477	105
%16 $CaCl_2$	6.4	13.0	72,093	116

TABLE 6.5: Eager Soil Corrosion Test Results

Treatment Level	pH	Resistivity Ohm-cm	Cl ppm	SO_4 ppm
No Treatment	8.1	1,100.0	115	51
%8 $CaCl_2$	6.9	23.0	21,070	54
%12 $CaCl_2$	6.7	20.0	58,656	63
%16 $CaCl_2$	6.5	16.0	84,874	93

Prior to the salt treatment, both soils would be considered corrosive due to the soil resistivity as outlined in NCHRP, 1978. After the salt treatments, both soils are considered to be very corrosive due to the soil resistivity decrease, the chloride content increase, and the pH decrease.

6.5. Conclusions

Presented within this chapter is the discussion of the laboratory results. Three soils were treated with varying amounts of salt and different results were observed. The results obtained from this research agrees well with the other authors when comparing the increase in Standard Proctor density and the reduction of the optimum moisture content.

The results when comparing the Atterberg Limits compare well with literature as well. When salt concentration was increased, a decrease in the plasticity index was observed in all soils which can be helpful if there is a project specification for plasticity index. Additionally, when comparing the precision and basis statement as outlined in the ASTM standard, the reduction seen with each treatment is statistically different since one operator performed the testing. The large reduction can be attributed to the hydrochloric acid that is produced with the calcium chloride is added to water. On the other hand, Lime when added to water produces calcium hydroxide. The hydrochloric acid decreases the liquid limit, while the calcium hydroxide increases the liquid limit and the plastic limit, which was observed in the literature as well as the two samples treated with Lime.

It was also observed the strength of the material did change as observed in the literature; however, a strength loss was observed in one of the soils, which could be attributed to the low clay content. The highest strength gain that occurred was approximately 2.7 times that of the untreated sample for the Anthem soil. This strength gain was not observed in the other two soils. The other two soils had a

marginal increase of 1.18 or a drastic decrease 0.6 in strength when treated with the salts.

When comparing the soil corrosive potential, the additional salt treatment showed promise for increasing strength, to an extent; however, it changes the chemical properties of the soil. The soils prior to treatment were corrosive, which could be managed with appropriate techniques, but the salt increased the values to levels that could be potentially cost prohibitive if salt was used by itself to treat the soil.

The addition of salt had the largest impacts on the soil properties of Atterberg limits, Proctor density, and soil corrosion potential, for all three soils.

The Eager soil was the most vulnerable to the acidic condition that the salt mix created and no improvement or benefit was observed for the pavement design structures analyzed. The Vineyard soil treated at 16% CaCl2 showed an improvement that is comparable to the Lime treatment. On the other hand, the Eager soil showed very little pavement performance improvement at 8% CaCl2; this goes back to the effect of acid on the Eager Clay mineralogy.

Chapter 7

Recommendations and Future Research

This study was limited to understanding and confirming structural changes due to treating soil with salt. It has been presented that the salt addition can reinforce the soil structure.

This chapter will list important recommendations to further research the sustainability of this treatment.

7.1. Chlorine Contamination of the Surrounding Environment

It was observed that after treatment, the chlorine levels in the soil increased exponentially such that, if not treated, can potentially have corrosive effects on buried structures. Additionally, as stated previously, high chlorine levels are also detrimental to the surrounding environment, including plants and animals. The added benefit of the salt treatment will need to be evaluated, addressing the following questions:

1. At what rate will the chlorine level leach into the surrounding untreated areas?
2. How far will the chlorine containment travel when the soil is constantly wetting and drying due to weather conditions?
3. Will the chlorine levels stabilize after certain number of cycles of wetting and drying of the soil?

7.2. Acid Treatment and Leaching

As the calcium chloride was added to water, hydrochloric acid was a byproduct of the reaction. The results of this study, indicated the pH of the soil decrease, and the soil environment became more acidic. Based on literature review, the acid counter effects soil reinforcement and can damage the clay mineralogy. After treatment, the hydrochloric acid will need to be chemically addressed in order to balance the soil

acidity. As part of future research, the research should evaluate the following questions:

1. How does the soil behave when treated with straight hydrochloric acid? Will similar results from this research be evident?

2. How can the hydrochloric acid be removed from the aqueous solution; can NaOH be chemically encouraged to increase PH?

7.3. Clay Content

As seen in the research three clay content levels were used; however, the clay mineralogy of the soils was not determined. As part of future research, the clay mineralogy should be determined for comparative purposes. Additionally, as the research is increased, additional clay contents should be evaluated, which should include clay contents ranging from 5% to 50% clay, as long as the 5% clay content has a high enough plasticity index that can cause a design concern. With future research regarding clay the following questions need to be addressed:

1. How does the treatment effect the different clay mineralogy structure and strength?
2. How does the percentage of clay within a sample effect the treatment outcome?

7.4. Highway Shoulders Stabilization

It is known that salt can saturate soil and create an environment that prevents the growth of majority of plants. However, as seen in the result, salt will reinforce the soil structure (depending on the clay structure, it could be very minimal) therefore, considering using salt by-products to stabilize highway shoulders could be ideal and

save a lot of maintenance money when it comes to removing unwanted vegetation. A salt saturated soil structure could help in dust control as well.

7.5. Developing Countries and Rural Roadways

The original idea of this research was initiated by a trip to Angola where dust was covering a majority of the city Luanda; mainly because of unpaved roadways. Despite some of the environmental challenges for salt leaching that could affect agriculture in developing countries, a localized treatment of these rural roadways will help in suppressing dust.

7.6. Combined Lime and Salt, and Calcium Carbonate as a Soil Stabilizer

As discussed in this study, Lime has traditionally been used as a soil stabilizer with certain detrimental environmental effects and is a manufactured product. Salt refuse is a viable soil stabilizer. In combination, manufactured Lime and salt refuse may prove to be an effective soil stabilizer. Future research is recommended to test the soil stabilizing properties of varying proportions of Lime and salt using the approach provided in this study. After treatment, a good portion of the Sodium Cation, Na+ will be displaced by Ca_2+.

7.7. Chloride Leaching and Exploring Other Salts

In the case of highway deicing, potential environmental impacts between calcium chloride and magnesium chloride are compared to sodium chloride (NaCl). Sodium chloride is less environmentally friendly as it tends to break down soil structure and decreases permeability; both calcium chloride and magnesium chloride improve soil structure and increase permeability (Oxycalciumchloride, 2017). Much of the concern related to the environmental impacts in the application of salts is the contamination of soil and water by chloride, sodium, magnesium and calcium. Although chloride is present in the natural environment, the use of these deicers can be measured in surface water, ground water and soils near roadways where they have

been used (Oxycalciumchloride, 2017). Chloride levels may negatively impact aquatic life (Oxycalciumchloride, 2017). In areas where the water table is more than 200 feet below the surface, even with corrosive soils, if used under pavement, Additional research regarding the environmental challenges might be considered.

7.8 Potential Saline Solution Sources

Other potential saline sources to be considered as soil stabilizers might be:

1. Seawater as a saline solution.
2. Analyze the potential effluents resulting from Nanofiltration and RO as a saline solution source (it is rich of divalent cations).
3. Potential Saline Waste Solutions analysis.
4. Wastewater Effluent.
5. Desalination plant by-products.
6. Water treatment plant brine waste.

REFERENCES

Abood,T.T, Kasa, A.B., and Chik, Z.B. 2007. Stabilization Of Silty Clay Soil Using Chloride Compounds. *Journal of Engineering Science and Technology:* 102 -110.

AASHTO, 1993. Guide for Design of Pavement Structures, American Association of State Highway and Transportation Officials, Washington, D.C.

ASTM Standard D1883-07. 2009. Standard Test Method for CBR (California Bearing Ratio) of Compacted Soils. West Conshohocken, PA.

ASU Office of Knowledge Enterprise Development. (2011, May 19). Facilities & Administrative (F&A) costs. Tempe, AZ. http://researchadmin.asu.edu/fa

Baron,P.(n.d.).Generation and Behavior of Airborne Particles (Aerosols). https://www.cdc.gov/niosh/topics/aerosols/pdfs/Aerosol_101.pdf

Balasubramanian, P. A Brief Review On Best Available Technologies For Reject Water (Brine) Management In Industries. 3rd ed. Tiruchirappalli,Trichy: N.p., 2013. Web.

California Test 301. (2000). California Test 301: Method For Determining The Resistance "R" Value Of Treated And Untreated Bases, Subbases, And Basement Soils By The Stabilometer. State Of California—Business, Transportation And Housing Agency. Sacramento, CA

Cao, X., Huang, X., Liang, P., Xiao, K., Zhou, Y., Zhang, X., & Logan, B. E. (2009). A New Method for Water Desalination Using Microbial Desalination Cells. *Environmental Science and Technology*: 7148-7152.

Carlson, Joby, Kamil Kaloush, Jay S. Golden, Mohamed Arab, and Claudia E. Zapata. "Evaluation of In Situ Temperatures, Water Infiltration and Regional Feasibility of Pervious Concrete Pavements." *International Journal of Pavements*. N.p., 31 Dec. 2007. Web. <https://trid.trb.org/view.aspx?id=1090747

Civil Engg. Dictionary. (n.d.). Determination of CBR Value http://aboutcivil.org/california-bearing-ratio-test.html#de

Coduto, D. P. (1999). *Geotechnical Engineering: Principles and Practices*. Upper Sattle River, New Jersey: Prentice-Hall.

Environmental Protection Agency. (2003).Dust Control and Stabilization. *Gravel Roads Maintenance and Design Manual*: Section IV https://www.epa.gov/sites/production/files/2015-10/documents/2003_07_24_nps_gravelroads_sec4_0.pdf

Environmental Protection Agency. (2011). National Ambient Air Quality Standards (NAAQS). *Air and Radiation*: http://www.epa.gov/air/criteria.html

Environmental Protection Agency. (2015, October). Retrieved from https://www.epa.gov/sites/production/files/2015-10/documents/2003_07_24_nps_gravelroads_sec4_0.pdf

Environmental Protection Agency. (2015, December 28). National Ambient Air Quality Standards (NAAQS). Retrieved from EPA.gov: http://www.epa.gov/criteria-air-pollutants/naaqs-table

Florineth, F., & Gerstgraser, C. (n.d.). Soil Bioengineering Measures for Hill and Slope Stabilization Works with Plants. Retrieved May 20, 2011, from FAO CorporateDocumentRepository: http://www.fao.org/docrep/X0622E/x0622e0s.htm

FHWA, (2009), Corrosion/Degradation of Soil Reinforcements for Mechanically Stabilized Earth Walls and Reinforced Soil Slopes

Greenhouse Gas Protocol, "Calculating CO2 Emissions from the Production of Lime" Version. 2. N.p.: n.p., n.d. PDF.

Grott, G. J. (2003). United States of America Patent No. 6651383 B2.

Health Canada. (2001). Priority Substances List Assessment Report for Road Salts. *Environment Canada Health Canada.* http://www.hc-sc.gc.ca/ewh-semt/pubs/contaminants/psl2-lsp2/road_salt_sels_voirie/index-eng.php

Horton Web Design. (2008). Water Management Solutions. Retrieved May 31, 2011, from Natural AG Solutions: http://www.naturalagsolutions.com/water.html

Industrial Resources Council. (c2008-2016). industrialresourcescouncil.org. Retrieved from http://www.industrialresourcescouncil.org/Applications/SoilStabilization/tabid/443/Default.aspx

Interactive, P. (2013, November 24th). Pavement Interactive. Retrieved from Resistance,http://www.pavementinteractive.org/article/resistance-value/#sthash.5u6d79Py.dpuf

International Decade for Action, Water For Life 2005 - 2015. (2011). Retrieved 2011, from United Nations: http://www.un.org/waterforlifedecade/scarcity.shtml

James K. Mitchell, K. S. (Third Edition). Fundamentals of Soil Behavior. John Wiley and Sons, INC.

Jones, James. Vitale. (2008, 11 13). Road Dust Management: State of the Practice. http://citeseerx.ist.psu.edu/viewdoc/download?doi=10.1.1.466.2805&rep=rep1&type=pdf

Kavazanjian, E. (2009). Biopolymer Soil Stabilization for Wind Erosion Control. Proceedings. 17th International Conference on Soil Mechanics and Geotechnical Engineering.

Krausz, J. (2016, November 7). www.newsmax.com/TheWire. Retrieved from www.newsmax.com: http://www.newsmax.com/TheWire/delhi-pollution-closes-schools/2016/11/07/id/757557/

Macpherson, J. (2008, November 17). North Dakota OKs spraying oil wastewater on roads. Retrieved May 26, 2011, from USA Today: http://www.usatoday.com/news/nation/2008-11-17-2428579857_x.htm

Marine 3 Technologies Ltd. (2008). Benefits. Retrieved May 28, 2011, from Dust Suppression: http://www.marine3technologies.com/ProductApplications/DustSuppression/tabid/84/Default.aspx

Martinet, M. C. (2008). Urban Stream Syndrome: The Future of Stream Ecosystems in Urban Watersheds. Sigma XI, The Scientific Research Society.

Michael J McCarthy, e. a. (2011). Clay-Lime Stabilization: Characterizing Fly Ash Effects in Minimizing the Risk of Sulfate Heave. 2011 Worldof Coal Ash (WOCA) Conference , (p. 15). Denver, CO.

Midwest Industrial Supply, Inc. (2011, February 17). Midwest Expands Dust Control Product Line with Dust Fyghter LN 100. Canton, Ohio.

NCHRP-50. (1978). Durability of Drainage Pipe, TRB, Washington, D.C.

"China Starts 2017 Engulfed by Smog, Issues Pollution Alerts." *Newsmax*. N.p., 02 Jan. 2017. Web. 01 May 2017. <http://www.newsmax.com/world/asia/as-china-smog/2017/01/02/id/766379>.

NLA - Soil Stabilization. (n.d.). Retrieved November 27, 2011, from National Lime Association: http://www.lime.org/uses_of_lime/construction/soil.asp

Occidental Chemical Corporation. (2009).

Onlelow & Okoafor. (2012, October). www.aprnjournals.com. Retrieved from http://www.arpnjournals.com/jes/research_papers/rp_2012/jes_1012_06.pdf

Osthoff, H. D., Roberts, J. M., Ravishankara, A. R., Williams, E. J., Lerner, B. M., Sommariva, R., Brown, S. S. (2008). High levels of nitryl chloride in the polluted subtropical marine boundary layer. Nature Geoscience, 324-328.

"Effect On Water And Natural Environment - Managing Impact - Highway Ice Melting - Oxychem Calcium Chloride". Oxycalciumchloride.com. N.p., 2017. Web.

Pavement Interactive. (2007, August 15). California Bearing Ratio. Retrieved from http://www.pavementinteractive.org/article/california-bearing-ratio/

Peng, X., Horn, R., Deery, D., Kirkham, M. B., & Blackwell, J. (2005). Influence of soil structure on the shrinkage behavior of a soil irrigated with saline-sodic water. Australian Journal of Soil Research, 555-563.

Prakash, S. and Arumairaj, P.D., (2013). Effects of Acid and Base Contamination on Geotechnical Properties of Clay. International Journal of Science and Research ISSN 2319-7064.

Rengasamy, P., & Olsson, K. A. (1991). Sodicity and Soil Structure. Austrailian Journal of Soil Research, 365-952.

Reske, H. J. (2011, May 23). Obama's EPA Moves to Regulate Dust. Retrieved May 24, 2011, from Newsmax.com: http://www.newsmax.com/InsideCover/epa-dust-farmers-regulation/2011/05/23/id/397445

Road Management & Engineering Journal. (1998, June 1). Retrieved from usroads.com: http://www.usroads.com/journals/rmej/9806/rm980604.htm

Salt Institute. (1982). Salt for Road Stabilization. Salt Institute.
Seed, H. B. (1967). Prediction of Flexible Pavement Deflections from laboratory Repeated Load Tests. NCHRP Rep. No. 35, National Cooperative Highway Research Program.

Senthilselvan, A., Zhang, Y., Dosman, J. A., BGarber, E. M., Holfeld, L. E., Kirychuk, S. P., . . . Rhodes, C. S. (1997). Positive Human Health Effects of Dust Suppression with Canola Oil in Swine Barns. American Journal of Respiratory and Critical Care Medicine, 410-417.

Sodic Soil Management. (n.d.). Sodic Soil Management. New South Wales, Australia *Department of Primary Industries*. http://www.dpi.nsw.gov.au/__data/assets/pdf_file/0009/127278/Sodic-soil-management.pdf: Chapter 6

Soilworks, LLC. (2011, June 2). Application Rates. Retrieved June 2, 2011, from Soiltac: http://www.soiltac.com/application-rates.aspx

Thorstensen Laboratory, Inc. (n.d.). Parameter Descriptions for Drinking Water. Retrieved May 26, 2011, from Thorstensen Laboratory: http://www.watertestonline.com/glossary.htm

The Constructor.org (n.d.). Proctors Test for Compaction of Soil-Procedures, Tools and Results. Retrieved from https://theconstructor.org/geotechnical/compaction-test-soil-proctors-test/3152

U.S. Roads. (1998, June 1). Road Management & Engineering Journal. Retrieved from http://www.usroads.com/journals/rmej/9806/rm980604.htm

U.S.Roads. (1998, June 1). Road management & Engineering Journal. Retrieved from http://www.usroads.com/journals/rmej/9806/rm980604.htm

University of Wisconsin. (1997, January). http://spdfiles.engr.wisc/pdf_web_files/bulletins. Retrieved from http://spdfiles.engr.wisc: http://spdfiles.engr.wisc/pdf_web_files/bulletins/Bltn_013_DustControl.pdf

Warrence, N. J., Bauder, J. W., & Peterson, K. E. (2004). Basics of Salinity and Sodicity Effects on Soil Physical Properties. Bozeman: Montana State University - Bozeman.

APPENDIX A

MEPDG GENERAL INPUT

Layer Information

Layer 1 Flexible : Default asphalt concrete

Asphalt		
Thickness (in)	5.4	
Unit weight (pcf)	150.0	
Poisson's ratio	Is Calculated?	False
	Ratio	0.35
	Parameter A	-
	Parameter B	-

Asphalt Dynamic Modulus (Input Level: 3)

Gradation	Percent Passing
3/4-inch sieve	100
3/8-inch sieve	77
No.4 sieve	60
No.200 sieve	6

Asphalt Binder

Parameter	Value
Grade	Superpave Performance Grade
Binder Type	76-16
A	10.015
VTS	-3.315

General Info

Name	Value
Reference temperature (°F)	70
Effective binder content (%)	5
Air voids (%)	5
Thermal conductivity (BTU/hr-ft-°F)	0.67
Heat capacity (BTU/lb-°F)	0.23

Identifiers

Field	Value
Display name/identifier	Default asphalt concrete
Description of object	
Author	
Date Created	10/29/2010 10:00:00 PM
Approver	
Date approved	10/29/2010 10:00:00 PM
State	
District	
County	
Highway	
Direction of Travel	
From station (miles)	
To station (miles)	
Province	
User defined field 2	
User defined field 3	
Revision Number	0

Layer 2 Non-stabilized Base : A-1-b

Unbound	
Layer thickness (in)	14.8
Poisson's ratio	0.35
Coefficient of lateral earth pressure (k0)	0.5

Modulus (Input Level: 3)

Analysis Type:	Modify input values by temperature/moisture
Method:	Resilient Modulus (psi)

Resilient Modulus (psi)
38000.0

Use Correction factor for NDT modulus?	-
NDT Correction Factor:	-

Identifiers

Field	Value
Display name/identifier	A-1-b
Description of object	Default material
Author	AASHTO
Date Created	1/1/2011 12:00:00 AM
Approver	
Date approved	1/1/2011 12:00:00 AM
State	
District	
County	
Highway	
Direction of Travel	
From station (miles)	
To station (miles)	
Province	
User defined field 2	
User defined field 3	
Revision Number	0

Sieve

Liquid Limit	11.0
Plasticity Index	1.0
Is layer compacted?	False

	Is User Defined?	Value
Maximum dry unit weight (pcf)	False	123.7
Saturated hydraulic conductivity (ft/hr)	False	2.303e-03
Specific gravity of solids	False	2.7
Optimum gravimetric water content (%)	False	9.1

User-defined Soil Water Characteristic Curve (SWCC)	
Is User Defined?	False
af	5.8206
bf	0.4621
cf	3.8497
hr	126.8000

Sieve Size	% Passing
0.001mm	
0.002mm	
0.020mm	
#200	13.4
#100	
#80	20.8
#60	
#50	
#40	37.6
#30	
#20	
#16	
#10	64.0
#8	
#4	74.2
3/8-in.	82.3
1/2-in.	85.8
3/4-in.	90.8
1-in.	93.6
1 1/2-in.	96.7
2-in.	98.4
2 1/2-in.	
3-in.	
3 1/2-in.	99.4

Structure 2

Layer Information

Layer 1 Flexible : Default asphalt concrete

Asphalt		
Thickness (in)	5.4	
Unit weight (pcf)	150.0	
Poisson's ratio	Is Calculated?	False
	Ratio	0.35
	Parameter A	-
	Parameter B	-

Asphalt Dynamic Modulus (Input Level: 3)

Gradation	Percent Passing
3/4-inch sieve	100
3/8-inch sieve	77
No.4 sieve	60
No.200 sieve	6

Asphalt Binder

Parameter	Value
Grade	Superpave Performance Grade
Binder Type	76-16
A	10.015
VTS	-3.315

General Info

Name	Value
Reference temperature (°F)	70
Effective binder content (%)	5
Air voids (%)	5
Thermal conductivity (BTU/hr-ft-°F)	0.67
Heat capacity (BTU/lb-°F)	0.23

Identifiers

Field	Value
Display name/identifier	Default asphalt concrete
Description of object	
Author	
Date Created	10/29/2010 10:00:00 PM
Approver	
Date approved	10/29/2010 10:00:00 PM
State	
District	
County	
Highway	
Direction of Travel	
From station (miles)	
To station (miles)	
Province	
User defined field 2	
User defined field 3	
Revision Number	0

Layer 2 Non-stabilized Base : A-1-b

Unbound	
Layer thickness (in)	14.8
Poisson's ratio	0.35
Coefficient of lateral earth pressure (k0)	0.5

Modulus (Input Level: 3)

Analysis Type:	Modify input values by temperature/moisture
Method:	Resilient Modulus (psi)

Resilient Modulus (psi)
38000.0

Use Correction factor for NDT modulus?	-
NDT Correction Factor:	-

Identifiers

Field	Value
Display name/identifier	A-1-b
Description of object	Default material
Author	AASHTO
Date Created	1/1/2011 12:00:00 AM
Approver	
Date approved	1/1/2011 12:00:00 AM
State	
District	
County	
Highway	
Direction of Travel	
From station (miles)	
To station (miles)	
Province	
User defined field 2	
User defined field 3	
Revision Number	0

Sieve

Liquid Limit	11.0
Plasticity Index	1.0
Is layer compacted?	False

	Is User Defined?	Value
Maximum dry unit weight (pcf)	False	123.7
Saturated hydraulic conductivity (ft/hr)	False	2.303e-03
Specific gravity of solids	False	2.7
Optimum gravimetric water content (%)	False	9.1

User-defined Soil Water Characteristic Curve (SWCC)	
Is User Defined?	False
af	5.8206
bf	0.4621
cf	3.8497
hr	126.8000

Sieve Size	% Passing
0.001mm	
0.002mm	
0.020mm	
#200	13.4
#100	
#80	20.8
#60	
#50	
#40	37.6
#30	
#20	
#16	
#10	64.0
#8	
#4	74.2
3/8-in.	82.3
1/2-in.	85.8
3/4-in.	90.8
1-in.	93.6
1 1/2-in.	96.7
2-in.	98.4
2 1/2-in.	
3-in.	
3 1/2-in.	99.4

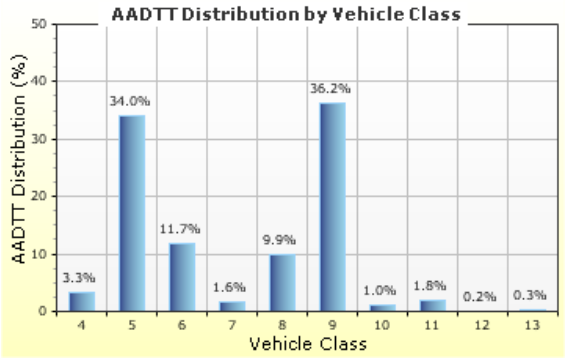
AADTT Distribution by Vehicle Class
AADTT Distribution (%)
3.3%
34.0%
11.7%
1.6%
9.9%
36.2%
1.0%
1.8%
0.2%
0.3%
Vehicle Class

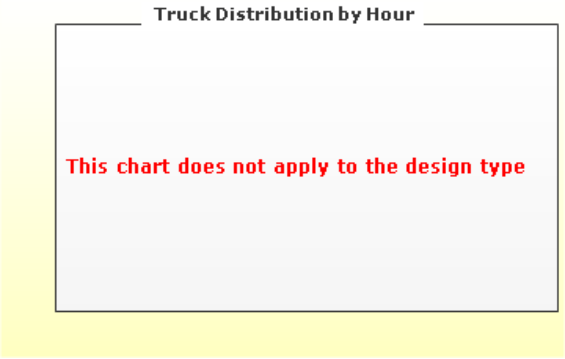
Truck Distribution by Hour
This chart does not apply to the design type

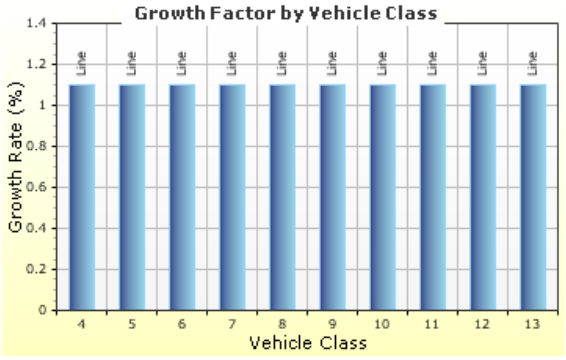
Growth Factor by Vehicle Class
Growth Rate (%)
Line
Vehicle Class

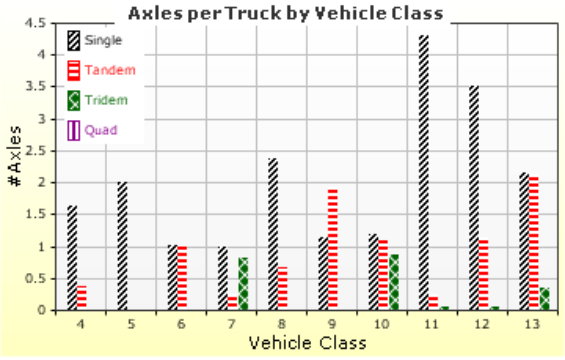
Axles per Truck by Vehicle Class
Single
Tandem
Tridem
Quad
#Axles
Vehicle Class

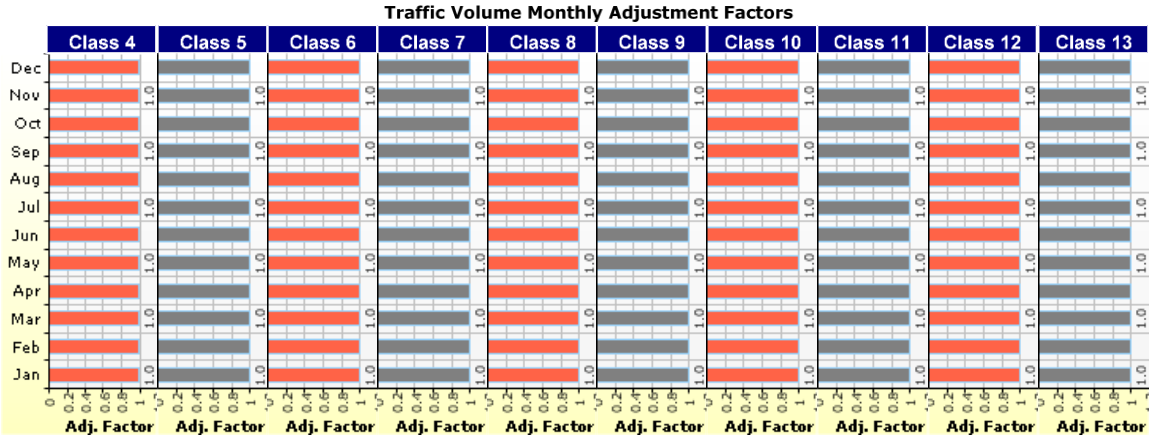
Traffic Volume Monthly Adjustment Factors
Class 4
Class 5
Class 6
Class 7
Class 8
Class 9
Class 10
Class 11
Class 12
Class 13
Dec
Nov
Oct
Sep
Aug
Jul
Jun
May
Apr
Mar
Feb
Jan
Adj. Factor

Tabular Representation of Traffic Inputs

Volume Monthly Adjustment Factors

Level 3: Default MAF

Month	Vehicle Class									
	4	5	6	7	8	9	10	11	12	13
January	1.0	1.0	1.0	1.0	1.0	1.0	1.0	1.0	1.0	1.0
February	1.0	1.0	1.0	1.0	1.0	1.0	1.0	1.0	1.0	1.0
March	1.0	1.0	1.0	1.0	1.0	1.0	1.0	1.0	1.0	1.0
April	1.0	1.0	1.0	1.0	1.0	1.0	1.0	1.0	1.0	1.0
May	1.0	1.0	1.0	1.0	1.0	1.0	1.0	1.0	1.0	1.0
June	1.0	1.0	1.0	1.0	1.0	1.0	1.0	1.0	1.0	1.0
July	1.0	1.0	1.0	1.0	1.0	1.0	1.0	1.0	1.0	1.0
August	1.0	1.0	1.0	1.0	1.0	1.0	1.0	1.0	1.0	1.0
September	1.0	1.0	1.0	1.0	1.0	1.0	1.0	1.0	1.0	1.0
October	1.0	1.0	1.0	1.0	1.0	1.0	1.0	1.0	1.0	1.0
November	1.0	1.0	1.0	1.0	1.0	1.0	1.0	1.0	1.0	1.0
December	1.0	1.0	1.0	1.0	1.0	1.0	1.0	1.0	1.0	1.0

Distributions by Vehicle Class

Vehicle Class	AADTT Distribution (%) (Level 3)	Growth Factor	
		Rate (%)	Function
Class 4	3.3%	1.1%	Linear
Class 5	34%	1.1%	Linear
Class 6	11.7%	1.1%	Linear
Class 7	1.6%	1.1%	Linear
Class 8	9.9%	1.1%	Linear
Class 9	36.2%	1.1%	Linear
Class 10	1%	1.1%	Linear
Class 11	1.8%	1.1%	Linear
Class 12	0.2%	1.1%	Linear
Class 13	0.3%	1.1%	Linear

Truck Distribution by Hour does not apply

Axle Configuration

Traffic Wander	
Mean wheel location (in)	18.0
Traffic wander standard deviation (in)	10.0
Design lane width (ft)	12.0

Axle Configuration	
Average axle width (ft)	8.5
Dual tire spacing (in)	12.0
Tire pressure (psi)	120.0

Average Axle Spacing	
Tandem axle spacing (in)	51.6
Tridem axle spacing (in)	49.2
Quad axle spacing (in)	49.2

Wheelbase does not apply

Number of Axles per Truck

Vehicle Class	Single Axle	Tandem Axle	Tridem Axle	Quad Axle
Class 4	1.62	0.39	0	0
Class 5	2	0	0	0
Class 6	1.02	0.99	0	0
Class 7	1	0.26	0.83	0
Class 8	2.38	0.67	0	0
Class 9	1.13	1.93	0	0
Class 10	1.19	1.09	0.89	0
Class 11	4.29	0.26	0.06	0
Class 12	3.52	1.14	0.06	0
Class 13	2.15	2.13	0.35	0

Traffic Inputs

Graphical Representation of Traffic Inputs

Initial two-way AADTT:

Number of lanes in design direction: 4,500 Percent of trucks in design direction (%): 50.0

AADTT (Average Annual Daily Truck Traffic) Growth

*** Traffic cap is not enforced**

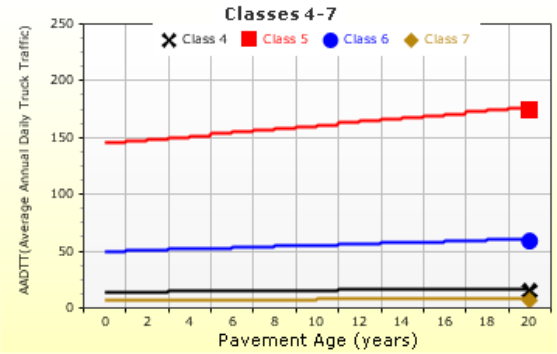

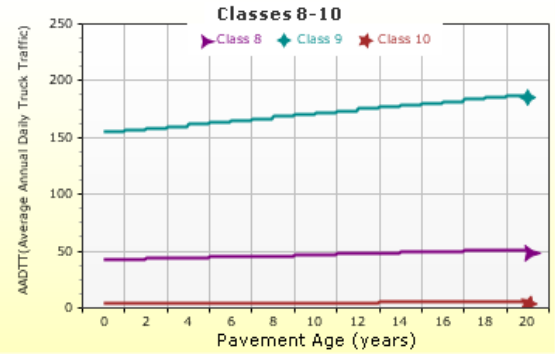

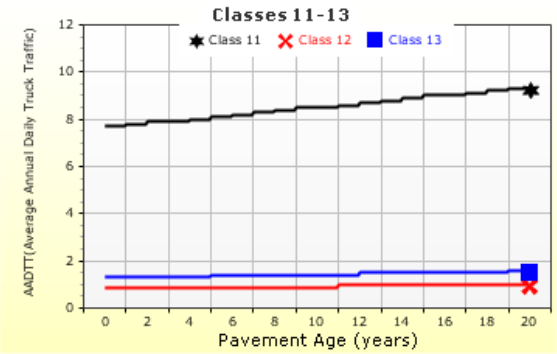

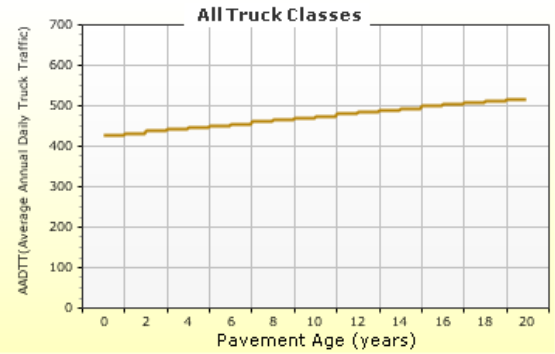

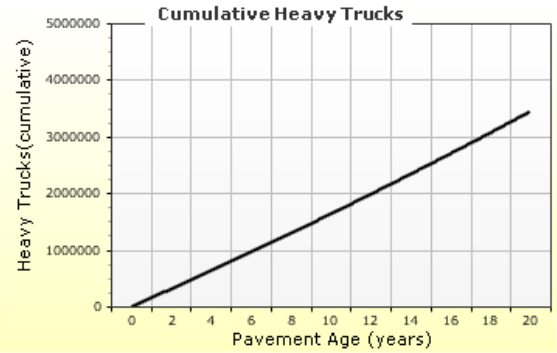

Traffic Inputs

Graphical Representation of Traffic Inputs

Initial two-way AADTT:

Number of lanes in design direction: 4,500 Percent of trucks in design direction (%): 50.0

AADTT (Average Annual Daily Truck Traffic) Growth

*** Traffic cap is not enforced**

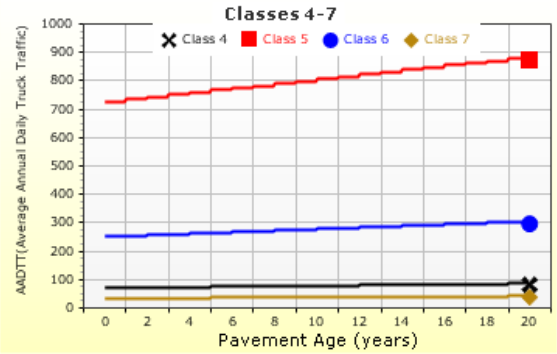

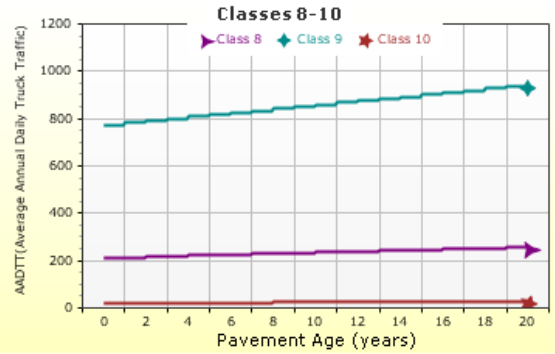

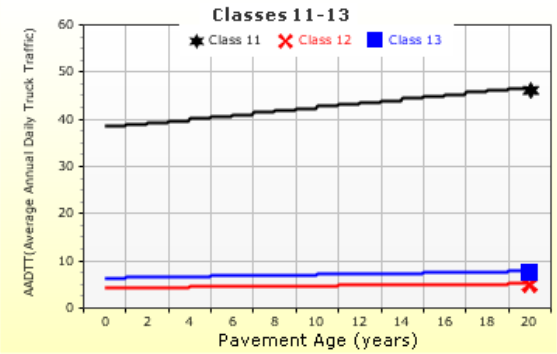

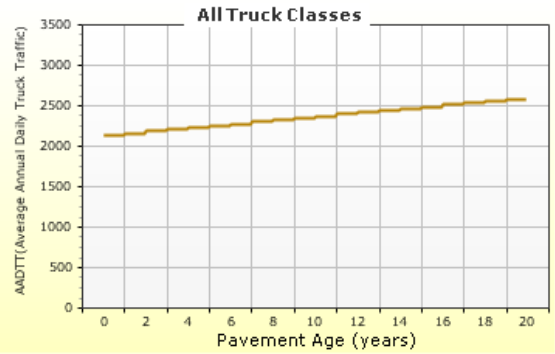

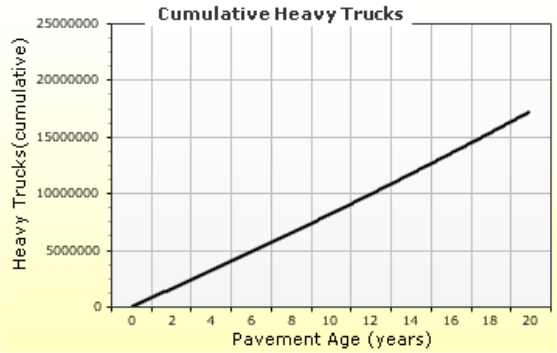

Traffic Inputs

Graphical Representation of Traffic Inputs

Initial two-way AADTT:

Number of lanes in design direction: 2,000 Percent of trucks in design direction (%): 50.0

AADTT (Average Annual Daily Truck Traffic) Growth

*** Traffic cap is not enforced**

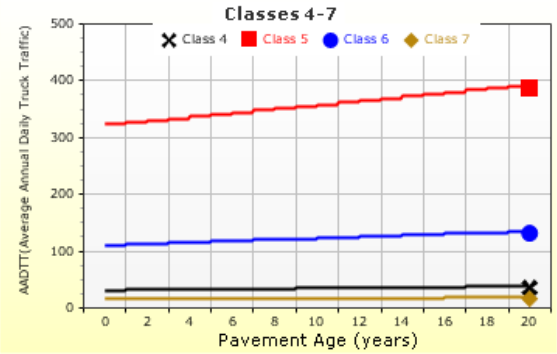

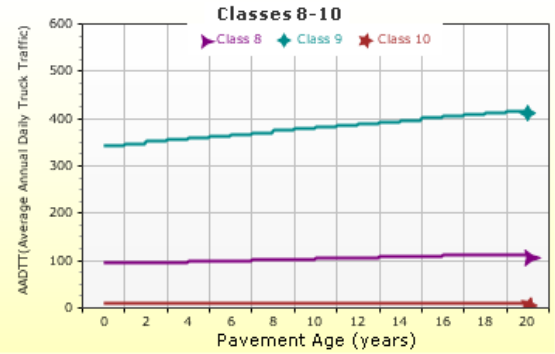

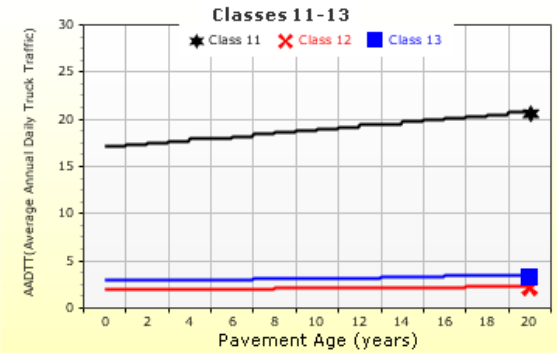

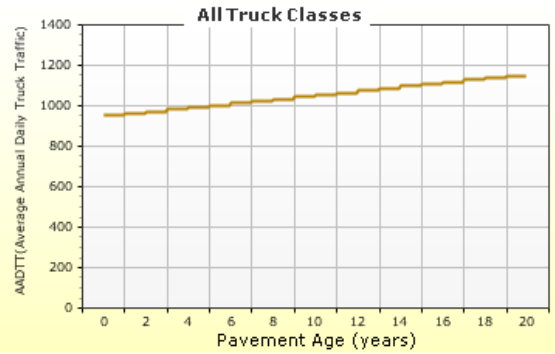

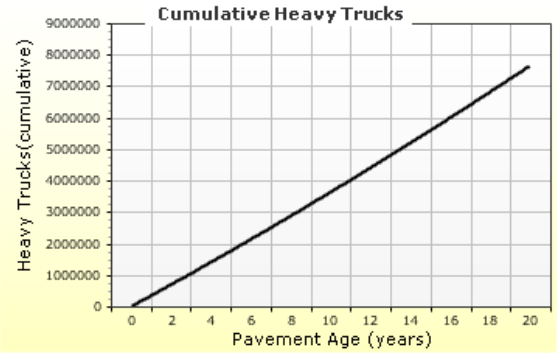

Traffic Inputs

Graphical Representation of Traffic Inputs

Initial two-way AADTT:

Number of lanes in design direction: 10,000 Percent of trucks in design direction (%): 50.0

AADTT (Average Annual Daily Truck Traffic) Growth

*** Traffic cap is not enforced**

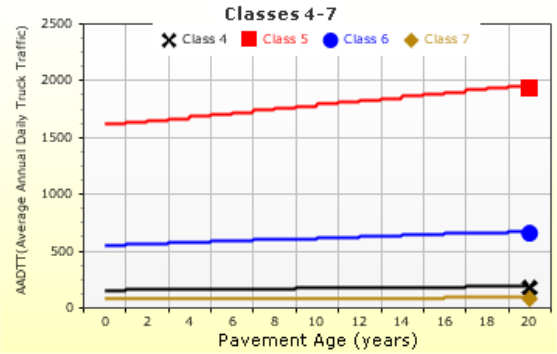

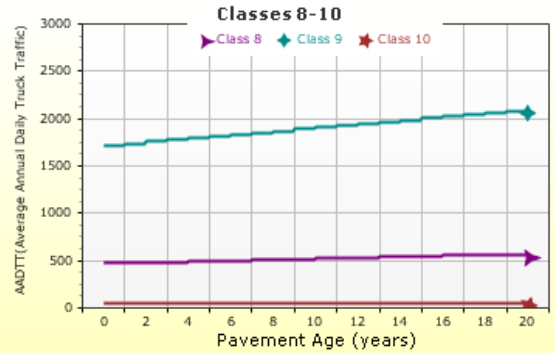

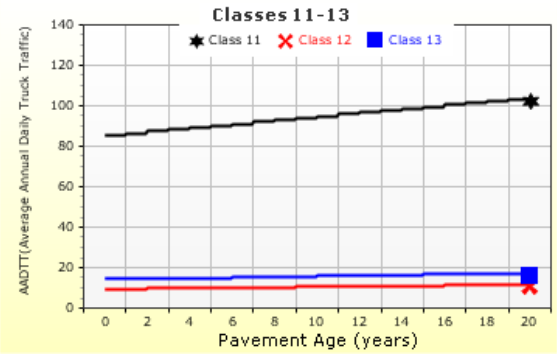

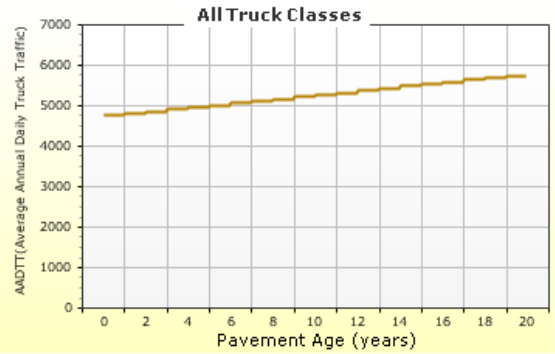

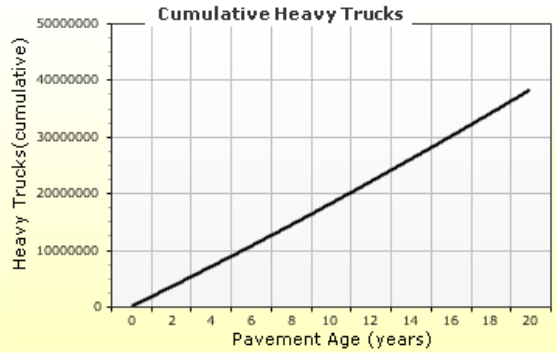

Climate Inputs

Climate Data Sources:

Climate Station Cities:	Location (lat lon elevation(ft))
PHOENIX, AZ	33.68800 -112.08200 1485

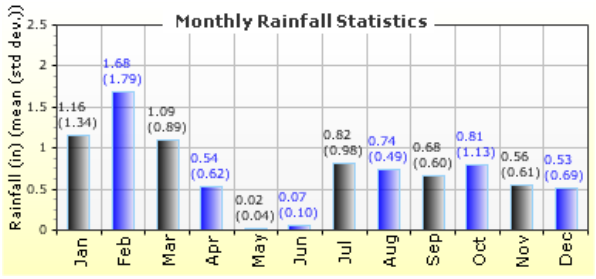

Annual Statistics:

Mean annual air temperature (ºF)	
Mean annual precipitation (in)	
Freezing index (ºF - days)	1.26
Average annual number of freeze/thaw cycles:	0.67

Water table depth (ft)	10.00

Monthly Climate Summary:

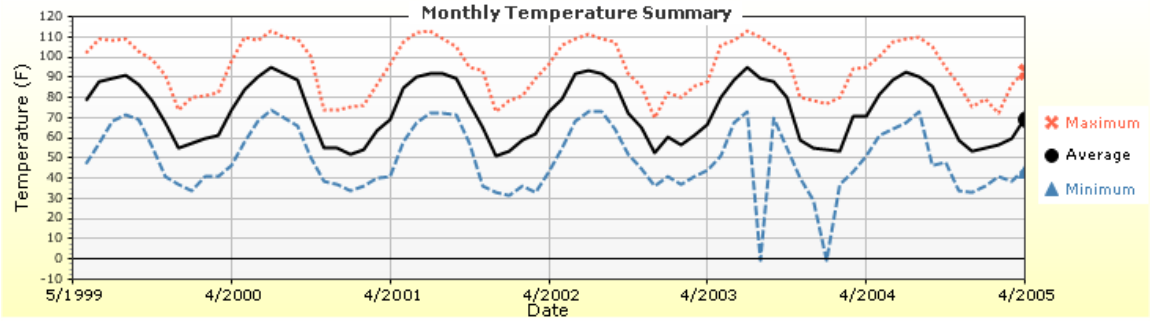

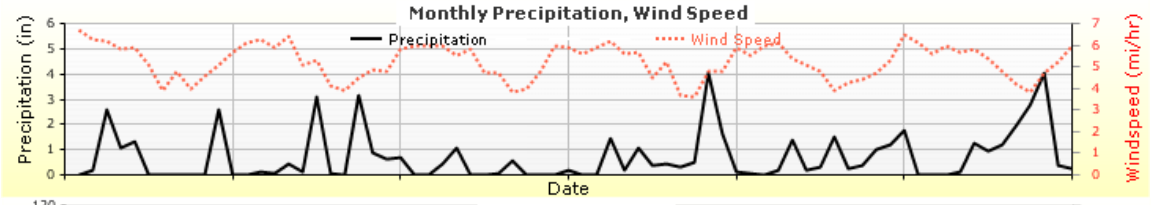

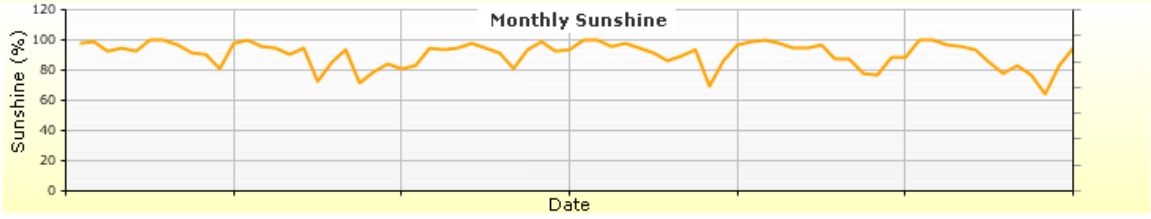

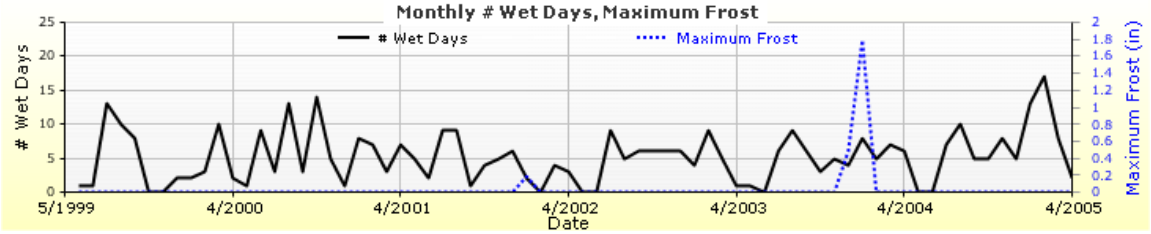

Calibration Coefficients

AC Fatigue

$$N_f = 0.00432 * C * \beta_{f1} k_1 \left(\frac{1}{\varepsilon_1}\right)^{k_2 \beta_{f2}} \left(\frac{1}{E}\right)^{k_3 \beta_{f3}}$$

$$C = 10^M$$

$$M = 4.84\left(\frac{V_b}{V_a + V_b} - 0.69\right)$$

k1: 0.007566	
k2: 3.9492	
k3: 1.281	
Bf1: 1	
Bf2: 1	
Bf3: 1	

AC Rutting

$$\frac{\varepsilon_p}{\varepsilon_r} = k_z \beta_{r1} 10^{k_1} T^{k_2 \beta_{r2}} N^{k_3 \beta_{r3}}$$

$$k_z = (C_1 + C_2 * depth) * 0.328196^{depth}$$

$$C_1 = -0.1039 * H_{ac}^2 + 2.4868 * H_{ac} - 17.342$$

$$C_2 = 0.0172 * H_{ac}^2 - 1.7331 * H_{ac} + 27.428$$

Where:

$H_{ac} = total\ AC\ thickness(in)$

$\varepsilon_p = plastic\ strain\left(^{in}/_{in}\right)$
$\varepsilon_r = resilient\ strain\left(^{in}/_{in}\right)$
$T = layer\ temperature\left(^{\circ}F\right)$
$N = number\ of\ load\ repetitions$

AC Rutting Standard Deviation	0.24 * Pow(RUT,0.8026) + 0.001	
AC Layer	K1:-3.35412 K2:1.5606 K3:0.4791	Br1:1 Br2:1 Br3:1

Thermal Fracture

$$C_f = 400 * N\left(\frac{\log C / h_{ac}}{\sigma}\right)$$

$$\Delta C = (k * \beta t)^{n+1} * A * \Delta K^n$$

$$A = 10^{(4.389 - 2.52 * \log(E * \sigma_m * n))}$$

$C_f = observed\ amount\ of\ thermal\ cracking(ft/500ft)$
$k = refression\ coefficient\ determined\ through\ field\ calibration$
$N() = standard\ normal\ distribution\ evaluated\ at()$
$\sigma = standard\ deviation\ of\ the \log\ of\ the\ depth\ of\ cracks\ in\ the\ pavments$
$C = crack\ depth(in)$
$h_{ac} = thickness\ of\ asphalt\ layer(in)$
$\Delta C = Change\ in\ the\ crack\ depth\ due\ to\ a\ cooling\ cycle$
$\Delta K = Change\ in\ the\ stress\ intensity\ factor\ due\ to\ a\ cooling\ cycle$
$A, n = Fracture\ parameters\ for\ the\ asphalt\ mixture$
$E = mixture\ stiffness$
$\sigma_M = Undamaged\ mixture\ tensile\ strength$
$\beta_t = Calibration\ parameter$

Level 1 K: 1.5	Level 1 Standard Deviation: 0.1468 * THERMAL + 65.027
Level 2 K: 0.5	Level 2 Standard Deviation: 0.2841 * THERMAL + 55.462
Level 3 K: 1.5	Level 3 Standard Deviation: 0.3972 * THERMAL + 20.422

CSM Fatigue

$$N_f = 10^{\left(\frac{k_1 \beta_{c1} \left(\frac{\sigma_s}{M_r}\right)}{k_2 \beta_{c2}}\right)}$$

$N_f = number\ of\ repetitions\ to\ fatigue\ cracking$
$\sigma_s = Tensile\ stress(psi)$
$M_r = modulus\ of\ rupture(psi)$

k1: 1	k2: 1	Bc1: 0.75	Bc2:1.1

Subgrade Rutting

$$\delta_a(N) = \beta_{s_1} k_1 \varepsilon_v h \left(\frac{\varepsilon_0}{\varepsilon_r}\right) \left| e^{-\left(\frac{\rho}{N}\right)^{\beta}} \right|$$

$\delta_a = permanent\ deformation\ for\ the\ layer$
$N = number\ of\ repetitions$
$\varepsilon_v = average\ veritcal\ strain(in/in)$
$\varepsilon_0, \beta, \rho = material\ properties$
$\varepsilon_r = resilient\ strain(in/in)$

Granular		Fine	
k1: 2.03	Bs1: 1	k1: 1.35	Bs1: 1
Standard Deviation (BASERUT) 0.1477 * Pow(BASERUT,0.6711) + 0.001		Standard Deviation (BASERUT) 0.1235 * Pow(SUBRUT,0.5012) + 0.001	

AC Cracking

AC Top Down Cracking

$$FC_{top} = \left(\frac{C_4}{1 + e^{(C_1 - C_2 * log_{10}(Damage))}}\right) * 10.56$$

c1: 7	c2: 3.5	c3: 0	c4: 1000

AC Cracking Top Standard Deviation

200 + 2300/(1+exp(1.072-2.1654*LOG10 (TOP+0.0001)))

AC Bottom Up Cracking

$$FC = \left(\frac{6000}{1 + e^{\left(C_1 * C_1' + C_2 * C_2' log_{10}(D * 100)\right)}}\right) * \left(\frac{1}{60}\right)$$

$$C_2' = -2.40874 - 39.748 * (1 + h_{ac})^{-2.856}$$

$$C_1' = -2 * C_2'$$

c1: 1	c2: 1	c3: 6000

AC Cracking Bottom Standard Deviation

1.13 + 13/(1+exp(7.57-15.5*LOG10 (BOTTOM+0.0001)))

CSM Cracking

$$FC_{ctb} = C_1 + \frac{C_2}{1 + e^{C_3 - C_4(Damage)}}$$

C1: 0	C2: 75	C3: 5	C4: 3

CSM Standard Deviation

CTB*1

IRI Flexible Pavements

C1 - Rutting
C2 - Fatigue Crack
C3 - Transverse Crack
C4 - Site Factors

C1: 40	C2: 0.4	C3: 0.008	C4: 0.015

APPENDIX B

MEPDG OUTPUT – EAGER SOIL – STRUCTURE 1

Case 1

Design Inputs

Design Life: 20 years
Design Type: Flexible Pavement
Base construction: May, 2018
Pavement construction: June, 2019
Traffic opening: September, 2019
Climate Data Sources (Lat/Lon): 33.688, -112.082

Design Structure

Layer type	Material Type	Thickness (in)
Flexible	Default asphalt concrete	5.4
NonStabilized	A-1-b	14.8
Subgrade	A-6	Semi-infinite

Volumetric at Construction:	
Effective binder content (%)	5.0
Air voids (%)	5.0

Traffic

Age (year)	Heavy Trucks (cumulative)
2019 (initial)	900
2029 (10 years)	1,638,740
2039 (20 years)	3,449,230

Design Outputs

Distress Prediction Summary

Distress Type	Distress @ Specified Reliability		Reliability (%)		Criterion Satisfied?
	Target	Predicted	Target	Achieved	
Terminal IRI (in/mile)	172.00	147.30	90.00	98.17	Pass
Permanent deformation - total pavement (in)	0.75	0.61	90.00	99.73	Pass
AC bottom-up fatigue cracking (% lane area)	25.00	22.69	90.00	92.59	Pass
AC thermal cracking (ft/mile)	1000.00	27.17	90.00	100.00	Pass
AC top-down fatigue cracking (ft/mile)	2000.00	4224.11	90.00	61.40	Fail
Permanent deformation - AC only (in)	0.25	0.33	90.00	58.90	Fail

Distress Charts

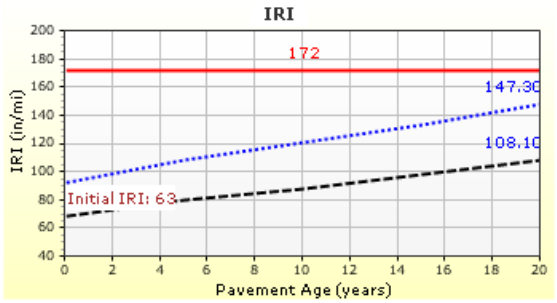

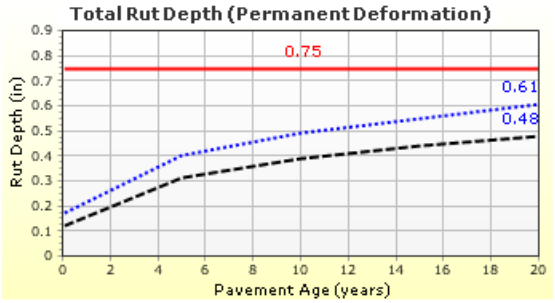

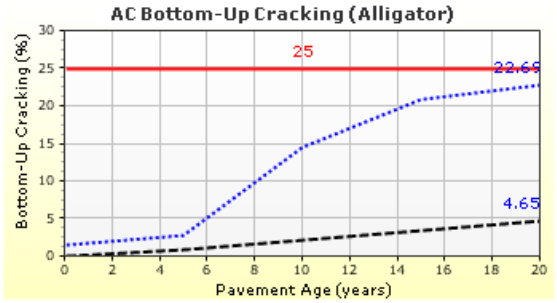

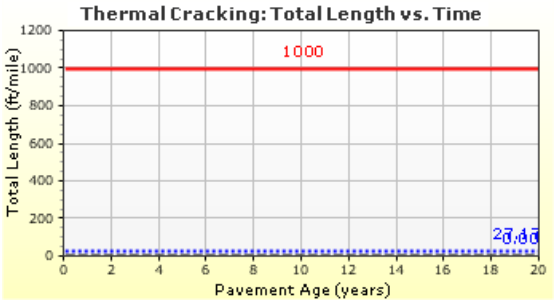

Threshold Value ····· @ Specified Reliability - - - @ 50% Reliability

Case 2

Design Inputs

Design Life: 20 years
Design Type: Flexible Pavement
Base construction: May, 2018
Pavement construction: June, 2019
Traffic opening: September, 2019
Climate Data Sources (Lat/Lon): 33.688, -112.082

Design Structure

Layer type	Material Type	Thickness (in)
Flexible	Default asphalt concrete	5.4
NonStabilized	A-1-b	14.8
Subgrade	A-6	Semi-infinite

Volumetric at Construction:	
Effective binder content (%)	5.0
Air voids (%)	5.0

Traffic

Age (year)	Heavy Trucks (cumulative)
2019 (initial)	900
2029 (10 years)	1,638,740
2039 (20 years)	3,449,230

Design Outputs

Distress Prediction Summary

Distress Type	Distress @ Specified Reliability		Reliability (%)		Criterion Satisfied?
	Target	Predicted	Target	Achieved	
Terminal IRI (in/mile)	172.00	143.86	90.00	98.68	Pass
Permanent deformation - total pavement (in)	0.75	0.53	90.00	99.99	Pass
AC bottom-up fatigue cracking (% lane area)	25.00	21.75	90.00	93.51	Pass
AC thermal cracking (ft/mile)	1000.00	27.17	90.00	100.00	Pass
AC top-down fatigue cracking (ft/mile)	2000.00	6110.31	90.00	32.19	Fail
Permanent deformation - AC only (in)	0.25	0.33	90.00	59.94	Fail

Distress Charts

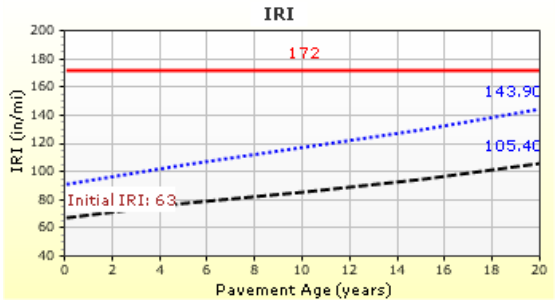

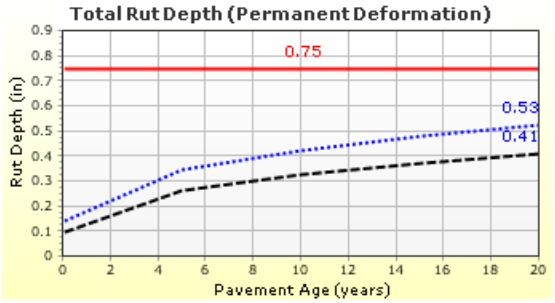

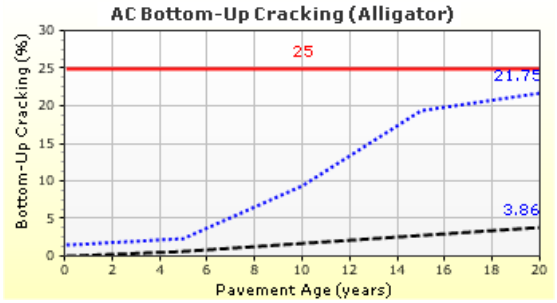

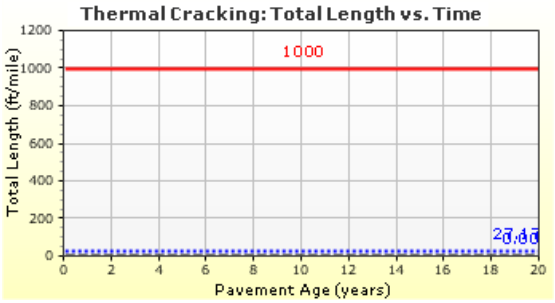

Design Inputs

Design Life: 20 years
Design Type: Flexible Pavement
Base construction: May, 2018
Pavement construction: June, 2019
Traffic opening: September, 2019
Climate Data Sources (Lat/Lon): 33.688, -112.082

Design Structure

Layer type	Material Type	Thickness (in)
Flexible	Default asphalt concrete	5.4
NonStabilized	A-1-b	14.8
Subgrade	A-6	Semi-infinite

Volumetric at Construction:	
Effective binder content (%)	5.0
Air voids (%)	5.0

Traffic

Age (year)	Heavy Trucks (cumulative)
2019 (initial)	900
2029 (10 years)	1,638,740
2039 (20 years)	3,449,230

Design Outputs

Distress Prediction Summary

Distress Type	Distress @ Specified Reliability		Reliability (%)		Criterion Satisfied?
	Target	Predicted	Target	Achieved	
Terminal IRI (in/mile)	172.00	162.64	90.00	94.12	Pass
Permanent deformation - total pavement (in)	0.75	0.95	90.00	33.10	Fail
AC bottom-up fatigue cracking (% lane area)	25.00	24.18	90.00	90.99	Pass
AC thermal cracking (ft/mile)	1000.00	27.17	90.00	100.00	Pass
AC top-down fatigue cracking (ft/mile)	2000.00	1296.22	90.00	97.66	Pass
Permanent deformation - AC only (in)	0.25	0.33	90.00	59.61	Fail

Distress Charts

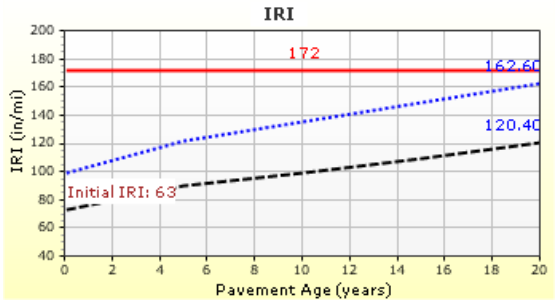

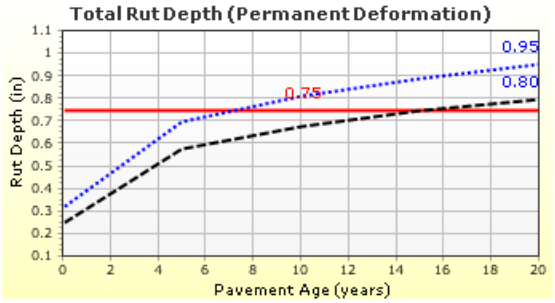

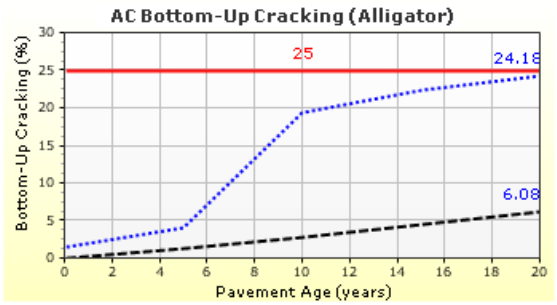

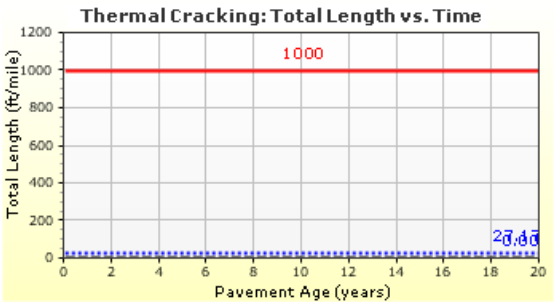

Case 4

Design Inputs

Design Life: 20 years
Design Type: Flexible Pavement
Base construction: May, 2018
Pavement construction: June, 2019
Traffic opening: September, 2019
Climate Data Sources (Lat/Lon): 33.688, -112.082

Design Structure

Layer type	Material Type	Thickness (in)
Flexible	Default asphalt concrete	5.4
NonStabilized	A-1-b	14.8
Subgrade	A-6	Semi-infinite

Volumetric at Construction:	
Effective binder content (%)	5.0
Air voids (%)	5.0

Traffic

Age (year)	Heavy Trucks (cumulative)
2019 (initial)	900
2029 (10 years)	1,638,740
2039 (20 years)	3,449,230

Design Outputs

Distress Prediction Summary

Distress Type	Distress @ Specified Reliability		Reliability (%)		Criterion Satisfied?
	Target	Predicted	Target	Achieved	
Terminal IRI (in/mile)	172.00	177.32	90.00	87.08	Fail
Permanent deformation - total pavement (in)	0.75	1.27	90.00	0.58	Fail
AC bottom-up fatigue cracking (% lane area)	25.00	25.12	90.00	89.85	Fail
AC thermal cracking (ft/mile)	1000.00	27.17	90.00	100.00	Pass
AC top-down fatigue cracking (ft/mile)	2000.00	291.02	90.00	100.00	Pass
Permanent deformation - AC only (in)	0.25	0.32	90.00	61.43	Fail

Distress Charts

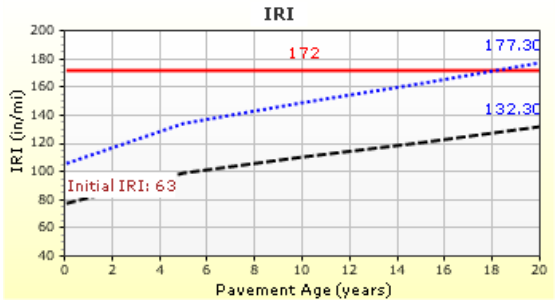

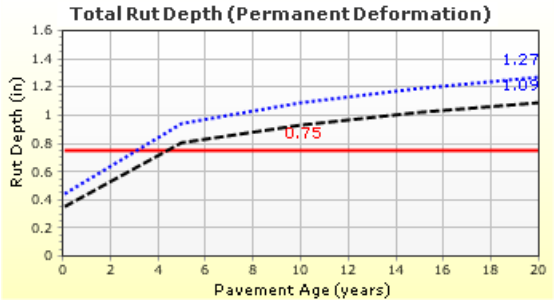

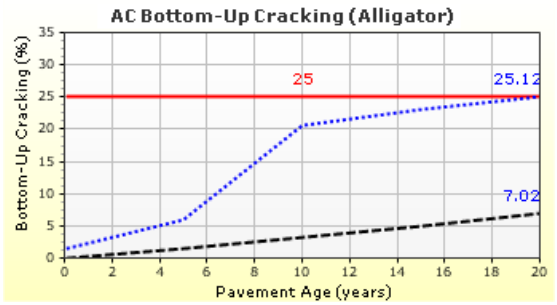

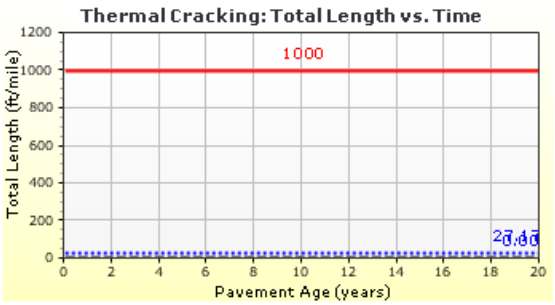

Design Inputs

Design Life: 20 years
Design Type: Flexible Pavement
Base construction: May, 2018
Pavement construction: June, 2019
Traffic opening: September, 2019
Climate Data Sources (Lat/Lon): 33.688, -112.082

Design Structure

Layer type	Material Type	Thickness (in)
Flexible	Default asphalt concrete	5.4
NonStabilized	A-1-b	14.8
Subgrade	A-6	Semi-infinite

Volumetric at Construction:	
Effective binder content (%)	5.0
Air voids (%)	5.0

Traffic

Age (year)	Heavy Trucks (cumulative)
2019 (initial)	900
2029 (10 years)	1,638,740
2039 (20 years)	3,449,230

Design Outputs

Distress Prediction Summary

Distress Type	Distress @ Specified Reliability		Reliability (%)		Criterion Satisfied?
	Target	Predicted	Target	Achieved	
Terminal IRI (in/mile)	172.00	188.35	90.00	79.83	Fail
Permanent deformation - total pavement (in)	0.75	1.50	90.00	0.01	Fail
AC bottom-up fatigue cracking (% lane area)	25.00	25.87	90.00	88.88	Fail
AC thermal cracking (ft/mile)	1000.00	27.17	90.00	100.00	Pass
AC top-down fatigue cracking (ft/mile)	2000.00	260.65	90.00	100.00	Pass
Permanent deformation - AC only (in)	0.25	0.32	90.00	62.98	Fail

Distress Charts

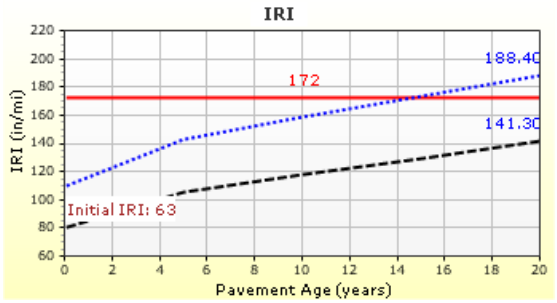

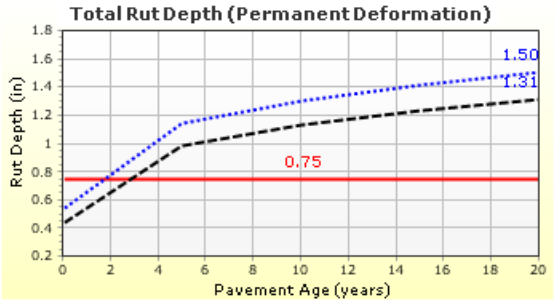

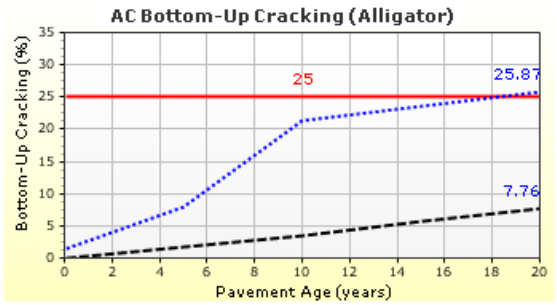

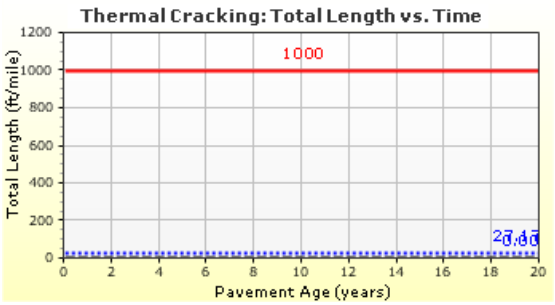

Case 6

Design Inputs

Design Life: 20 years | Base construction: May, 2018 | Climate Data Sources (Lat/Lon): 33.688, -112.082

Design Type: Flexible Pavement | Pavement construction: June, 2019

Traffic opening: September, 2019

Design Structure

Layer type	Material Type	Thickness (in)
Flexible	Default asphalt concrete	5.4
NonStabilized	A-1-b	14.8
Subgrade	A-6	Semi-infinite

Volumetric at Construction:	
Effective binder content (%)	5.0
Air voids (%)	5.0

Traffic

Age (year)	Heavy Trucks (cumulative)
2019 (initial)	900
2029 (10 years)	1,638,740
2039 (20 years)	3,449,230

Design Outputs

Distress Prediction Summary

Distress Type	Distress @ Specified Reliability		Reliability (%)		Criterion Satisfied?
	Target	Predicted	Target	Achieved	
Terminal IRI (in/mile)	172.00	147.56	90.00	98.12	Pass
Permanent deformation - total pavement (in)	0.75	0.61	90.00	99.65	Pass
AC bottom-up fatigue cracking (% lane area)	25.00	22.75	90.00	92.52	Pass
AC thermal cracking (ft/mile)	1000.00	27.17	90.00	100.00	Pass
AC top-down fatigue cracking (ft/mile)	2000.00	4084.48	90.00	63.52	Fail
Permanent deformation - AC only (in)	0.25	0.33	90.00	58.90	Fail

Distress Charts

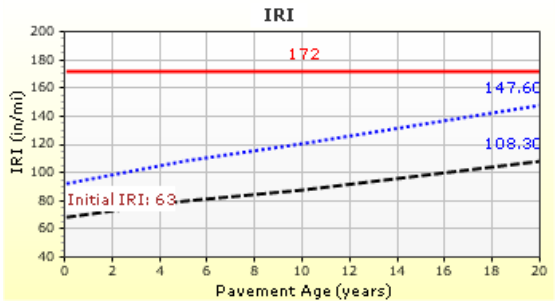

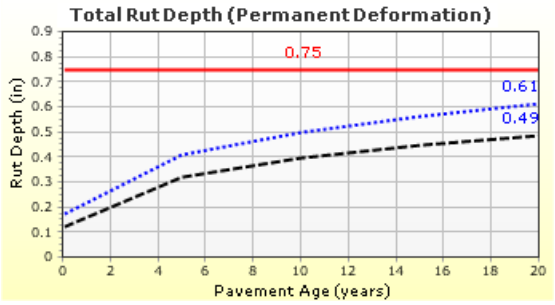

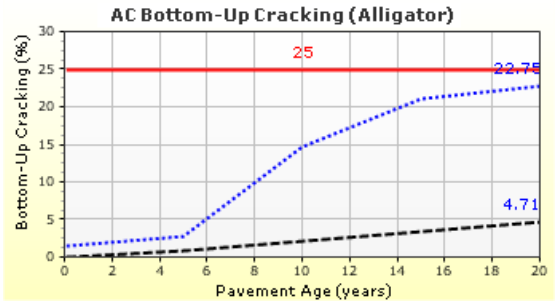

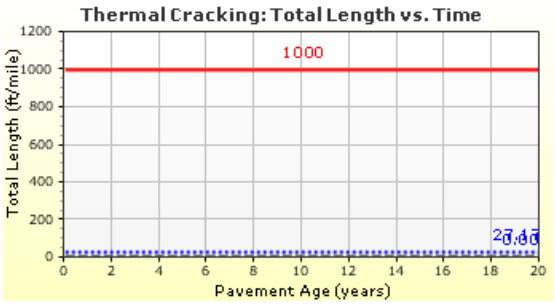

Case 8

Design Inputs

Design Life: 20 years
Design Type: Flexible Pavement
Base construction: May, 2018
Pavement construction: June, 2019
Traffic opening: September, 2019
Climate Data Sources (Lat/Lon): 33.688, -112.082

Design Structure

Layer type	Material Type	Thickness (in)
Flexible	Default asphalt concrete	5.4
NonStabilized	A-1-b	14.8
Subgrade	A-6	Semi-infinite

Volumetric at Construction:	
Effective binder content (%)	5.0
Air voids (%)	5.0

Traffic

Age (year)	Heavy Trucks (cumulative)
2019 (initial)	900
2029 (10 years)	1,638,740
2039 (20 years)	3,449,230

Design Outputs

Distress Prediction Summary

Distress Type	Distress @ Specified Reliability		Reliability (%)		Criterion Satisfied?
	Target	Predicted	Target	Achieved	
Terminal IRI (in/mile)	172.00	147.19	90.00	98.19	Pass
Permanent deformation - total pavement (in)	0.75	0.60	90.00	99.79	Pass
AC bottom-up fatigue cracking (% lane area)	25.00	22.31	90.00	92.97	Pass
AC thermal cracking (ft/mile)	1000.00	27.17	90.00	100.00	Pass
AC top-down fatigue cracking (ft/mile)	2000.00	5090.69	90.00	47.76	Fail
Permanent deformation - AC only (in)	0.25	0.33	90.00	59.12	Fail

Distress Charts

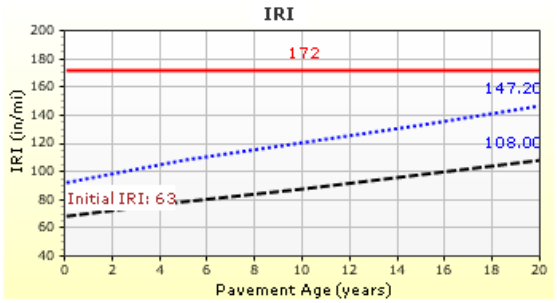

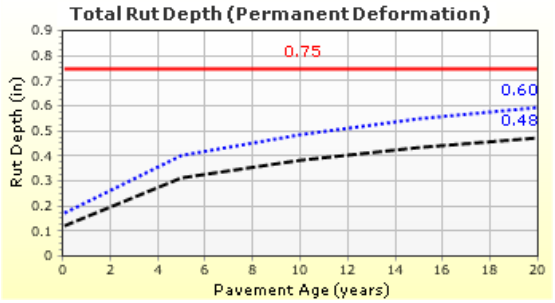

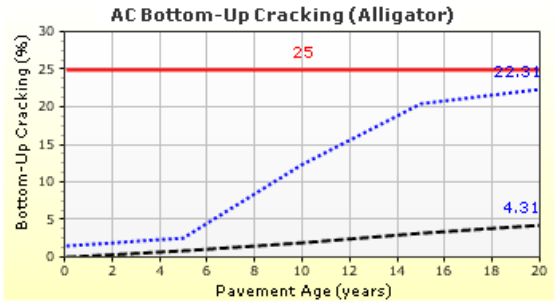

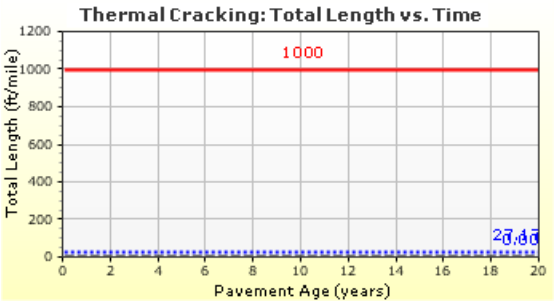

Case 9

Design Inputs

Design Life: 20 years
Design Type: Flexible Pavement
Base construction: May, 2018
Pavement construction: June, 2019
Traffic opening: September, 2019
Climate Data Sources (Lat/Lon): 33.688, -112.082

Design Structure

Layer type	Material Type	Thickness (in)
Flexible	Default asphalt concrete	5.4
NonStabilized	A-1-b	14.8
Subgrade	A-6	Semi-infinite

Volumetric at Construction:	
Effective binder content (%)	5.0
Air voids (%)	5.0

Traffic

Age (year)	Heavy Trucks (cumulative)
2019 (initial)	900
2029 (10 years)	1,638,740
2039 (20 years)	3,449,230

Design Outputs

Distress Prediction Summary

Distress Type	Distress @ Specified Reliability		Reliability (%)		Criterion Satisfied?
	Target	Predicted	Target	Achieved	
Terminal IRI (in/mile)	172.00	149.80	90.00	97.72	Pass
Permanent deformation - total pavement (in)	0.75	0.67	90.00	98.01	Pass
AC bottom-up fatigue cracking (% lane area)	25.00	22.79	90.00	92.49	Pass
AC thermal cracking (ft/mile)	1000.00	27.17	90.00	100.00	Pass
AC top-down fatigue cracking (ft/mile)	2000.00	3965.96	90.00	65.29	Fail
Permanent deformation - AC only (in)	0.25	0.33	90.00	58.74	Fail

Distress Charts

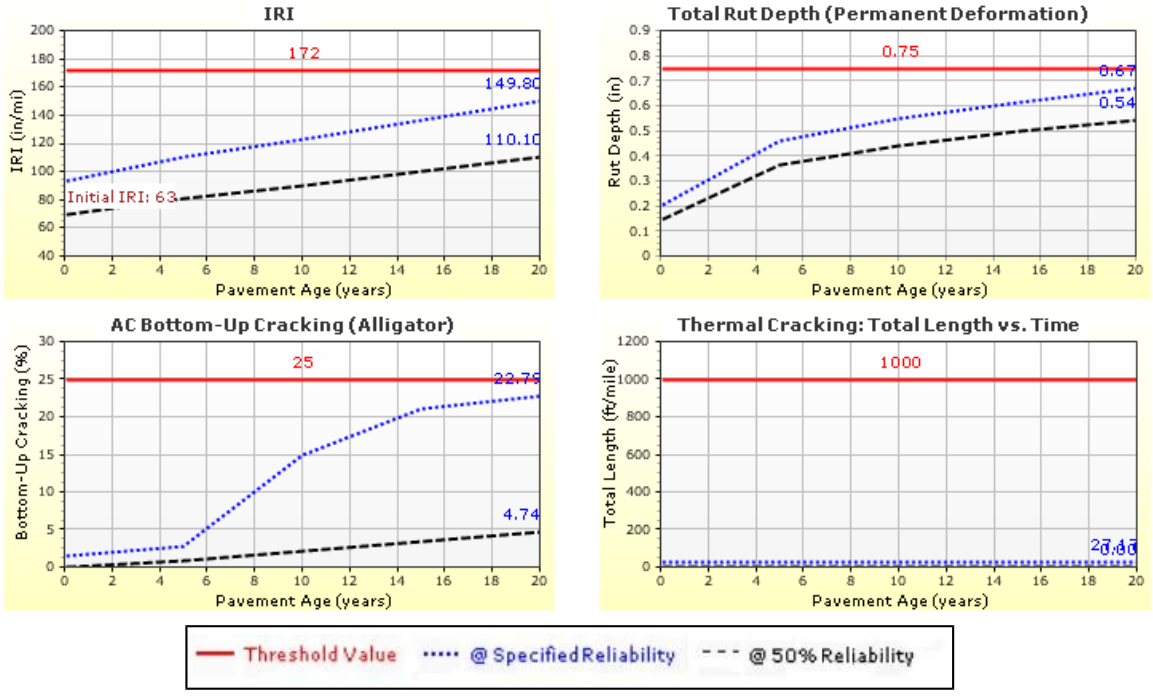

Design Inputs

Design Life: 20 years
Design Type: Flexible Pavement
Base construction: May, 2018
Pavement construction: June, 2019
Traffic opening: September, 2019
Climate Data Sources (Lat/Lon): 33.688, -112.082

Design Structure

Layer type	Material Type	Thickness (in)
Flexible	Default asphalt concrete	5.4
NonStabilized	A-1-b	14.8
Subgrade	A-6	Semi-infinite

Volumetric at Construction:	
Effective binder content (%)	5.0
Air voids (%)	5.0

Traffic

Age (year)	Heavy Trucks (cumulative)
2019 (initial)	900
2029 (10 years)	1,638,740
2039 (20 years)	3,449,230

Design Outputs

Distress Prediction Summary

Distress Type	Distress @ Specified Reliability		Reliability (%)		Criterion Satisfied?
	Target	Predicted	Target	Achieved	
Terminal IRI (in/mile)	172.00	148.33	90.00	97.99	Pass
Permanent deformation - total pavement (in)	0.75	0.63	90.00	99.31	Pass
AC bottom-up fatigue cracking (% lane area)	25.00	22.60	90.00	92.68	Pass
AC thermal cracking (ft/mile)	1000.00	27.17	90.00	100.00	Pass
AC top-down fatigue cracking (ft/mile)	2000.00	4440.86	90.00	58.05	Fail
Permanent deformation - AC only (in)	0.25	0.33	90.00	58.68	Fail

Distress Charts

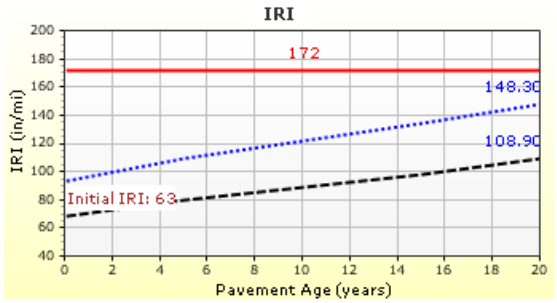

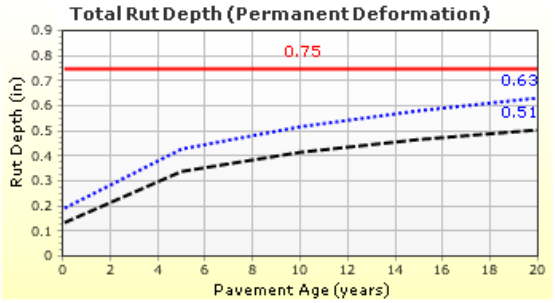

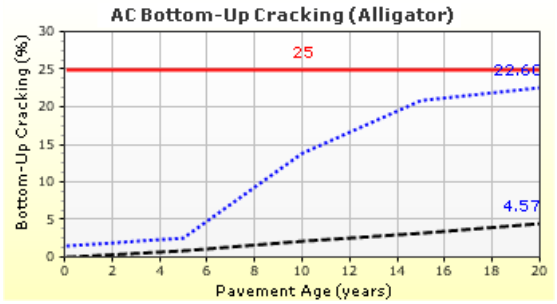

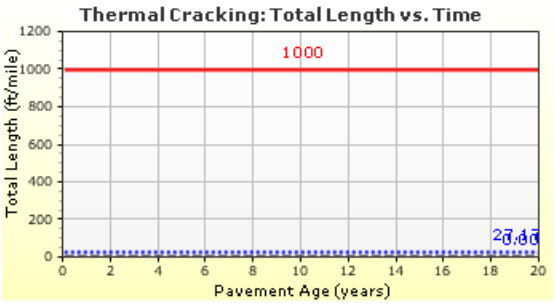

Design Inputs

Design Life: 20 years
Design Type: Flexible Pavement
Base construction: May, 2018
Pavement construction: June, 2019
Traffic opening: September, 2019
Climate Data Sources (Lat/Lon): 33.688, -112.082

Design Structure

Layer type	Material Type	Thickness (in)
Flexible	Default asphalt concrete	5.4
NonStabilized	A-1-b	14.8
Subgrade	A-6	Semi-infinite

Volumetric at Construction:	
Effective binder content (%)	5.0
Air voids (%)	5.0

Traffic

Age (year)	Heavy Trucks (cumulative)
2019 (initial)	4,500
2029 (10 years)	8,193,680
2039 (20 years)	17,246,100

Design Outputs

Distress Prediction Summary

Distress Type	Distress @ Specified Reliability		Reliability (%)		Criterion Satisfied?
	Target	Predicted	Target	Achieved	
Terminal IRI (in/mile)	172.00	177.94	90.00	86.74	Fail
Permanent deformation - total pavement (in)	0.75	1.02	90.00	32.80	Fail
AC bottom-up fatigue cracking (% lane area)	25.00	41.31	90.00	55.07	Fail
AC thermal cracking (ft/mile)	1000.00	27.17	90.00	100.00	Pass
AC top-down fatigue cracking (ft/mile)	2000.00	9764.09	90.00	2.85	Fail
Permanent deformation - AC only (in)	0.25	0.68	90.00	3.45	Fail

Distress Charts

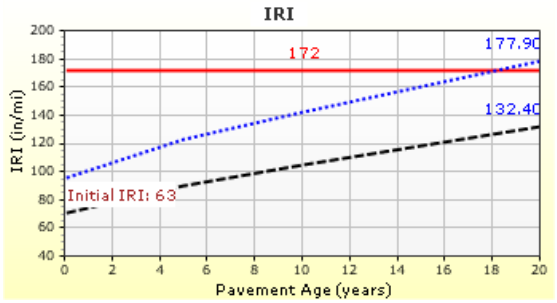

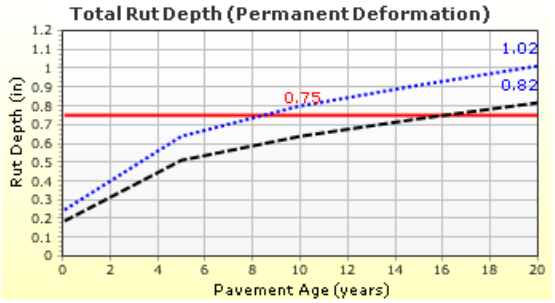

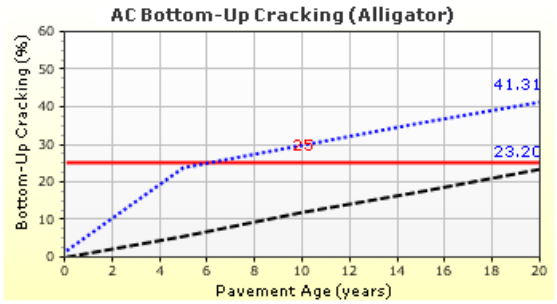

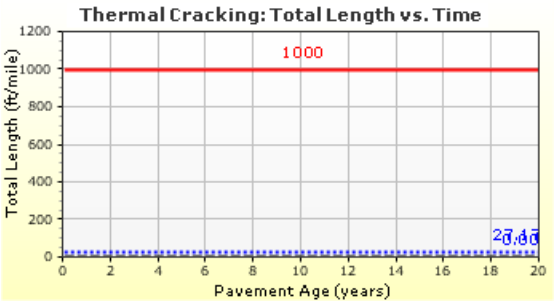

Design Inputs

Design Life: 20 years
Design Type: Flexible Pavement
Base construction: May, 2018
Pavement construction: June, 2019
Traffic opening: September, 2019
Climate Data Sources (Lat/Lon): 33.688, -112.082

Design Structure

Layer type	Material Type	Thickness (in)
Flexible	Default asphalt concrete	5.4
NonStabilized	A-1-b	14.8
Subgrade	A-6	Semi-infinite

Volumetric at Construction:	
Effective binder content (%)	5.0
Air voids (%)	5.0

Traffic

Age (year)	Heavy Trucks (cumulative)
2019 (initial)	4,500
2029 (10 years)	8,193,680
2039 (20 years)	17,246,100

Design Outputs

Distress Prediction Summary

Distress Type	Distress @ Specified Reliability		Reliability (%)		Criterion Satisfied?
	Target	Predicted	Target	Achieved	
Terminal IRI (in/mile)	172.00	172.58	90.00	89.70	Fail
Permanent deformation - total pavement (in)	0.75	0.92	90.00	56.74	Fail
AC bottom-up fatigue cracking (% lane area)	25.00	38.01	90.00	64.09	Fail
AC thermal cracking (ft/mile)	1000.00	27.17	90.00	100.00	Pass
AC top-down fatigue cracking (ft/mile)	2000.00	11891.48	90.00	0.32	Fail
Permanent deformation - AC only (in)	0.25	0.68	90.00	3.59	Fail

Distress Charts

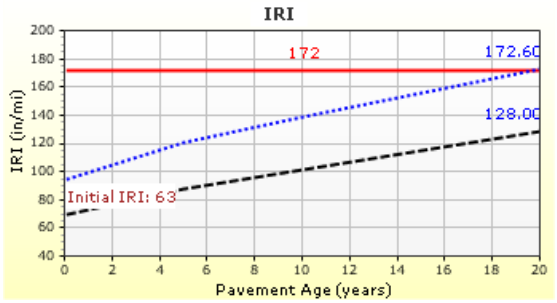

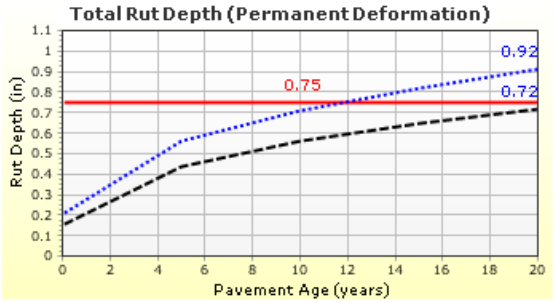

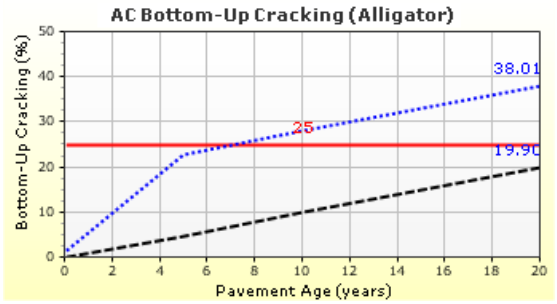

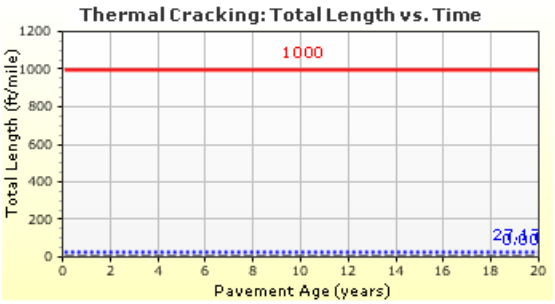

Design Inputs

Design Life: 20 years
Design Type: Flexible Pavement
Base construction: May, 2018
Pavement construction: June, 2019
Traffic opening: September, 2019
Climate Data Sources (Lat/Lon): 33.688, -112.082

Design Structure

Layer type	Material Type	Thickness (in)
Flexible	Default asphalt concrete	5.4
NonStabilized	A-1-b	14.8
Subgrade	A-6	Semi-infinite

Volumetric at Construction:	
Effective binder content (%)	5.0
Air voids (%)	5.0

Traffic

Age (year)	Heavy Trucks (cumulative)
2019 (initial)	4,500
2029 (10 years)	8,193,680
2039 (20 years)	17,246,100

Design Outputs

Distress Prediction Summary

Distress Type	Distress @ Specified Reliability		Reliability (%)		Criterion Satisfied?
	Target	Predicted	Target	Achieved	
Terminal IRI (in/mile)	172.00	194.15	90.00	75.62	Fail
Permanent deformation - total pavement (in)	0.75	1.43	90.00	0.38	Fail
AC bottom-up fatigue cracking (% lane area)	25.00	46.71	90.00	39.94	Fail
AC thermal cracking (ft/mile)	1000.00	27.17	90.00	100.00	Pass
AC top-down fatigue cracking (ft/mile)	2000.00	2560.01	90.00	83.52	Fail
Permanent deformation - AC only (in)	0.25	0.68	90.00	3.55	Fail

Distress Charts

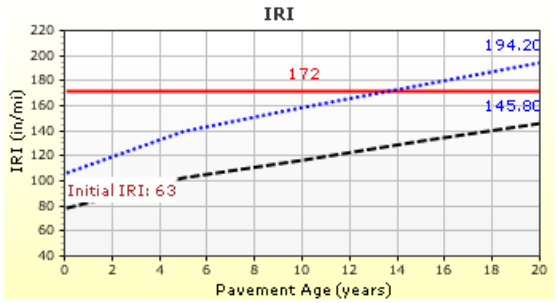

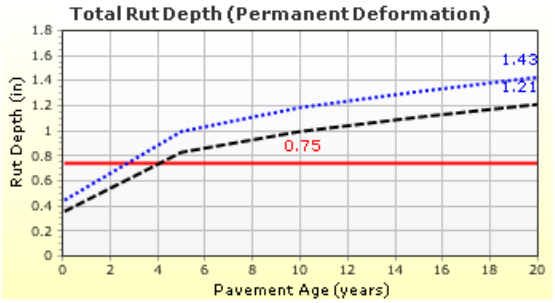

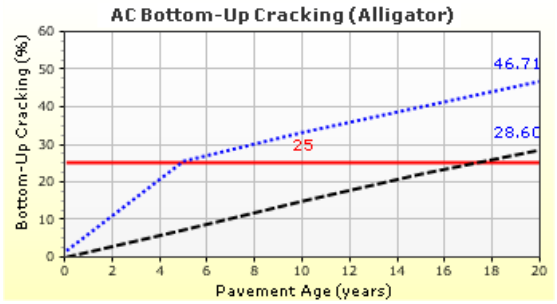

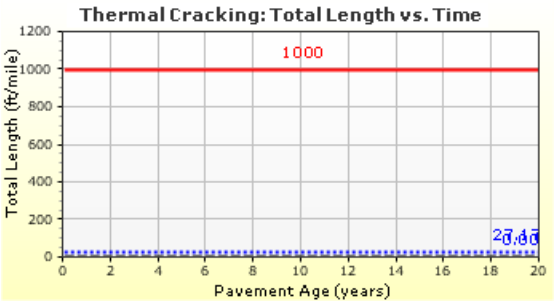

Design Inputs

Design Life: 20 years
Design Type: Flexible Pavement
Base construction: May, 2018
Pavement construction: June, 2019
Traffic opening: September, 2019
Climate Data Sources (Lat/Lon): 33.688, -112.082

Design Structure

Layer type	Material Type	Thickness (in)
Flexible	Default asphalt concrete	5.4
NonStabilized	A-1-b	14.8
Subgrade	A-6	Semi-infinite

Volumetric at Construction:	
Effective binder content (%)	5.0
Air voids (%)	5.0

Traffic

Age (year)	Heavy Trucks (cumulative)
2019 (initial)	4,500
2029 (10 years)	8,193,680
2039 (20 years)	17,246,100

Design Outputs

Distress Prediction Summary

Distress Type	Distress @ Specified Reliability		Reliability (%)		Criterion Satisfied?
	Target	Predicted	Target	Achieved	
Terminal IRI (in/mile)	172.00	212.60	90.00	60.53	Fail
Permanent deformation - total pavement (in)	0.75	1.81	90.00	0.00	Fail
AC bottom-up fatigue cracking (% lane area)	25.00	49.91	90.00	31.52	Fail
AC thermal cracking (ft/mile)	1000.00	27.17	90.00	100.00	Pass
AC top-down fatigue cracking (ft/mile)	2000.00	407.59	90.00	100.00	Pass
Permanent deformation - AC only (in)	0.25	0.67	90.00	3.80	Fail

Distress Charts

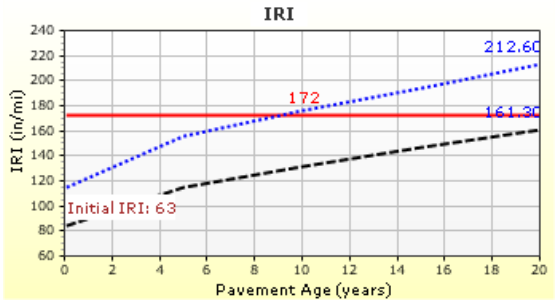

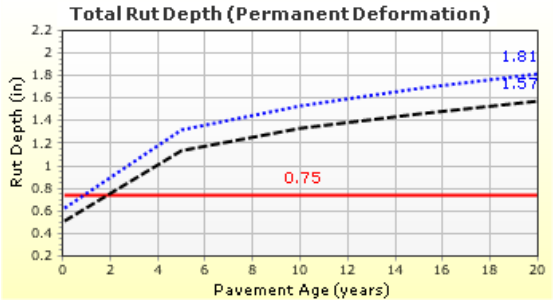

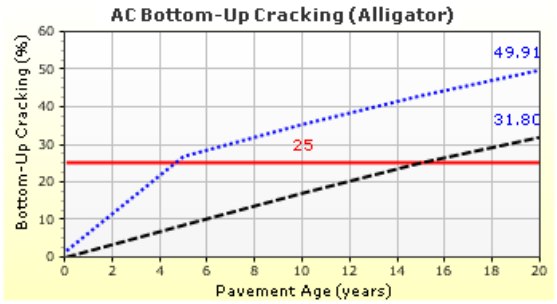

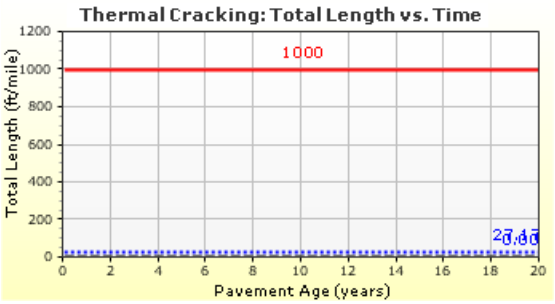

Design Inputs

Design Life: 20 years
Design Type: Flexible Pavement
Base construction: May, 2018
Pavement construction: June, 2019
Traffic opening: September, 2019
Climate Data Sources (Lat/Lon): 33.688, -112.082

Design Structure

Layer type	Material Type	Thickness (in)
Flexible	Default asphalt concrete	5.4
NonStabilized	A-1-b	14.8
Subgrade	A-6	Semi-infinite

Volumetric at Construction:	
Effective binder content (%)	5.0
Air voids (%)	5.0

Traffic

Age (year)	Heavy Trucks (cumulative)
2019 (initial)	4,500
2029 (10 years)	8,193,680
2039 (20 years)	17,246,100

Design Outputs

Distress Prediction Summary

Distress Type	Distress @ Specified Reliability		Reliability (%)		Criterion Satisfied?
	Target	Predicted	Target	Achieved	
Terminal IRI (in/mile)	172.00	226.83	90.00	48.66	Fail
Permanent deformation - total pavement (in)	0.75	2.10	90.00	0.00	Fail
AC bottom-up fatigue cracking (% lane area)	25.00	52.31	90.00	25.75	Fail
AC thermal cracking (ft/mile)	1000.00	27.17	90.00	100.00	Pass
AC top-down fatigue cracking (ft/mile)	2000.00	275.40	90.00	100.00	Pass
Permanent deformation - AC only (in)	0.25	0.66	90.00	4.03	Fail

Distress Charts

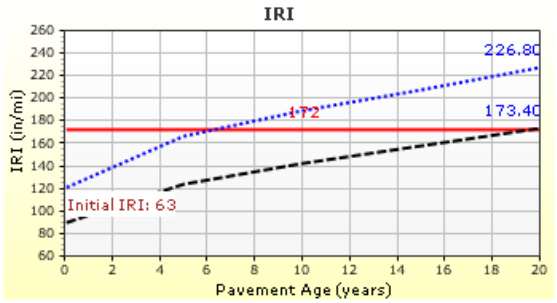

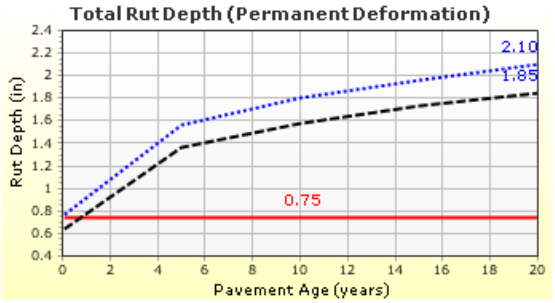

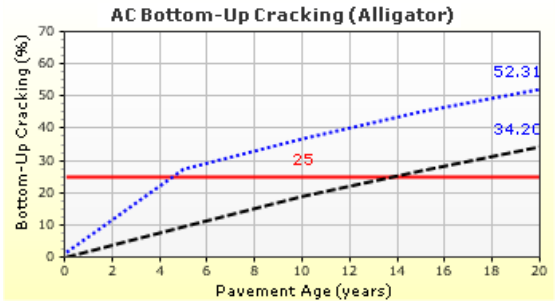

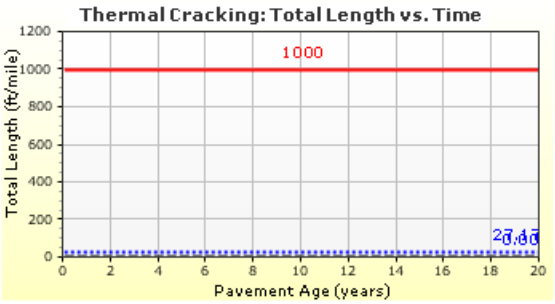

Design Inputs

Design Life: 20 years
Design Type: Flexible Pavement
Base construction: May, 2018
Pavement construction: June, 2019
Traffic opening: September, 2019
Climate Data Sources (Lat/Lon): 33.688, -112.082

Design Structure

Layer type	Material Type	Thickness (in)
Flexible	Default asphalt concrete	5.4
NonStabilized	A-1-b	14.8
Subgrade	A-6	Semi-infinite

Volumetric at Construction:	
Effective binder content (%)	5.0
Air voids (%)	5.0

Traffic

Age (year)	Heavy Trucks (cumulative)
2019 (initial)	4,500
2029 (10 years)	8,193,680
2039 (20 years)	17,246,100

Design Outputs

Distress Prediction Summary

Distress Type	Distress @ Specified Reliability		Reliability (%)		Criterion Satisfied?
	Target	Predicted	Target	Achieved	
Terminal IRI (in/mile)	172.00	178.23	90.00	86.57	Fail
Permanent deformation - total pavement (in)	0.75	1.03	90.00	30.92	Fail
AC bottom-up fatigue cracking (% lane area)	25.00	41.51	90.00	54.51	Fail
AC thermal cracking (ft/mile)	1000.00	27.17	90.00	100.00	Pass
AC top-down fatigue cracking (ft/mile)	2000.00	9499.13	90.00	3.60	Fail
Permanent deformation - AC only (in)	0.25	0.68	90.00	3.46	Fail

Distress Charts

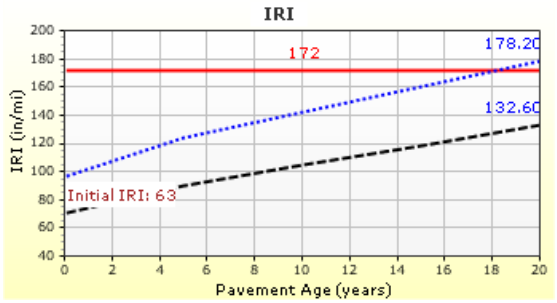

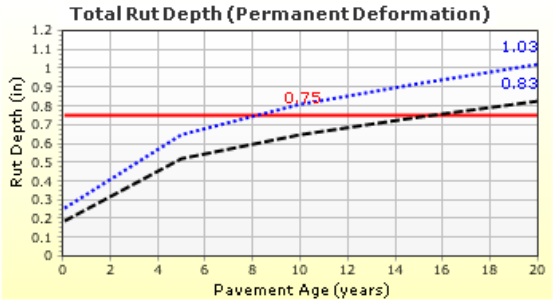

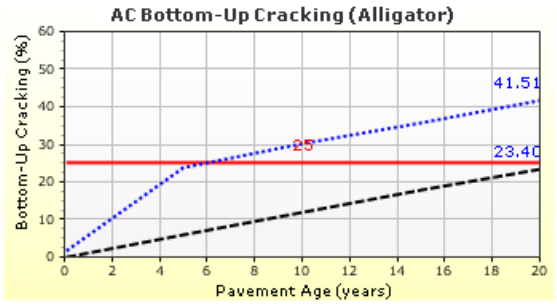

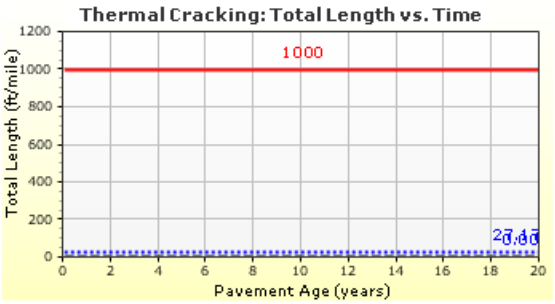

Case 18

Design Inputs

Design Life: 20 years
Design Type: Flexible Pavement
Base construction: May, 2018
Pavement construction: June, 2019
Traffic opening: September, 2019
Climate Data Sources (Lat/Lon): 33.688, -112.082

Design Structure

Layer type	Material Type	Thickness (in)
Flexible	Default asphalt concrete	5.4
NonStabilized	A-1-b	14.8
Subgrade	A-6	Semi-infinite

Volumetric at Construction:	
Effective binder content (%)	5.0
Air voids (%)	5.0

Traffic

Age (year)	Heavy Trucks (cumulative)
2019 (initial)	4,500
2029 (10 years)	8,193,680
2039 (20 years)	17,246,100

Design Outputs

Distress Prediction Summary

Distress Type	Distress @ Specified Reliability		Reliability (%)		Criterion Satisfied?
	Target	Predicted	Target	Achieved	
Terminal IRI (in/mile)	172.00	177.29	90.00	87.13	Fail
Permanent deformation - total pavement (in)	0.75	1.00	90.00	36.16	Fail
AC bottom-up fatigue cracking (% lane area)	25.00	39.91	90.00	58.96	Fail
AC thermal cracking (ft/mile)	1000.00	27.17	90.00	100.00	Pass
AC top-down fatigue cracking (ft/mile)	2000.00	11016.79	90.00	0.84	Fail
Permanent deformation - AC only (in)	0.25	0.68	90.00	3.49	Fail

Distress Charts

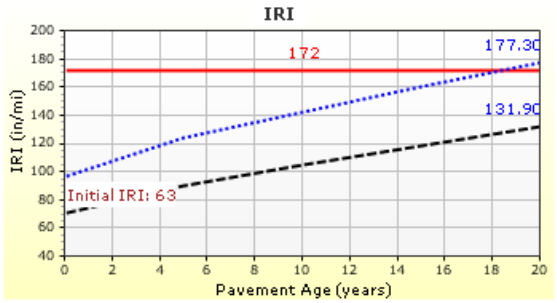

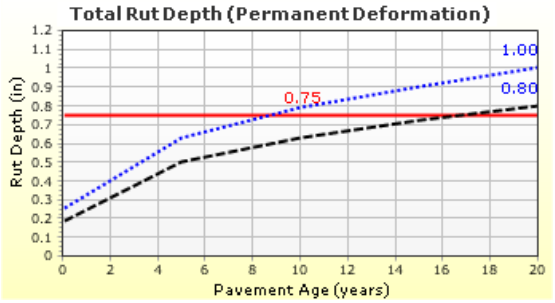

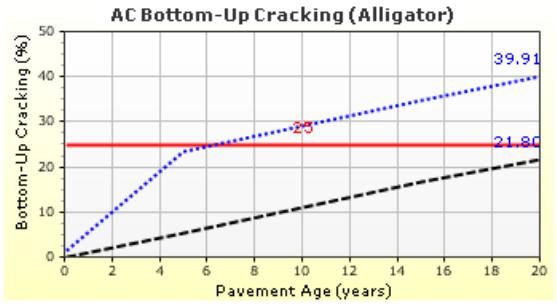

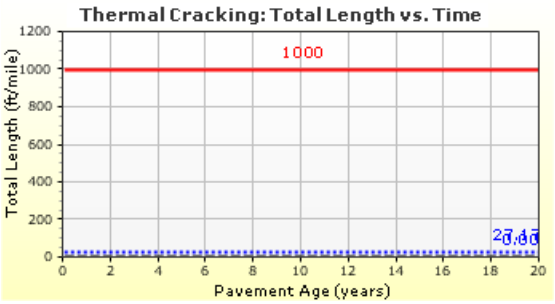

Design Inputs

Design Life: 20 years
Design Type: Flexible Pavement
Base construction: May, 2018
Pavement construction: June, 2019
Traffic opening: September, 2019
Climate Data Sources (Lat/Lon): 33.688, -112.082

Design Structure

Layer type	Material Type	Thickness (in)
Flexible	Default asphalt concrete	5.4
NonStabilized	A-1-b	14.8
Subgrade	A-6	Semi-infinite

Volumetric at Construction:	
Effective binder content (%)	5.0
Air voids (%)	5.0

Traffic

Age (year)	Heavy Trucks (cumulative)
2019 (initial)	4,500
2029 (10 years)	8,193,680
2039 (20 years)	17,246,100

Design Outputs

Distress Prediction Summary

Distress Type	Distress @ Specified Reliability		Reliability (%)		Criterion Satisfied?
	Target	Predicted	Target	Achieved	
Terminal IRI (in/mile)	172.00	180.75	90.00	85.04	Fail
Permanent deformation - total pavement (in)	0.75	1.09	90.00	18.86	Fail
AC bottom-up fatigue cracking (% lane area)	25.00	41.71	90.00	53.95	Fail
AC thermal cracking (ft/mile)	1000.00	27.17	90.00	100.00	Pass
AC top-down fatigue cracking (ft/mile)	2000.00	9172.82	90.00	4.73	Fail
Permanent deformation - AC only (in)	0.25	0.68	90.00	3.43	Fail

Distress Charts

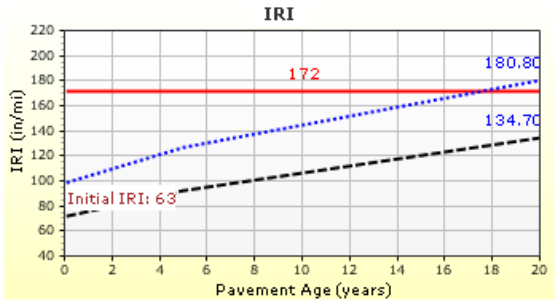

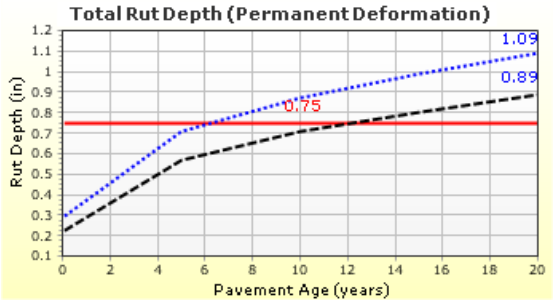

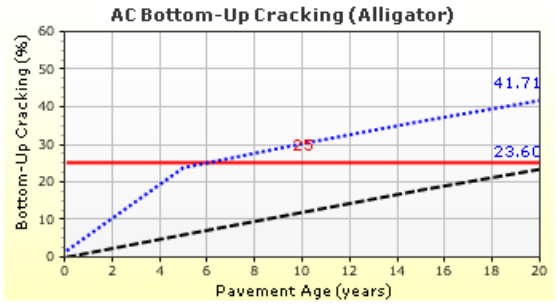

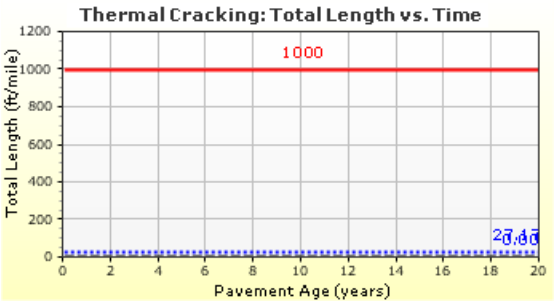

Design Inputs

Design Life: 20 years
Design Type: Flexible Pavement
Base construction: May, 2018
Pavement construction: June, 2019
Traffic opening: September, 2019
Climate Data Sources (Lat/Lon): 33.688, -112.082

Design Structure

Layer type	Material Type	Thickness (in)
Flexible	Default asphalt concrete	5.4
NonStabilized	A-1-b	14.8
Subgrade	A-6	Semi-infinite

Volumetric at Construction:	
Effective binder content (%)	5.0
Air voids (%)	5.0

Traffic

Age (year)	Heavy Trucks (cumulative)
2019 (initial)	4,500
2029 (10 years)	8,193,680
2039 (20 years)	17,246,100

Design Outputs

Distress Prediction Summary

Distress Type	Distress @ Specified Reliability		Reliability (%)		Criterion Satisfied?
	Target	Predicted	Target	Achieved	
Terminal IRI (in/mile)	172.00	178.97	90.00	86.13	Fail
Permanent deformation - total pavement (in)	0.75	1.04	90.00	27.11	Fail
AC bottom-up fatigue cracking (% lane area)	25.00	40.91	90.00	56.19	Fail
AC thermal cracking (ft/mile)	1000.00	27.17	90.00	100.00	Pass
AC top-down fatigue cracking (ft/mile)	2000.00	10141.57	90.00	2.02	Fail
Permanent deformation - AC only (in)	0.25	0.68	90.00	3.42	Fail

Distress Charts

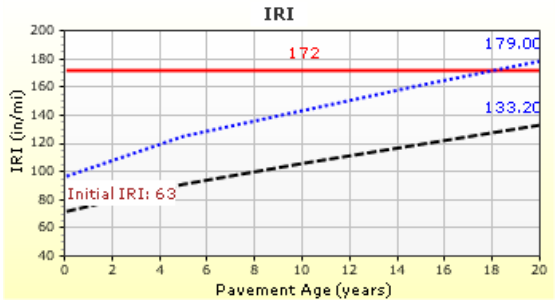

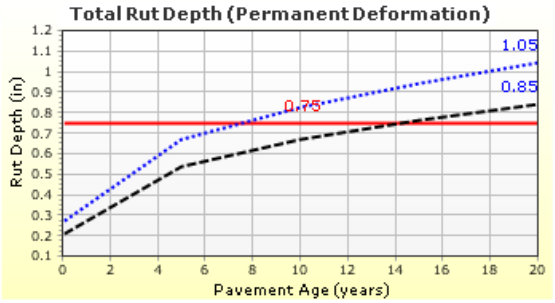

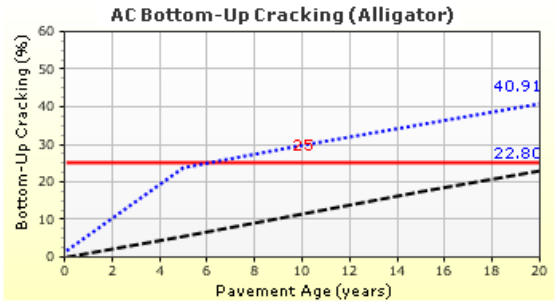

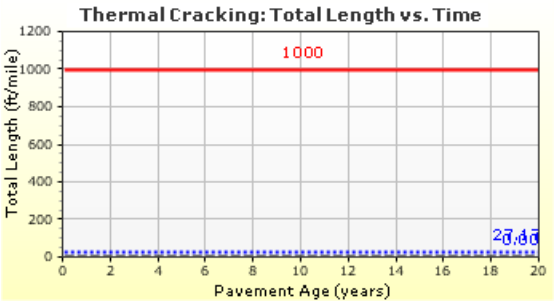

APPENDIX C

MEPDG OUTPUT – EAGER SOIL – STRUCTURE 2

Design Inputs

Design Life: 20 years
Design Type: Flexible Pavement
Base construction: May, 2018
Pavement construction: June, 2019
Traffic opening: September, 2019
Climate Data Sources (Lat/Lon): 33.688, -112.082

Design Structure

Layer type	Material Type	Thickness (in)
Flexible	Default asphalt concrete	13.0
NonStabilized	A-1-b	6.0
Subgrade	A-6	Semi-infinite

Volumetric at Construction:	
Effective binder content (%)	5.0
Air voids (%)	5.0

Traffic

Age (year)	Heavy Trucks (cumulative)
2019 (initial)	2,000
2029 (10 years)	3,641,630
2039 (20 years)	7,664,950

Design Outputs

Distress Prediction Summary

Distress Type	Distress @ Specified Reliability		Reliability (%)		Criterion Satisfied?
	Target	Predicted	Target	Achieved	
Terminal IRI (in/mile)	172.00	135.37	90.00	99.52	Pass
Permanent deformation - total pavement (in)	0.75	0.43	90.00	100.00	Pass
AC bottom-up fatigue cracking (% lane area)	25.00	1.62	90.00	100.00	Pass
AC thermal cracking (ft/mile)	1000.00	27.17	90.00	100.00	Pass
AC top-down fatigue cracking (ft/mile)	2000.00	288.25	90.00	100.00	Pass
Permanent deformation - AC only (in)	0.25	0.25	90.00	89.83	Fail

Distress Charts

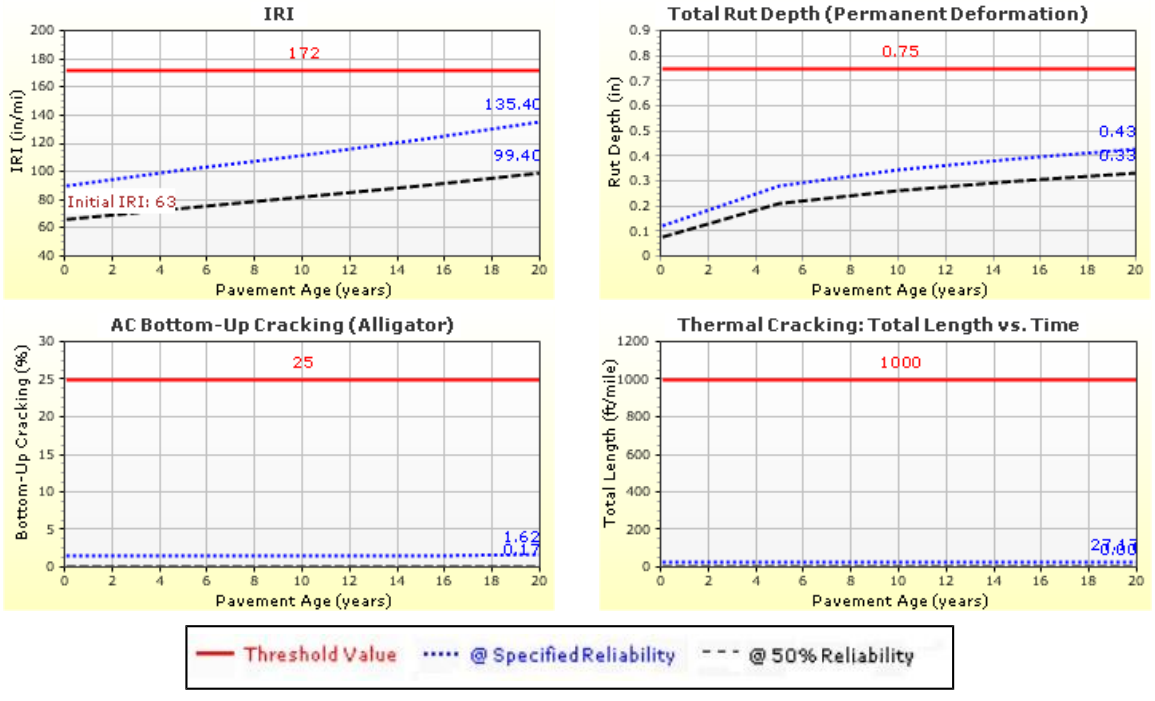

Case 22

Design Inputs

Design Life: 20 years
Design Type: Flexible Pavement
Base construction: May, 2018
Pavement construction: June, 2019
Traffic opening: September, 2019
Climate Data Sources (Lat/Lon): 33.688, -112.082

Design Structure

Layer type	Material Type	Thickness (in)
Flexible	Default asphalt concrete	13.0
NonStabilized	A-1-b	6.0
Subgrade	A-6	Semi-infinite

Volumetric at Construction:	
Effective binder content (%)	5.0
Air voids (%)	5.0

Traffic

Age (year)	Heavy Trucks (cumulative)
2019 (initial)	2,000
2029 (10 years)	3,641,630
2039 (20 years)	7,664,950

Design Outputs

Distress Prediction Summary

Distress Type	Distress @ Specified Reliability		Reliability (%)		Criterion Satisfied?
	Target	Predicted	Target	Achieved	
Terminal IRI (in/mile)	172.00	131.42	90.00	99.72	Pass
Permanent deformation - total pavement (in)	0.75	0.37	90.00	100.00	Pass
AC bottom-up fatigue cracking (% lane area)	25.00	1.53	90.00	100.00	Pass
AC thermal cracking (ft/mile)	1000.00	27.17	90.00	100.00	Pass
AC top-down fatigue cracking (ft/mile)	2000.00	517.77	90.00	100.00	Pass
Permanent deformation - AC only (in)	0.25	0.25	90.00	89.46	Fail

Distress Charts

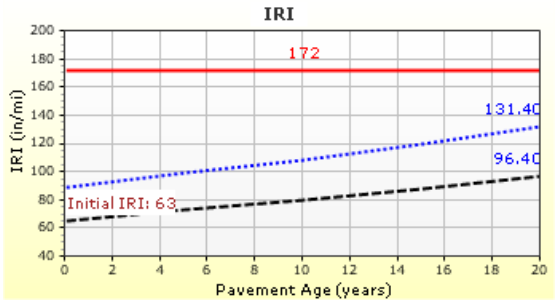

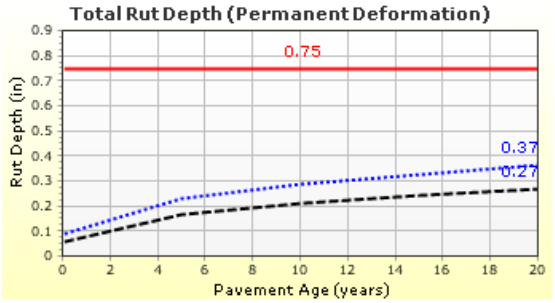

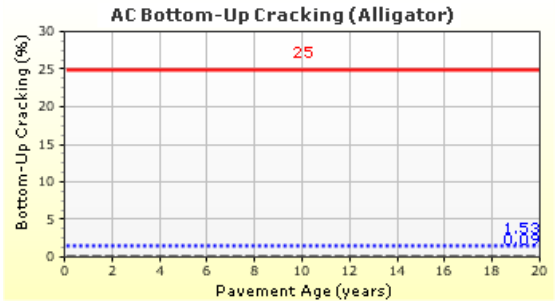

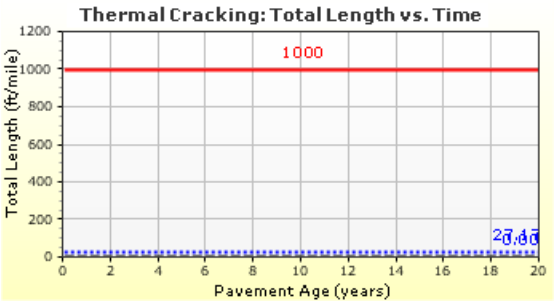

Design Inputs

Design Life: 20 years
Design Type: Flexible Pavement
Base construction: May, 2018
Pavement construction: June, 2019
Traffic opening: September, 2019
Climate Data Sources (Lat/Lon): 33.688, -112.082

Design Structure

Layer type	Material Type	Thickness (in)
Flexible	Default asphalt concrete	13.0
NonStabilized	A-1-b	6.0
Subgrade	A-6	Semi-infinite

Volumetric at Construction:	
Effective binder content (%)	5.0
Air voids (%)	5.0

Traffic

Age (year)	Heavy Trucks (cumulative)
2019 (initial)	2,000
2029 (10 years)	3,641,630
2039 (20 years)	7,664,950

Design Outputs

Distress Prediction Summary

Distress Type	Distress @ Specified Reliability		Reliability (%)		Criterion Satisfied?
	Target	Predicted	Target	Achieved	
Terminal IRI (in/mile)	172.00	148.88	90.00	97.95	Pass
Permanent deformation - total pavement (in)	0.75	0.73	90.00	93.55	Pass
AC bottom-up fatigue cracking (% lane area)	25.00	1.93	90.00	100.00	Pass
AC thermal cracking (ft/mile)	1000.00	27.17	90.00	100.00	Pass
AC top-down fatigue cracking (ft/mile)	2000.00	256.58	90.00	100.00	Pass
Permanent deformation - AC only (in)	0.25	0.25	90.00	91.25	Pass

Distress Charts

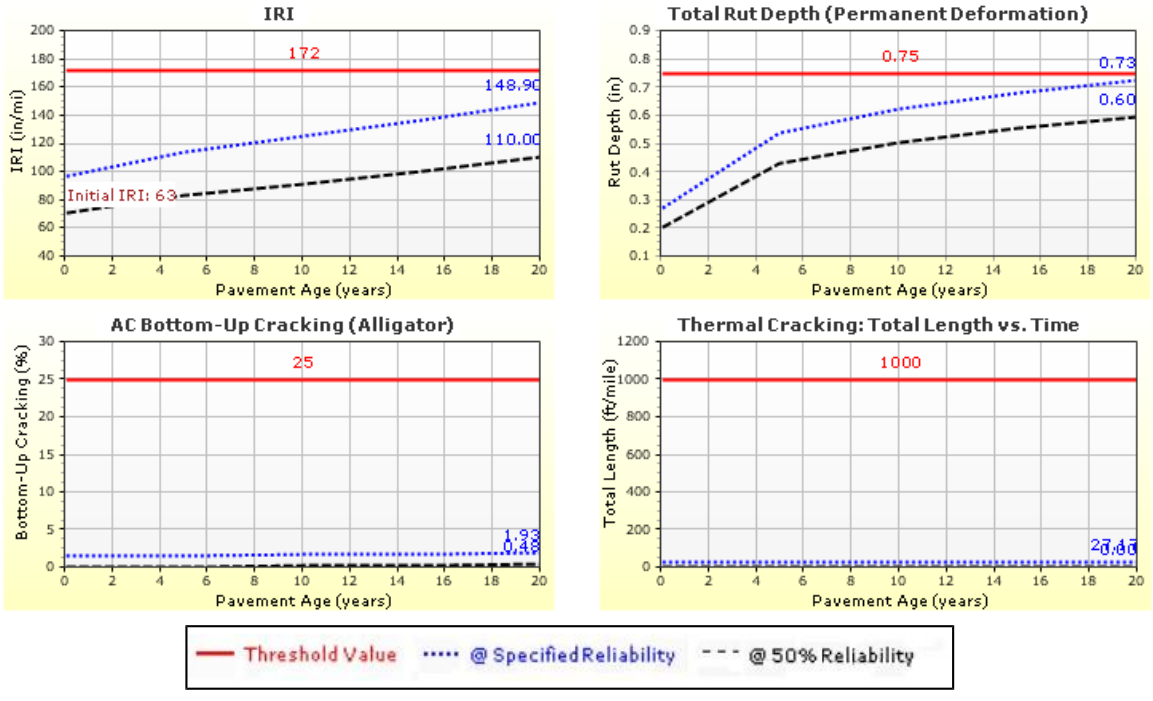

Design Inputs

Design Life: 20 years
Design Type: Flexible Pavement
Base construction: May, 2018
Pavement construction: June, 2019
Traffic opening: September, 2019
Climate Data Sources (Lat/Lon): 33.688, -112.082

Design Structure

Layer type	Material Type	Thickness (in)
Flexible	Default asphalt concrete	13.0
NonStabilized	A-1-b	6.0
Subgrade	A-6	Semi-infinite

Volumetric at Construction:	
Effective binder content (%)	5.0
Air voids (%)	5.0

Traffic

Age (year)	Heavy Trucks (cumulative)
2019 (initial)	2,000
2029 (10 years)	3,641,630
2039 (20 years)	7,664,950

Design Outputs

Distress Prediction Summary

Distress Type	Distress @ Specified Reliability		Reliability (%)		Criterion Satisfied?
	Target	Predicted	Target	Achieved	
Terminal IRI (in/mile)	172.00	160.94	90.00	94.78	Pass
Permanent deformation - total pavement (in)	0.75	0.99	90.00	22.73	Fail
AC bottom-up fatigue cracking (% lane area)	25.00	2.27	90.00	100.00	Pass
AC thermal cracking (ft/mile)	1000.00	27.17	90.00	100.00	Pass
AC top-down fatigue cracking (ft/mile)	2000.00	256.48	90.00	100.00	Pass
Permanent deformation - AC only (in)	0.25	0.24	90.00	92.63	Pass

Distress Charts

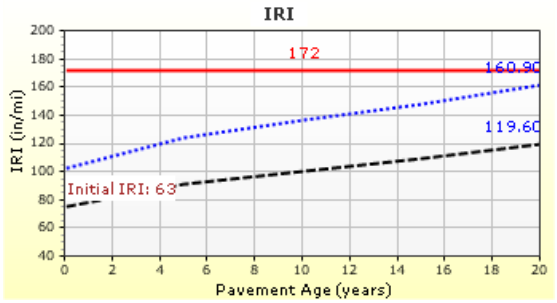

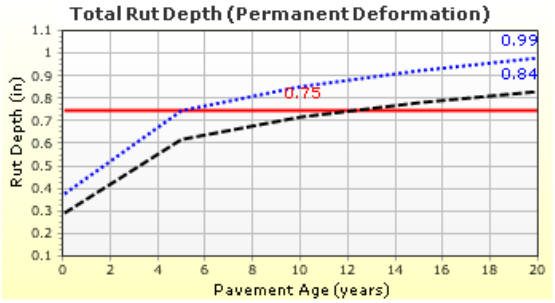

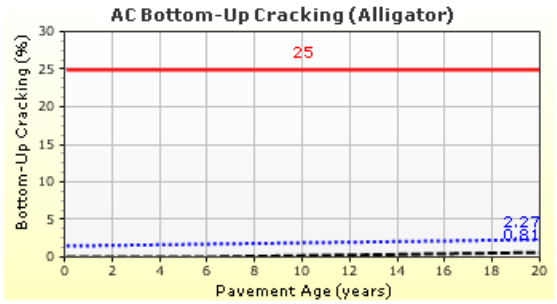

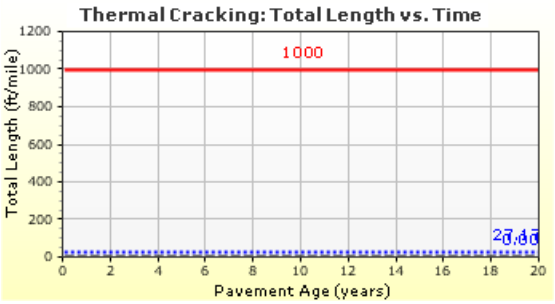

Design Inputs

Design Life: 20 years
Design Type: Flexible Pavement
Base construction: May, 2018
Pavement construction: June, 2019
Traffic opening: September, 2019
Climate Data Sources (Lat/Lon): 33.688, -112.082

Design Structure

Layer type	Material Type	Thickness (in)
Flexible	Default asphalt concrete	13.0
NonStabilized	A-1-b	6.0
Subgrade	A-6	Semi-infinite

Volumetric at Construction:	
Effective binder content (%)	5.0
Air voids (%)	5.0

Traffic

Age (year)	Heavy Trucks (cumulative)
2019 (initial)	2,000
2029 (10 years)	3,641,630
2039 (20 years)	7,664,950

Design Outputs

Distress Prediction Summary

Distress Type	Distress @ Specified Reliability		Reliability (%)		Criterion Satisfied?
	Target	Predicted	Target	Achieved	
Terminal IRI (in/mile)	172.00	170.13	90.00	90.94	Pass
Permanent deformation - total pavement (in)	0.75	1.18	90.00	1.79	Fail
AC bottom-up fatigue cracking (% lane area)	25.00	2.74	90.00	100.00	Pass
AC thermal cracking (ft/mile)	1000.00	27.17	90.00	100.00	Pass
AC top-down fatigue cracking (ft/mile)	2000.00	256.48	90.00	100.00	Pass
Permanent deformation - AC only (in)	0.25	0.24	90.00	93.67	Pass

Distress Charts

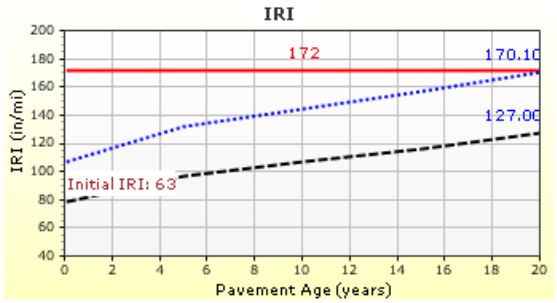

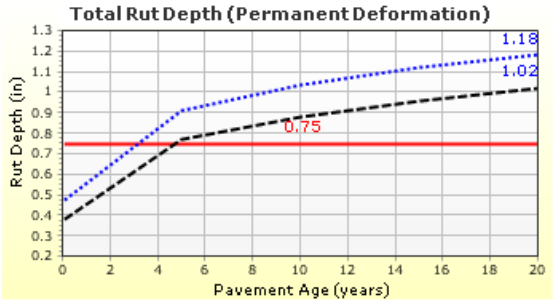

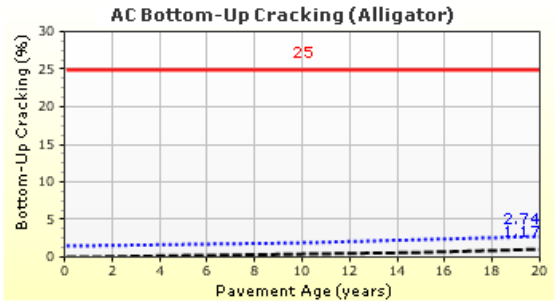

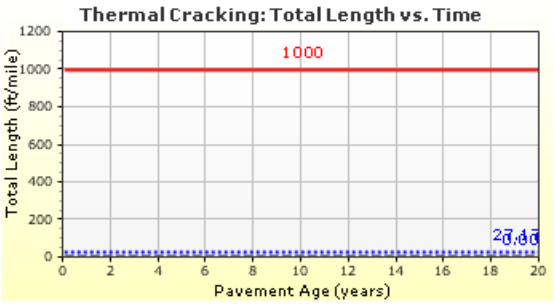

Design Inputs

Design Life: 20 years
Design Type: Flexible Pavement
Base construction: May, 2018
Pavement construction: June, 2019
Traffic opening: September, 2019
Climate Data Sources (Lat/Lon): 33.688, -112.082

Design Structure

Layer type	Material Type	Thickness (in)
Flexible	Default asphalt concrete	13.0
NonStabilized	A-1-b	6.0
Subgrade	A-6	Semi-infinite

Volumetric at Construction:	
Effective binder content (%)	5.0
Air voids (%)	5.0

Traffic

Age (year)	Heavy Trucks (cumulative)
2019 (initial)	2,000
2029 (10 years)	3,704,090
2039 (20 years)	7,928,660

Design Outputs

Distress Prediction Summary

Distress Type	Distress @ Specified Reliability		Reliability (%)		Criterion Satisfied?
	Target	Predicted	Target	Achieved	
Terminal IRI (in/mile)	172.00	135.86	90.00	99.49	Pass
Permanent deformation - total pavement (in)	0.75	0.44	90.00	100.00	Pass
AC bottom-up fatigue cracking (% lane area)	25.00	1.63	90.00	100.00	Pass
AC thermal cracking (ft/mile)	1000.00	27.17	90.00	100.00	Pass
AC top-down fatigue cracking (ft/mile)	2000.00	284.18	90.00	100.00	Pass
Permanent deformation - AC only (in)	0.25	0.25	90.00	88.64	Fail

Distress Charts

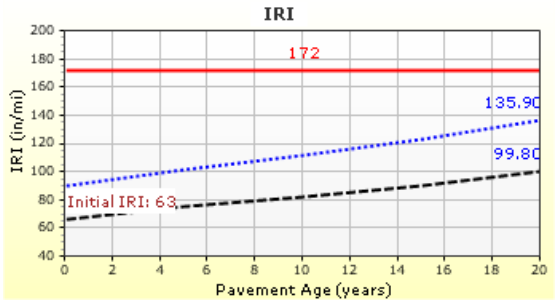

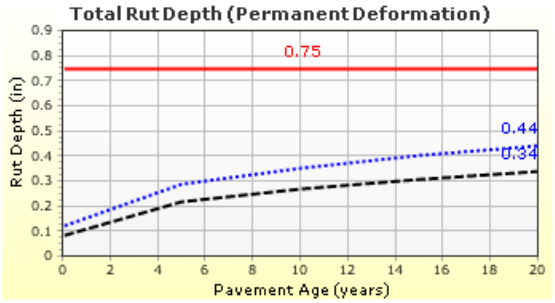

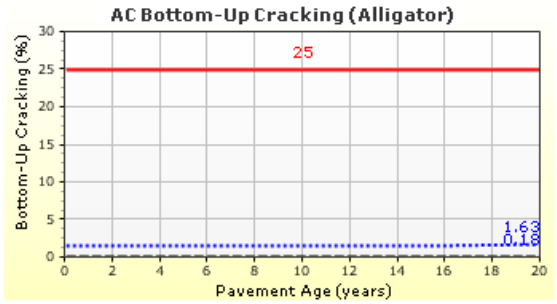

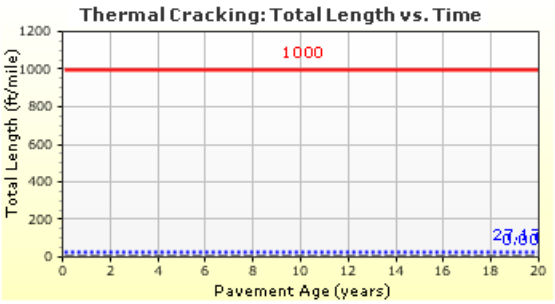

Design Inputs

Design Life: 20 years
Design Type: Flexible Pavement
Base construction: May, 2018
Pavement construction: June, 2019
Traffic opening: September, 2019
Climate Data Sources (Lat/Lon): 33.688, -112.082

Design Structure

Layer type	Material Type	Thickness (in)
Flexible	Default asphalt concrete	13.0
NonStabilized	A-1-b	6.0
Subgrade	A-6	Semi-infinite

Volumetric at Construction:	
Effective binder content (%)	5.0
Air voids (%)	5.0

Traffic

Age (year)	Heavy Trucks (cumulative)
2019 (initial)	2,000
2029 (10 years)	3,641,630
2039 (20 years)	7,664,950

Design Outputs

Distress Prediction Summary

Distress Type	Distress @ Specified Reliability		Reliability (%)		Criterion Satisfied?
	Target	Predicted	Target	Achieved	
Terminal IRI (in/mile)	172.00	134.85	90.00	99.55	Pass
Permanent deformation - total pavement (in)	0.75	0.43	90.00	100.00	Pass
AC bottom-up fatigue cracking (% lane area)	25.00	1.57	90.00	100.00	Pass
AC thermal cracking (ft/mile)	1000.00	27.17	90.00	100.00	Pass
AC top-down fatigue cracking (ft/mile)	2000.00	341.71	90.00	100.00	Pass
Permanent deformation - AC only (in)	0.25	0.25	90.00	89.62	Fail

Distress Charts

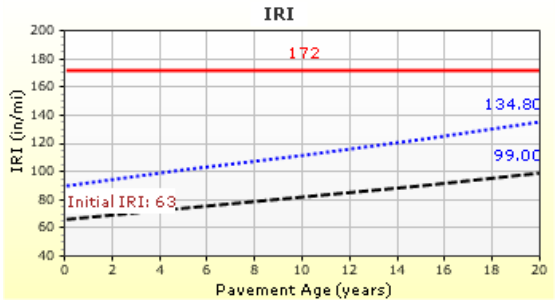

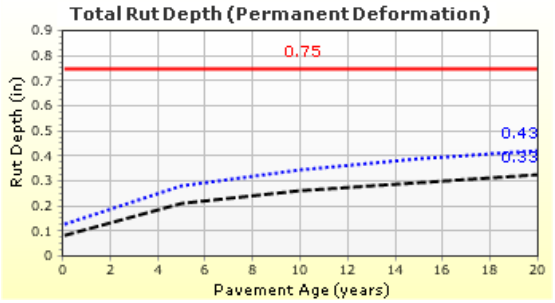

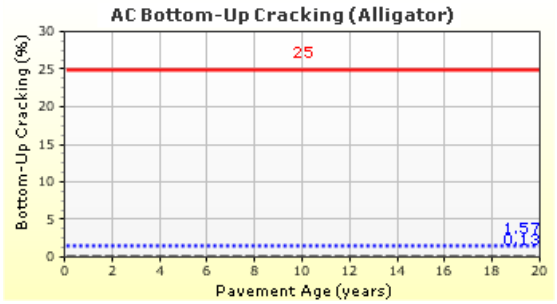

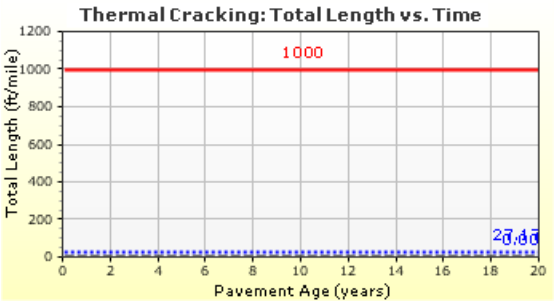

Design Inputs

Design Life: 20 years
Design Type: Flexible Pavement
Base construction: May, 2018
Pavement construction: June, 2019
Traffic opening: September, 2019
Climate Data Sources (Lat/Lon): 33.688, -112.082

Design Structure

Layer type	Material Type	Thickness (in)
Flexible	Default asphalt concrete	13.0
NonStabilized	A-1-b	6.0
Subgrade	A-6	Semi-infinite

Volumetric at Construction:	
Effective binder content (%)	5.0
Air voids (%)	5.0

Traffic

Age (year)	Heavy Trucks (cumulative)
2019 (initial)	2,000
2029 (10 years)	3,641,630
2039 (20 years)	7,664,950

Design Outputs

Distress Prediction Summary

Distress Type	Distress @ Specified Reliability		Reliability (%)		Criterion Satisfied?
	Target	Predicted	Target	Achieved	
Terminal IRI (in/mile)	172.00	137.68	90.00	99.36	Pass
Permanent deformation - total pavement (in)	0.75	0.49	90.00	100.00	Pass
AC bottom-up fatigue cracking (% lane area)	25.00	1.63	90.00	100.00	Pass
AC thermal cracking (ft/mile)	1000.00	27.17	90.00	100.00	Pass
AC top-down fatigue cracking (ft/mile)	2000.00	278.99	90.00	100.00	Pass
Permanent deformation - AC only (in)	0.25	0.25	90.00	89.75	Fail

Distress Charts

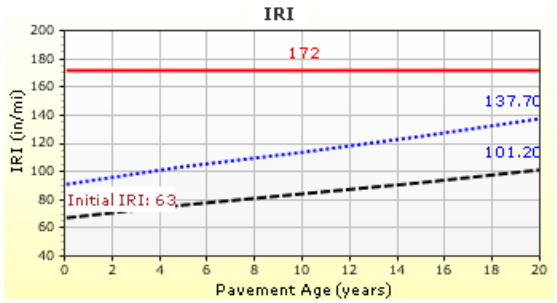

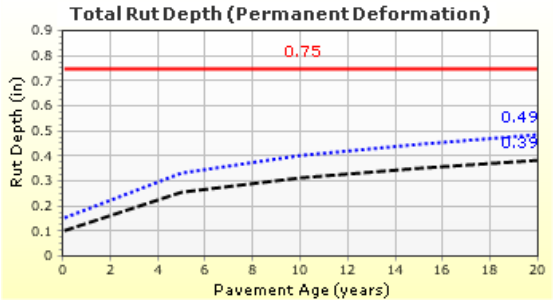

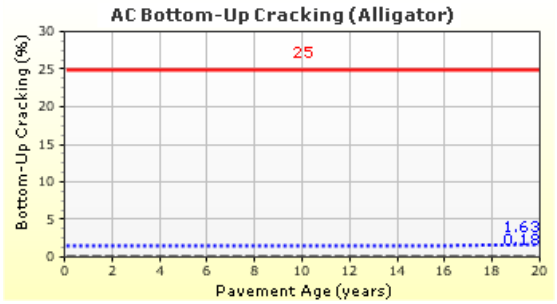

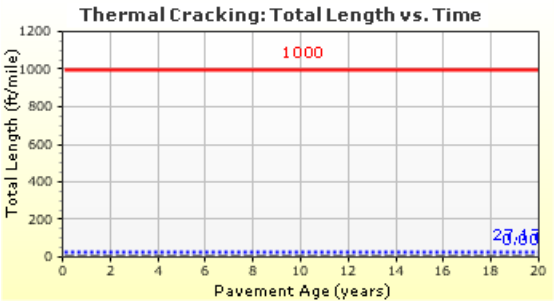

Design Inputs

Design Life: 20 years
Design Type: Flexible Pavement
Base construction: May, 2018
Pavement construction: June, 2019
Traffic opening: September, 2019
Climate Data Sources (Lat/Lon): 33.688, -112.082

Design Structure

Layer type	Material Type	Thickness (in)
Flexible	Default asphalt concrete	13.0
NonStabilized	A-1-b	6.0
Subgrade	A-6	Semi-infinite

Volumetric at Construction:	
Effective binder content (%)	5.0
Air voids (%)	5.0

Traffic

Age (year)	Heavy Trucks (cumulative)
2019 (initial)	2,000
2029 (10 years)	3,641,630
2039 (20 years)	7,664,950

Design Outputs

Distress Prediction Summary

Distress Type	Distress @ Specified Reliability		Reliability (%)		Criterion Satisfied?
	Target	Predicted	Target	Achieved	
Terminal IRI (in/mile)	172.00	136.12	90.00	99.47	Pass
Permanent deformation - total pavement (in)	0.75	0.46	90.00	100.00	Pass
AC bottom-up fatigue cracking (% lane area)	25.00	1.60	90.00	100.00	Pass
AC thermal cracking (ft/mile)	1000.00	27.17	90.00	100.00	Pass
AC top-down fatigue cracking (ft/mile)	2000.00	298.42	90.00	100.00	Pass
Permanent deformation - AC only (in)	0.25	0.25	90.00	89.66	Fail

Distress Charts

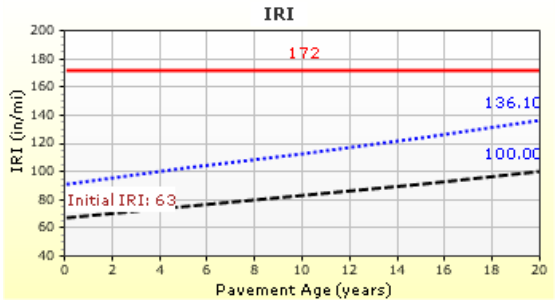

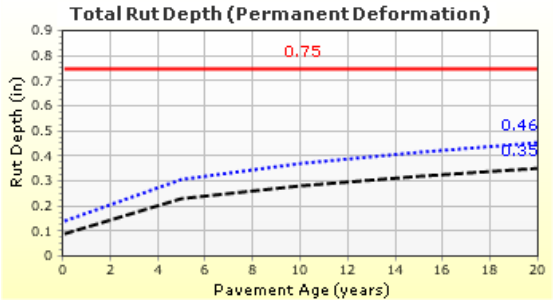

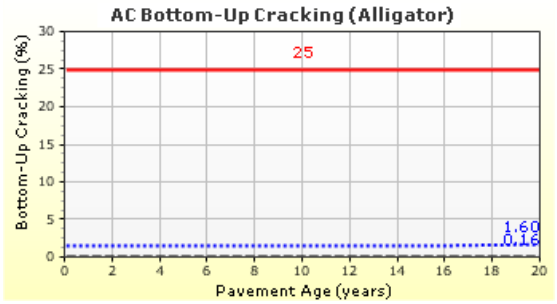

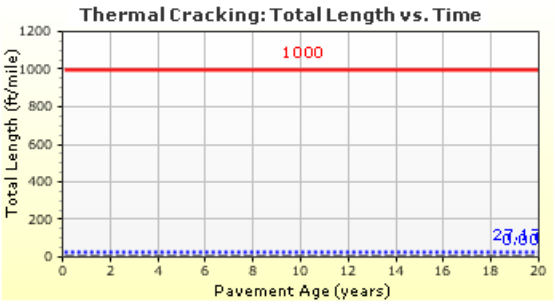

Design Inputs

Design Life: 20 years
Design Type: Flexible Pavement
Base construction: May, 2018
Pavement construction: June, 2019
Traffic opening: September, 2019
Climate Data Sources (Lat/Lon): 33.688, -112.082

Design Structure

Layer type	Material Type	Thickness (in)
Flexible	Default asphalt concrete	13.0
NonStabilized	A-1-b	6.0
Subgrade	A-6	Semi-infinite

Volumetric at Construction:	
Effective binder content (%)	5.0
Air voids (%)	5.0

Traffic

Age (year)	Heavy Trucks (cumulative)
2019 (initial)	10,000
2029 (10 years)	18,208,200
2039 (20 years)	38,324,800

Design Outputs

Distress Prediction Summary

Distress Type	Distress @ Specified Reliability		Reliability (%)		Criterion Satisfied?
	Target	Predicted	Target	Achieved	
Terminal IRI (in/mile)	172.00	148.48	90.00	98.01	Pass
Permanent deformation - total pavement (in)	0.75	0.74	90.00	91.93	Pass
AC bottom-up fatigue cracking (% lane area)	25.00	2.38	90.00	100.00	Pass
AC thermal cracking (ft/mile)	1000.00	27.17	90.00	100.00	Pass
AC top-down fatigue cracking (ft/mile)	2000.00	395.92	90.00	100.00	Pass
Permanent deformation - AC only (in)	0.25	0.52	90.00	12.77	Fail

Distress Charts

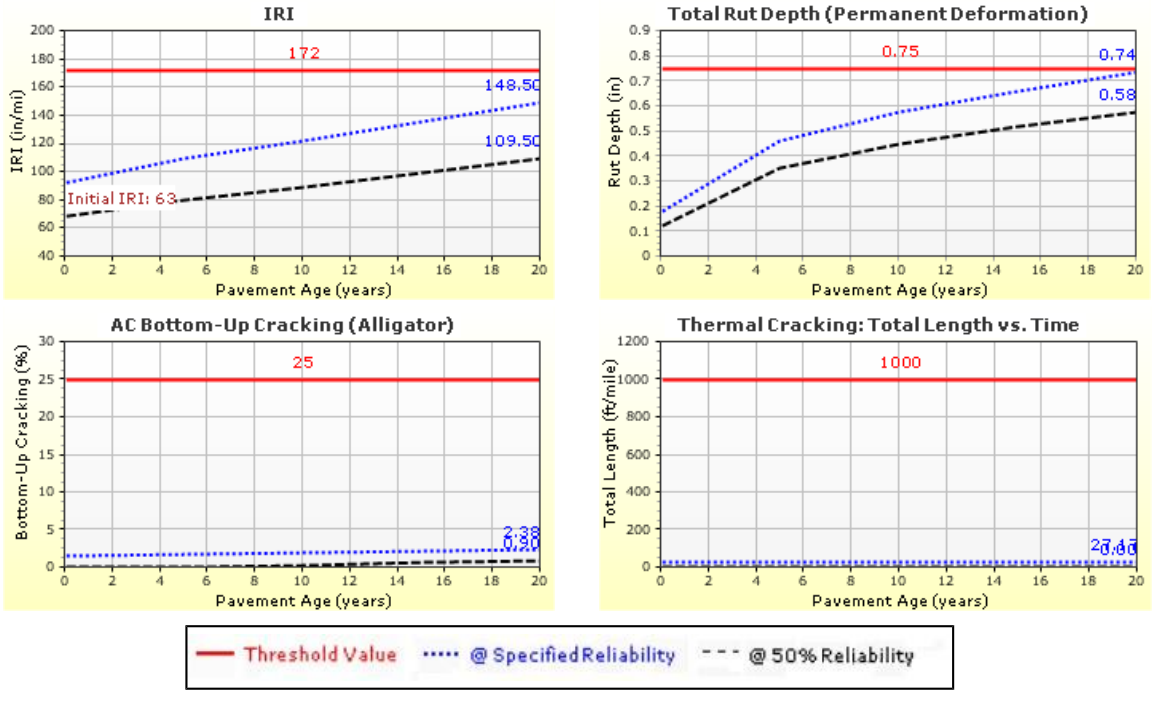

Case 32

Design Inputs

Design Life: 20 years
Design Type: Flexible Pavement
Base construction: May, 2018
Pavement construction: June, 2019
Traffic opening: September, 2019
Climate Data Sources (Lat/Lon): 33.688, -112.082

Design Structure

Layer type	Material Type	Thickness (in)
Flexible	Default asphalt concrete	13.0
NonStabilized	A-1-b	6.0
Subgrade	A-6	Semi-infinite

Volumetric at Construction:	
Effective binder content (%)	5.0
Air voids (%)	5.0

Traffic

Age (year)	Heavy Trucks (cumulative)
2019 (initial)	10,000
2029 (10 years)	18,208,200
2039 (20 years)	38,324,800

Design Outputs

Distress Prediction Summary

Distress Type	Distress @ Specified Reliability		Reliability (%)		Criterion Satisfied?
	Target	Predicted	Target	Achieved	
Terminal IRI (in/mile)	172.00	143.63	90.00	98.75	Pass
Permanent deformation - total pavement (in)	0.75	0.65	90.00	98.14	Pass
AC bottom-up fatigue cracking (% lane area)	25.00	1.92	90.00	100.00	Pass
AC thermal cracking (ft/mile)	1000.00	27.17	90.00	100.00	Pass
AC top-down fatigue cracking (ft/mile)	2000.00	1168.72	90.00	98.63	Pass
Permanent deformation - AC only (in)	0.25	0.52	90.00	12.52	Fail

Distress Charts

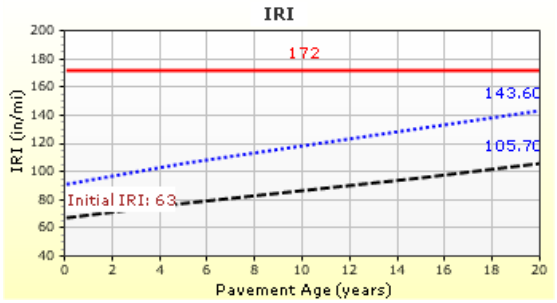

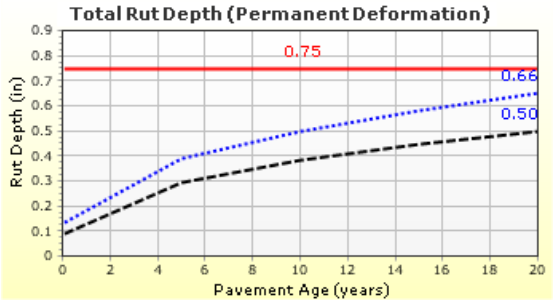

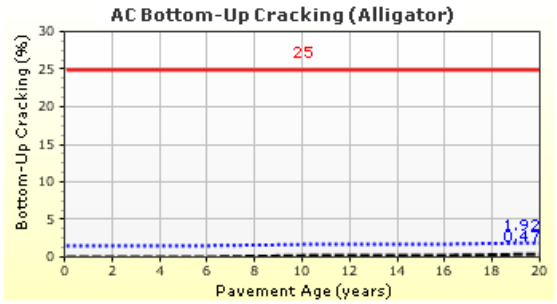

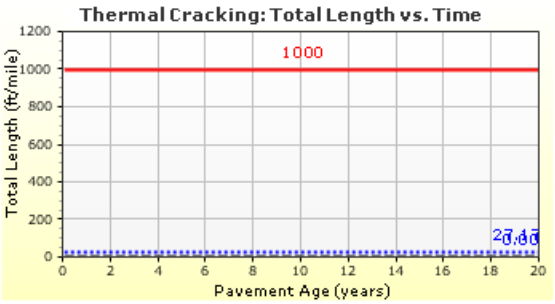

Case 33

Design Inputs

Design Life: 20 years
Design Type: Flexible Pavement
Base construction: May, 2018
Pavement construction: June, 2019
Traffic opening: September, 2019
Climate Data Sources (Lat/Lon): 33.688, -112.082

Design Structure

Layer type	Material Type	Thickness (in)
Flexible	Default asphalt concrete	13.0
NonStabilized	A-1-b	6.0
Subgrade	A-6	Semi-infinite

Volumetric at Construction:	
Effective binder content (%)	5.0
Air voids (%)	5.0

Traffic

Age (year)	Heavy Trucks (cumulative)
2019 (initial)	10,000
2029 (10 years)	18,208,200
2039 (20 years)	38,324,800

Design Outputs

Distress Prediction Summary

Distress Type	Distress @ Specified Reliability		Reliability (%)		Criterion Satisfied?
	Target	Predicted	Target	Achieved	
Terminal IRI (in/mile)	172.00	165.50	90.00	93.02	Pass
Permanent deformation - total pavement (in)	0.75	1.08	90.00	14.20	Fail
AC bottom-up fatigue cracking (% lane area)	25.00	13.14	90.00	99.67	Pass
AC thermal cracking (ft/mile)	1000.00	27.17	90.00	100.00	Pass
AC top-down fatigue cracking (ft/mile)	2000.00	256.95	90.00	100.00	Pass
Permanent deformation - AC only (in)	0.25	0.51	90.00	13.93	Fail

Distress Charts

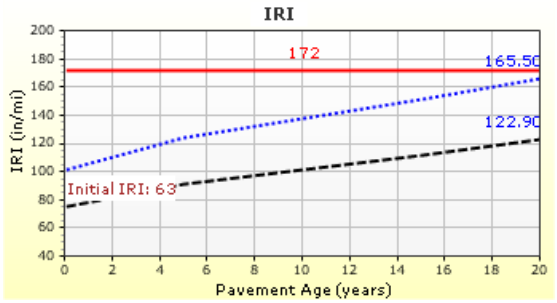

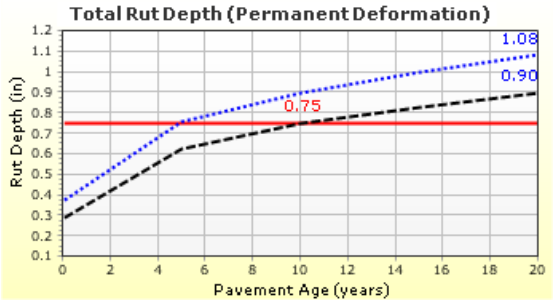

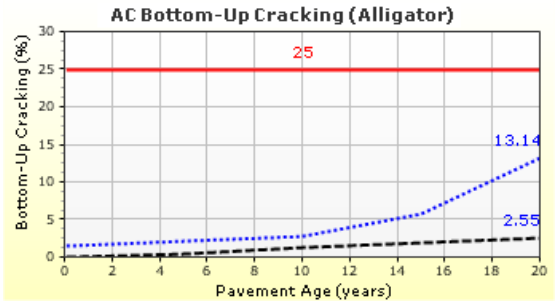

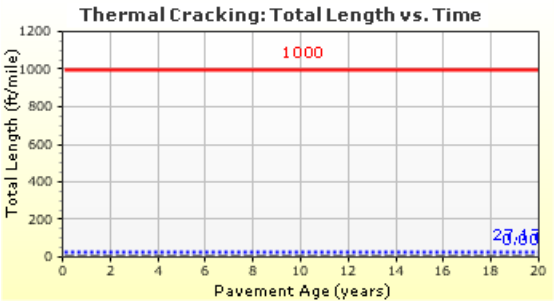

Design Inputs

Design Life: 20 years
Design Type: Flexible Pavement
Base construction: May, 2018
Pavement construction: June, 2019
Traffic opening: September, 2019
Climate Data Sources (Lat/Lon): 33.688, -112.082

Design Structure

Layer type	Material Type	Thickness (in)
Flexible	Default asphalt concrete	13.0
NonStabilized	A-1-b	6.0
Subgrade	A-6	Semi-infinite

Volumetric at Construction:	
Effective binder content (%)	5.0
Air voids (%)	5.0

Traffic

Age (year)	Heavy Trucks (cumulative)
2019 (initial)	10,000
2029 (10 years)	18,208,200
2039 (20 years)	38,324,800

Design Outputs

Distress Prediction Summary

Distress Type	Distress @ Specified Reliability		Reliability (%)		Criterion Satisfied?
	Target	Predicted	Target	Achieved	
Terminal IRI (in/mile)	172.00	180.99	90.00	84.84	Fail
Permanent deformation - total pavement (in)	0.75	1.39	90.00	0.21	Fail
AC bottom-up fatigue cracking (% lane area)	25.00	21.97	90.00	93.34	Pass
AC thermal cracking (ft/mile)	1000.00	27.17	90.00	100.00	Pass
AC top-down fatigue cracking (ft/mile)	2000.00	256.48	90.00	100.00	Pass
Permanent deformation - AC only (in)	0.25	0.50	90.00	15.30	Fail

Distress Charts

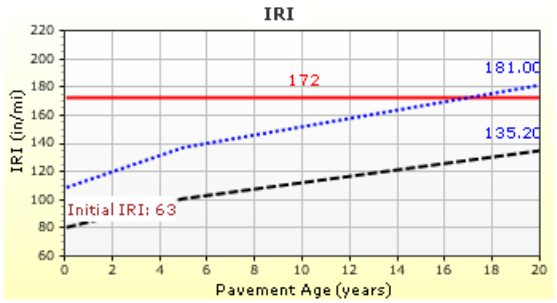

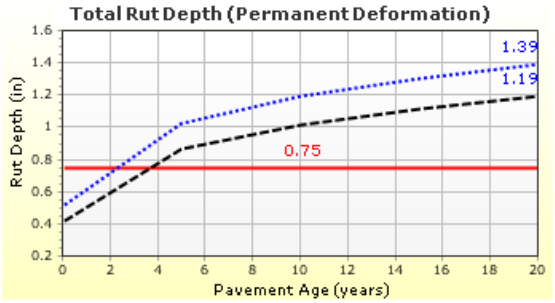

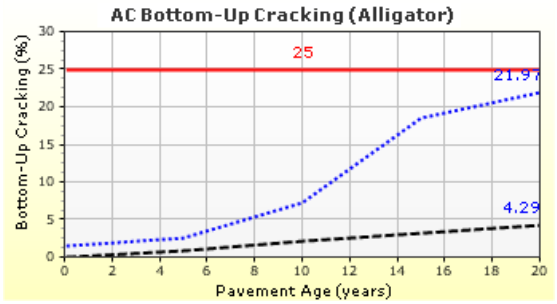

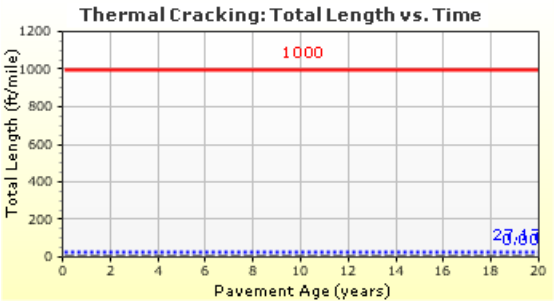

Design Inputs

Design Life: 20 years
Design Type: Flexible Pavement
Base construction: May, 2018
Pavement construction: June, 2019
Traffic opening: September, 2019
Climate Data Sources (Lat/Lon): 33.688, -112.082

Design Structure

Layer type	Material Type	Thickness (in)
Flexible	Default asphalt concrete	13.0
NonStabilized	A-1-b	6.0
Subgrade	A-6	Semi-infinite

Volumetric at Construction:	
Effective binder content (%)	5.0
Air voids (%)	5.0

Traffic

Age (year)	Heavy Trucks (cumulative)
2019 (initial)	10,000
2029 (10 years)	18,208,200
2039 (20 years)	38,324,800

Design Outputs

Distress Prediction Summary

Distress Type	Distress @ Specified Reliability		Reliability (%)		Criterion Satisfied?
	Target	Predicted	Target	Achieved	
Terminal IRI (in/mile)	172.00	192.98	90.00	76.42	Fail
Permanent deformation - total pavement (in)	0.75	1.63	90.00	0.00	Fail
AC bottom-up fatigue cracking (% lane area)	25.00	24.12	90.00	91.05	Pass
AC thermal cracking (ft/mile)	1000.00	27.17	90.00	100.00	Pass
AC top-down fatigue cracking (ft/mile)	2000.00	256.48	90.00	100.00	Pass
Permanent deformation - AC only (in)	0.25	0.49	90.00	16.49	Fail

Distress Charts

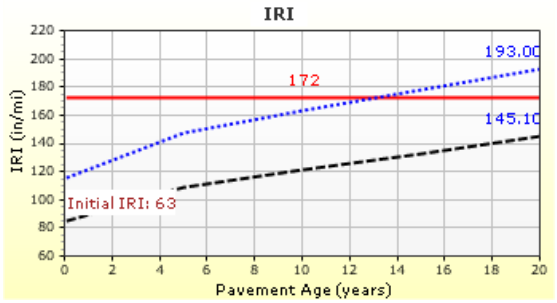

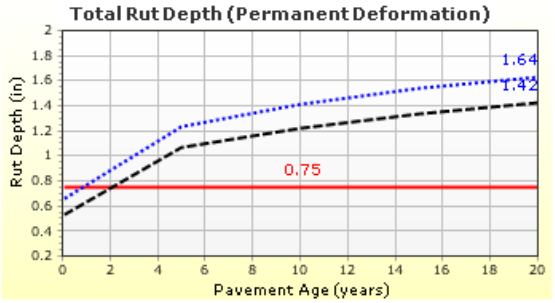

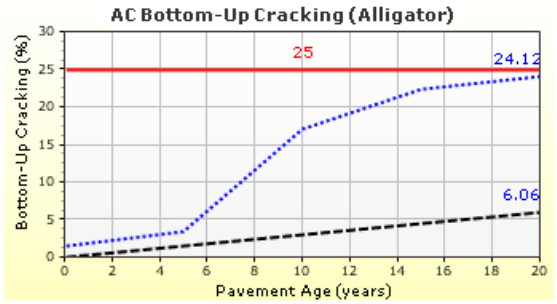

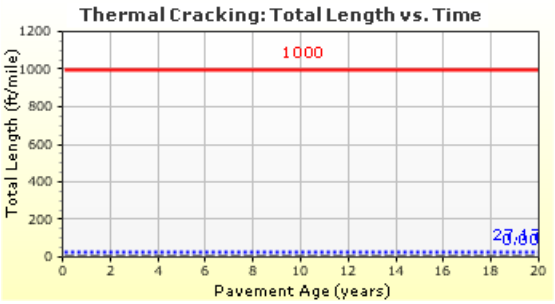

Case 36

Design Inputs

Design Life: 20 years
Design Type: Flexible Pavement
Base construction: May, 2018
Pavement construction: June, 2019
Traffic opening: September, 2019
Climate Data Sources (Lat/Lon): 33.688, -112.082

Design Structure

Layer type	Material Type	Thickness (in)
Flexible	Default asphalt concrete	13.0
NonStabilized	A-1-b	6.0
Subgrade	A-6	Semi-infinite

Volumetric at Construction:	
Effective binder content (%)	5.0
Air voids (%)	5.0

Traffic

Age (year)	Heavy Trucks (cumulative)
2019 (initial)	10,000
2029 (10 years)	18,208,200
2039 (20 years)	38,324,800

Design Outputs

Distress Prediction Summary

Distress Type	Distress @ Specified Reliability		Reliability (%)		Criterion Satisfied?
	Target	Predicted	Target	Achieved	
Terminal IRI (in/mile)	172.00	148.87	90.00	97.93	Pass
Permanent deformation - total pavement (in)	0.75	0.74	90.00	90.92	Pass
AC bottom-up fatigue cracking (% lane area)	25.00	2.43	90.00	100.00	Pass
AC thermal cracking (ft/mile)	1000.00	27.17	90.00	100.00	Pass
AC top-down fatigue cracking (ft/mile)	2000.00	375.12	90.00	100.00	Pass
Permanent deformation - AC only (in)	0.25	0.52	90.00	12.76	Fail

Distress Charts

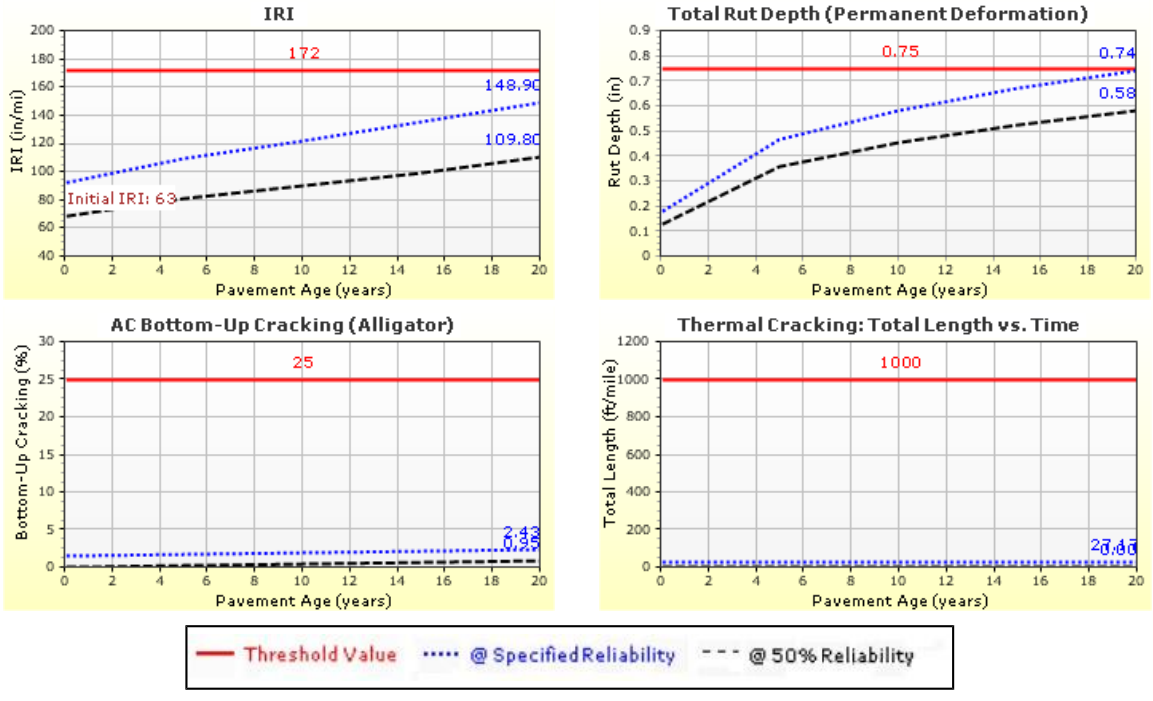

Design Inputs

Design Life: 20 years
Design Type: Flexible Pavement
Base construction: May, 2018
Pavement construction: June, 2019
Traffic opening: September, 2019
Climate Data Sources (Lat/Lon): 33.688, -112.082

Design Structure

Layer type	Material Type	Thickness (in)
Flexible	Default asphalt concrete	13.0
NonStabilized	A-1-b	6.0
Subgrade	A-6	Semi-infinite

Volumetric at Construction:	
Effective binder content (%)	5.0
Air voids (%)	5.0

Traffic

Age (year)	Heavy Trucks (cumulative)
2019 (initial)	10,000
2029 (10 years)	18,208,200
2039 (20 years)	38,324,800

Design Outputs

Distress Prediction Summary

Distress Type	Distress @ Specified Reliability		Reliability (%)		Criterion Satisfied?
	Target	Predicted	Target	Achieved	
Terminal IRI (in/mile)	172.00	147.58	90.00	98.16	Pass
Permanent deformation - total pavement (in)	0.75	0.72	90.00	93.21	Pass
AC bottom-up fatigue cracking (% lane area)	25.00	2.13	90.00	100.00	Pass
AC thermal cracking (ft/mile)	1000.00	27.17	90.00	100.00	Pass
AC top-down fatigue cracking (ft/mile)	2000.00	609.29	90.00	100.00	Pass
Permanent deformation - AC only (in)	0.25	0.52	90.00	12.63	Fail

Distress Charts

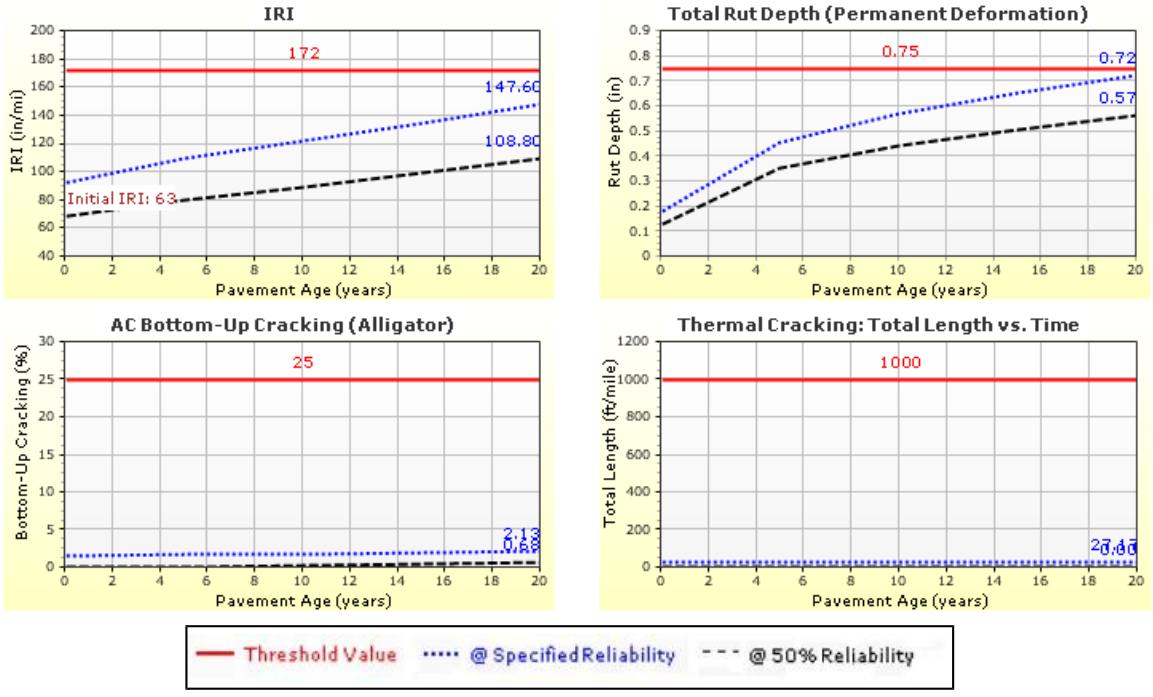

Case 39

Design Inputs

Design Life: 20 years
Design Type: Flexible Pavement
Base construction: May, 2018
Pavement construction: June, 2019
Traffic opening: September, 2019
Climate Data Sources (Lat/Lon): 33.688, -112.082

Design Structure

Layer type	Material Type	Thickness (in)
Flexible	Default asphalt concrete	13.0
NonStabilized	A-1-b	6.0
Subgrade	A-6	Semi-infinite

Volumetric at Construction:	
Effective binder content (%)	5.0
Air voids (%)	5.0

Traffic

Age (year)	Heavy Trucks (cumulative)
2019 (initial)	10,000
2029 (10 years)	18,208,200
2039 (20 years)	38,324,800

Design Outputs

Distress Prediction Summary

Distress Type	Distress @ Specified Reliability		Reliability (%)		Criterion Satisfied?
	Target	Predicted	Target	Achieved	
Terminal IRI (in/mile)	172.00	151.13	90.00	97.49	Pass
Permanent deformation - total pavement (in)	0.75	0.80	90.00	81.45	Fail
AC bottom-up fatigue cracking (% lane area)	25.00	2.48	90.00	100.00	Pass
AC thermal cracking (ft/mile)	1000.00	27.17	90.00	100.00	Pass
AC top-down fatigue cracking (ft/mile)	2000.00	356.34	90.00	100.00	Pass
Permanent deformation - AC only (in)	0.25	0.52	90.00	12.74	Fail

Distress Charts

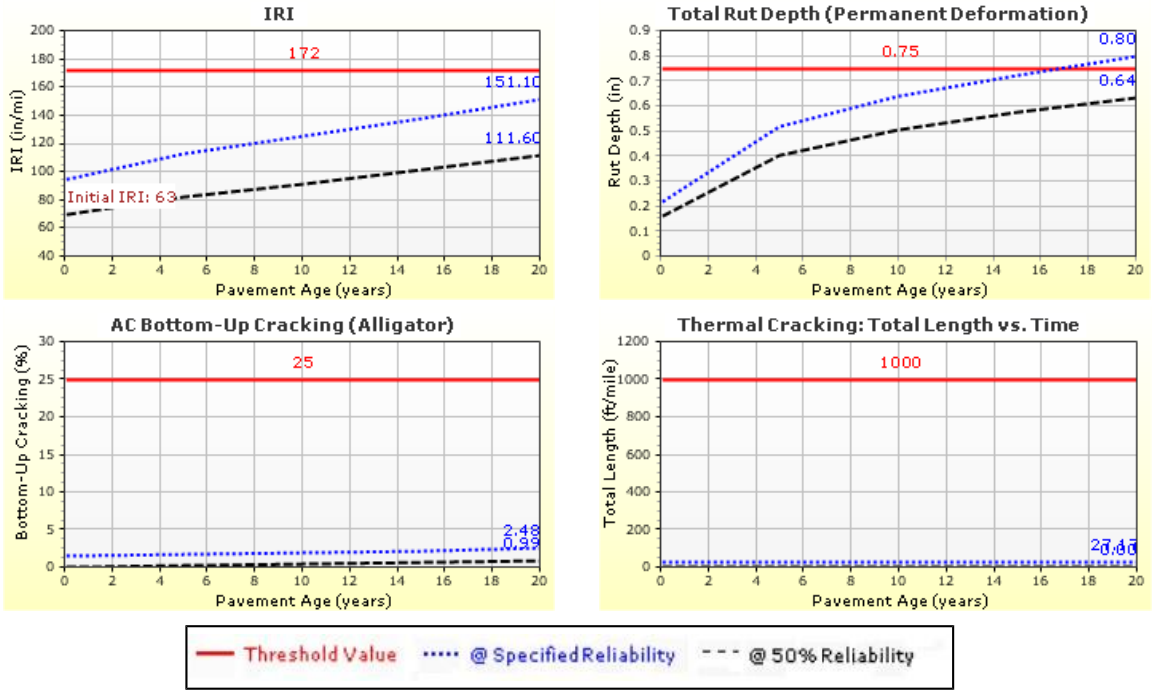

Design Inputs

Design Life: 20 years
Design Type: Flexible Pavement
Base construction: May, 2018
Pavement construction: June, 2019
Traffic opening: September, 2019
Climate Data Sources (Lat/Lon): 33.688, -112.082

Design Structure

Layer type	Material Type	Thickness (in)
Flexible	Default asphalt concrete	13.0
NonStabilized	A-1-b	6.0
Subgrade	A-6	Semi-infinite

Volumetric at Construction:	
Effective binder content (%)	5.0
Air voids (%)	5.0

Traffic

Age (year)	Heavy Trucks (cumulative)
2019 (initial)	10,000
2029 (10 years)	18,208,200
2039 (20 years)	38,324,800

Design Outputs

Distress Prediction Summary

Distress Type	Distress @ Specified Reliability		Reliability (%)		Criterion Satisfied?
	Target	Predicted	Target	Achieved	
Terminal IRI (in/mile)	172.00	149.22	90.00	97.87	Pass
Permanent deformation - total pavement (in)	0.75	0.76	90.00	88.58	Fail
AC bottom-up fatigue cracking (% lane area)	25.00	2.30	90.00	100.00	Pass
AC thermal cracking (ft/mile)	1000.00	27.17	90.00	100.00	Pass
AC top-down fatigue cracking (ft/mile)	2000.00	438.91	90.00	100.00	Pass
Permanent deformation - AC only (in)	0.25	0.52	90.00	12.66	Fail

Distress Charts

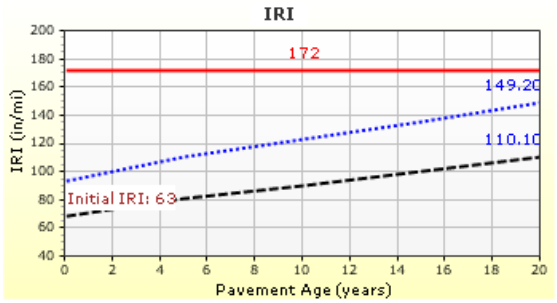

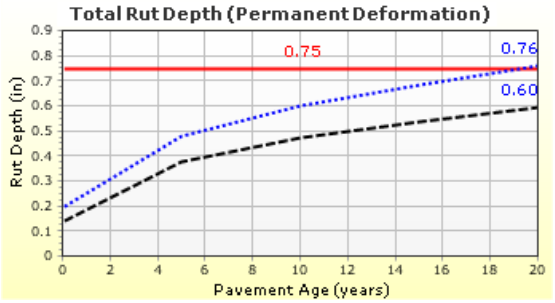

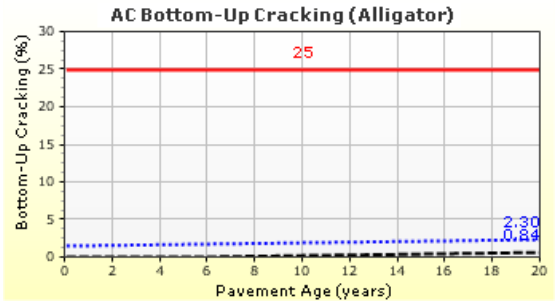

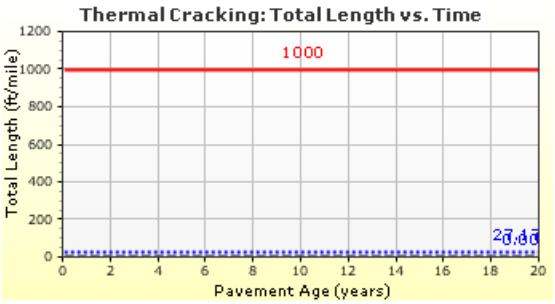

APPENDIX D

MEPDG OUTPUT – VINEYARD SOIL – STRUCTURE 1

Case 1

Design Inputs

Design Life: 20 years
Design Type: Flexible Pavement
Base construction: May, 2018
Pavement construction: June, 2019
Traffic opening: September, 2019
Climate Data Sources (Lat/Lon): 33.688, -112.082

Design Structure

Layer type	Material Type	Thickness (in)
Flexible	Default asphalt concrete	5.4
NonStabilized	A-1-b	14.8
Subgrade	A-6	Semi-infinite

Volumetric at Construction:	
Effective binder content (%)	5.0
Air voids (%)	5.0

Traffic

Age (year)	Heavy Trucks (cumulative)
2019 (initial)	900
2029 (10 years)	1,638,740
2039 (20 years)	3,449,230

Design Outputs

Distress Prediction Summary

Distress Type	Distress @ Specified Reliability		Reliability (%)		Criterion Satisfied?
	Target	Predicted	Target	Achieved	
Terminal IRI (in/mile)	172.00	154.46	90.00	96.67	Pass
Permanent deformation - total pavement (in)	0.75	0.77	90.00	85.51	Fail
AC bottom-up fatigue cracking (% lane area)	25.00	23.53	90.00	91.71	Pass
AC thermal cracking (ft/mile)	1000.00	27.17	90.00	100.00	Pass
AC top-down fatigue cracking (ft/mile)	2000.00	2568.04	90.00	83.42	Fail
Permanent deformation - AC only (in)	0.25	0.33	90.00	59.17	Fail

Distress Charts

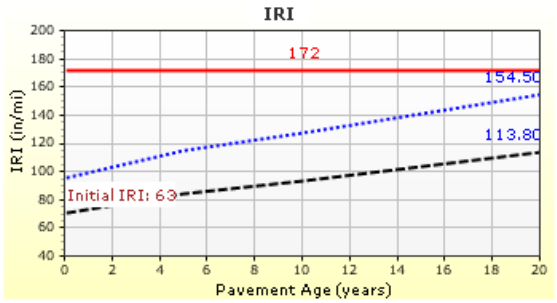

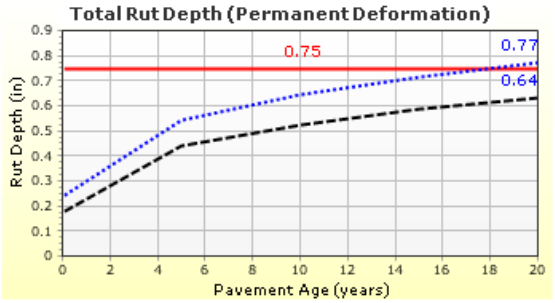

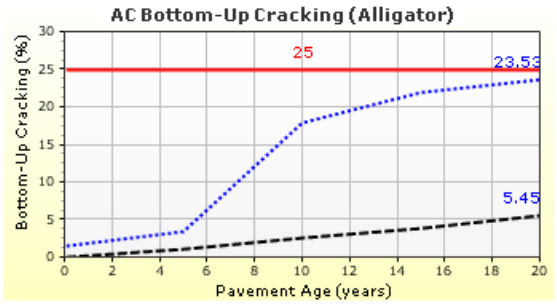

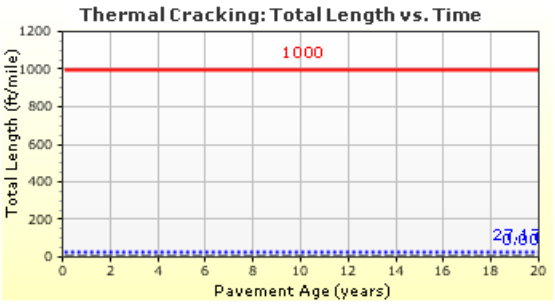

Case 2

Design Inputs

Design Life: 20 years
Design Type: Flexible Pavement
Base construction: May, 2018
Pavement construction: June, 2019
Traffic opening: September, 2019
Climate Data Sources (Lat/Lon): 33.688, -112.082

Design Structure

Layer type	Material Type	Thickness (in)
Flexible	Default asphalt concrete	5.4
NonStabilized	A-1-b	14.8
Subgrade	A-6	Semi-infinite

Volumetric at Construction:	
Effective binder content (%)	5.0
Air voids (%)	5.0

Traffic

Age (year)	Heavy Trucks (cumulative)
2019 (initial)	900
2029 (10 years)	1,638,740
2039 (20 years)	3,449,230

Design Outputs

Distress Prediction Summary

Distress Type	Distress @ Specified Reliability		Reliability (%)		Criterion Satisfied?
	Target	Predicted	Target	Achieved	
Terminal IRI (in/mile)	172.00	146.63	90.00	98.28	Pass
Permanent deformation - total pavement (in)	0.75	0.60	90.00	99.81	Pass
AC bottom-up fatigue cracking (% lane area)	25.00	22.76	90.00	92.51	Pass
AC thermal cracking (ft/mile)	1000.00	27.17	90.00	100.00	Pass
AC top-down fatigue cracking (ft/mile)	2000.00	4224.11	90.00	61.40	Fail
Permanent deformation - AC only (in)	0.25	0.33	90.00	59.34	Fail

Distress Charts

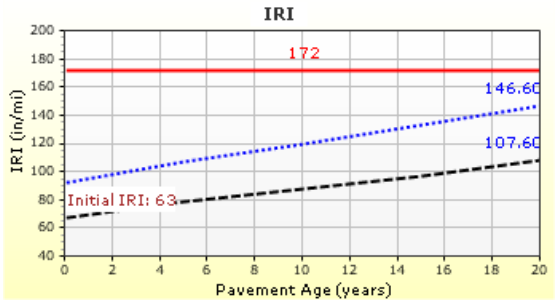

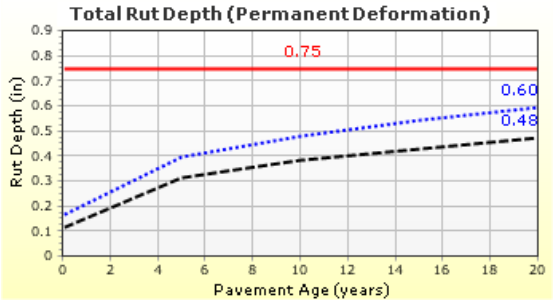

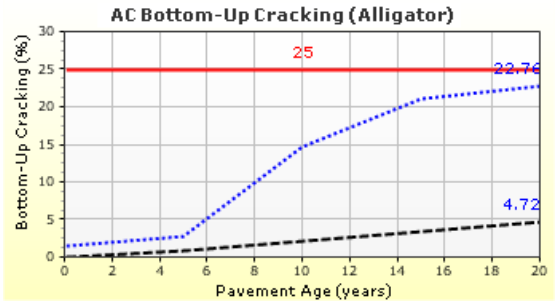

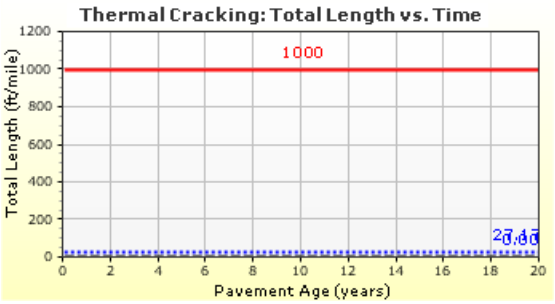

Case 3

Design Inputs

Design Life: 20 years
Design Type: Flexible Pavement
Base construction: May, 2018
Pavement construction: June, 2019
Traffic opening: September, 2019
Climate Data Sources (Lat/Lon): 33.688, -112.082

Design Structure

Layer type	Material Type	Thickness (in)
Flexible	Default asphalt concrete	5.4
NonStabilized	A-1-b	14.8
Subgrade	A-6	Semi-infinite

Volumetric at Construction:	
Effective binder content (%)	5.0
Air voids (%)	5.0

Traffic

Age (year)	Heavy Trucks (cumulative)
2019 (initial)	900
2029 (10 years)	1,638,740
2039 (20 years)	3,449,230

Design Outputs

Distress Prediction Summary

Distress Type	Distress @ Specified Reliability		Reliability (%)		Criterion Satisfied?
	Target	Predicted	Target	Achieved	
Terminal IRI (in/mile)	172.00	173.22	90.00	89.37	Fail
Permanent deformation - total pavement (in)	0.75	1.18	90.00	2.33	Fail
AC bottom-up fatigue cracking (% lane area)	25.00	24.66	90.00	90.42	Pass
AC thermal cracking (ft/mile)	1000.00	27.17	90.00	100.00	Pass
AC top-down fatigue cracking (ft/mile)	2000.00	532.31	90.00	100.00	Pass
Permanent deformation - AC only (in)	0.25	0.33	90.00	60.60	Fail

Distress Charts

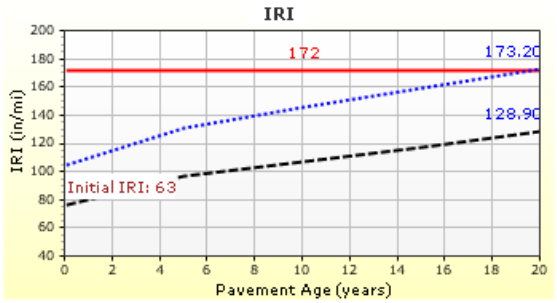

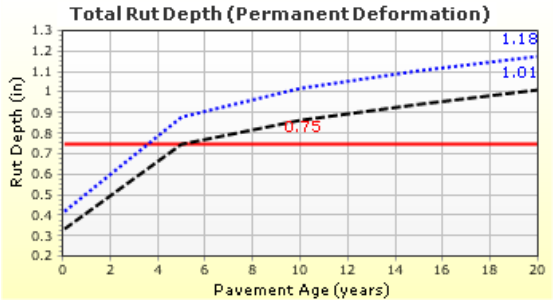

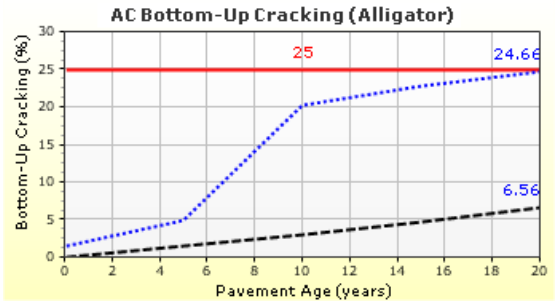

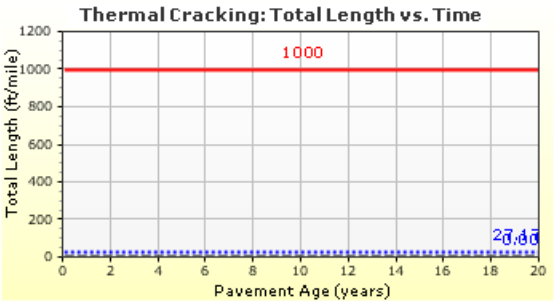

Case 4

Design Inputs

Design Life: 20 years
Design Type: Flexible Pavement
Base construction: May, 2018
Pavement construction: June, 2019
Traffic opening: September, 2019
Climate Data Sources (Lat/Lon): 33.688, -112.082

Design Structure

Layer type	Material Type	Thickness (in)
Flexible	Default asphalt concrete	5.4
NonStabilized	A-1-b	14.8
Subgrade	A-6	Semi-infinite

Volumetric at Construction:	
Effective binder content (%)	5.0
Air voids (%)	5.0

Traffic

Age (year)	Heavy Trucks (cumulative)
2019 (initial)	900
2029 (10 years)	1,638,740
2039 (20 years)	3,449,230

Design Outputs

Distress Prediction Summary

Distress Type	Distress @ Specified Reliability		Reliability (%)		Criterion Satisfied?
	Target	Predicted	Target	Achieved	
Terminal IRI (in/mile)	172.00	160.30	90.00	94.95	Pass
Permanent deformation - total pavement (in)	0.75	0.91	90.00	46.70	Fail
AC bottom-up fatigue cracking (% lane area)	25.00	23.76	90.00	91.46	Pass
AC thermal cracking (ft/mile)	1000.00	27.17	90.00	100.00	Pass
AC top-down fatigue cracking (ft/mile)	2000.00	2084.64	90.00	89.01	Fail
Permanent deformation - AC only (in)	0.25	0.33	90.00	59.01	Fail

Distress Charts

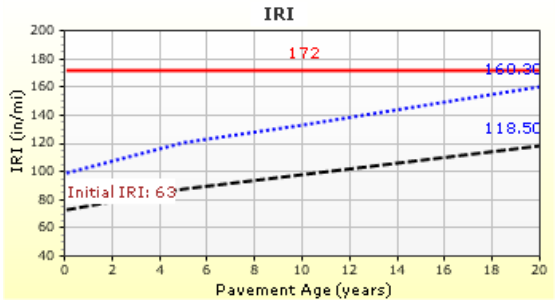

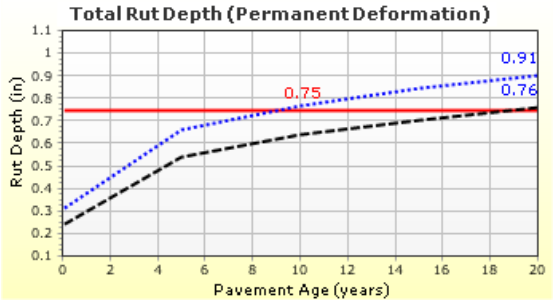

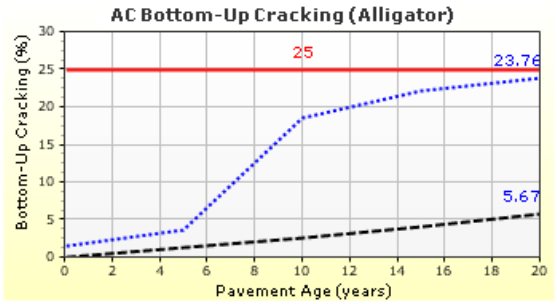

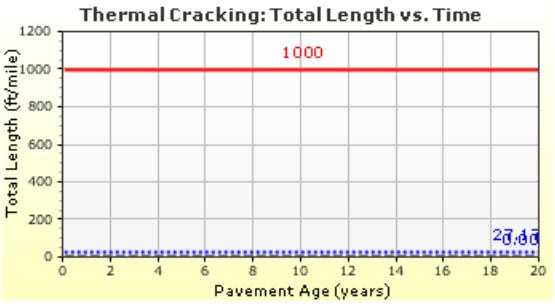

Case 5

Design Inputs

Design Life: 20 years
Design Type: Flexible Pavement
Base construction: May, 2018
Pavement construction: June, 2019
Traffic opening: September, 2019
Climate Data Sources (Lat/Lon): 33.688, -112.082

Design Structure

Layer type	Material Type	Thickness (in)
Flexible	Default asphalt concrete	5.4
NonStabilized	A-1-b	14.8
Subgrade	A-6	Semi-infinite

Volumetric at Construction:	
Effective binder content (%)	5.0
Air voids (%)	5.0

Traffic

Age (year)	Heavy Trucks (cumulative)
2019 (initial)	900
2029 (10 years)	1,638,740
2039 (20 years)	3,449,230

Design Outputs

Distress Prediction Summary

Distress Type	Distress @ Specified Reliability		Reliability (%)		Criterion Satisfied?
	Target	Predicted	Target	Achieved	
Terminal IRI (in/mile)	172.00	156.61	90.00	96.09	Pass
Permanent deformation - total pavement (in)	0.75	0.83	90.00	71.43	Fail
AC bottom-up fatigue cracking (% lane area)	25.00	23.43	90.00	91.82	Pass
AC thermal cracking (ft/mile)	1000.00	27.17	90.00	100.00	Pass
AC top-down fatigue cracking (ft/mile)	2000.00	2670.04	90.00	82.24	Fail
Permanent deformation - AC only (in)	0.25	0.33	90.00	58.85	Fail

Distress Charts

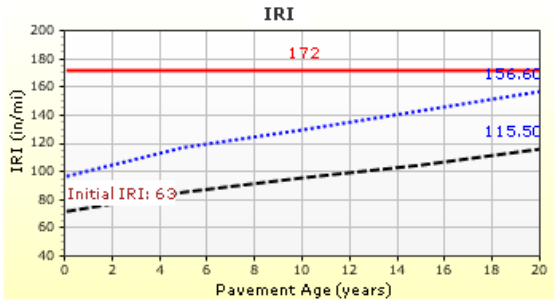

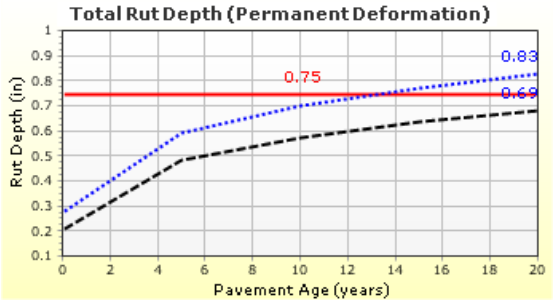

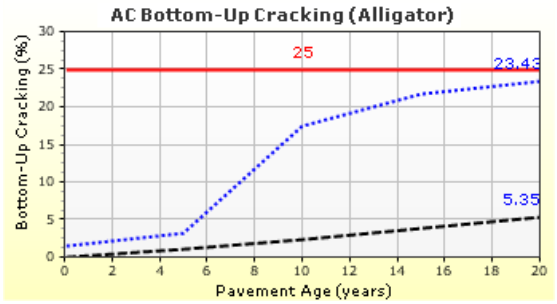

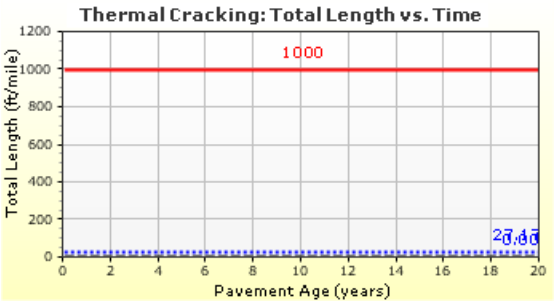

Case 6

Design Inputs

Design Life: 20 years
Design Type: Flexible Pavement
Base construction: May, 2018
Pavement construction: June, 2019
Traffic opening: September, 2019
Climate Data Sources (Lat/Lon): 33.688, -112.082

Design Structure

Layer type	Material Type	Thickness (in)
Flexible	Default asphalt concrete	5.4
NonStabilized	A-1-b	14.8
Subgrade	A-6	Semi-infinite

Volumetric at Construction:	
Effective binder content (%)	5.0
Air voids (%)	5.0

Traffic

Age (year)	Heavy Trucks (cumulative)
2019 (initial)	900
2029 (10 years)	1,638,740
2039 (20 years)	3,449,230

Design Outputs

Distress Prediction Summary

Distress Type	Distress @ Specified Reliability		Reliability (%)		Criterion Satisfied?
	Target	Predicted	Target	Achieved	
Terminal IRI (in/mile)	172.00	151.41	90.00	97.39	Pass
Permanent deformation - total pavement (in)	0.75	0.70	90.00	95.86	Pass
AC bottom-up fatigue cracking (% lane area)	25.00	23.01	90.00	92.26	Pass
AC thermal cracking (ft/mile)	1000.00	27.17	90.00	100.00	Pass
AC top-down fatigue cracking (ft/mile)	2000.00	3500.66	90.00	71.89	Fail
Permanent deformation - AC only (in)	0.25	0.33	90.00	58.90	Fail

Distress Charts

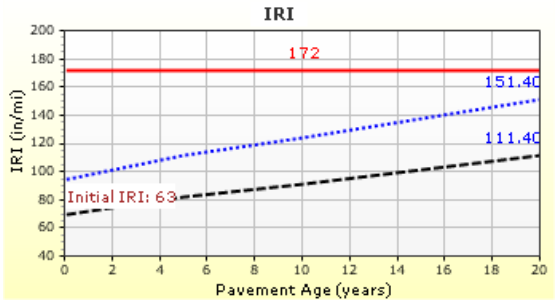

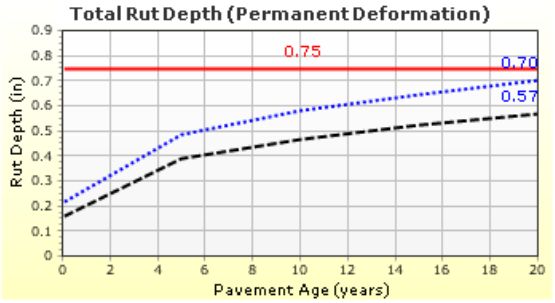

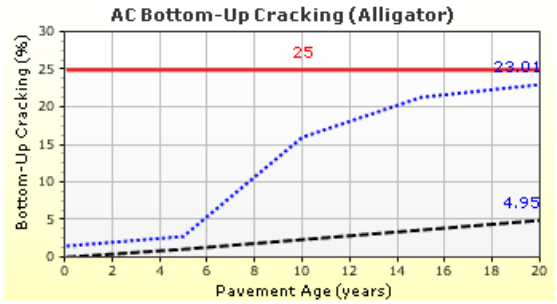

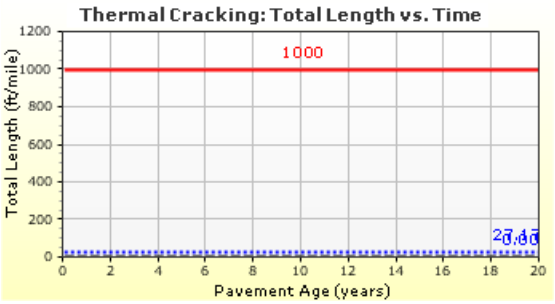

Case 8

Design Inputs

Design Life: 20 years
Design Type: Flexible Pavement
Base construction: May, 2018
Pavement construction: June, 2019
Traffic opening: September, 2019
Climate Data Sources (Lat/Lon): 33.688, -112.082

Design Structure

Layer type	Material Type	Thickness (in)
Flexible	Default asphalt concrete	5.4
NonStabilized	A-1-b	14.8
Subgrade	A-6	Semi-infinite

Volumetric at Construction:	
Effective binder content (%)	5.0
Air voids (%)	5.0

Traffic

Age (year)	Heavy Trucks (cumulative)
2019 (initial)	900
2029 (10 years)	1,638,740
2039 (20 years)	3,449,230

Design Outputs

Distress Prediction Summary

Distress Type	Distress @ Specified Reliability		Reliability (%)		Criterion Satisfied?
	Target	Predicted	Target	Achieved	
Terminal IRI (in/mile)	172.00	150.81	90.00	97.51	Pass
Permanent deformation - total pavement (in)	0.75	0.69	90.00	96.95	Pass
AC bottom-up fatigue cracking (% lane area)	25.00	22.75	90.00	92.52	Pass
AC thermal cracking (ft/mile)	1000.00	27.17	90.00	100.00	Pass
AC top-down fatigue cracking (ft/mile)	2000.00	4072.27	90.00	63.70	Fail
Permanent deformation - AC only (in)	0.25	0.33	90.00	59.01	Fail

Distress Charts

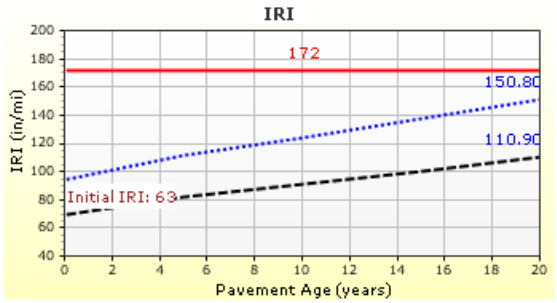

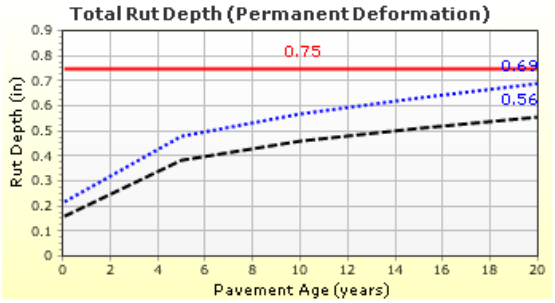

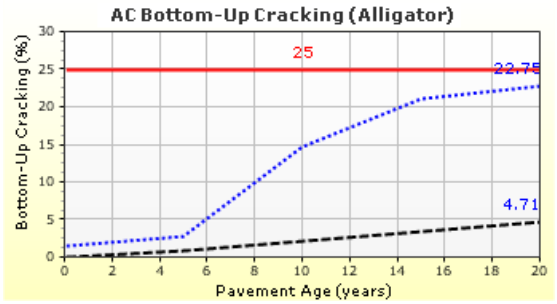

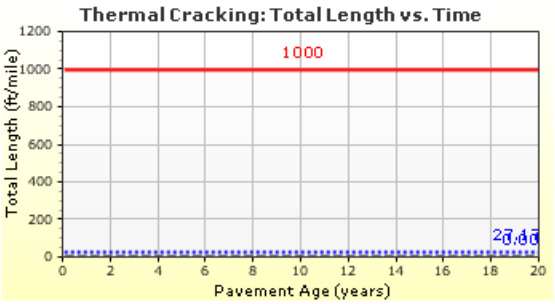

Design Inputs

Design Life: 20 years
Design Type: Flexible Pavement
Base construction: May, 2018
Pavement construction: June, 2019
Traffic opening: September, 2019
Climate Data Sources (Lat/Lon): 33.688, -112.082

Design Structure

Layer type	Material Type	Thickness (in)
Flexible	Default asphalt concrete	5.4
NonStabilized	A-1-b	14.8
Subgrade	A-6	Semi-infinite

Volumetric at Construction:	
Effective binder content (%)	5.0
Air voids (%)	5.0

Traffic

Age (year)	Heavy Trucks (cumulative)
2019 (initial)	900
2029 (10 years)	1,638,740
2039 (20 years)	3,449,230

Design Outputs

Distress Prediction Summary

Distress Type	Distress @ Specified Reliability		Reliability (%)		Criterion Satisfied?
	Target	Predicted	Target	Achieved	
Terminal IRI (in/mile)	172.00	148.31	90.00	97.99	Pass
Permanent deformation - total pavement (in)	0.75	0.63	90.00	99.45	Pass
AC bottom-up fatigue cracking (% lane area)	25.00	22.34	90.00	92.93	Pass
AC thermal cracking (ft/mile)	1000.00	27.17	90.00	100.00	Pass
AC top-down fatigue cracking (ft/mile)	2000.00	4971.54	90.00	49.65	Fail
Permanent deformation - AC only (in)	0.25	0.33	90.00	59.07	Fail

Distress Charts

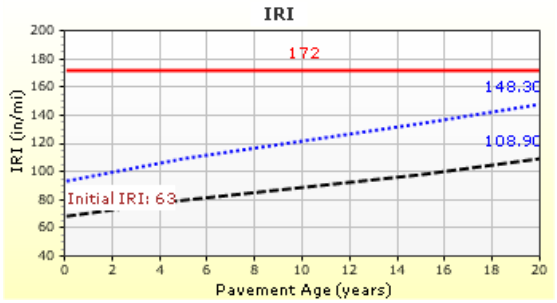

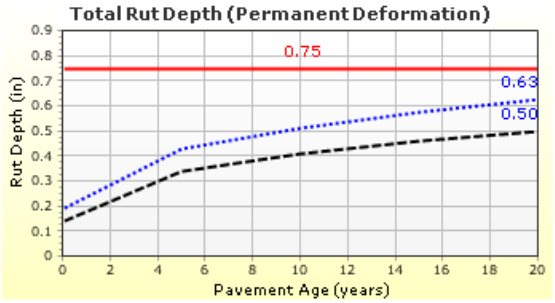

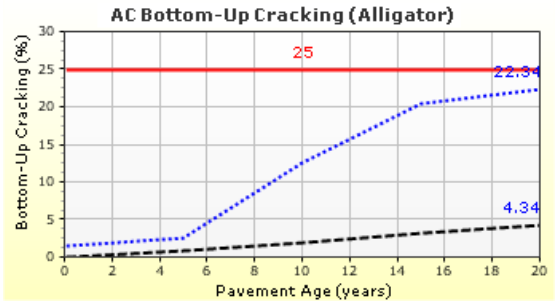

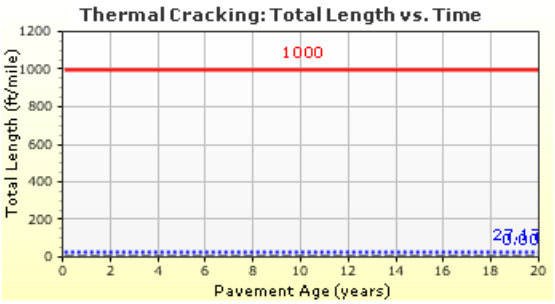

Case 10

Design Inputs

Design Life: 20 years
Design Type: Flexible Pavement
Base construction: May, 2018
Pavement construction: June, 2019
Traffic opening: September, 2019
Climate Data Sources (Lat/Lon): 33.688, -112.082

Design Structure

Layer type	Material Type	Thickness (in)
Flexible	Default asphalt concrete	5.4
NonStabilized	A-1-b	14.8
Subgrade	A-6	Semi-infinite

Volumetric at Construction:	
Effective binder content (%)	5.0
Air voids (%)	5.0

Traffic

Age (year)	Heavy Trucks (cumulative)
2019 (initial)	900
2029 (10 years)	1,638,740
2039 (20 years)	3,449,230

Design Outputs

Distress Prediction Summary

Distress Type	Distress @ Specified Reliability		Reliability (%)		Criterion Satisfied?
	Target	Predicted	Target	Achieved	
Terminal IRI (in/mile)	172.00	147.03	90.00	98.21	Pass
Permanent deformation - total pavement (in)	0.75	0.59	90.00	99.84	Pass
AC bottom-up fatigue cracking (% lane area)	25.00	22.06	90.00	93.21	Pass
AC thermal cracking (ft/mile)	1000.00	27.17	90.00	100.00	Pass
AC top-down fatigue cracking (ft/mile)	2000.00	5614.80	90.00	39.54	Fail
Permanent deformation - AC only (in)	0.25	0.33	90.00	59.34	Fail

Distress Charts

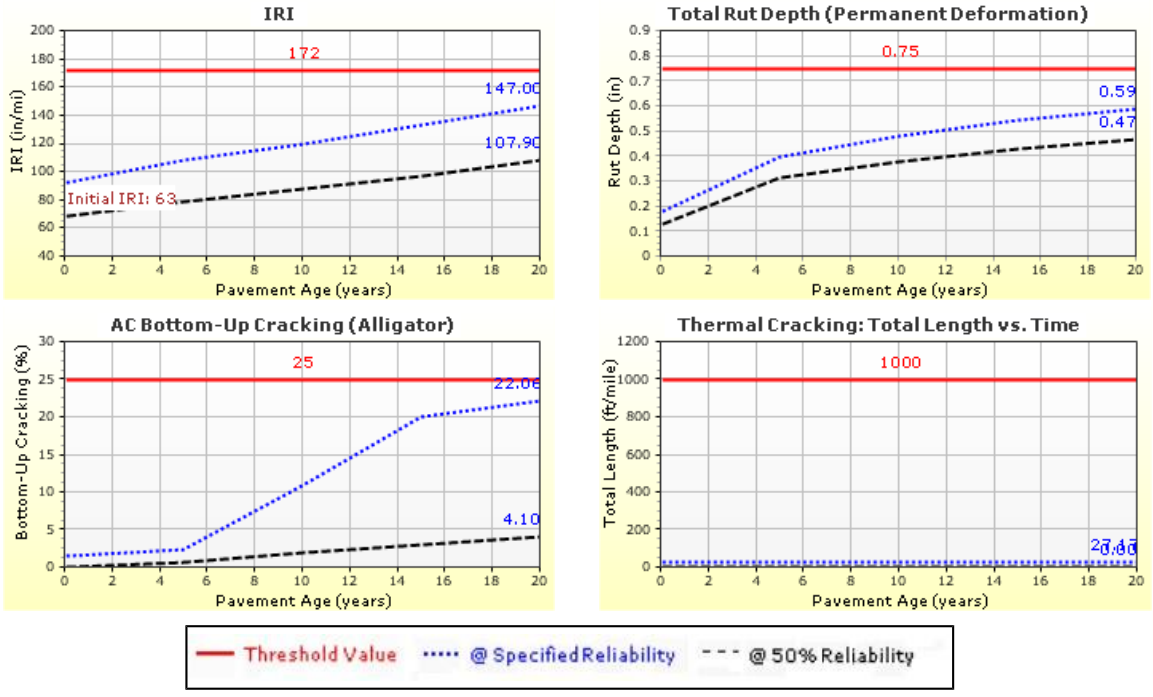

Design Inputs

Design Life: 20 years
Design Type: Flexible Pavement
Base construction: May, 2018
Pavement construction: June, 2019
Traffic opening: September, 2019
Climate Data Sources (Lat/Lon): 33.688, -112.082

Design Structure

Layer type	Material Type	Thickness (in)
Flexible	Default asphalt concrete	5.4
NonStabilized	A-1-b	14.8
Subgrade	A-6	Semi-infinite

Volumetric at Construction:	
Effective binder content (%)	5.0
Air voids (%)	5.0

Traffic

Age (year)	Heavy Trucks (cumulative)
2019 (initial)	4,500
2029 (10 years)	8,193,680
2039 (20 years)	17,246,100

Design Outputs

Distress Prediction Summary

Distress Type	Distress @ Specified Reliability		Reliability (%)		Criterion Satisfied?
	Target	Predicted	Target	Achieved	
Terminal IRI (in/mile)	172.00	184.97	90.00	82.28	Fail
Permanent deformation - total pavement (in)	0.75	1.22	90.00	5.78	Fail
AC bottom-up fatigue cracking (% lane area)	25.00	44.41	90.00	46.33	Fail
AC thermal cracking (ft/mile)	1000.00	27.17	90.00	100.00	Pass
AC top-down fatigue cracking (ft/mile)	2000.00	5069.12	90.00	48.10	Fail
Permanent deformation - AC only (in)	0.25	0.68	90.00	3.49	Fail

Distress Charts

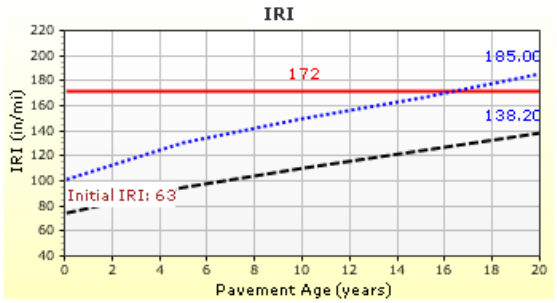

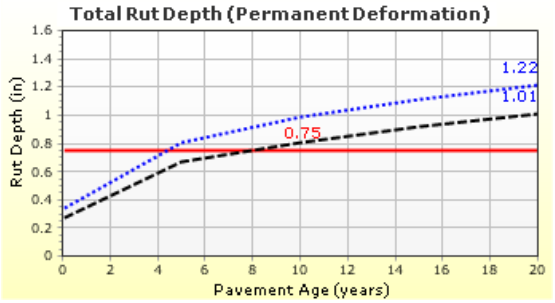

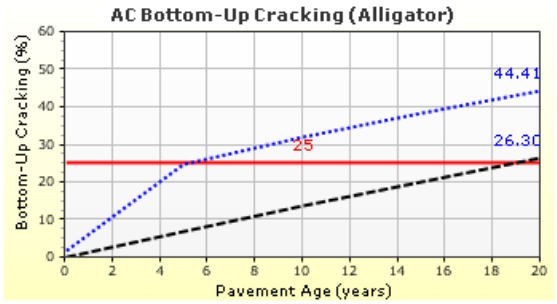

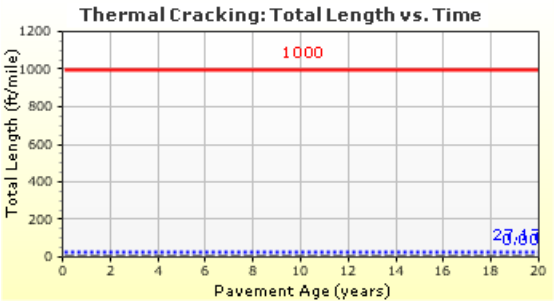

Design Inputs

Design Life: 20 years
Design Type: Flexible Pavement
Base construction: May, 2018
Pavement construction: June, 2019
Traffic opening: September, 2019
Climate Data Sources (Lat/Lon): 33.688, -112.082

Design Structure

Layer type	Material Type	Thickness (in)
Flexible	Default asphalt concrete	5.4
NonStabilized	A-1-b	14.8
Subgrade	A-6	Semi-infinite

Volumetric at Construction:	
Effective binder content (%)	5.0
Air voids (%)	5.0

Traffic

Age (year)	Heavy Trucks (cumulative)
2019 (initial)	4,500
2029 (10 years)	8,193,680
2039 (20 years)	17,246,100

Design Outputs

Distress Prediction Summary

Distress Type	Distress @ Specified Reliability		Reliability (%)		Criterion Satisfied?
	Target	Predicted	Target	Achieved	
Terminal IRI (in/mile)	172.00	175.15	90.00	88.33	Fail
Permanent deformation - total pavement (in)	0.75	0.96	90.00	46.49	Fail
AC bottom-up fatigue cracking (% lane area)	25.00	38.61	90.00	62.49	Fail
AC thermal cracking (ft/mile)	1000.00	27.17	90.00	100.00	Pass
AC top-down fatigue cracking (ft/mile)	2000.00	11698.14	90.00	0.40	Fail
Permanent deformation - AC only (in)	0.25	0.68	90.00	3.58	Fail

Distress Charts

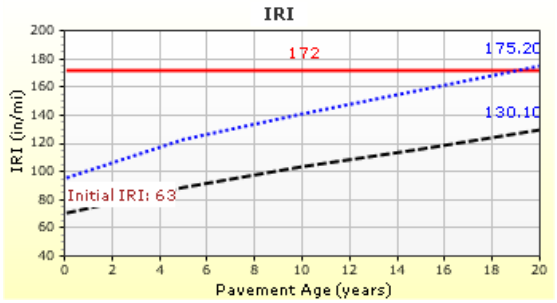

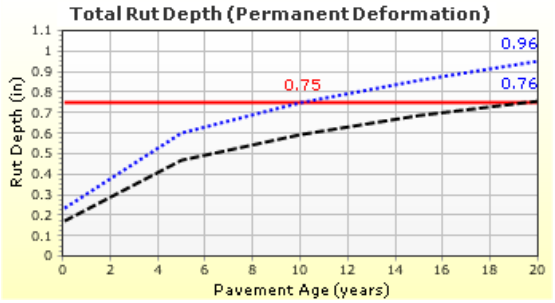

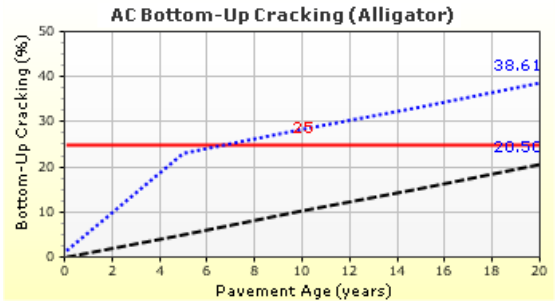

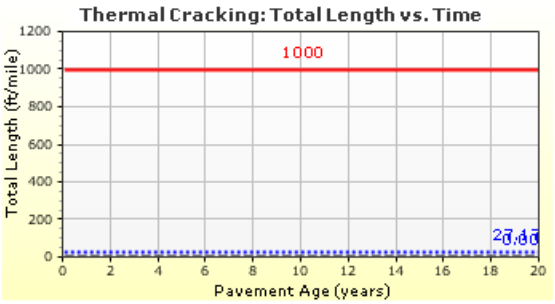

Design Inputs

Design Life: 20 years
Design Type: Flexible Pavement
Base construction: May, 2018
Pavement construction: June, 2019
Traffic opening: September, 2019
Climate Data Sources (Lat/Lon): 33.688, -112.082

Design Structure

Layer type	Material Type	Thickness (in)
Flexible	Default asphalt concrete	5.4
NonStabilized	A-1-b	14.8
Subgrade	A-6	Semi-infinite

Volumetric at Construction:	
Effective binder content (%)	5.0
Air voids (%)	5.0

Traffic

Age (year)	Heavy Trucks (cumulative)
2019 (initial)	4,500
2029 (10 years)	8,193,680
2039 (20 years)	17,246,100

Design Outputs

Distress Prediction Summary

Distress Type	Distress @ Specified Reliability		Reliability (%)		Criterion Satisfied?
	Target	Predicted	Target	Achieved	
Terminal IRI (in/mile)	172.00	206.67	90.00	65.52	Fail
Permanent deformation - total pavement (in)	0.75	1.69	90.00	0.01	Fail
AC bottom-up fatigue cracking (% lane area)	25.00	48.41	90.00	35.38	Fail
AC thermal cracking (ft/mile)	1000.00	27.17	90.00	100.00	Pass
AC top-down fatigue cracking (ft/mile)	2000.00	1209.90	90.00	98.34	Pass
Permanent deformation - AC only (in)	0.25	0.67	90.00	3.68	Fail

Distress Charts

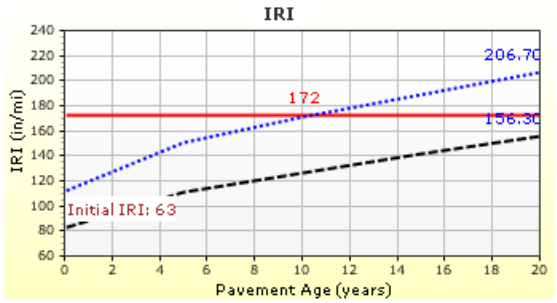

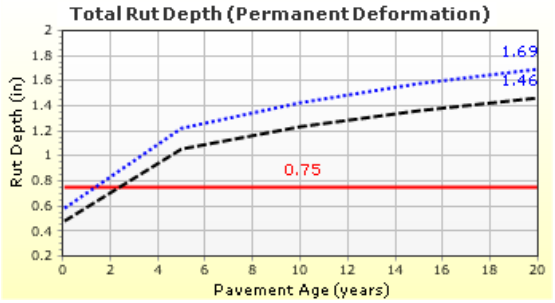

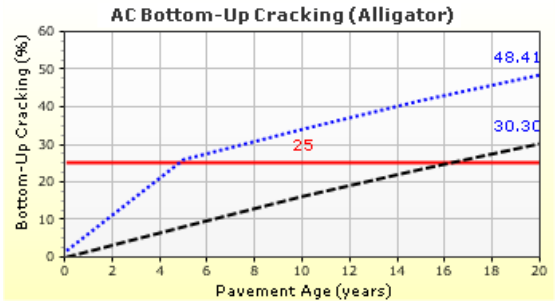

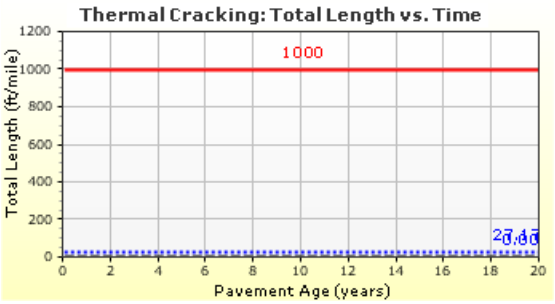

Design Inputs

Design Life: 20 years
Design Type: Flexible Pavement
Base construction: May, 2018
Pavement construction: June, 2019
Traffic opening: September, 2019
Climate Data Sources (Lat/Lon): 33.688, -112.082

Design Structure

Layer type	Material Type	Thickness (in)
Flexible	Default asphalt concrete	5.4
NonStabilized	A-1-b	14.8
Subgrade	A-6	Semi-infinite

Volumetric at Construction:	
Effective binder content (%)	5.0
Air voids (%)	5.0

Traffic

Age (year)	Heavy Trucks (cumulative)
2019 (initial)	4,500
2029 (10 years)	8,193,680
2039 (20 years)	17,246,100

Design Outputs

Distress Prediction Summary

Distress Type	Distress @ Specified Reliability		Reliability (%)		Criterion Satisfied?
	Target	Predicted	Target	Achieved	
Terminal IRI (in/mile)	172.00	191.12	90.00	77.91	Fail
Permanent deformation - total pavement (in)	0.75	1.37	90.00	0.92	Fail
AC bottom-up fatigue cracking (% lane area)	25.00	45.21	90.00	44.09	Fail
AC thermal cracking (ft/mile)	1000.00	27.17	90.00	100.00	Pass
AC top-down fatigue cracking (ft/mile)	2000.00	3819.74	90.00	67.42	Fail
Permanent deformation - AC only (in)	0.25	0.68	90.00	3.47	Fail

Distress Charts

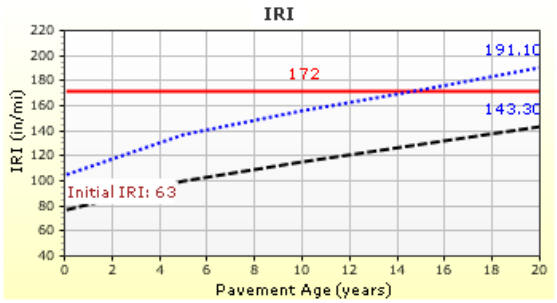

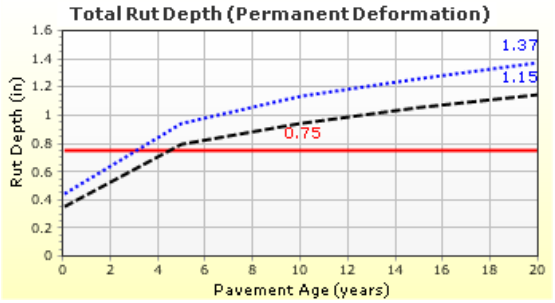

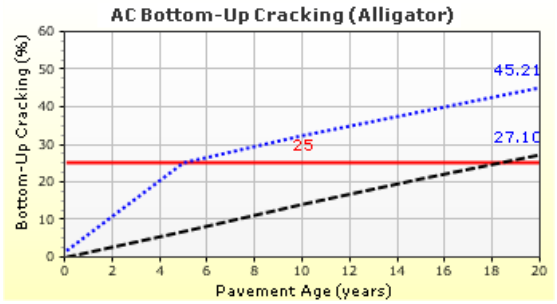

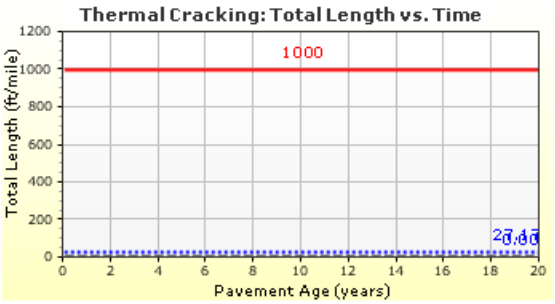

Design Inputs

Design Life: 20 years
Design Type: Flexible Pavement
Base construction: May, 2018
Pavement construction: June, 2019
Traffic opening: September, 2019
Climate Data Sources (Lat/Lon): 33.688, -112.082

Design Structure

Layer type	Material Type	Thickness (in)
Flexible	Default asphalt concrete	5.4
NonStabilized	A-1-b	14.8
Subgrade	A-6	Semi-infinite

Volumetric at Construction:	
Effective binder content (%)	5.0
Air voids (%)	5.0

Traffic

Age (year)	Heavy Trucks (cumulative)
2019 (initial)	4,500
2029 (10 years)	8,193,680
2039 (20 years)	17,246,100

Design Outputs

Distress Prediction Summary

Distress Type	Distress @ Specified Reliability		Reliability (%)		Criterion Satisfied?
	Target	Predicted	Target	Achieved	
Terminal IRI (in/mile)	172.00	187.26	90.00	80.70	Fail
Permanent deformation - total pavement (in)	0.75	1.27	90.00	3.06	Fail
AC bottom-up fatigue cracking (% lane area)	25.00	44.01	90.00	47.46	Fail
AC thermal cracking (ft/mile)	1000.00	27.17	90.00	100.00	Pass
AC top-down fatigue cracking (ft/mile)	2000.00	5391.47	90.00	43.01	Fail
Permanent deformation - AC only (in)	0.25	0.68	90.00	3.45	Fail

Distress Charts

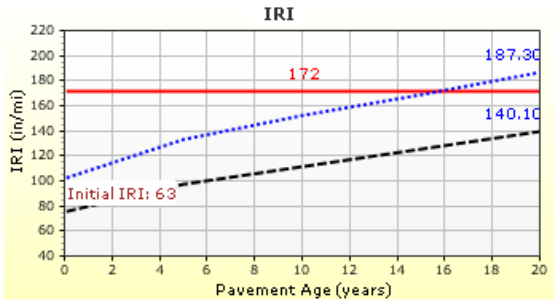

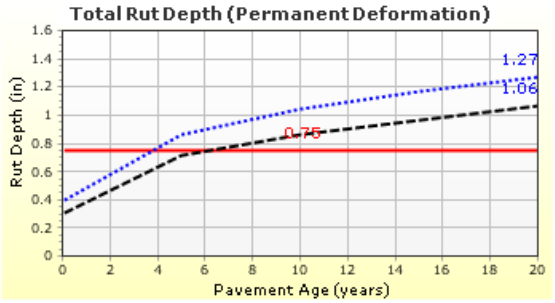

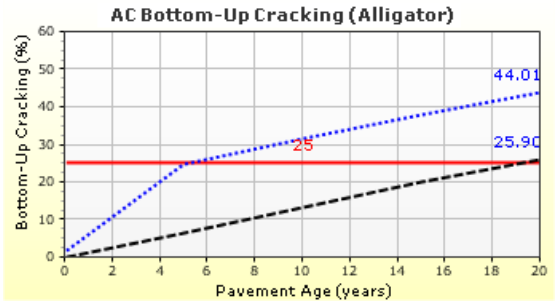

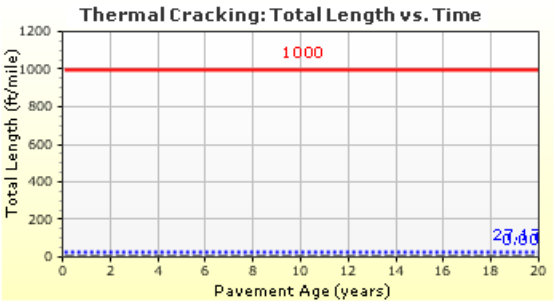

Design Inputs

Design Life: 20 years
Design Type: Flexible Pavement
Base construction: May, 2018
Pavement construction: June, 2019
Traffic opening: September, 2019
Climate Data Sources (Lat/Lon): 33.688, -112.082

Design Structure

Layer type	Material Type	Thickness (in)
Flexible	Default asphalt concrete	5.4
NonStabilized	A-1-b	14.8
Subgrade	A-6	Semi-infinite

Volumetric at Construction:	
Effective binder content (%)	5.0
Air voids (%)	5.0

Traffic

Age (year)	Heavy Trucks (cumulative)
2019 (initial)	4,500
2029 (10 years)	8,193,680
2039 (20 years)	17,246,100

Design Outputs

Distress Prediction Summary

Distress Type	Distress @ Specified Reliability		Reliability (%)		Criterion Satisfied?
	Target	Predicted	Target	Achieved	
Terminal IRI (in/mile)	172.00	182.25	90.00	84.08	Fail
Permanent deformation - total pavement (in)	0.75	1.13	90.00	13.93	Fail
AC bottom-up fatigue cracking (% lane area)	25.00	42.51	90.00	51.69	Fail
AC thermal cracking (ft/mile)	1000.00	27.17	90.00	100.00	Pass
AC top-down fatigue cracking (ft/mile)	2000.00	8077.38	90.00	10.73	Fail
Permanent deformation - AC only (in)	0.25	0.68	90.00	3.46	Fail

Distress Charts

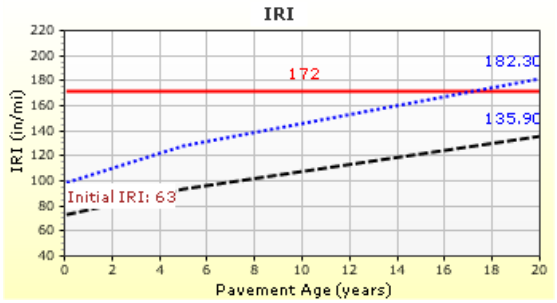

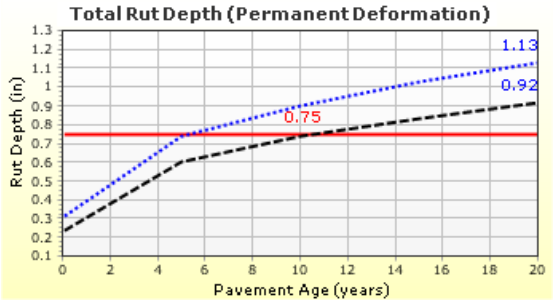

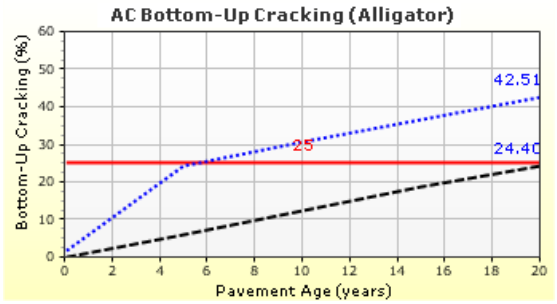

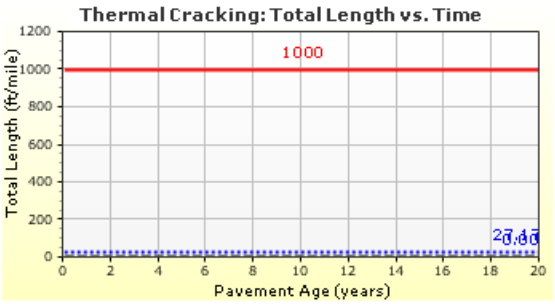

Design Inputs

Design Life: 20 years
Design Type: Flexible Pavement
Base construction: May, 2018
Pavement construction: June, 2019
Traffic opening: September, 2019
Climate Data Sources (Lat/Lon): 33.688, -112.082

Design Structure

Layer type	Material Type	Thickness (in)
Flexible	Default asphalt concrete	5.4
NonStabilized	A-1-b	14.8
Subgrade	A-6	Semi-infinite

Volumetric at Construction:	
Effective binder content (%)	5.0
Air voids (%)	5.0

Traffic

Age (year)	Heavy Trucks (cumulative)
2019 (initial)	4,500
2029 (10 years)	8,193,680
2039 (20 years)	17,246,100

Design Outputs

Distress Prediction Summary

Distress Type	Distress @ Specified Reliability		Reliability (%)		Criterion Satisfied?
	Target	Predicted	Target	Achieved	
Terminal IRI (in/mile)	172.00	181.66	90.00	84.46	Fail
Permanent deformation - total pavement (in)	0.75	1.11	90.00	16.78	Fail
AC bottom-up fatigue cracking (% lane area)	25.00	41.51	90.00	54.51	Fail
AC thermal cracking (ft/mile)	1000.00	27.17	90.00	100.00	Pass
AC top-down fatigue cracking (ft/mile)	2000.00	9468.54	90.00	3.69	Fail
Permanent deformation - AC only (in)	0.25	0.68	90.00	3.47	Fail

Distress Charts

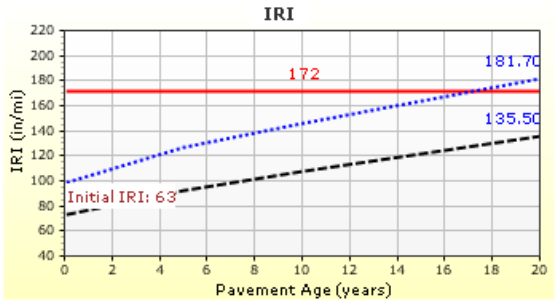

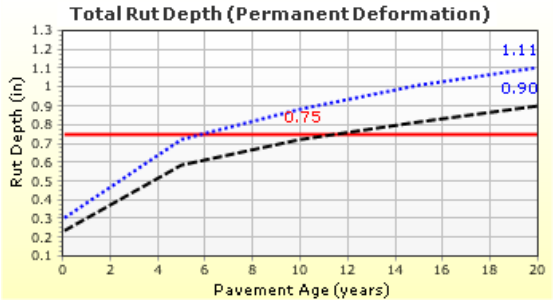

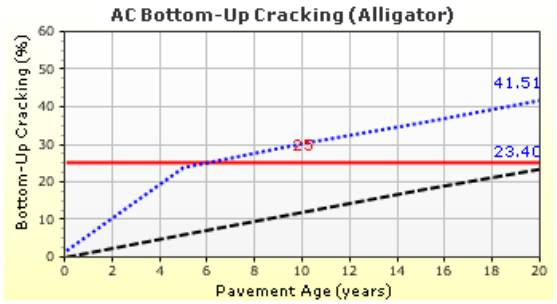

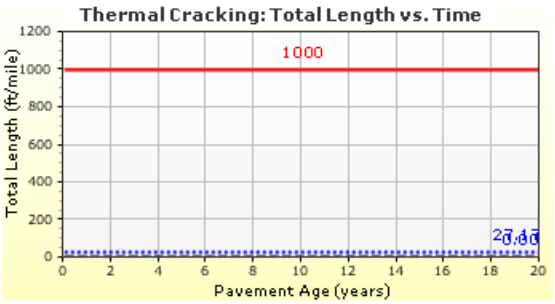

Design Inputs

Design Life: 20 years
Design Type: Flexible Pavement
Base construction: May, 2018
Pavement construction: June, 2019
Traffic opening: September, 2019
Climate Data Sources (Lat/Lon): 33.688, -112.082

Design Structure

Layer type	Material Type	Thickness (in)
Flexible	Default asphalt concrete	5.4
NonStabilized	A-1-b	14.8
Subgrade	A-6	Semi-infinite

Volumetric at Construction:	
Effective binder content (%)	5.0
Air voids (%)	5.0

Traffic

Age (year)	Heavy Trucks (cumulative)
2019 (initial)	4,500
2029 (10 years)	8,193,680
2039 (20 years)	17,246,100

Design Outputs

Distress Prediction Summary

Distress Type	Distress @ Specified Reliability		Reliability (%)		Criterion Satisfied?
	Target	Predicted	Target	Achieved	
Terminal IRI (in/mile)	172.00	178.54	90.00	86.39	Fail
Permanent deformation - total pavement (in)	0.75	1.03	90.00	29.58	Fail
AC bottom-up fatigue cracking (% lane area)	25.00	40.01	90.00	58.68	Fail
AC thermal cracking (ft/mile)	1000.00	27.17	90.00	100.00	Pass
AC top-down fatigue cracking (ft/mile)	2000.00	10874.36	90.00	0.98	Fail
Permanent deformation - AC only (in)	0.25	0.68	90.00	3.47	Fail

Distress Charts

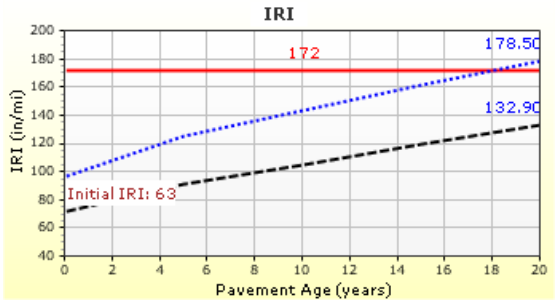

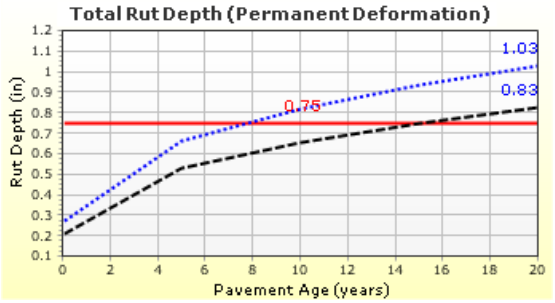

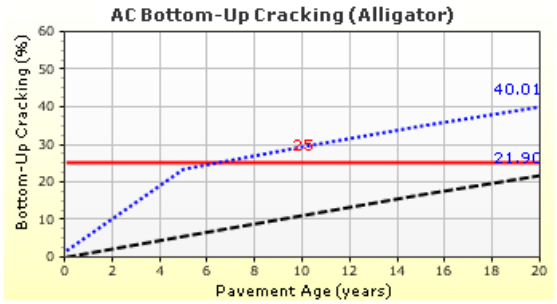

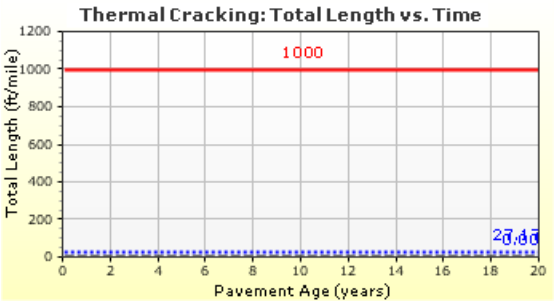

Design Inputs

Design Life: 20 years
Design Type: Flexible Pavement
Base construction: May, 2018
Pavement construction: June, 2019
Traffic opening: September, 2019
Climate Data Sources (Lat/Lon): 33.688, -112.082

Design Structure

Layer type	Material Type	Thickness (in)
Flexible	Default asphalt concrete	5.4
NonStabilized	A-1-b	14.8
Subgrade	A-6	Semi-infinite

Volumetric at Construction:	
Effective binder content (%)	5.0
Air voids (%)	5.0

Traffic

Age (year)	Heavy Trucks (cumulative)
2019 (initial)	4,500
2029 (10 years)	8,193,680
2039 (20 years)	17,246,100

Design Outputs

Distress Prediction Summary

Distress Type	Distress @ Specified Reliability		Reliability (%)		Criterion Satisfied?
	Target	Predicted	Target	Achieved	
Terminal IRI (in/mile)	172.00	176.57	90.00	87.54	Fail
Permanent deformation - total pavement (in)	0.75	0.99	90.00	38.80	Fail
AC bottom-up fatigue cracking (% lane area)	25.00	39.01	90.00	61.42	Fail
AC thermal cracking (ft/mile)	1000.00	27.17	90.00	100.00	Pass
AC top-down fatigue cracking (ft/mile)	2000.00	11515.16	90.00	0.49	Fail
Permanent deformation - AC only (in)	0.25	0.68	90.00	3.51	Fail

Distress Charts

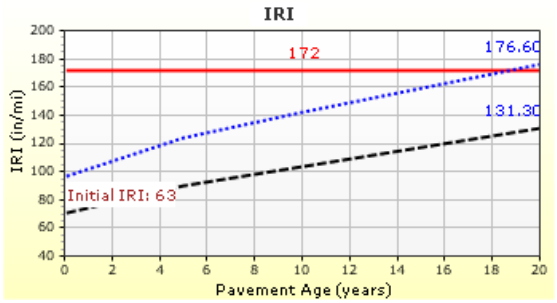

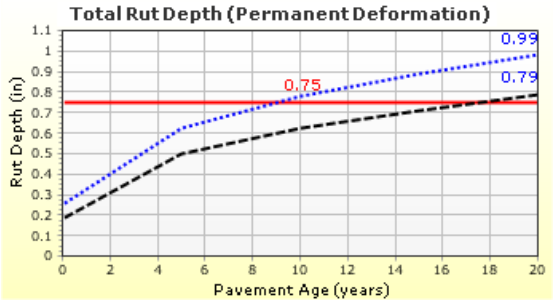

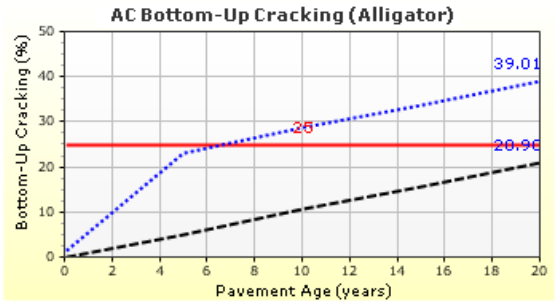

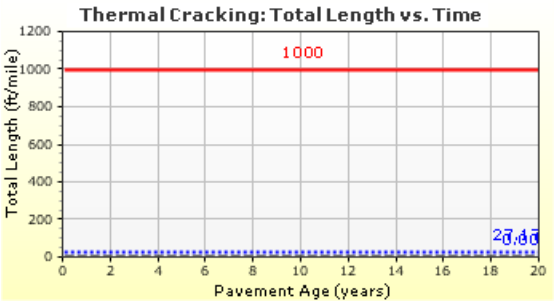

APPENDIX E

MEPDG OUTPUT – VINEYARD SOIL – STRUCTURE 2

Case 21

Design Inputs

Design Life: 20 years
Design Type: Flexible Pavement
Base construction: May, 2018
Pavement construction: June, 2019
Traffic opening: September, 2019
Climate Data Sources (Lat/Lon): 33.688, -112.082

Design Structure

Layer type	Material Type	Thickness (in)
Flexible	Default asphalt concrete	13.0
NonStabilized	A-1-b	6.0
Subgrade	A-6	Semi-infinite

Volumetric at Construction:	
Effective binder content (%)	5.0
Air voids (%)	5.0

Traffic

Age (year)	Heavy Trucks (cumulative)
2019 (initial)	2,000
2029 (10 years)	3,641,630
2039 (20 years)	7,664,950

Design Outputs

Distress Prediction Summary

Distress Type	Distress @ Specified Reliability		Reliability (%)		Criterion Satisfied?
	Target	Predicted	Target	Achieved	
Terminal IRI (in/mile)	172.00	142.01	90.00	98.95	Pass
Permanent deformation - total pavement (in)	0.75	0.57	90.00	99.94	Pass
AC bottom-up fatigue cracking (% lane area)	25.00	1.76	90.00	100.00	Pass
AC thermal cracking (ft/mile)	1000.00	27.17	90.00	100.00	Pass
AC top-down fatigue cracking (ft/mile)	2000.00	258.41	90.00	100.00	Pass
Permanent deformation - AC only (in)	0.25	0.25	90.00	90.53	Pass

Distress Charts

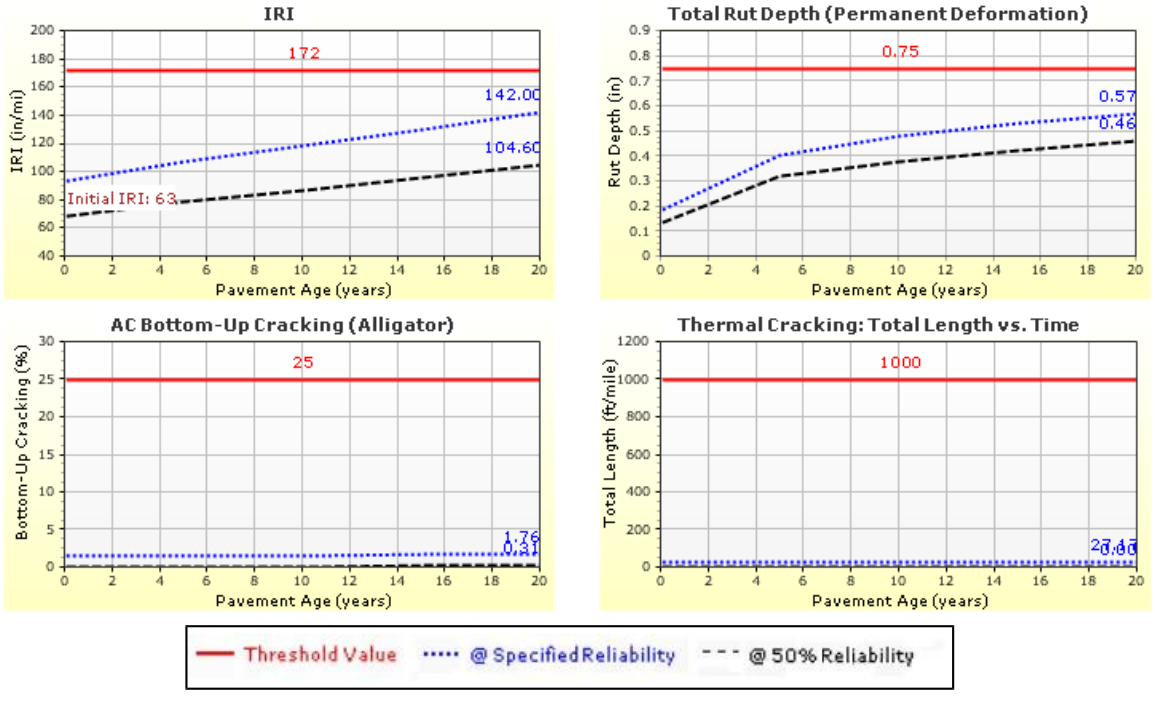

Case 22

Design Inputs

Design Life: 20 years
Design Type: Flexible Pavement
Base construction: May, 2018
Pavement construction: June, 2019
Traffic opening: September, 2019
Climate Data Sources (Lat/Lon): 33.688, -112.082

Design Structure

Layer type	Material Type	Thickness (in)
Flexible	Default asphalt concrete	13.0
NonStabilized	A-1-b	6.0
Subgrade	A-6	Semi-infinite

Volumetric at Construction:	
Effective binder content (%)	5.0
Air voids (%)	5.0

Traffic

Age (year)	Heavy Trucks (cumulative)
2019 (initial)	2,000
2029 (10 years)	3,641,630
2039 (20 years)	7,664,950

Design Outputs

Distress Prediction Summary

Distress Type	Distress @ Specified Reliability		Reliability (%)		Criterion Satisfied?
	Target	Predicted	Target	Achieved	
Terminal IRI (in/mile)	172.00	134.61	90.00	99.56	Pass
Permanent deformation - total pavement (in)	0.75	0.42	90.00	100.00	Pass
AC bottom-up fatigue cracking (% lane area)	25.00	1.62	90.00	100.00	Pass
AC thermal cracking (ft/mile)	1000.00	27.17	90.00	100.00	Pass
AC top-down fatigue cracking (ft/mile)	2000.00	285.93	90.00	100.00	Pass
Permanent deformation - AC only (in)	0.25	0.25	90.00	90.02	Pass

Distress Charts

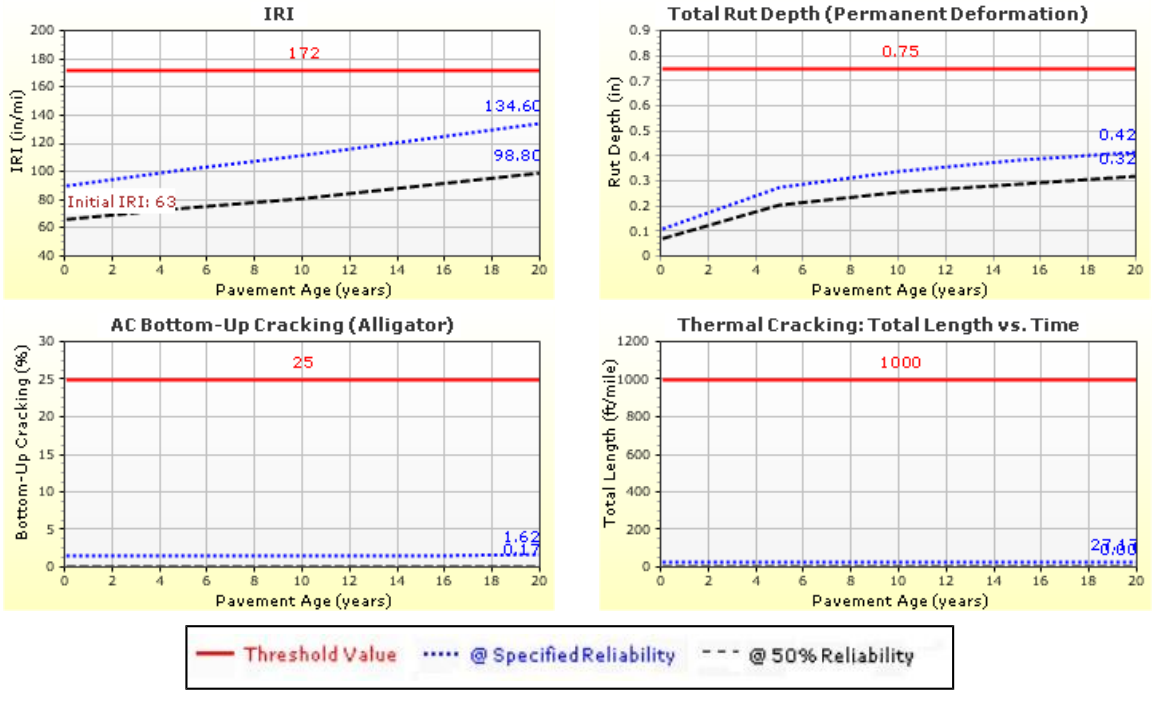

Design Inputs

Design Life: 20 years
Design Type: Flexible Pavement
Base construction: May, 2018
Pavement construction: June, 2019
Traffic opening: September, 2019
Climate Data Sources (Lat/Lon): 33.688, -112.082

Design Structure

Layer type	Material Type	Thickness (in)
Flexible	Default asphalt concrete	13.0
NonStabilized	A-1-b	6.0
Subgrade	A-6	Semi-infinite

Volumetric at Construction:	
Effective binder content (%)	5.0
Air voids (%)	5.0

Traffic

Age (year)	Heavy Trucks (cumulative)
2019 (initial)	2,000
2029 (10 years)	3,641,630
2039 (20 years)	7,664,950

Design Outputs

Distress Prediction Summary

Distress Type	Distress @ Specified Reliability		Reliability (%)		Criterion Satisfied?
	Target	Predicted	Target	Achieved	
Terminal IRI (in/mile)	172.00	157.65	90.00	95.85	Pass
Permanent deformation - total pavement (in)	0.75	0.91	90.00	42.82	Fail
AC bottom-up fatigue cracking (% lane area)	25.00	2.08	90.00	100.00	Pass
AC thermal cracking (ft/mile)	1000.00	27.17	90.00	100.00	Pass
AC top-down fatigue cracking (ft/mile)	2000.00	256.49	90.00	100.00	Pass
Permanent deformation - AC only (in)	0.25	0.24	90.00	91.94	Pass

Distress Charts

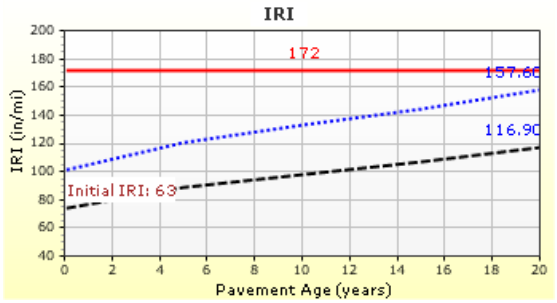

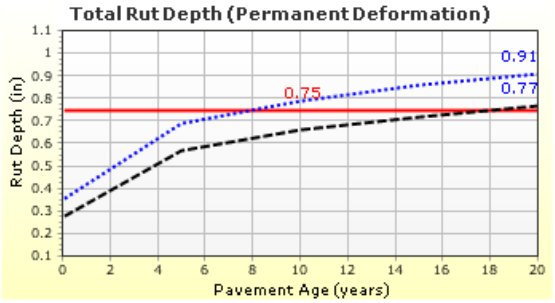

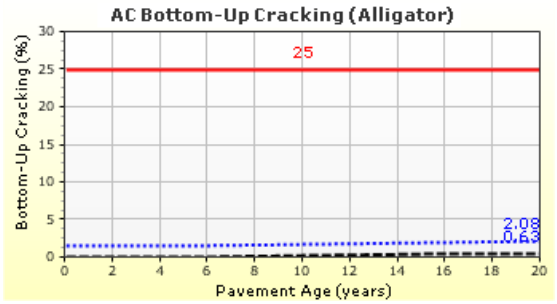

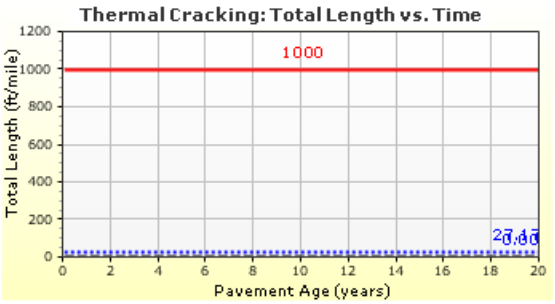

Design Inputs

Design Life: 20 years
Design Type: Flexible Pavement
Base construction: May, 2018
Pavement construction: June, 2019
Traffic opening: September, 2019
Climate Data Sources (Lat/Lon): 33.688, -112.082

Design Structure

Layer type	Material Type	Thickness (in)
Flexible	Default asphalt concrete	13.0
NonStabilized	A-1-b	6.0
Subgrade	A-6	Semi-infinite

Volumetric at Construction:	
Effective binder content (%)	5.0
Air voids (%)	5.0

Traffic

Age (year)	Heavy Trucks (cumulative)
2019 (initial)	2,000
2029 (10 years)	3,641,630
2039 (20 years)	7,664,950

Design Outputs

Distress Prediction Summary

Distress Type	Distress @ Specified Reliability		Reliability (%)		Criterion Satisfied?
	Target	Predicted	Target	Achieved	
Terminal IRI (in/mile)	172.00	147.02	90.00	98.27	Pass
Permanent deformation - total pavement (in)	0.75	0.69	90.00	97.15	Pass
AC bottom-up fatigue cracking (% lane area)	25.00	1.82	90.00	100.00	Pass
AC thermal cracking (ft/mile)	1000.00	27.17	90.00	100.00	Pass
AC top-down fatigue cracking (ft/mile)	2000.00	257.21	90.00	100.00	Pass
Permanent deformation - AC only (in)	0.25	0.25	90.00	90.68	Pass

Distress Charts

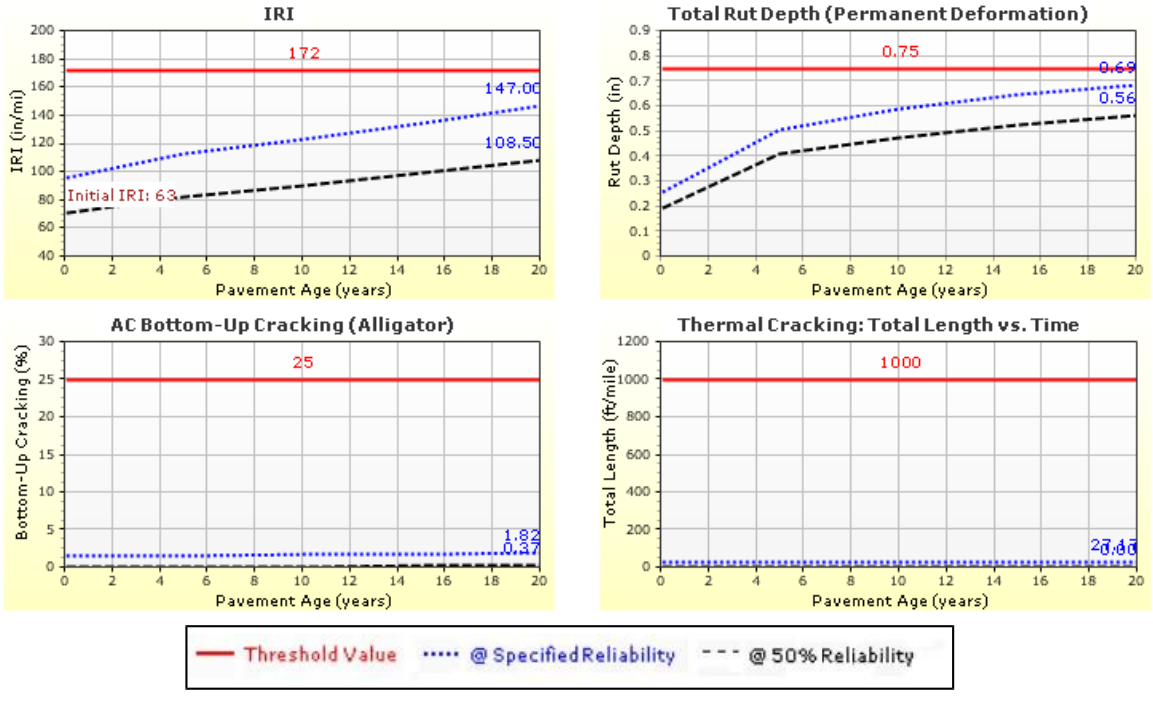

Design Inputs

Design Life: 20 years
Design Type: Flexible Pavement
Base construction: May, 2018
Pavement construction: June, 2019
Traffic opening: September, 2019
Climate Data Sources (Lat/Lon): 33.688, -112.082

Design Structure

Layer type	Material Type	Thickness (in)
Flexible	Default asphalt concrete	13.0
NonStabilized	A-1-b	6.0
Subgrade	A-6	Semi-infinite

Volumetric at Construction:	
Effective binder content (%)	5.0
Air voids (%)	5.0

Traffic

Age (year)	Heavy Trucks (cumulative)
2019 (initial)	2,000
2029 (10 years)	3,641,630
2039 (20 years)	7,664,950

Design Outputs

Distress Prediction Summary

Distress Type	Distress @ Specified Reliability		Reliability (%)		Criterion Satisfied?
	Target	Predicted	Target	Achieved	
Terminal IRI (in/mile)	172.00	143.90	90.00	98.72	Pass
Permanent deformation - total pavement (in)	0.75	0.62	90.00	99.59	Pass
AC bottom-up fatigue cracking (% lane area)	25.00	1.75	90.00	100.00	Pass
AC thermal cracking (ft/mile)	1000.00	27.17	90.00	100.00	Pass
AC top-down fatigue cracking (ft/mile)	2000.00	258.62	90.00	100.00	Pass
Permanent deformation - AC only (in)	0.25	0.25	90.00	90.26	Pass

Distress Charts

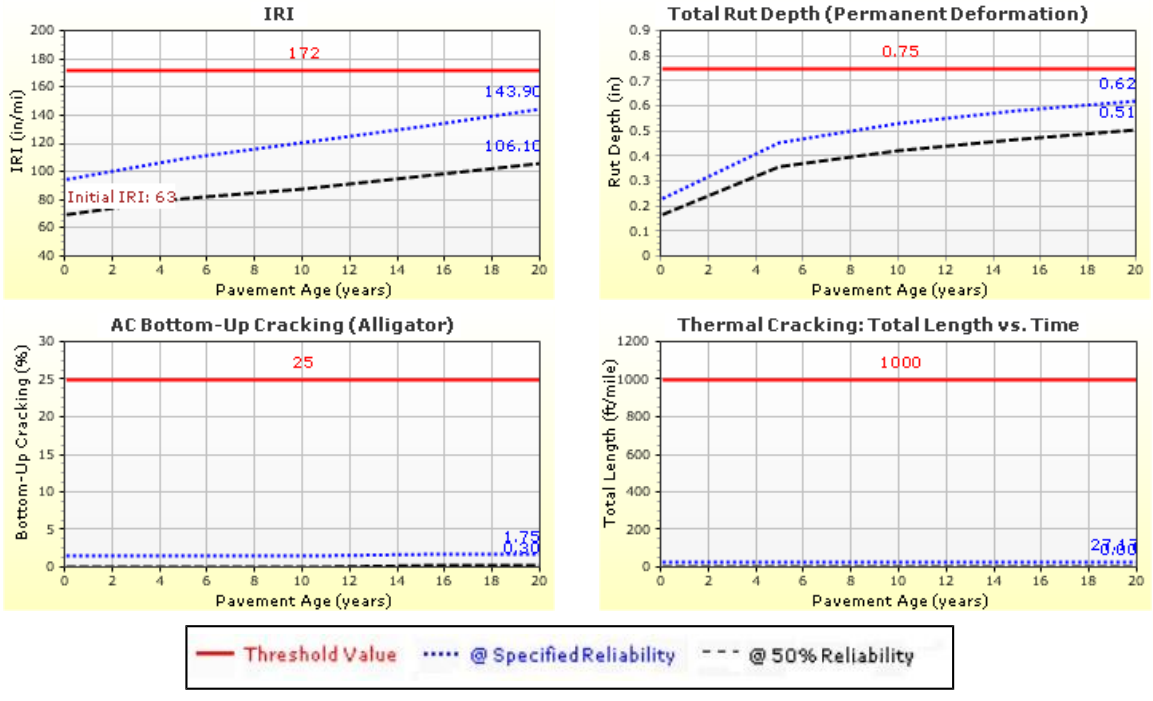

Design Inputs

Design Life: 20 years
Design Type: Flexible Pavement
Base construction: May, 2018
Pavement construction: June, 2019
Traffic opening: September, 2019
Climate Data Sources (Lat/Lon): 33.688, -112.082

Design Structure

Layer type	Material Type	Thickness (in)
Flexible	Default asphalt concrete	13.0
NonStabilized	A-1-b	6.0
Subgrade	A-6	Semi-infinite

Volumetric at Construction:	
Effective binder content (%)	5.0
Air voids (%)	5.0

Traffic

Age (year)	Heavy Trucks (cumulative)
2019 (initial)	2,000
2029 (10 years)	3,641,630
2039 (20 years)	7,664,950

Design Outputs

Distress Prediction Summary

Distress Type	Distress @ Specified Reliability		Reliability (%)		Criterion Satisfied?
	Target	Predicted	Target	Achieved	
Terminal IRI (in/mile)	172.00	139.23	90.00	99.23	Pass
Permanent deformation - total pavement (in)	0.75	0.52	90.00	100.00	Pass
AC bottom-up fatigue cracking (% lane area)	25.00	1.66	90.00	100.00	Pass
AC thermal cracking (ft/mile)	1000.00	27.17	90.00	100.00	Pass
AC top-down fatigue cracking (ft/mile)	2000.00	267.19	90.00	100.00	Pass
Permanent deformation - AC only (in)	0.25	0.25	90.00	89.98	Fail

Distress Charts

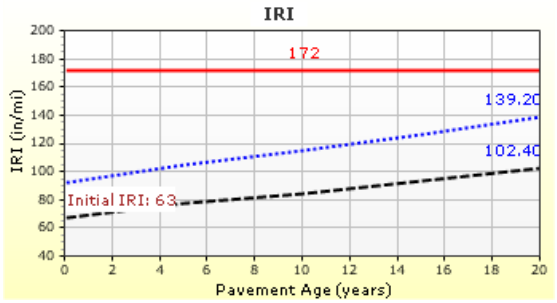

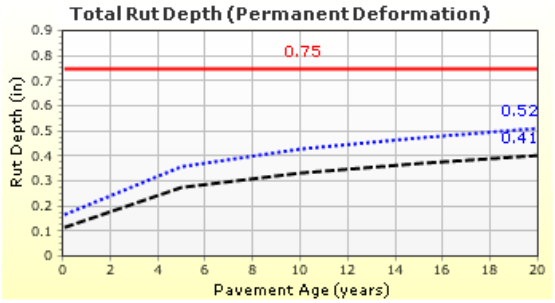

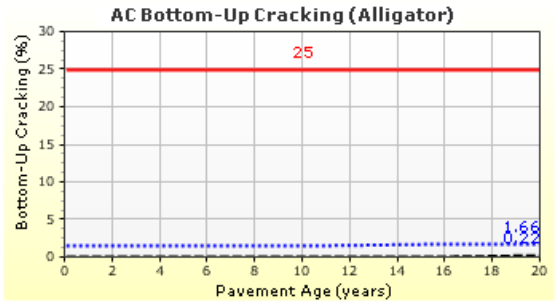

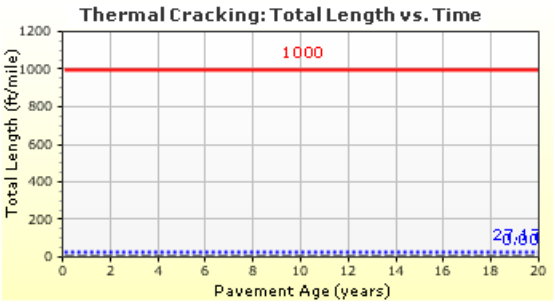

Design Inputs

Design Life: 20 years
Design Type: Flexible Pavement
Base construction: May, 2018
Pavement construction: June, 2019
Traffic opening: September, 2019
Climate Data Sources (Lat/Lon): 33.688, -112.082

Design Structure

Layer type	Material Type	Thickness (in)
Flexible	Default asphalt concrete	13.0
NonStabilized	A-1-b	6.0
Subgrade	A-6	Semi-infinite

Volumetric at Construction:	
Effective binder content (%)	5.0
Air voids (%)	5.0

Traffic

Age (year)	Heavy Trucks (cumulative)
2019 (initial)	2,000
2029 (10 years)	3,641,630
2039 (20 years)	7,664,950

Design Outputs

Distress Prediction Summary

Distress Type	Distress @ Specified Reliability		Reliability (%)		Criterion Satisfied?
	Target	Predicted	Target	Achieved	
Terminal IRI (in/mile)	172.00	138.43	90.00	99.30	Pass
Permanent deformation - total pavement (in)	0.75	0.50	90.00	100.00	Pass
AC bottom-up fatigue cracking (% lane area)	25.00	1.62	90.00	100.00	Pass
AC thermal cracking (ft/mile)	1000.00	27.17	90.00	100.00	Pass
AC top-down fatigue cracking (ft/mile)	2000.00	282.89	90.00	100.00	Pass
Permanent deformation - AC only (in)	0.25	0.25	90.00	89.87	Fail

Distress Charts

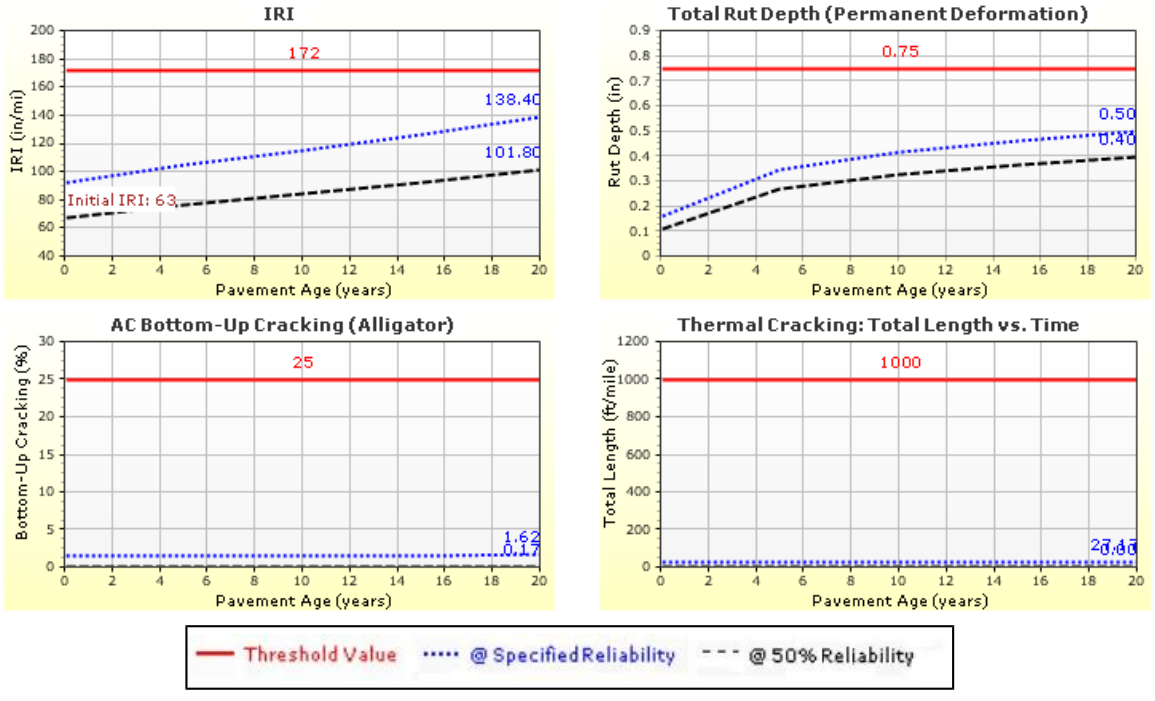

Design Inputs

Design Life: 20 years
Design Type: Flexible Pavement
Base construction: May, 2018
Pavement construction: June, 2019
Traffic opening: September, 2019
Climate Data Sources (Lat/Lon): 33.688, -112.082

Design Structure

Layer type	Material Type	Thickness (in)
Flexible	Default asphalt concrete	13.0
NonStabilized	A-1-b	6.0
Subgrade	A-6	Semi-infinite

Volumetric at Construction:	
Effective binder content (%)	5.0
Air voids (%)	5.0

Traffic

Age (year)	Heavy Trucks (cumulative)
2019 (initial)	2,000
2029 (10 years)	3,641,630
2039 (20 years)	7,664,950

Design Outputs

Distress Prediction Summary

Distress Type	Distress @ Specified Reliability		Reliability (%)		Criterion Satisfied?
	Target	Predicted	Target	Achieved	
Terminal IRI (in/mile)	172.00	135.89	90.00	99.48	Pass
Permanent deformation - total pavement (in)	0.75	0.45	90.00	100.00	Pass
AC bottom-up fatigue cracking (% lane area)	25.00	1.58	90.00	100.00	Pass
AC thermal cracking (ft/mile)	1000.00	27.17	90.00	100.00	Pass
AC top-down fatigue cracking (ft/mile)	2000.00	333.17	90.00	100.00	Pass
Permanent deformation - AC only (in)	0.25	0.25	90.00	89.54	Fail

Distress Charts

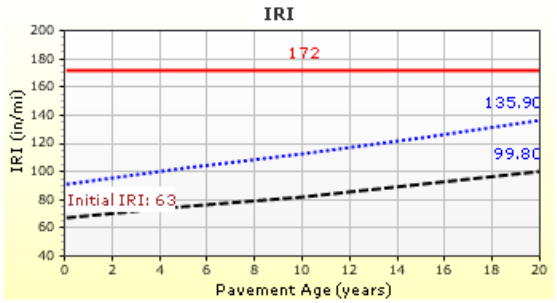

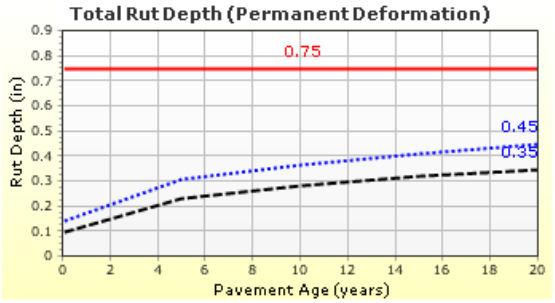

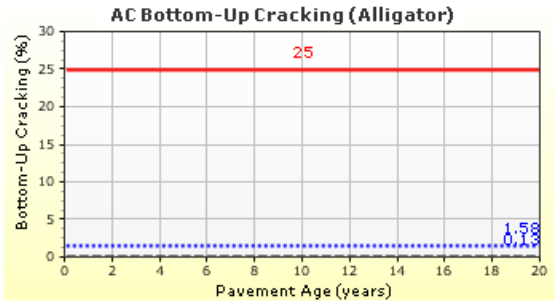

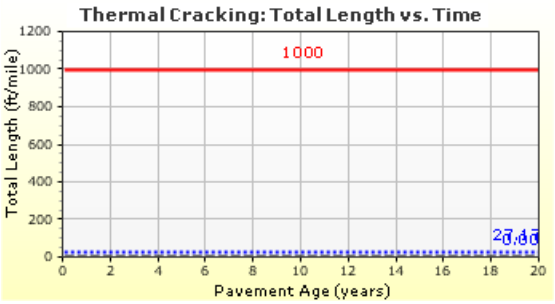

Design Inputs

Design Life: 20 years
Design Type: Flexible Pavement
Base construction: May, 2018
Pavement construction: June, 2019
Traffic opening: September, 2019
Climate Data Sources (Lat/Lon): 33.688, -112.082

Design Structure

Layer type	Material Type	Thickness (in)
Flexible	Default asphalt concrete	13.0
NonStabilized	A-1-b	6.0
Subgrade	A-6	Semi-infinite

Volumetric at Construction:	
Effective binder content (%)	5.0
Air voids (%)	5.0

Traffic

Age (year)	Heavy Trucks (cumulative)
2019 (initial)	2,000
2029 (10 years)	3,641,630
2039 (20 years)	7,664,950

Design Outputs

Distress Prediction Summary

Distress Type	Distress @ Specified Reliability		Reliability (%)		Criterion Satisfied?
	Target	Predicted	Target	Achieved	
Terminal IRI (in/mile)	172.00	134.43	90.00	99.57	Pass
Permanent deformation - total pavement (in)	0.75	0.42	90.00	100.00	Pass
AC bottom-up fatigue cracking (% lane area)	25.00	1.55	90.00	100.00	Pass
AC thermal cracking (ft/mile)	1000.00	27.17	90.00	100.00	Pass
AC top-down fatigue cracking (ft/mile)	2000.00	404.69	90.00	100.00	Pass
Permanent deformation - AC only (in)	0.25	0.25	90.00	89.58	Fail

Distress Charts

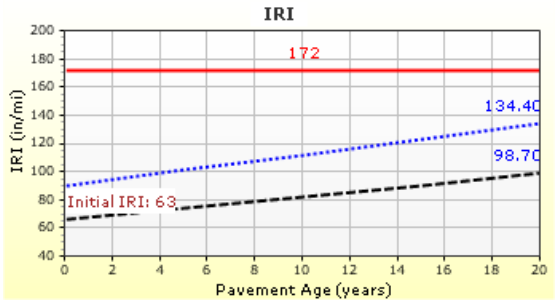

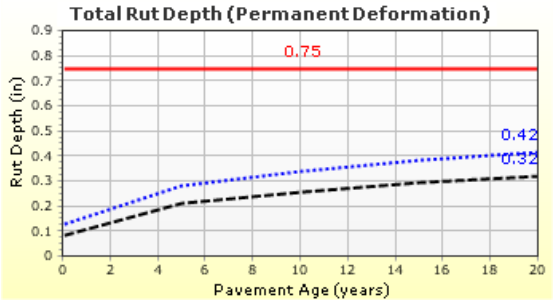

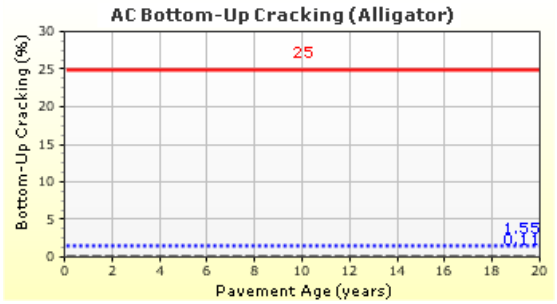

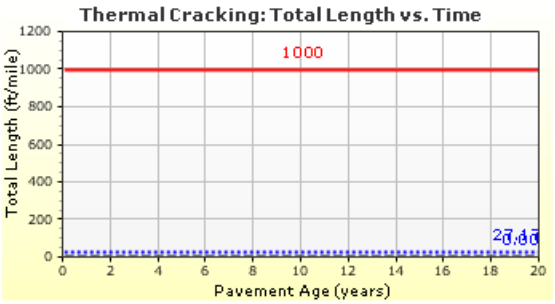

Case 31

Design Inputs

Design Life: 20 years
Design Type: Flexible Pavement
Base construction: May, 2018
Pavement construction: June, 2019
Traffic opening: September, 2019
Climate Data Sources (Lat/Lon): 33.688, -112.082

Design Structure

Layer type	Material Type	Thickness (in)
Flexible	Default asphalt concrete	13.0
NonStabilized	A-1-b	6.0
Subgrade	A-6	Semi-infinite

Volumetric at Construction:	
Effective binder content (%)	5.0
Air voids (%)	5.0

Traffic

Age (year)	Heavy Trucks (cumulative)
2019 (initial)	10,000
2029 (10 years)	18,208,200
2039 (20 years)	38,324,800

Design Outputs

Distress Prediction Summary

Distress Type	Distress @ Specified Reliability		Reliability (%)		Criterion Satisfied?
	Target	Predicted	Target	Achieved	
Terminal IRI (in/mile)	172.00	156.70	90.00	96.11	Pass
Permanent deformation - total pavement (in)	0.75	0.90	90.00	55.21	Fail
AC bottom-up fatigue cracking (% lane area)	25.00	4.38	90.00	100.00	Pass
AC thermal cracking (ft/mile)	1000.00	27.17	90.00	100.00	Pass
AC top-down fatigue cracking (ft/mile)	2000.00	265.35	90.00	100.00	Pass
Permanent deformation - AC only (in)	0.25	0.51	90.00	13.34	Fail

Distress Charts

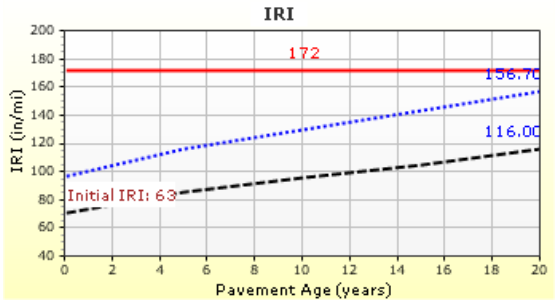

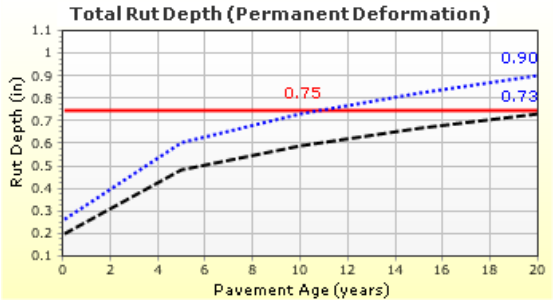

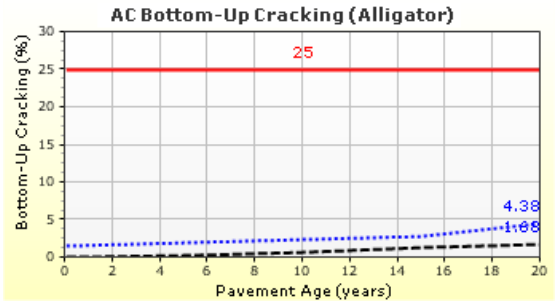

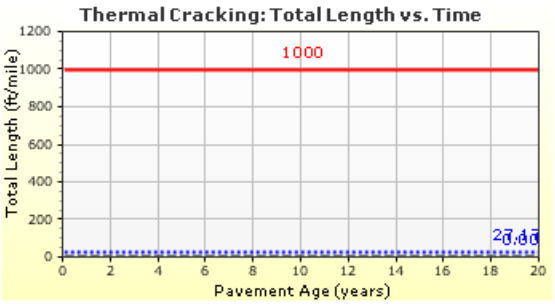

Design Inputs

Design Life: 20 years
Design Type: Flexible Pavement
Base construction: May, 2018
Pavement construction: June, 2019
Traffic opening: September, 2019
Climate Data Sources (Lat/Lon): 33.688, -112.082

Design Structure

Layer type	Material Type	Thickness (in)
Flexible	Default asphalt concrete	13.0
NonStabilized	A-1-b	6.0
Subgrade	A-6	Semi-infinite

Volumetric at Construction:	
Effective binder content (%)	5.0
Air voids (%)	5.0

Traffic

Age (year)	Heavy Trucks (cumulative)
2019 (initial)	10,000
2029 (10 years)	18,208,200
2039 (20 years)	38,324,800

Design Outputs

Distress Prediction Summary

Distress Type	Distress @ Specified Reliability		Reliability (%)		Criterion Satisfied?
	Target	Predicted	Target	Achieved	
Terminal IRI (in/mile)	172.00	145.78	90.00	98.45	Pass
Permanent deformation - total pavement (in)	0.75	0.69	90.00	96.37	Pass
AC bottom-up fatigue cracking (% lane area)	25.00	1.97	90.00	100.00	Pass
AC thermal cracking (ft/mile)	1000.00	27.17	90.00	100.00	Pass
AC top-down fatigue cracking (ft/mile)	2000.00	971.78	90.00	99.60	Pass
Permanent deformation - AC only (in)	0.25	0.52	90.00	12.62	Fail

Distress Charts

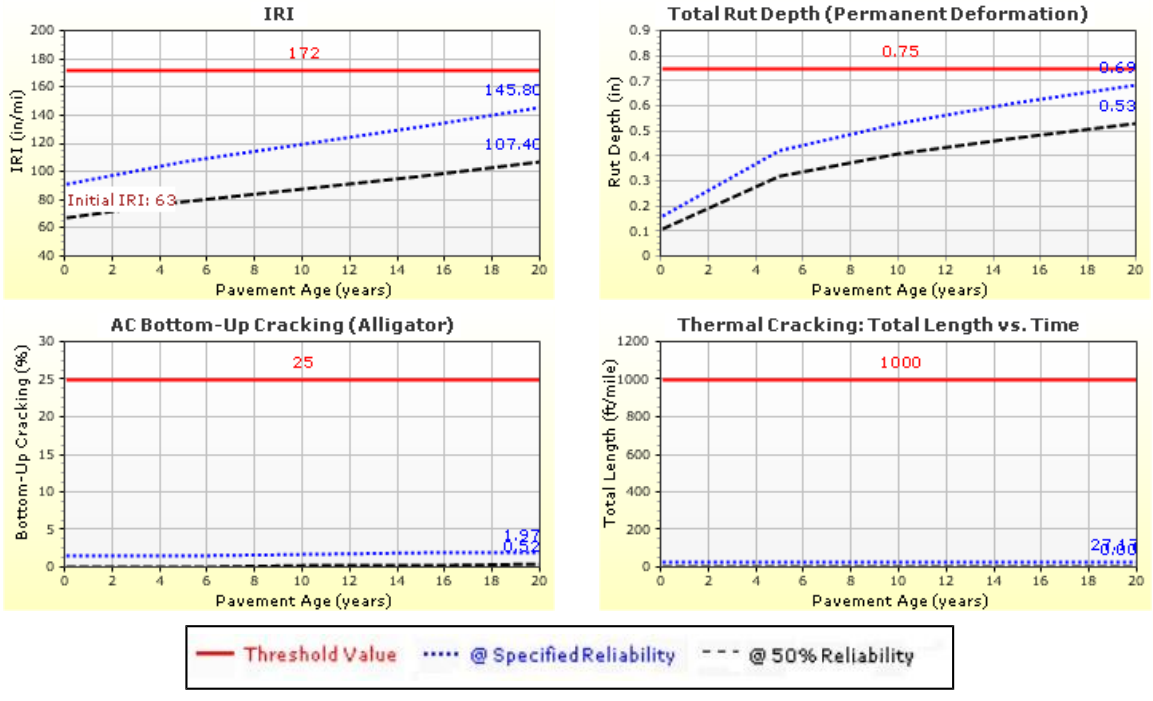

Design Inputs

Design Life: 20 years
Design Type: Flexible Pavement
Base construction: May, 2018
Pavement construction: June, 2019
Traffic opening: September, 2019
Climate Data Sources (Lat/Lon): 33.688, -112.082

Design Structure

Layer type	Material Type	Thickness (in)
Flexible	Default asphalt concrete	13.0
NonStabilized	A-1-b	6.0
Subgrade	A-6	Semi-infinite

Volumetric at Construction:	
Effective binder content (%)	5.0
Air voids (%)	5.0

Traffic

Age (year)	Heavy Trucks (cumulative)
2019 (initial)	10,000
2029 (10 years)	18,208,200
2039 (20 years)	38,324,800

Design Outputs

Distress Prediction Summary

Distress Type	Distress @ Specified Reliability		Reliability (%)		Criterion Satisfied?
	Target	Predicted	Target	Achieved	
Terminal IRI (in/mile)	172.00	176.12	90.00	87.77	Fail
Permanent deformation - total pavement (in)	0.75	1.30	90.00	0.97	Fail
AC bottom-up fatigue cracking (% lane area)	25.00	19.39	90.00	95.81	Pass
AC thermal cracking (ft/mile)	1000.00	27.17	90.00	100.00	Pass
AC top-down fatigue cracking (ft/mile)	2000.00	256.49	90.00	100.00	Pass
Permanent deformation - AC only (in)	0.25	0.50	90.00	14.59	Fail

Distress Charts

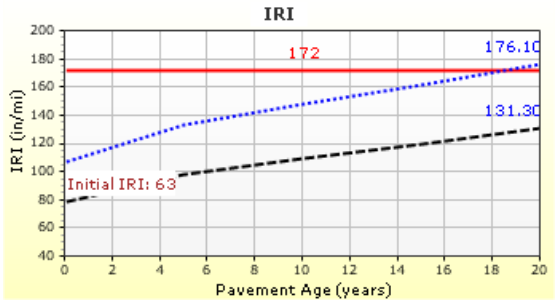

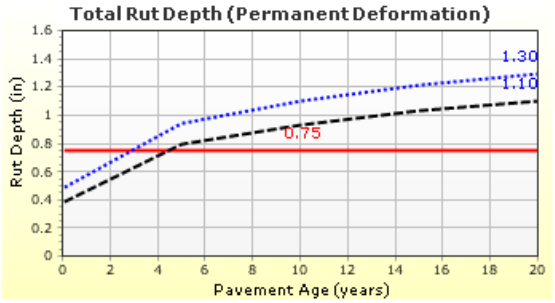

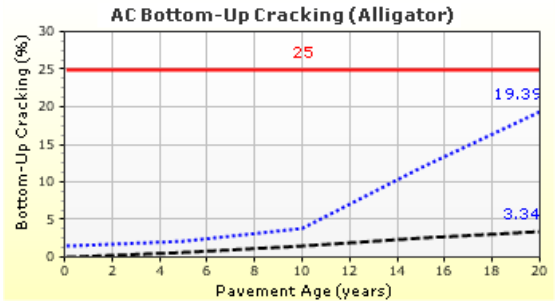

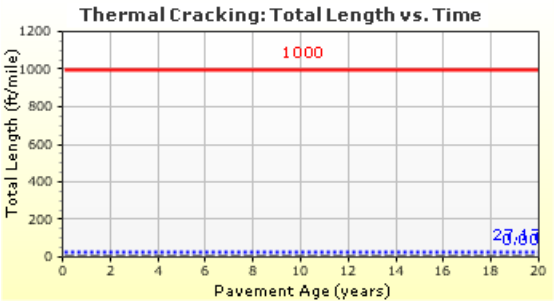

Case 34

Design Inputs

Design Life: 20 years
Design Type: Flexible Pavement
Base construction: May, 2018
Pavement construction: June, 2019
Traffic opening: September, 2019
Climate Data Sources (Lat/Lon): 33.688, -112.082

Design Structure

Layer type	Material Type	Thickness (in)
Flexible	Default asphalt concrete	13.0
NonStabilized	A-1-b	6.0
Subgrade	A-6	Semi-infinite

Volumetric at Construction:	
Effective binder content (%)	5.0
Air voids (%)	5.0

Traffic

Age (year)	Heavy Trucks (cumulative)
2019 (initial)	10,000
2029 (10 years)	18,208,200
2039 (20 years)	38,324,800

Design Outputs

Distress Prediction Summary

Distress Type	Distress @ Specified Reliability		Reliability (%)		Criterion Satisfied?
	Target	Predicted	Target	Achieved	
Terminal IRI (in/mile)	172.00	162.60	90.00	94.17	Pass
Permanent deformation - total pavement (in)	0.75	1.03	90.00	22.76	Fail
AC bottom-up fatigue cracking (% lane area)	25.00	6.66	90.00	100.00	Pass
AC thermal cracking (ft/mile)	1000.00	27.17	90.00	100.00	Pass
AC top-down fatigue cracking (ft/mile)	2000.00	259.86	90.00	100.00	Pass
Permanent deformation - AC only (in)	0.25	0.51	90.00	13.47	Fail

Distress Charts

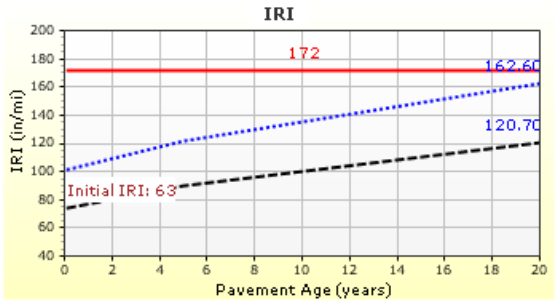

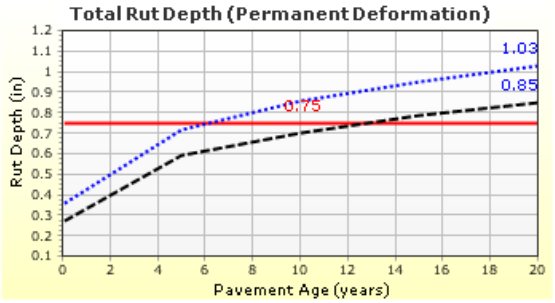

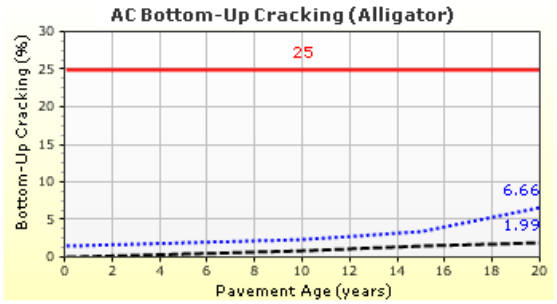

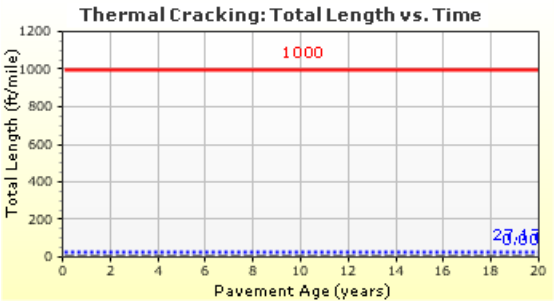

Design Inputs

Design Life: 20 years
Design Type: Flexible Pavement
Base construction: May, 2018
Pavement construction: June, 2019
Traffic opening: September, 2019
Climate Data Sources (Lat/Lon): 33.688, -112.082

Design Structure

Layer type	Material Type	Thickness (in)
Flexible	Default asphalt concrete	13.0
NonStabilized	A-1-b	6.0
Subgrade	A-6	Semi-infinite

Volumetric at Construction:	
Effective binder content (%)	5.0
Air voids (%)	5.0

Traffic

Age (year)	Heavy Trucks (cumulative)
2019 (initial)	10,000
2029 (10 years)	18,208,200
2039 (20 years)	38,324,800

Design Outputs

Distress Prediction Summary

Distress Type	Distress @ Specified Reliability		Reliability (%)		Criterion Satisfied?
	Target	Predicted	Target	Achieved	
Terminal IRI (in/mile)	172.00	158.71	90.00	95.51	Pass
Permanent deformation - total pavement (in)	0.75	0.95	90.00	40.92	Fail
AC bottom-up fatigue cracking (% lane area)	25.00	4.01	90.00	100.00	Pass
AC thermal cracking (ft/mile)	1000.00	27.17	90.00	100.00	Pass
AC top-down fatigue cracking (ft/mile)	2000.00	266.31	90.00	100.00	Pass
Permanent deformation - AC only (in)	0.25	0.51	90.00	13.14	Fail

Distress Charts

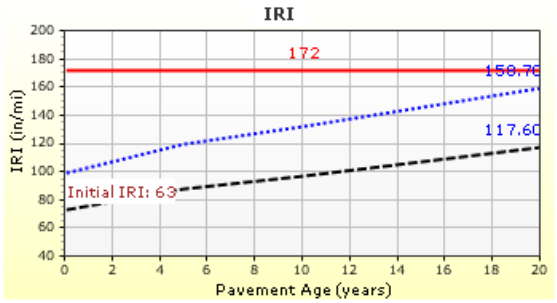

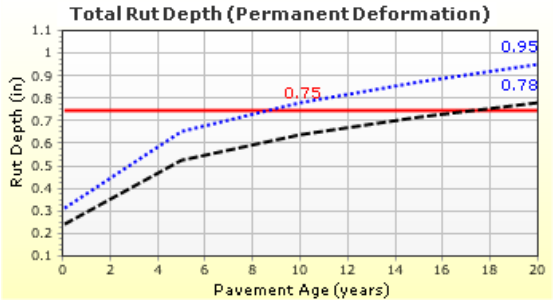

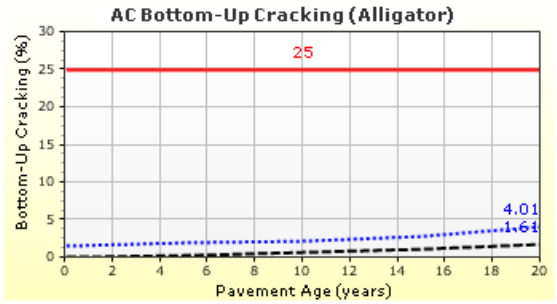

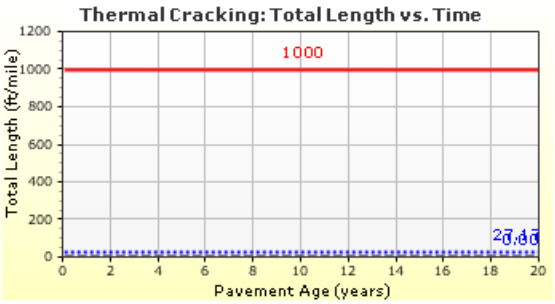

Case 36

Design Inputs

Design Life: 20 years
Design Type: Flexible Pavement
Base construction: May, 2018
Pavement construction: June, 2019
Traffic opening: September, 2019
Climate Data Sources (Lat/Lon): 33.688, -112.082

Design Structure

Layer type	Material Type	Thickness (in)
Flexible	Default asphalt concrete	13.0
NonStabilized	A-1-b	6.0
Subgrade	A-6	Semi-infinite

Volumetric at Construction:	
Effective binder content (%)	5.0
Air voids (%)	5.0

Traffic

Age (year)	Heavy Trucks (cumulative)
2019 (initial)	10,000
2029 (10 years)	18,208,200
2039 (20 years)	38,324,800

Design Outputs

Distress Prediction Summary

Distress Type	Distress @ Specified Reliability		Reliability (%)		Criterion Satisfied?
	Target	Predicted	Target	Achieved	
Terminal IRI (in/mile)	172.00	153.00	90.00	97.07	Pass
Permanent deformation - total pavement (in)	0.75	0.83	90.00	74.73	Fail
AC bottom-up fatigue cracking (% lane area)	25.00	2.73	90.00	100.00	Pass
AC thermal cracking (ft/mile)	1000.00	27.17	90.00	100.00	Pass
AC top-down fatigue cracking (ft/mile)	2000.00	304.70	90.00	100.00	Pass
Permanent deformation - AC only (in)	0.25	0.52	90.00	12.90	Fail

Distress Charts

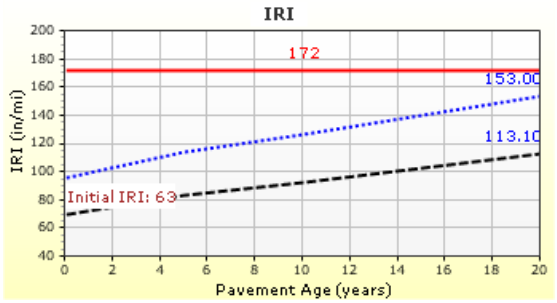

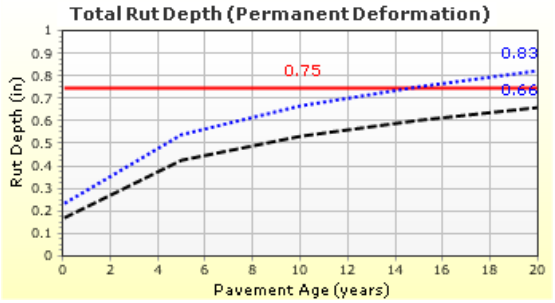

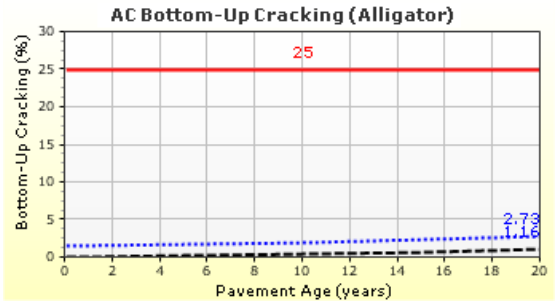

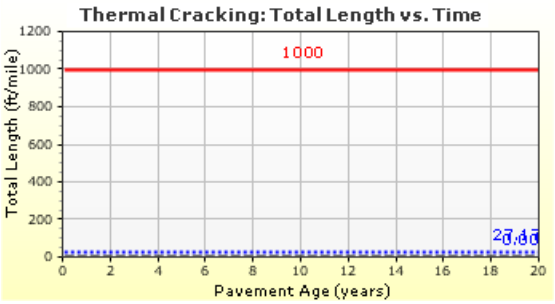

Design Inputs

Design Life: 20 years
Design Type: Flexible Pavement
Base construction: May, 2018
Pavement construction: June, 2019
Traffic opening: September, 2019
Climate Data Sources (Lat/Lon): 33.688, -112.082

Design Structure

Layer type	Material Type	Thickness (in)
Flexible	Default asphalt concrete	13.0
NonStabilized	A-1-b	6.0
Subgrade	A-6	Semi-infinite

Volumetric at Construction:	
Effective binder content (%)	5.0
Air voids (%)	5.0

Traffic

Age (year)	Heavy Trucks (cumulative)
2019 (initial)	10,000
2029 (10 years)	18,208,200
2039 (20 years)	38,324,800

Design Outputs

Distress Prediction Summary

Distress Type	Distress @ Specified Reliability		Reliability (%)		Criterion Satisfied?
	Target	Predicted	Target	Achieved	
Terminal IRI (in/mile)	172.00	151.82	90.00	97.34	Pass
Permanent deformation - total pavement (in)	0.75	0.81	90.00	78.89	Fail
AC bottom-up fatigue cracking (% lane area)	25.00	2.43	90.00	100.00	Pass
AC thermal cracking (ft/mile)	1000.00	27.17	90.00	100.00	Pass
AC top-down fatigue cracking (ft/mile)	2000.00	373.11	90.00	100.00	Pass
Permanent deformation - AC only (in)	0.25	0.52	90.00	12.83	Fail

Distress Charts

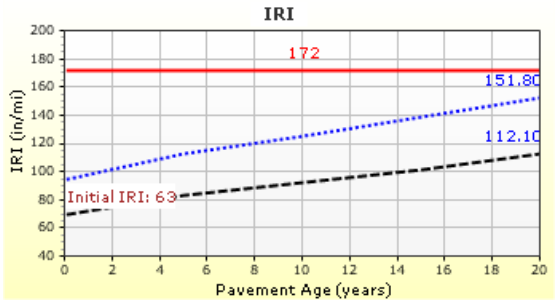

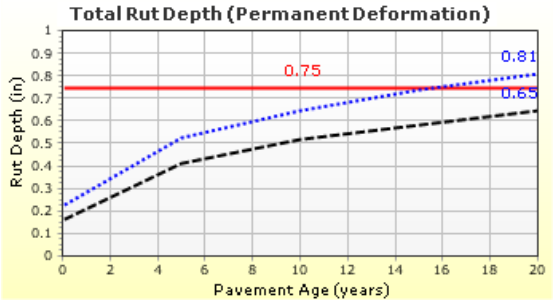

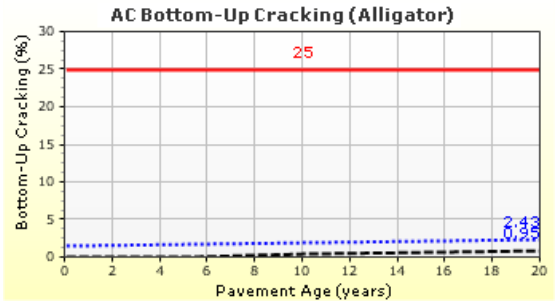

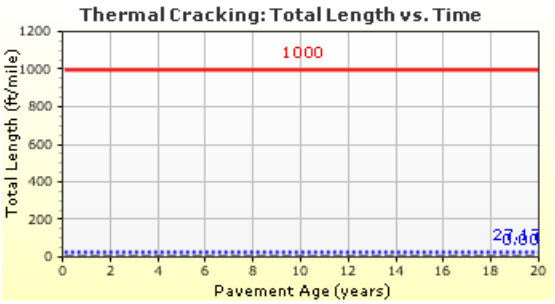

Design Inputs

Design Life: 20 years
Design Type: Flexible Pavement
Base construction: May, 2018
Pavement construction: June, 2019
Traffic opening: September, 2019
Climate Data Sources (Lat/Lon): 33.688, -112.082

Design Structure

Layer type	Material Type	Thickness (in)
Flexible	Default asphalt concrete	13.0
NonStabilized	A-1-b	6.0
Subgrade	A-6	Semi-infinite

Volumetric at Construction:	
Effective binder content (%)	5.0
Air voids (%)	5.0

Traffic

Age (year)	Heavy Trucks (cumulative)
2019 (initial)	10,000
2029 (10 years)	18,208,200
2039 (20 years)	38,324,800

Design Outputs

Distress Prediction Summary

Distress Type	Distress @ Specified Reliability		Reliability (%)		Criterion Satisfied?
	Target	Predicted	Target	Achieved	
Terminal IRI (in/mile)	172.00	148.75	90.00	97.96	Pass
Permanent deformation - total pavement (in)	0.75	0.75	90.00	89.88	Fail
AC bottom-up fatigue cracking (% lane area)	25.00	2.16	90.00	100.00	Pass
AC thermal cracking (ft/mile)	1000.00	27.17	90.00	100.00	Pass
AC top-down fatigue cracking (ft/mile)	2000.00	577.21	90.00	100.00	Pass
Permanent deformation - AC only (in)	0.25	0.52	90.00	12.58	Fail

Distress Charts

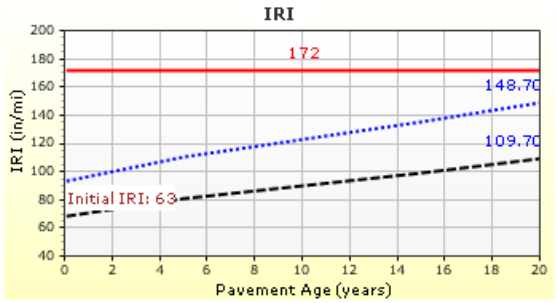

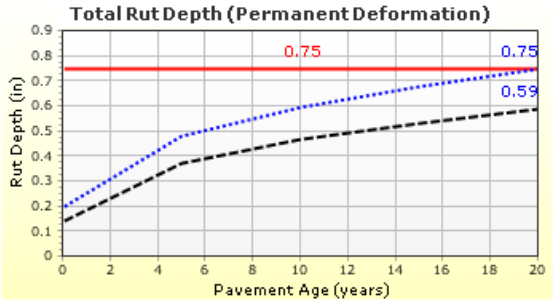

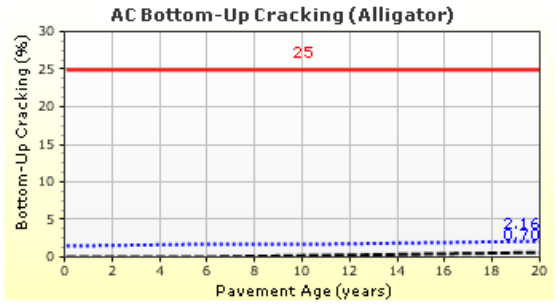

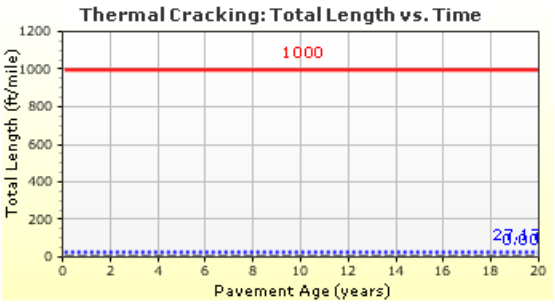

Design Inputs

Design Life: 20 years
Design Type: Flexible Pavement
Base construction: May, 2018
Pavement construction: June, 2019
Traffic opening: September, 2019
Climate Data Sources (Lat/Lon): 33.688, -112.082

Design Structure

Layer type	Material Type	Thickness (in)
Flexible	Default asphalt concrete	13.0
NonStabilized	A-1-b	6.0
Subgrade	A-6	Semi-infinite

Volumetric at Construction:	
Effective binder content (%)	5.0
Air voids (%)	5.0

Traffic

Age (year)	Heavy Trucks (cumulative)
2019 (initial)	10,000
2029 (10 years)	18,208,200
2039 (20 years)	38,324,800

Design Outputs

Distress Prediction Summary

Distress Type	Distress @ Specified Reliability		Reliability (%)		Criterion Satisfied?
	Target	Predicted	Target	Achieved	
Terminal IRI (in/mile)	172.00	146.95	90.00	98.27	Pass
Permanent deformation - total pavement (in)	0.75	0.72	90.00	94.15	Pass
AC bottom-up fatigue cracking (% lane area)	25.00	2.02	90.00	100.00	Pass
AC thermal cracking (ft/mile)	1000.00	27.17	90.00	100.00	Pass
AC top-down fatigue cracking (ft/mile)	2000.00	831.97	90.00	99.90	Pass
Permanent deformation - AC only (in)	0.25	0.52	90.00	12.60	Fail

Distress Charts

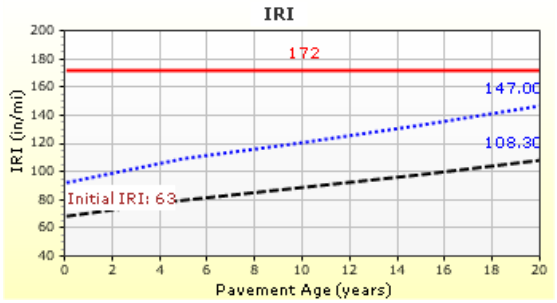

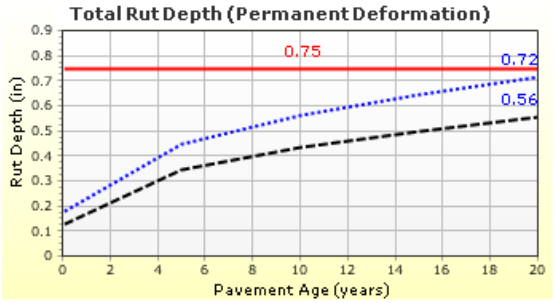

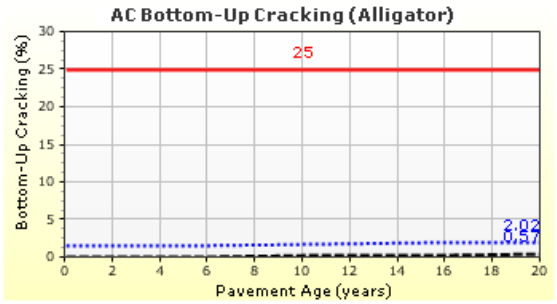

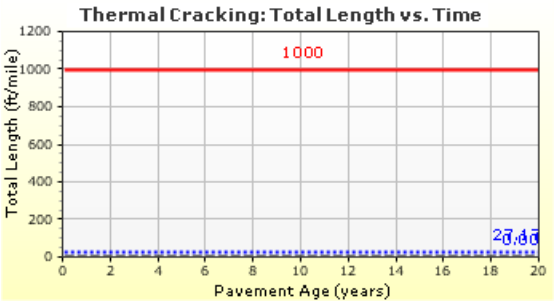

APPENDIX F

ANTHEM SOIL – SUMMARY

Anthem Soil

Run	Structure	Traffic AADTT	Condition	Treatment	LL	PL	PI	γdry
1	1	2000	Soaked	Control	48.7	21.3	27.4	106.7
2	1	2000	Soaked	%16 CaO			0	
3	1	2000	Soaked	2%CaCl2	44.2	20.9	23.3	
4	1	2000	Soaked	4%CaCl2	42.5	19.8	22.7	
5	1	2000	Soaked	8%CaCl2	39.9	19.2	20.7	
6	1	2000	Unsoaked	Control	48.7	21.3	27.4	106.7
7	1	2000	Unsoaked	%16 CaO			0	
8	1	2000	Unsoaked	8%CaCl2	44.2	20.9	23.3	
9	1	2000	Unsoaked	12%CaCl2	42.5	19.8	22.7	
10	1	2000	Unsoaked	16%CaCl2	39.9	19.2	20.7	
11	1	5000	Soaked	Control	48.7	21.3	27.4	106.7
12	1	5000	Soaked	%16 CaO			0	
13	1	5000	Soaked	8%CaCl2	44.2	20.9	23.3	
14	1	5000	Soaked	12%CaCl2	42.5	19.8	22.7	
15	1	5000	Soaked	16%CaCl2	39.9	19.2	20.7	
16	1	5000	Unsoaked	Control	48.7	21.3	27.4	106.7
17	1	5000	Unsoaked	%16 CaO			0	
18	1	5000	Unsoaked	8%CaCl2	44.2	20.9	23.3	
19	1	5000	Unsoaked	12%CaCl2	42.5	19.8	22.7	
20	1	5000	Unsoaked	16%CaCl2	39.9	19.2	20.7	
21	2	2000	Soaked	Control	48.7	21.3	27.4	106.7
22	2	2000	Soaked	%16 CaO			0	
23	2	2000	Soaked	8%CaCl2	44.2	20.9	23.3	
24	2	2000	Soaked	12%CaCl2	42.5	19.8	22.7	
25	2	2000	Soaked	16%CaCl2	39.9	19.2	20.7	
26	2	2000	Unsoaked	Control	48.7	21.3	27.4	106.7
27	2	2000	Unsoaked	%16 CaO			0	
28	2	2000	Unsoaked	8%CaCl2	44.2	20.9	23.3	
29	2	2000	Unsoaked	12%CaCl2	42.5	19.8	22.7	
30	2	2000	Unsoaked	16%CaCl2	39.9	19.2	20.7	
31	2	5000	Soaked	Control	48.7	21.3	27.4	106.7
32	2	5000	Soaked	%16 CaO			0	
33	2	5000	Soaked	8%CaCl2	44.2	20.9	23.3	
34	2	5000	Soaked	12%CaCl2	42.5	19.8	22.7	

35	2	5000	Soaked	16%CaCl2	39.9	19.2	20.7	
36	2	5000	Unsoaked	Control	48.7	21.3	27.4	106.7
37	2	5000	Unsoaked	%16 CaO			0	
38	2	5000	Unsoaked	8%CaCl2	44.2	20.9	23.3	
39	2	5000	Unsoaked	12%CaCl2	42.5	19.8	22.7	
40	2	5000	Unsoaked	16%CaCl2	39.9	19.2	20.7	

APPENDIX G

EAGER SOIL – SUMMARY

Eager Soil

Run	Structure	Traffic AADTT	Condition	Treatment	LL	PL	PI	γdry max
1	1	900	Soaked	Control	49.8	22.5	27.3	97.1
2	1	900	Soaked	%16 CaO	53.2	36.7	16.5	--
3	1	900	Soaked	8%CaCl2	46.1	22.7	23.4	109.2
4	1	900	Soaked	12%CaCl2	43.1	21.4	21.7	110.9
5	1	900	Soaked	16%CaCl2	43.1	21.1	22	108.6
6	1	900	Unsoaked	Control	49.8	22.5	27.3	97.1
7	1	900	Unsoaked	%16 CaO	53.2	36.7	16.5	--
8	1	900	Unsoaked	8%CaCl2	46.1	22.7	23.4	109.2
9	1	900	Unsoaked	12%CaCl2	43.1	21.4	21.7	110.9
10	1	900	Unsoaked	16%CaCl2	43.1	21.1	22	108.6
11	1	4500	Soaked	Control	49.8	22.5	27.3	97.1
12	1	4500	Soaked	%16 CaO	53.2	36.7	16.5	--
13	1	4500	Soaked	8%CaCl2	46.1	22.7	23.4	109.2
14	1	4500	Soaked	12%CaCl2	43.1	21.4	21.7	110.9
15	1	4500	Soaked	16%CaCl2	43.1	21.1	22	108.6
16	1	4500	Unsoaked	Control	49.8	22.5	27.3	97.1
17	1	4500	Unsoaked	%16 CaO	53.2	36.7	16.5	--
18	1	4500	Unsoaked	8%CaCl2	46.1	22.7	23.4	109.2
19	1	4500	Unsoaked	12%CaCl2	43.1	21.4	21.7	110.9
20	1	4500	Unsoaked	16%CaCl2	43.1	21.1	22	108.6
1-2	2	2000	Soaked	Control	49.8	22.5	27.3	97.1
2-2	2	2000	Soaked	%16 CaO	53.2	36.7	16.5	--
3-2	2	2000	Soaked	8%CaCl2	46.1	22.7	23.4	109.2
4-2	2	2000	Soaked	12%CaCl2	43.1	21.4	21.7	110.9
5-2	2	2000	Soaked	16%CaCl2	43.1	21.1	22	108.6
6-2	2	2000	Unsoaked	Control	49.8	22.5	27.3	97.1
7-2	2	2000	Unsoaked	%16 CaO	53.2	36.7	16.5	--
8-2	2	2000	Unsoaked	8%CaCl2	46.1	22.7	23.4	109.2
9-2	2	2000	Unsoaked	12%CaCl2	43.1	21.4	21.7	110.9
10-2	2	2000	Unsoaked	16%CaCl2	43.1	21.1	22	108.6
11-2	2	10000	Soaked	Control	49.8	22.5	27.3	97.1

12-2	2	10000	Soaked	%16 CaO	53.2	36.7	16.5	--
13-2	2	10000	Soaked	8%CaCl2	46.1	22.7	23.4	109.2
14-2	2	10000	Soaked	12%CaCl2	43.1	21.4	21.7	110.9
15-2	2	10000	Soaked	16%CaCl2	43.1	21.1	22	108.6
16-2	2	10000	Unsoaked	Control	49.8	22.5	27.3	97.1
17-2	2	10000	Unsoaked	%16 CaO	53.2	36.7	16.5	--
18-2	2	10000	Unsoaked	8%CaCl2	46.1	22.7	23.4	109.2
19-2	2	10000	Unsoaked	12%CaCl2	43.1	21.4	21.7	110.9
20-2	2	10000	Unsoaked	16%CaCl2	43.1	21.1	22	108.6

Eager Soil

Run	wopt	Compacted γdry	Compacted MC	CBR	Mr
1	23.1	1001.1	21.8	13.3	13,386
2	--	88.1	23.6	33.7	24,270
3	17.7	100.7	22.6	1.8	3,722
4	15.1	101.2	22.6	1.1	2,716
5	17.5	104.7	22.7	0.4	1,421
6	23.1	98.6	23.3	12.3	12,733
7	--	--	--	--	--
8	17.7	106.7	15.9	17.6	16,015
9	15.1	102.4	13.1	14.8	14,334
10	17.5	96.2	16	13.6	13,579
11	23.1	1001.1	21.8	13.3	13,386
12	--	88.1	23.6	33.7	24,270
13	17.7	100.7	22.6	1.8	3,722
14	15.1	101.2	22.6	1.1	2,716
15	17.5	104.7	22.7	0.4	1,421
16	23.1	98.6	23.3	12.3	12,733
17	--	--	--	--	--
18	17.7	106.7	15.9	17.6	16,015
19	15.1	102.4	13.1	14.8	14,334
20	17.5	96.2	16	13.6	13,579
1-2	23.1	1001.1	21.8	13.3	13,386
2-2	--	88.1	23.6	33.7	24,270
3-2	17.7	100.7	22.6	1.8	3,722
4-2	15.1	101.2	22.6	1.1	2,716
5-2	17.5	104.7	22.7	0.4	1,421
6-2	23.1	98.6	23.3	12.3	12,733
7-2	--	--	--	--	--
8-2	17.7	106.7	15.9	17.6	16,015
9-2	15.1	102.4	13.1	14.8	14,334
10-2	17.5	96.2	16	13.6	13,579
11-2	23.1	1001.1	21.8	13.3	13,386

12-2	--	88.1	23.6	33.7	24,270
13-2	17.7	100.7	22.6	1.8	3,722
14-2	15.1	101.2	22.6	1.1	2,716
15-2	17.5	104.7	22.7	0.4	1,421
16-2	23.1	98.6	23.3	12.3	12,733
17-2	--	--	--	--	--
18-2	17.7	106.7	15.9	17.6	16,015
19-2	15.1	102.4	13.1	14.8	14,334
20-2	17.5	96.2	16	13.6	13,579

Eager Soil

Run	Terminal IRI (in/mile)	Permanent deformation Total pavement (in)	AC bottom up cracking (% lane area)
1	147.3	0.61	22.69
2	143.86	0.53	21.75
3	162.64	0.95	24.18
4	177.32	1.27	25.12
5	188.35	1.5	25.87
6	147.56	0.61	22.75
7	--	--	--
8	147.19	0.6	22.31
9	149.8	0.67	22.79
10	148.33	0.63	22.6
11	177.94	1.02	41.31
12	172.58	0.92	38.01
13	194.15	1.43	46.71
14	212.6	1.81	49.91
15	226.83	2.1	52.31
16	178.23	1.03	41.51
17	--	--	--
18	177.29	1	39.91
19	180.75	1.09	41.71
20	178.97	1.04	40.91
1-2	135.37	0.43	1.62
2-2	131.42	0.37	1.53
3-2	148.88	0.73	1.93
4-2	160.94	0.99	2.27
5-2	170.13	1.18	2.74
6-2	135.86	0.44	1.63
7-2	--	--	--
8-2	134.85	0.43	1.57
9-2	137.68	0.49	1.63
10-2	136.12	0.46	1.6
11-2	148.48	0.74	2.38

12-2	143.63	0.65	1.92
13-2	165.5	1.08	13.14
14-2	180.99	1.39	21.97
15-2	192.98	1.63	24.12
16-2	148.87	0.74	2.43
17-2	--	--	--
18-2	147.58	0.72	2.13
19-2	151.13	0.8	2.48
20-2	149.22	0.76	2.3

APPENDIX H

VINEYARD SOIL – SUMMARY

Vineyard Soil

Run	Structure	Traffic AADTT	Condition	Treatment	LL	PL	PI	γdry max	wopt
1	1	900	Soaked	Control	38.5	17.2	21.3	110.0	15.7
2	1	900	Soaked	%16 CaO	42.5	24.3	18.2	--	--
3	1	900	Soaked	8%CaCl2	33.5	14.9	18.6	117.6	11.7
4	1	900	Soaked	12%CaCl2	33.4	16	17.4	116.3	14.0
5	1	900	Soaked	16%CaCl2	31.9	15	16.9	116.3	14.7
6	1	900	Unsoaked	Control	38.5	17.2	21.3	110.0	15.7
7	1	900	Unsoaked	%16 CaO	42.5	24.3	18.2	--	--
8	1	900	Unsoaked	8%CaCl2	33.5	14.9	18.6	117.6	11.7
9	1	900	Unsoaked	12%CaCl2	33.4	16	17.4	116.3	14.0
10	1	900	Unsoaked	16%CaCl2	31.9	15	16.9	116.3	14.7
11	1	4500	Soaked	Control	38.5	17.2	21.3	110.0	15.7
12	1	4500	Soaked	%16 CaO	42.5	24.3	18.2	--	--
13	1	4500	Soaked	8%CaCl2	33.5	14.9	18.6	117.6	11.7
14	1	4500	Soaked	12%CaCl2	33.4	16	17.4	116.3	14.0
15	1	4500	Soaked	16%CaCl2	31.9	15	16.9	116.3	14.7
16	1	4500	Unsoaked	Control	38.5	17.2	21.3	110.0	15.7
17	1	4500	Unsoaked	%16 CaO	42.5	24.3	18.2	--	--
18	1	4500	Unsoaked	8%CaCl2	33.5	14.9	18.6	117.6	11.7
19	1	4500	Unsoaked	12%CaCl2	33.4	16	17.4	116.3	14.0
20	1	4500	Unsoaked	16%CaCl2	31.9	15	16.9	116.3	14.7
1-2	2	2000	Soaked	Control	38.5	17.2	21.3	110.0	15.7
2-2	2	2000	Soaked	%16 CaO	42.5	24.3	18.2	--	--
3-2	2	2000	Soaked	8%CaCl2	33.5	14.9	18.6	117.6	11.7
4-2	2	2000	Soaked	12%CaCl2	33.4	16	17.4	116.3	14.0
5-2	2	2000	Soaked	16%CaCl2	31.9	15	16.9	116.3	14.7
6-2	2	2000	Unsoaked	Control	38.5	17.2	21.3	110.0	15.7
7-2	2	2000	Unsoaked	%16 CaO	42.5	24.3	18.2	--	--
8-2	2	2000	Unsoaked	8%CaCl2	33.5	14.9	18.6	117.6	11.7
9-2	2	2000	Unsoaked	12%CaCl2	33.4	16	17.4	116.3	14.0
10-2	2	2000	Unsoaked	16%CaCl2	31.9	15	16.9	116.3	14.7
11-2	2	10000	Soaked	Control	38.5	17.2	21.3	110.0	15.7
12-2	2	10000	Soaked	%16 CaO	42.5	24.3	18.2	--	--

13-2	2	10000	Soaked	8%CaCl2	33.5	14.9	18.6	117.6	11.7
14-2	2	10000	Soaked	12%CaCl2	33.4	16	17.4	116.3	14.0
15-2	2	10000	Soaked	16%CaCl2	31.9	15	16.9	116.3	14.7
16-2	2	10000	Unsoaked	Control	38.5	17.2	21.3	110.0	15.7
17-2	2	10000	Unsoaked	%16 CaO	42.5	24.3	18.2	--	--
18-2	2	10000	Unsoaked	8%CaCl2	33.5	14.9	18.6	117.6	11.7
19-2	2	10000	Unsoaked	12%CaCl2	33.4	16	17.4	116.3	14.0
20-2	2	10000	Unsoaked	16%CaCl2	31.9	15	16.9	116.3	14.7

Vineyard Soil

Run	Compacted γdry	Compacted MC	CBR	Mr
1	111.5	15.7	8.8	10,277
2	93.8	15.7	42.0	27,943
3	114.8	15.3	2.3	4,354
4	115.0	15.0	3.3	5,486
5	113.3	15.0	3.8	6,004
6	110.2	15.7	11.1	11,923
7	`	--	--	--
8	115.5	10.1	20.9	17,877
9	112.1	12.0	19.4	17,044
10	94.4	12.8	22.3	18,634
11	111.5	15.7	8.8	10,277
12	93.8	15.7	42.0	27,943
13	114.8	15.3	2.3	4,354
14	115.0	15.0	3.3	5,486
15	113.3	15.0	3.8	6,004
16	110.2	15.7	11.1	11,923
17	--	--	--	--
18	115.5	10.1	20.9	17,877
19	112.1	12.0	19.4	17,044
20	94.4	12.8	22.3	18,634
1-2	111.5	15.7	8.8	10,277
2-2	93.8	15.7	42.0	27,943
3-2	114.8	15.3	2.3	4,354
4-2	115.0	15.0	3.3	5,486
5-2	113.3	15.0	3.8	6,004
6-2	110.2	15.7	11.1	11,923
7-2	--	--	--	--
8-2	115.5	10.1	20.9	17,877
9-2	112.1	12.0	19.4	17,044
10-2	94.4	12.8	22.3	18,634
11-2	111.5	15.7	8.8	10,277
12-2	93.8	15.7	42.0	27,943

13-2	114.8	15.3	2.3	4,354
14-2	115.0	15.0	3.3	5,486
15-2	113.3	15.0	3.8	6,004
16-2	110.2	15.7	11.1	11,923
17-2	--	--	--	--
18-2	115.5	10.1	20.9	17,877
19-2	112.1	12.0	19.4	17,044
20-2	94.4	12.8	22.3	18,634

Vineyard Soil

Run	Terminal IRI (in/mile)	Permanent deformation Total pavement (in)	AC bottom up cracking (% lane area)
1	154.5	0.8	23.5
2	146.6	0.6	22.76
3	173.22	1.18	24.66
4	160.3	0.91	23.76
5	156.61	0.83	23.43
6	151.41	0.7	23.01
7	--	--	--
8	150.81	0.69	22.75
9	148.31	0.63	22.34
10	147.03	0.59	22.06
11	184.97	1.22	44.41
12	175.15	0.96	38.61
13	206.67	1.68	48.41
14	191.12	1.37	45.21
15	187.26	1.27	44.01
16	182.25	1.13	42.51
17	--	--	--
18	181.66	1.11	41.51
19	178.54	1.03	40.01
20	176.57	0.99	39.01
1-2	142.01	0.57	1.76
2-2	134.61	0.42	1.62
3-2	157.65	0.91	2.08
4-2	147.02	0.69	1.82
5-2	143.9	0.62	1.75
6-2	139.23	0.52	1.66
7-2	--	--	--
8-2	138.43	0.5	1.62
9-2	135.89	0.45	1.58
10-2	134.43	0.42	1.55
11-2	156.7	0.9	4.38

12-2	145.78	0.69	1.97
13-2	176.12	1.3	19.39
14-2	162.6	1.03	6.66
15-2	158.71	0.95	4.01
16-2	153	0.83	2.73
17-2	--	--	--
18-2	151.82	0.81	2.43
19-2	148.75	0.75	2.16
20-2	146.95	0.72	2.02

APPENDIX I

EAGER SOIL – STRUCTURE / TRAFFIC RESULTS

Structure 1 -Traffic 1

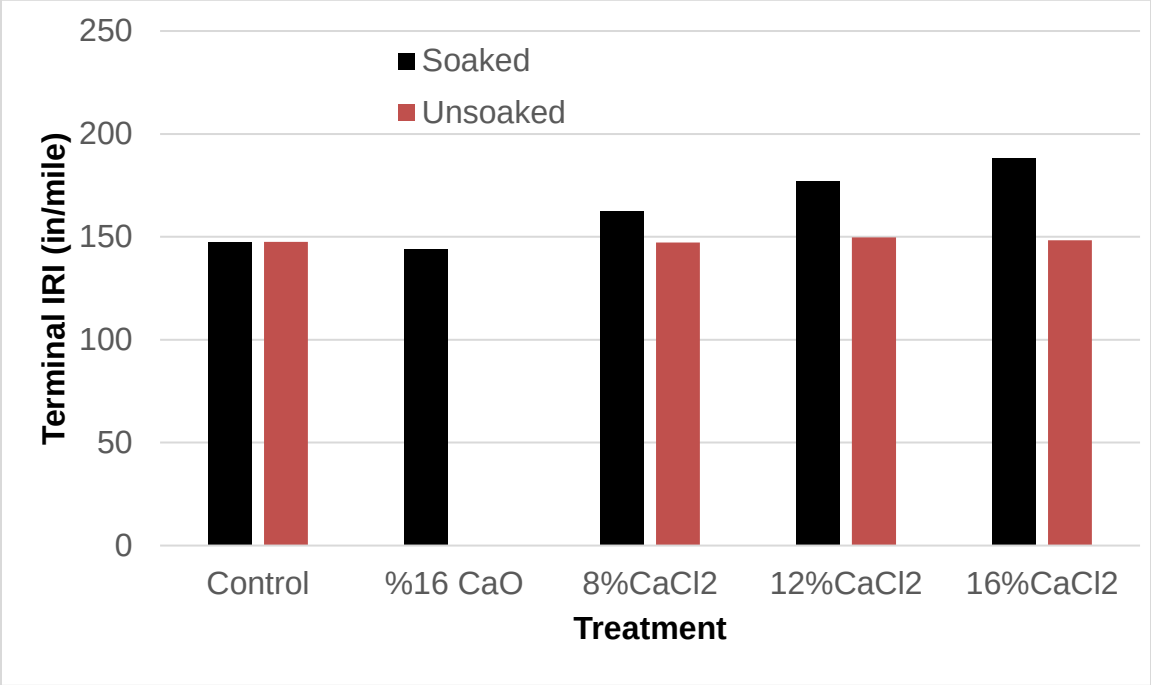

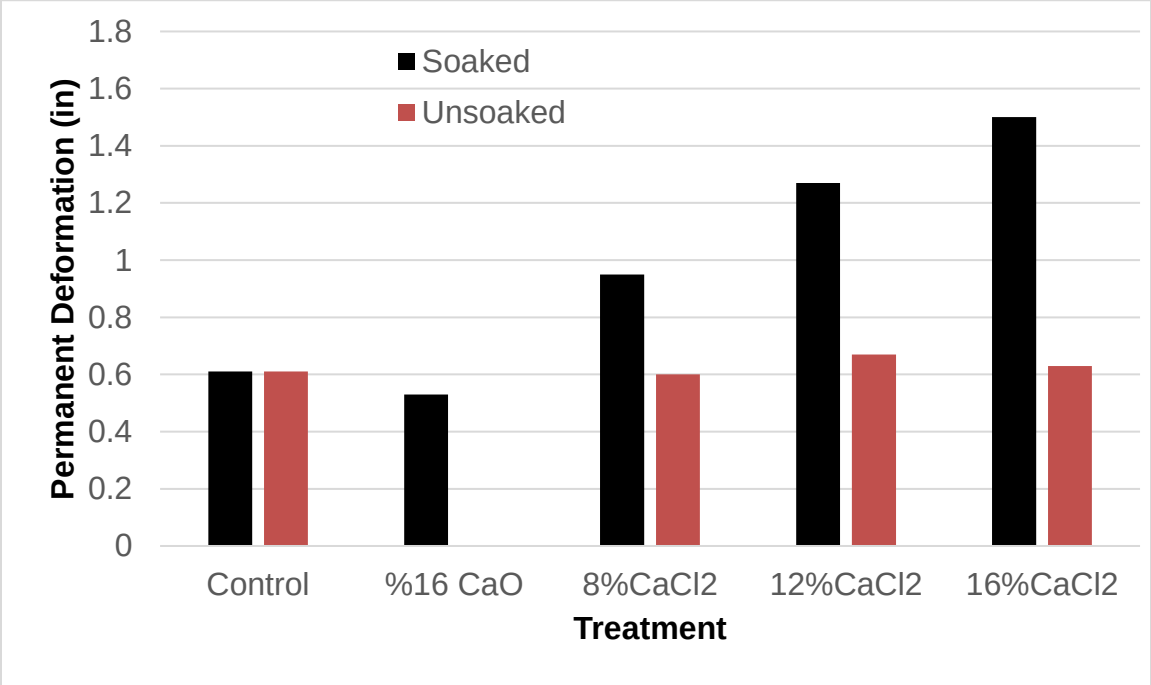

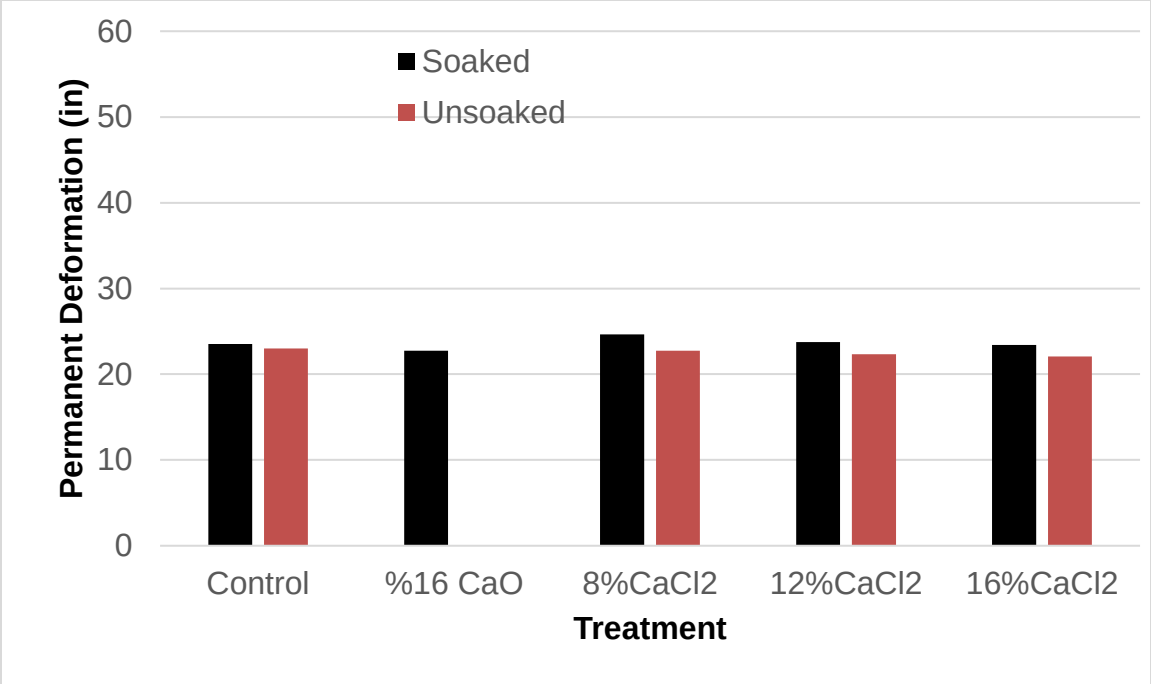
60
50
40
30
20
10
0
Permanent Deformation (in)
Soaked
Unsoaked
Control
%16 CaO
8%CaCl2
12%CaCl2
16%CaCl2
Treatment

Structure 1 - Traffic 2

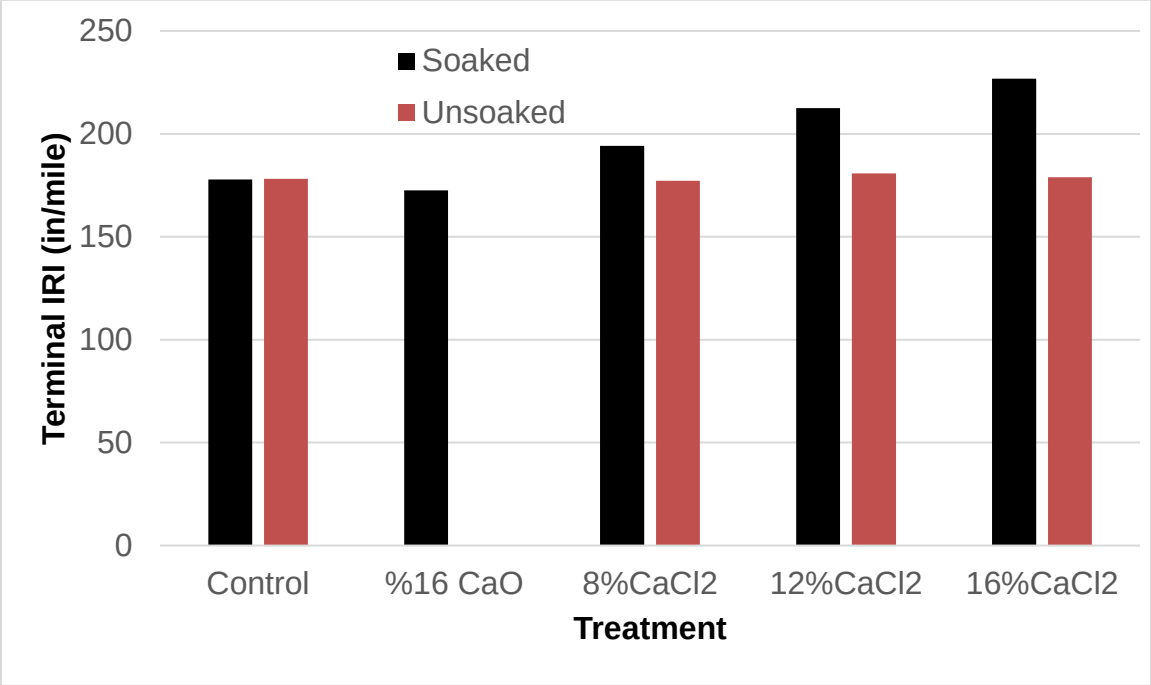

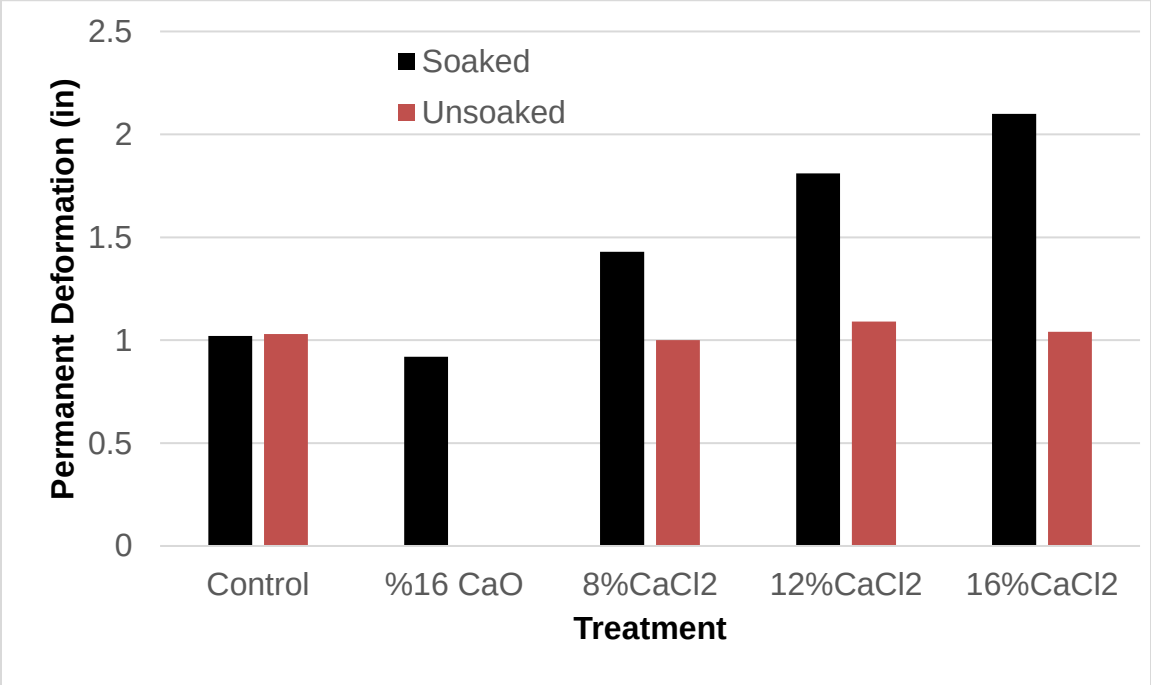

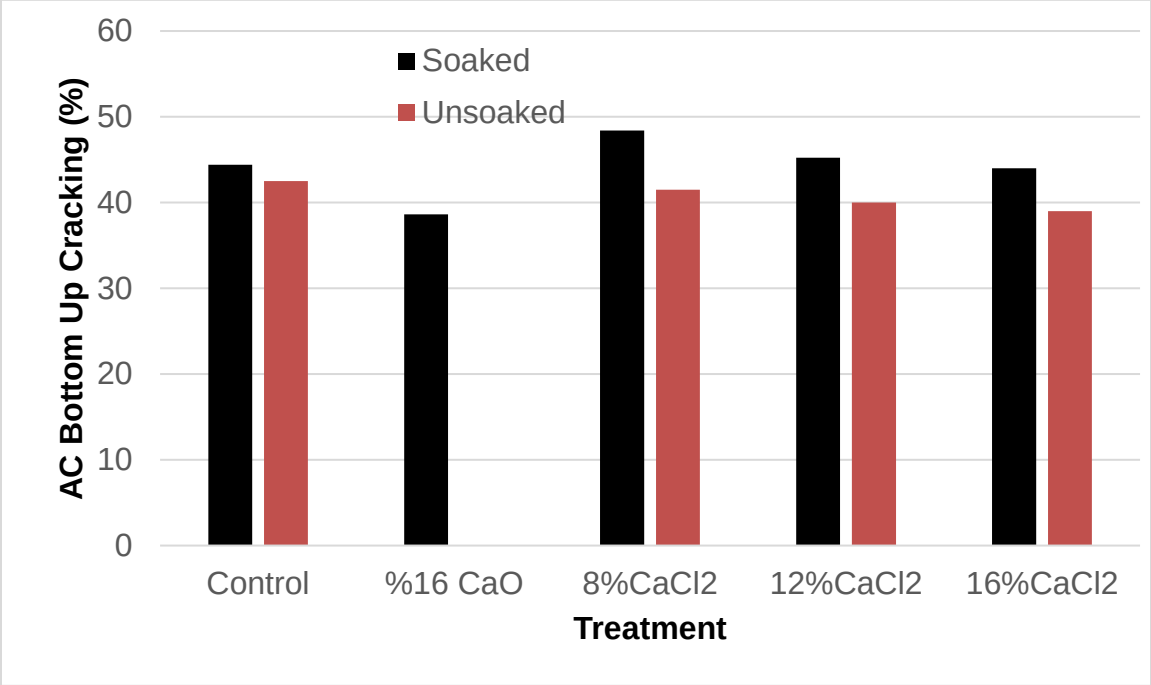
60
50
40
30
20
10
0
Soaked
Unsoaked
AC Bottom Up Cracking (%)
Control
%16 CaO
8%CaCl2
12%CaCl2
16%CaCl2
Treatment

Structure 2 - Traffic 1

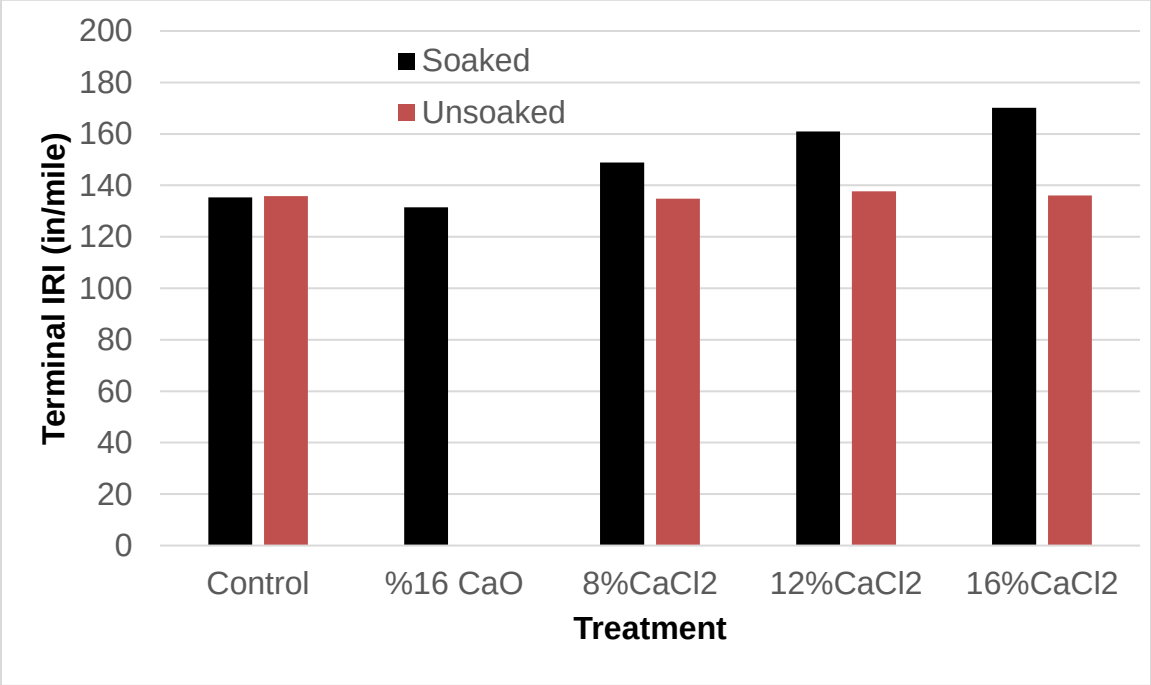

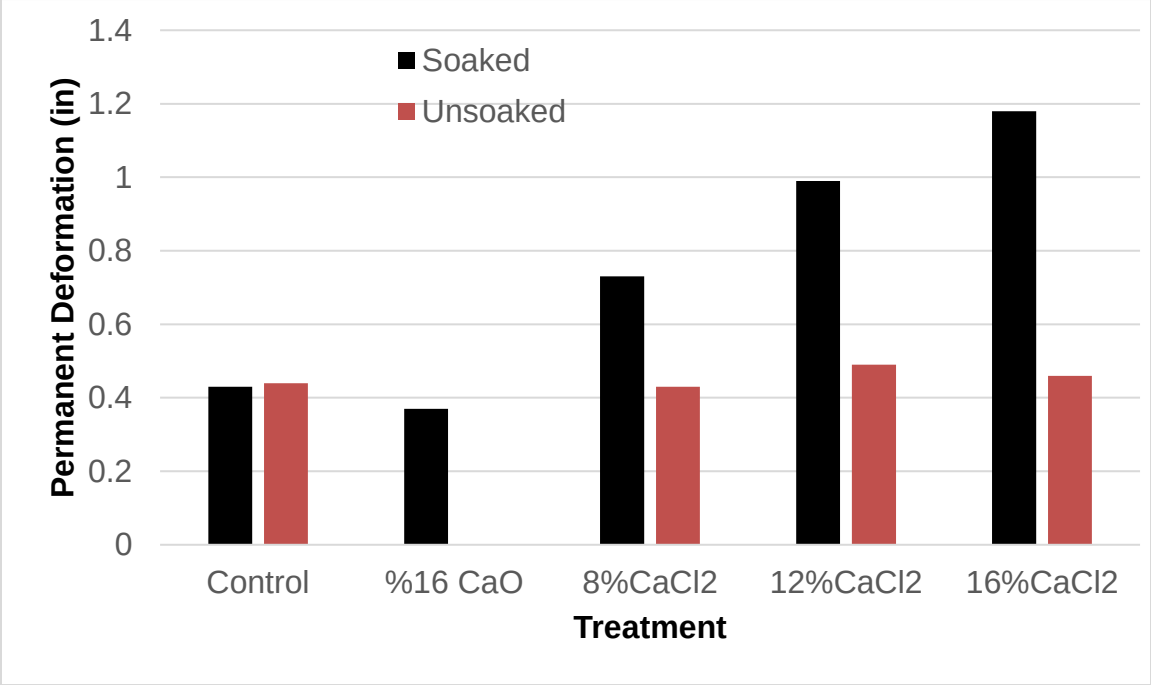

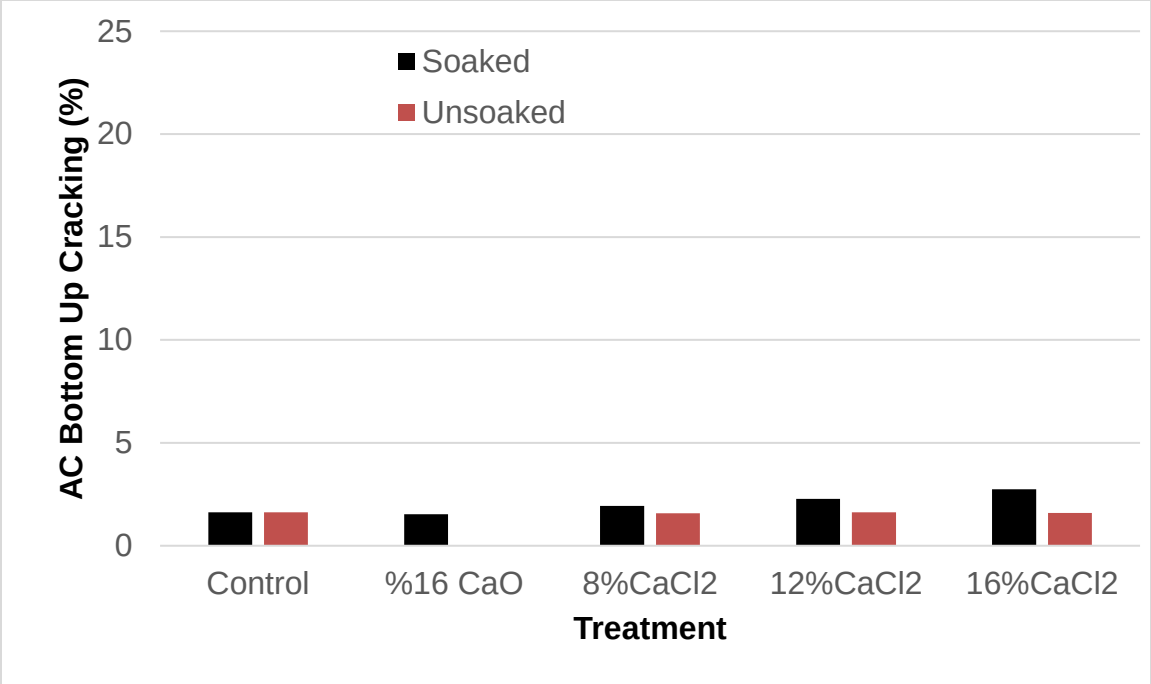
25
20
15
10
5
0
AC Bottom Up Cracking (%)
Soaked
Unsoaked
Control
%16 CaO
8%CaCl2
12%CaCl2
16%CaCl2
Treatment

Structure 2 - Traffic 2

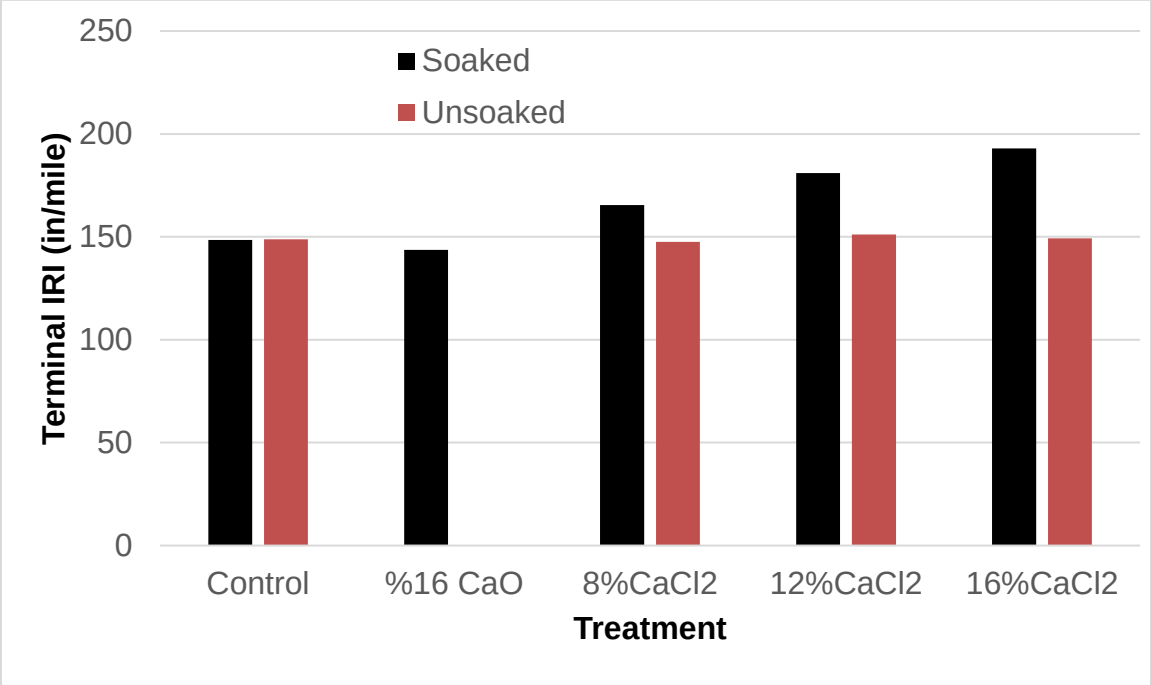

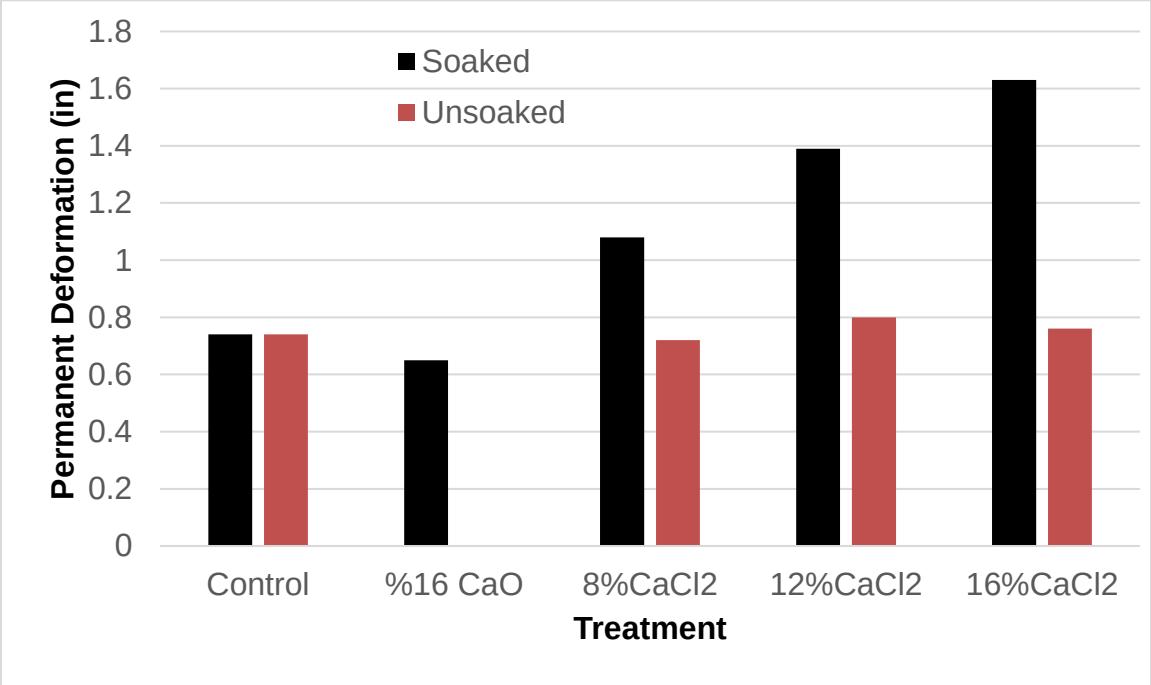

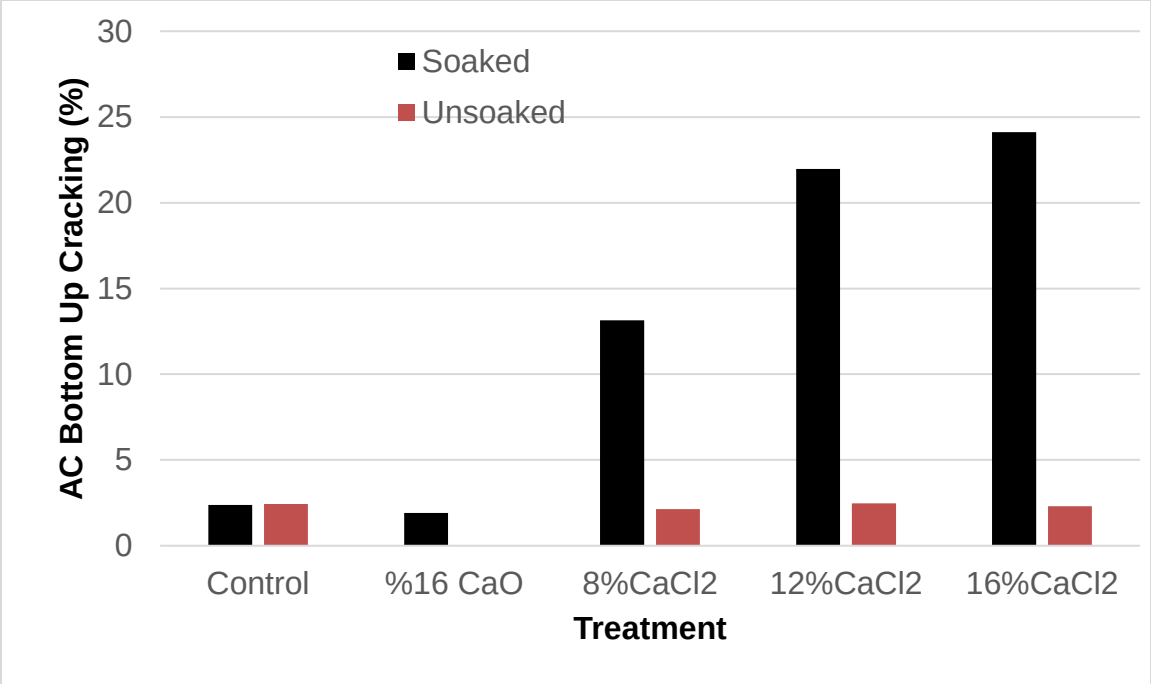
30
25
20
15
10
5
0
AC Bottom Up Cracking (%)
Soaked
Unsoaked
Control
%16 CaO
8%CaCl2
12%CaCl2
16%CaCl2
Treatment

APPENDIX J

VINEYARD SOIL – STRUCTURE / TRAFFIC RESULTS

Structure 1 - Traffic 1

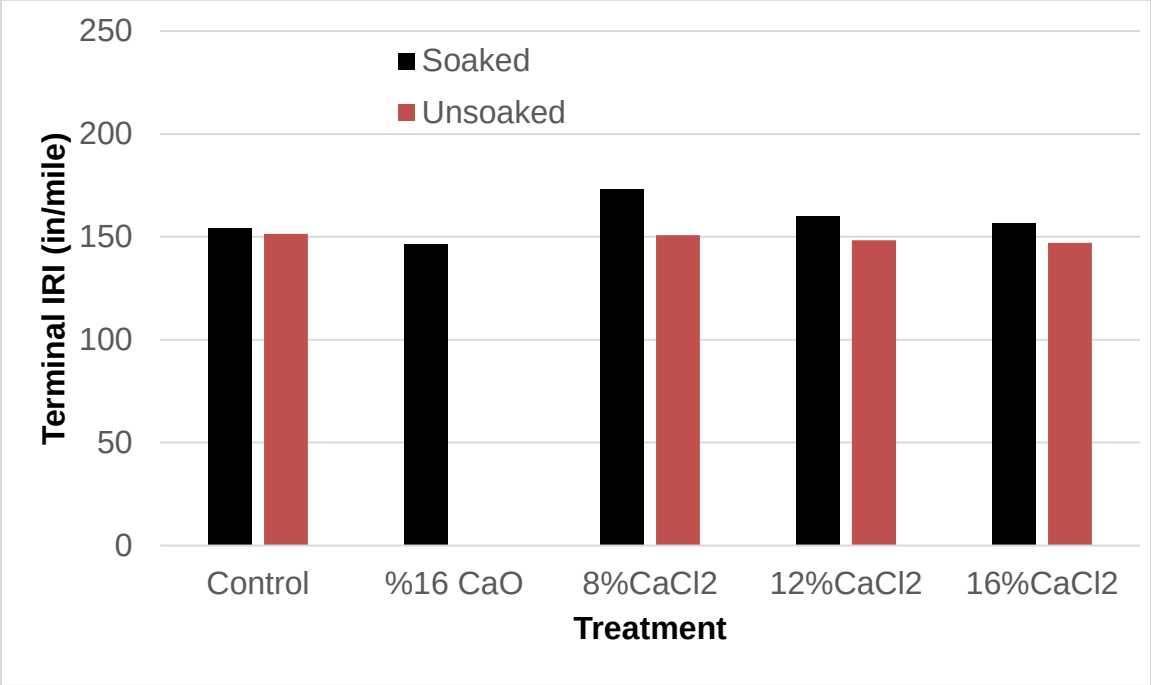

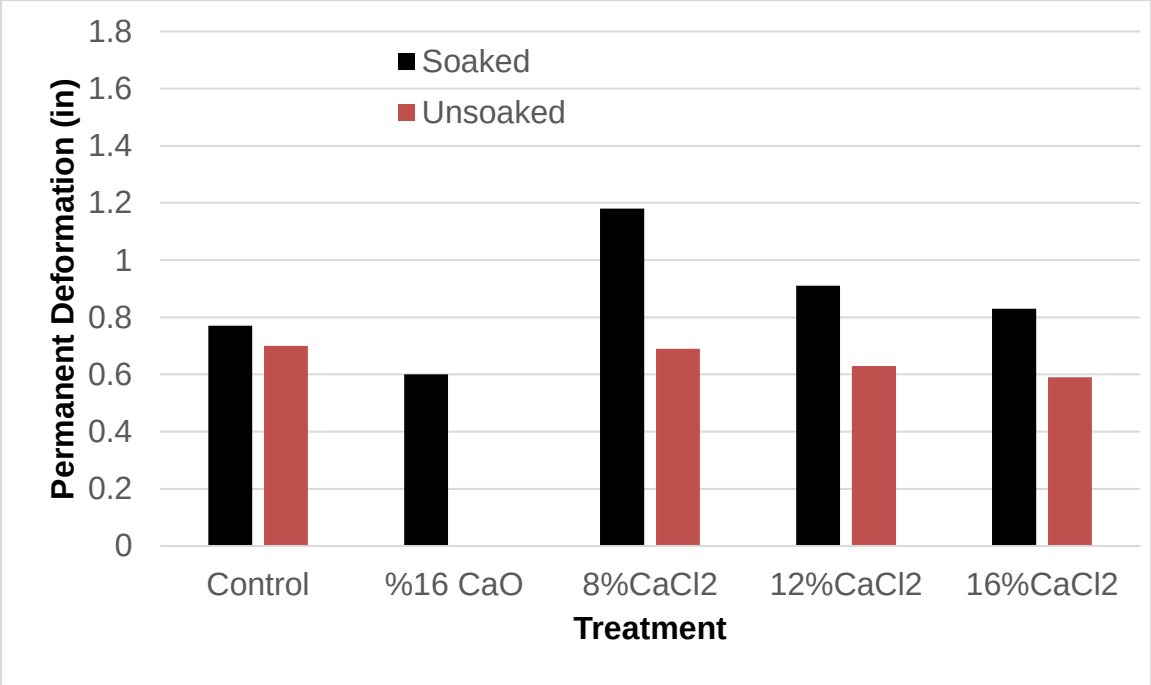

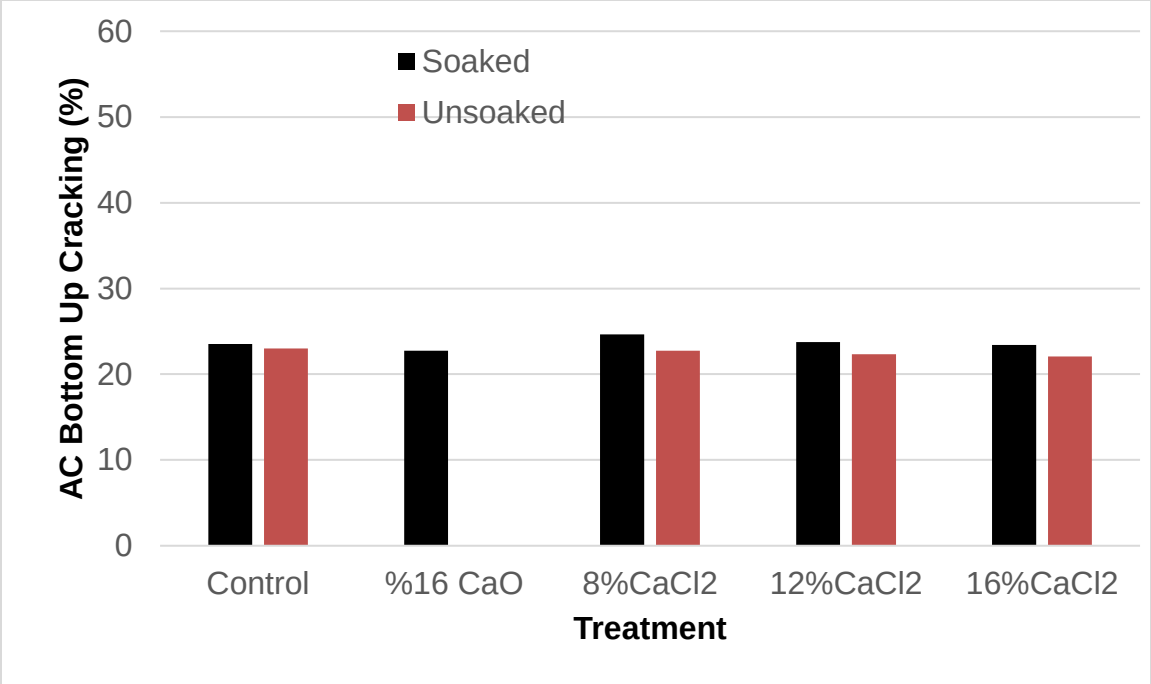
60
50
40
30
20
10
0
AC Bottom Up Cracking (%)
Soaked
Unsoaked
Control
%16 CaO
8%CaCl2
12%CaCl2
16%CaCl2
Treatment

Structure 1 - Traffic 2

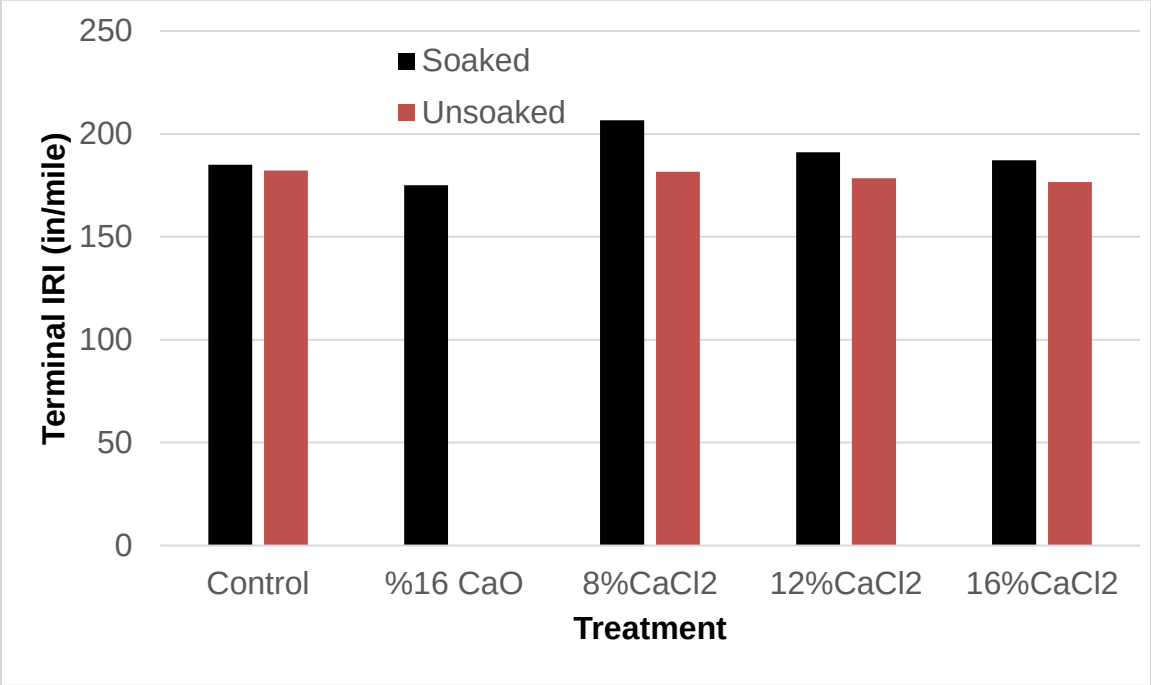

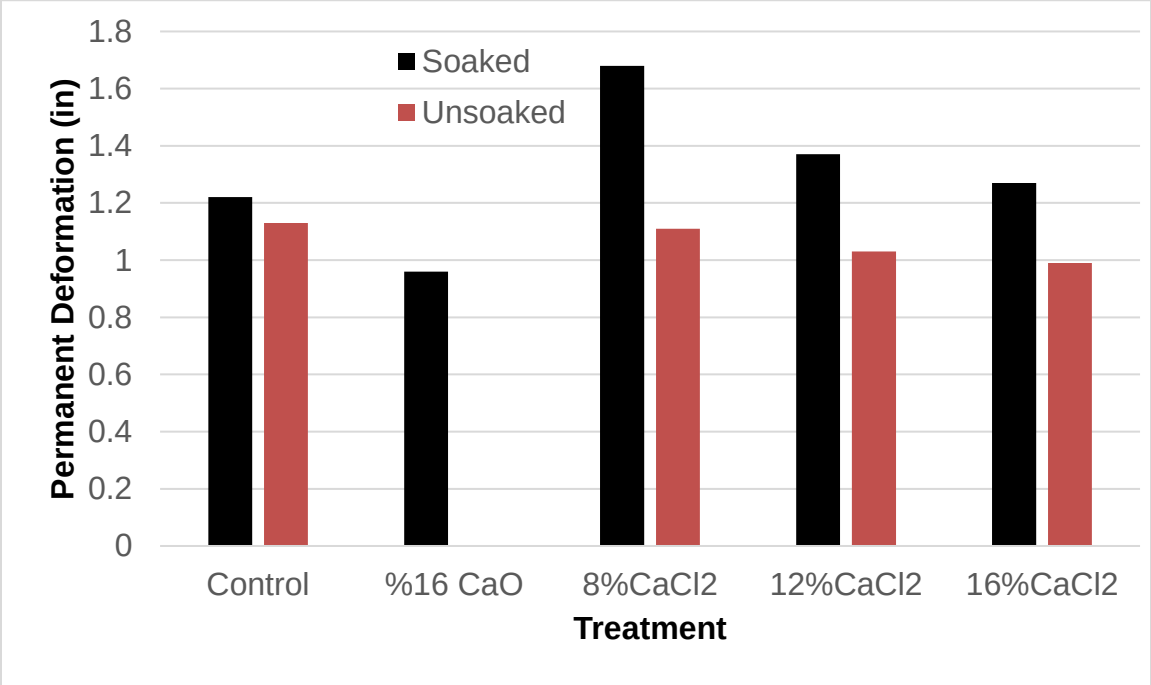

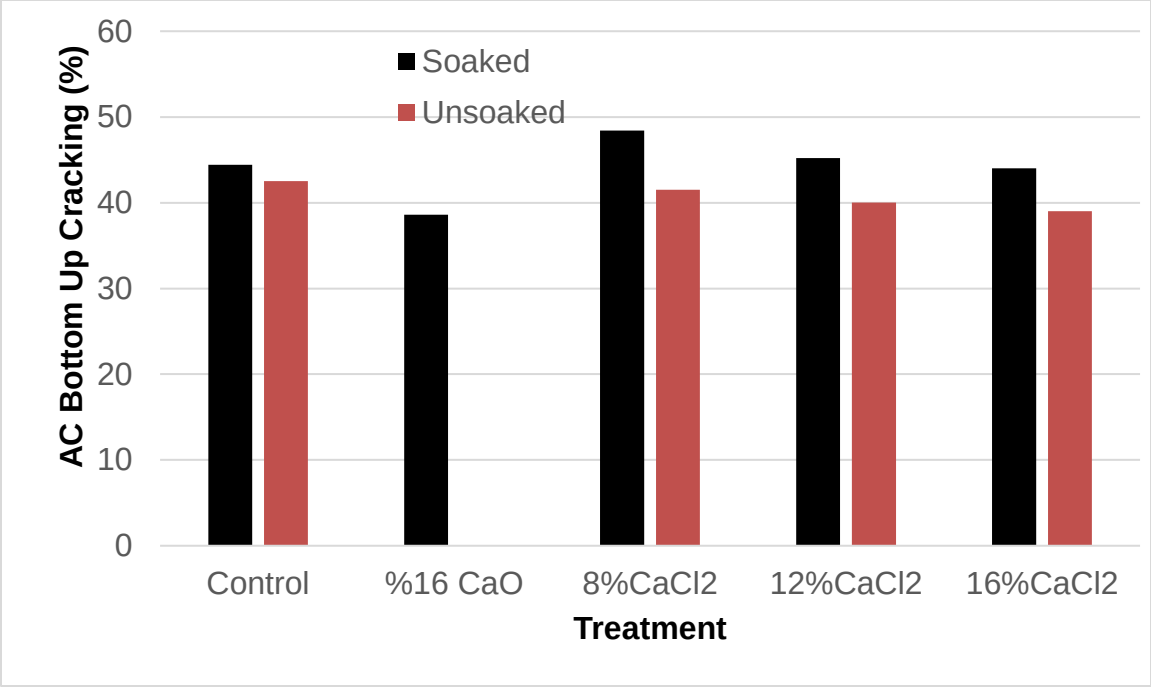
AC Bottom Up Cracking (%)
60
50
40
30
20
10
0
Soaked
Unsoaked
Control
%16 CaO
8%CaCl2
12%CaCl2
16%CaCl2
Treatment

Structure 2 - Traffic 1

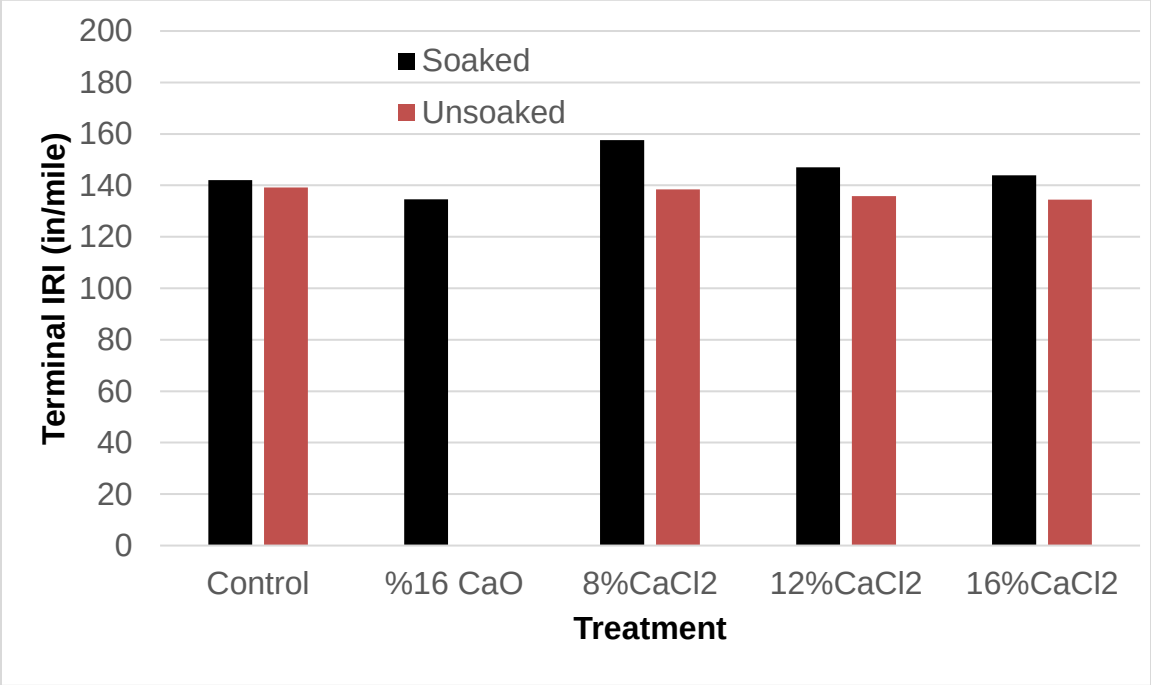

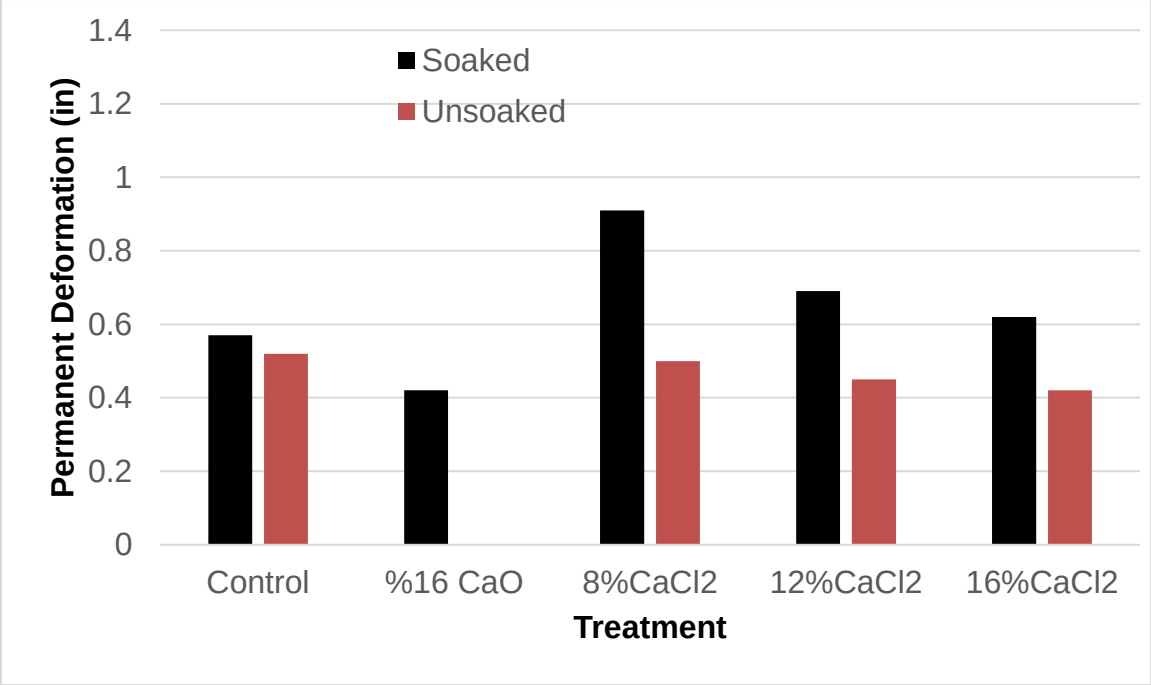

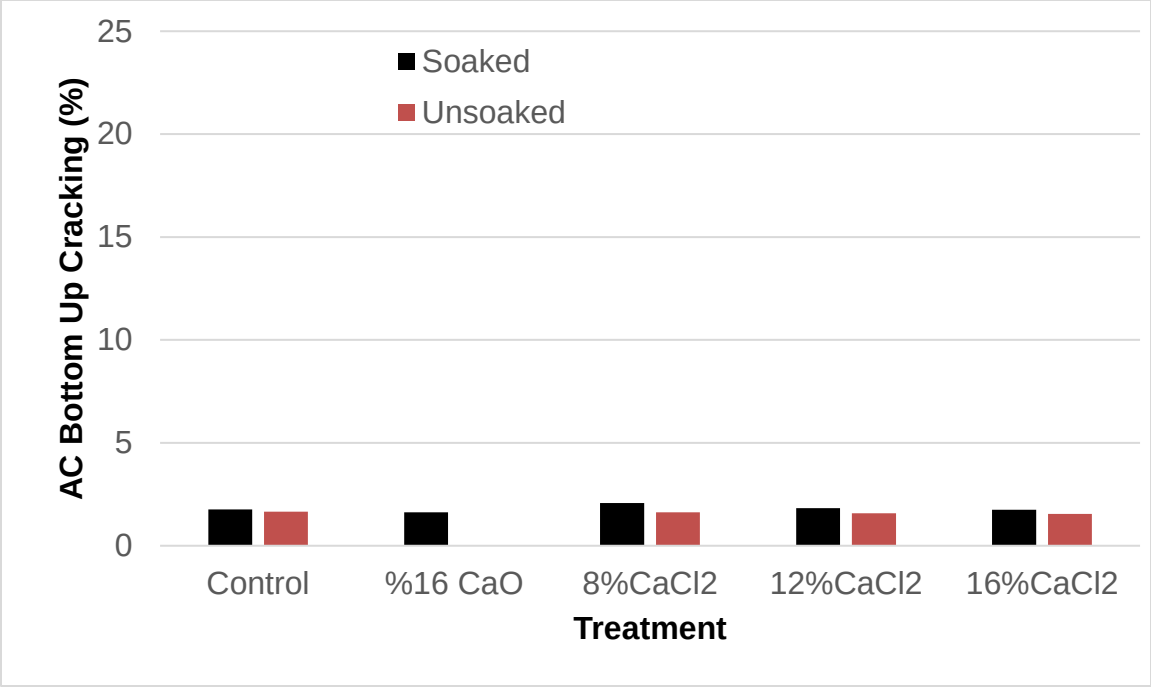
25
20
15
10
5
0
AC Bottom Up Cracking (%)
Soaked
Unsoaked
Control
%16 CaO
8%CaCl2
12%CaCl2
16%CaCl2
Treatment

Structure 2 - Traffic 2

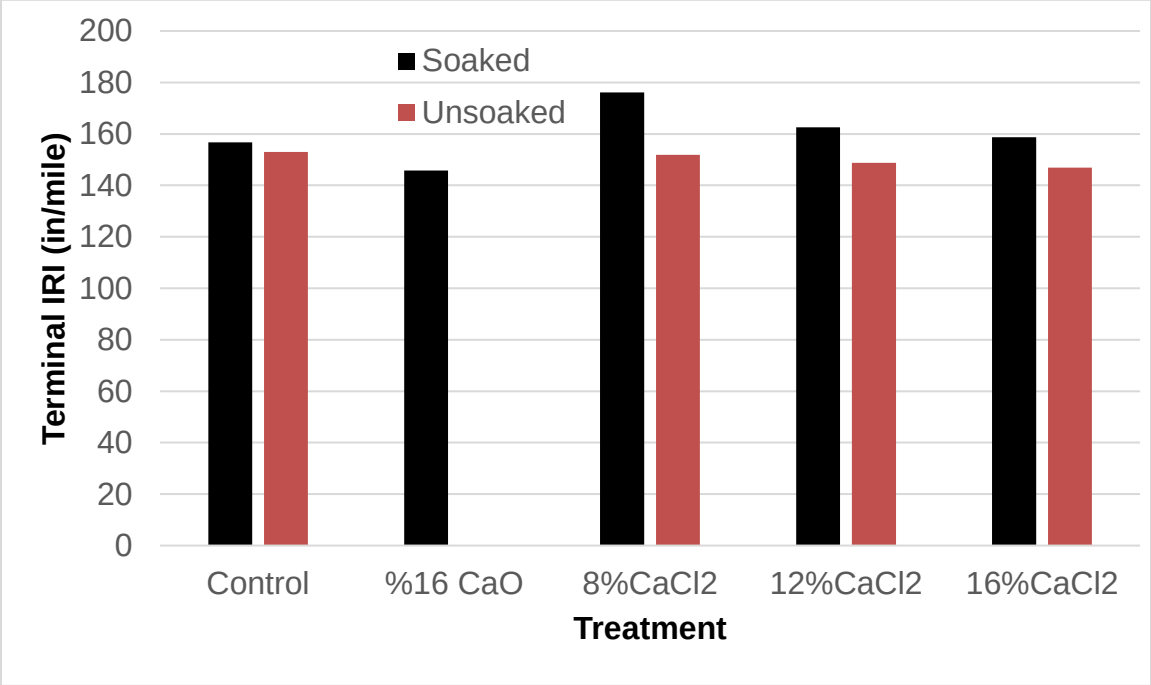

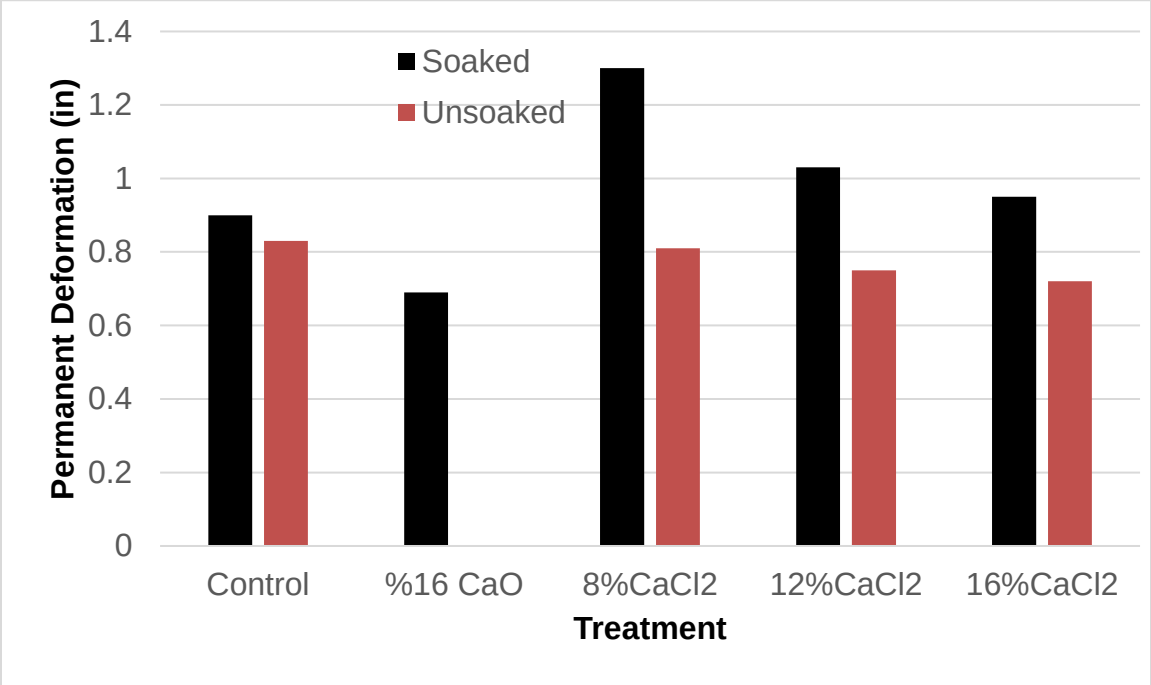

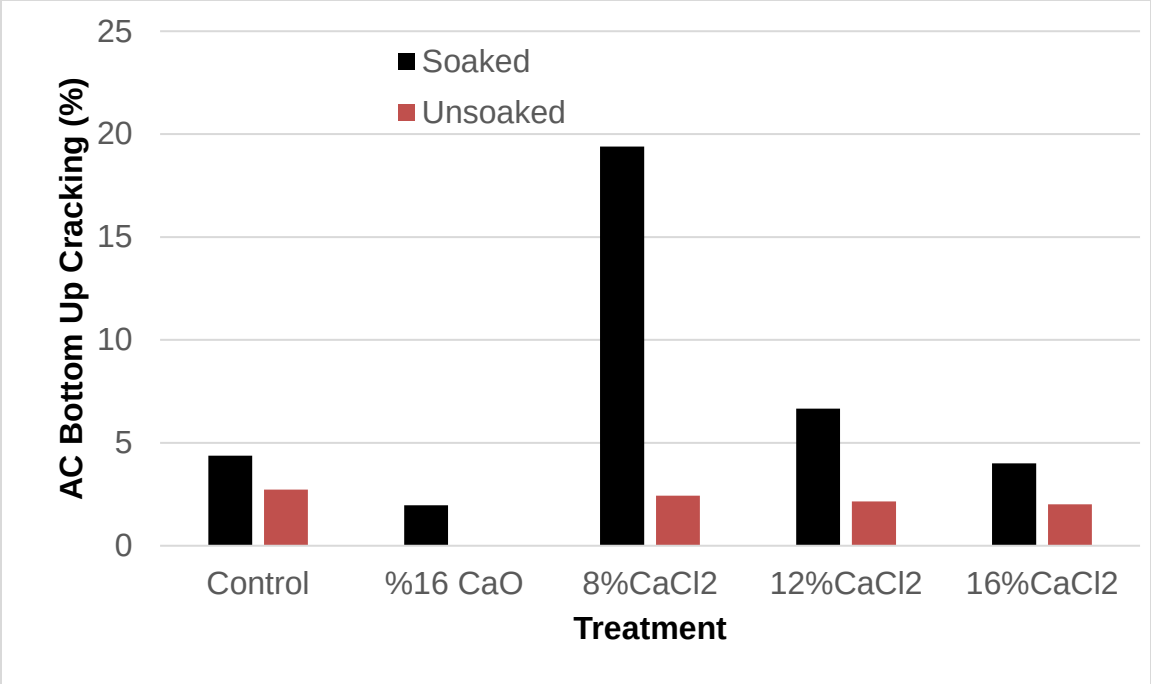
25
20
15
10
5
0
AC Bottom Up Cracking (%)
Soaked
Unsoaked
Control
%16 CaO
8%CaCl2
12%CaCl2
16%CaCl2
Treatment